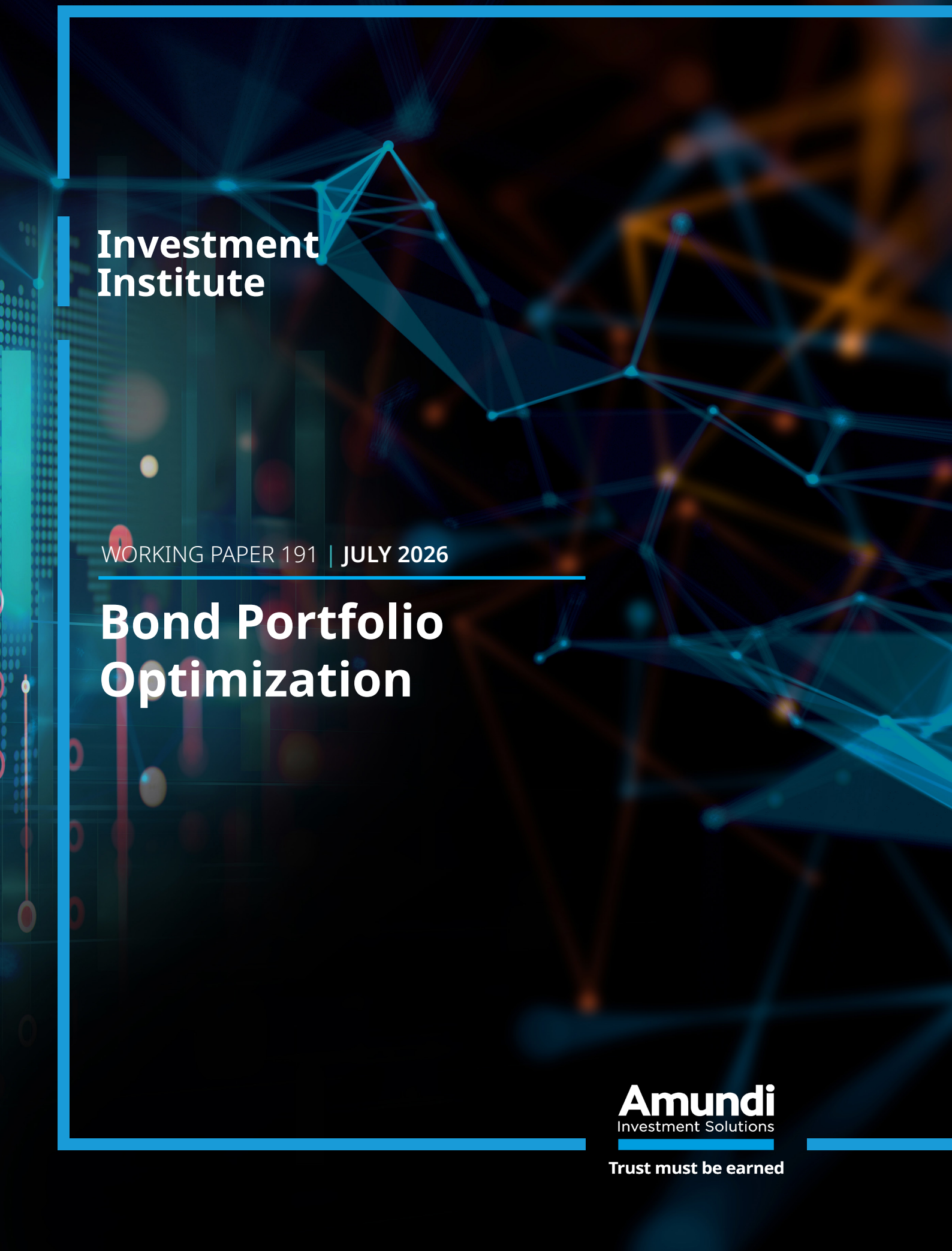

Investment Institute

WORKING PAPER 191 | JULY 2026

Bond Portfolio Optimization

Amundi
Investment Solutions

Trust must be earned

Bond Portfolio Optimization

Mohamed BEN SLIMANE
Amundi Investment Institute
mohamed.benslimane@amundi.com

Amina CHERIEF
Amundi Investment Institute
amina.cherief@amundi.com

Thierry RONCALLI
Amundi Investment Institute
thierry.roncalli@amundi.com

Jiali XU
Amundi Investment Institute
jiali.xu@amundi.com

Abstract

Although bond portfolio optimization is one of the oldest applications of the mean-variance framework, it is considerably less developed and adopted than its equity and multi-asset counterparts. This paper presents a comprehensive framework for bond portfolio optimization applied to investment universes composed of individual securities. We first identify the challenges that distinguish bond portfolio optimization from equity portfolio optimization. We then develop a family of optimization problems with and without a benchmark under alternative risk factor models. In particular, we focus on a two-factor risk model based on interest rates and credit risk. We also distinguish between l1-norm and l2-norm optimization problems, and show how these formulations can be cast into linear programming and quadratic programming problems using the properties of quadratic and extended linear forms. Beyond these standard formulations, we consider advanced optimization problems combining both l1 and l2 risk measures. We pay particular attention to active share constraints, which play a central role in fixed-income portfolio management.

The second part of the paper is dedicated to empirical applications using the ICE BofA Corporate Bond indices (Global, EUR, and USD). We first illustrate the differences between l1-norm and l2-norm optimization and their impact on tracking error volatility. We then apply the Barra multi-factor risk model and decompose portfolio risk into common factor and specific risk contributions. The third application addresses active portfolio management, where we decompose expected excess returns into carry, rolldown, and repricing components. The fourth application considers the classical problem of portfolio decarbonization. The fifth application examines the sensitivity of portfolio construction to alternative clustering and bucketing methodologies. The sixth and final application illustrates the practical challenges of constructing investable portfolios and demonstrates that the difference between model and investable portfolios is a primary issue in fixed-income optimization.

Acknowledgement

The authors are very grateful to Jean-Marie Dumas and Hamza Fredj for their helpful comments. The opinions expressed in this research are those of the authors and are not meant to represent the opinions or official positions of Amundi Asset Management. The authors used an AI-based language model to assist with English language polishing. The authors remain fully responsible for the content of the paper.

Keywords: Bond, fixed-income, active ETF, portfolio optimization, multi-factor risk model, tracking error, modified duration, duration times spread, clustering, quadratic programming, linear programming, lp norm, ADMM, carry, rolldown, repricing, quantamental investing.

JEL classification: C61, G11, G12.

About the authors

Mohamed BEN SLIMANE

Mohamed Ben Slimane is the Head of Fixed Income Quant Portfolio Strategy within Amundi Institute. On top of the long-term research subjects of the team, Mohamed specialises in designing new thinking for problems which have not yet been solved within investment platforms for active or passive fixed income management from the upper stages down to prototyping and testing.

He joined the Quantitative Research team of Amundi in 2016 as a Quantitative Analyst. Prior to his current position, he was the Head of Credit and Counterparty Risks (2013-2015), Head of Regulatory Risk for Fixed Income and Structured Funds (2010-2013), and Head of Regulatory Risk at Société Générale AM (2005-2010). Before joining Amundi he was an IT consultant with Altran (2002-2005) and a software engineer at Sungard Systems (2001-2002). He started his working career with Cap Gemini in 1999 as a software engineer.

Mohamed holds an engineering degree from the Ecole Nationale de l'Aviation Civile (1999). He is a certified international investment analyst CIIA (2010) and FRM charterholder (2013).

Amina CHERIEF

Amina Cherief is a Fixed Income Quant Researcher at Amundi Investment Institute. Amina joined Amundi's Quantitative Research Team in April 2017 to work on the development of a multi-factor risk and performance analysis tool. She worked from 2017 to 2018 as a Financial Engineer at Natixis AM and from 2018 to 2019 as a Cross-Asset Strategist at Natixis CIB where she was in charge of support and research (equity & commodity strategies, new portfolio allocation) for the QIS team. In 2019, Amina joined SG CIB in New York as a Cross-Asset Financial Engineer in the QIS team for two years; she was in charge of research and portfolio construction of systematic equity and commodity strategies. She developed tools for sales and traders. Amina re-joined Amundi as a Quantitative Researcher in December 2020. Her areas of research are factor investing, sustainable investing and AI-ML in both fixed-income and equities. Recent advanced topics covered by Amina have been the integration of machine learning algorithms in the investment process of a fixed income team or the creation of innovative allocation in portfolios.

Amina holds a Master's Degree (with honors) in Risk and Asset Management from Paris-Saclay University.

Thierry RONCALLI

Thierry Roncalli is Head of Quant Portfolio Strategy at Amundi Investment Institute. In this role, he steers the quantitative research towards the best interests and ambitions of Amundi and its clients. He is also involved in the development of client relationships and innovative investment solutions.

Prior to his current position, he was Head of Research and Development at Lyxor Asset Management (2009-2016), Head of Investment Products and Strategies at SGAM AI, Société Générale (2005-2009), and Head of Risk Analytics at the Operational Research Group of Crédit Agricole SA (2004-2005). He was also a member of the Industry Technical Working Group on Operational Risk (ITWGOR) from 2001 to 2003. Thierry started his professional career at Crédit Lyonnais in 1999 as a financial engineer. Previously, Thierry was a researcher at the University of Bordeaux and then a research fellow at the Financial Econometrics Research Centre at Cass Business School. During his five-year academic career, he also worked as a consultant on option pricing models for several banks.

Since February 2017, he has been a member of the Scientific Advisory Board of the AMF, the French securities and financial markets regulator, while from 2014 to 2018 he was a member of the Group of Economic Advisers (GEA), ESMA's Committee for Economic and Market Analysis (CEMA). Thierry is also an Adjunct Professor of Economics at the University of Paris-Saclay (Evry), Department of Economics. He holds a Ph.D. in Economics from the University of Bordeaux, France. He is the author of numerous academic articles in scientific journals and has published several books on risk and asset management. His last two books are "Introduction to Risk Parity and Budgeting", published by Chapman & Hall in 2013 and translated into Chinese by China Financial Publishing House in 2016, and "Handbook of Financial Risk Management", published by Chapman & Hall in 2020.

Jiali XU

Jiali Xu is Head of Multi-Asset Quantitative Research in Quant Portfolio Strategy at Amundi Investment Institute. He joined Amundi in 2018 and is responsible for developing multi-asset quantitative investment strategies and investment applications of advanced optimization and machine learning techniques. His research focuses on factor investing, portfolio construction, and the application of advanced statistical methods in portfolio management.

Previously, from 2014 to 2018, he was a quantitative analyst in the risk analytics and solutions team at Société Générale. A graduate of Ecole des Ponts ParisTech, he also holds a Master's degree in Financial Mathematics from the University of Paris-Est Marne-la-Vallée

1 Introduction

Portfolio optimization is one of the most widely used tools for asset allocation in the investment industry. Since the pioneering work of Harry Markowitz, the mean-variance framework has profoundly influenced the theory and practice of portfolio construction (Elton *et al.*, 2014). Over the past decades, a vast literature has emerged around portfolio optimization, covering applications ranging from equity portfolio management (Fabozzi *et al.*, 2010) and multi-asset investing (Bessler *et al.*, 2017) to trend-following strategies (Jusselin *et al.*, 2017), carry strategies (Koijen *et al.*, 2018), strategic asset allocation (Bekkers *et al.*, 2009), and Fama-French risk factors (DeMiguel *et al.*, 2009). By contrast, bond portfolio optimization has received comparatively less attention outside specialized fixed-income circles[1]. While the fixed-income literature is rich in topics such as duration management, immunization, yield curve positioning, and liability-driven investment, the portfolio optimization framework is less frequently discussed in the context of bond investing. As a result, the concept of bond portfolio optimization remains less visible and standardized than its equity counterpart.

The optimization framework used by most practitioners has a common structure. It begins with a standard mean-variance optimization problem, typically calibrated with a three- to five-year empirical covariance matrix. The main differences across applications lie in how expected returns are determined. For trend-following and momentum strategies, expected returns are estimated from past realized returns over time horizons ranging from one month to two years, depending on whether the strategy targets long, medium, or short-term trends. More sophisticated trend estimation methods also exist (Bruder *et al.*, 2011). For contrarian or mean-reverting strategies, expected returns are set to the opposite of recent trends or calculated using econometric models such as time series and cointegration models (Roncalli, 2017). For carry strategies, expected returns are proxied by the carry itself, such as currency carry, equity dividend yields, or futures curve measures like contango and backwardation. Finally, for strategic asset allocation, expected returns are based on capital market assumptions derived from long-term macrofinance models. Beyond these standard implementations, the mean-variance framework has been extended in many ways, including Merton's continuous-time portfolio model, covariance factor models, robust optimization techniques (Tütüncü and Koenig, 2004), covariance shrinkage estimators (Ledoit and Wolf, 2004), and various denoising approaches designed to improve the stability of portfolio allocations (Laloux *et al.*, 1999). A comprehensive list of these extensions[2] can be found in Kolm *et al.* (2014), which illustrates how rapidly portfolio optimization techniques have evolved over the past decades.

In contrast to equity and multi-asset portfolio optimization, applications to fixed-income securities remain relatively sparse. In fact, the most common applications focus on liquid bond futures or generic sovereign bonds, where the investment universe is defined by country and standard maturity buckets (*e.g.*, 1Y, 3Y, 5Y, 7Y, and 10Y). Applications at the level of individual (sovereign or corporate) bonds are considerably more limited[3]. Indeed, a broad survey of the literature[4] suggests that relatively few academic contributions explicitly address portfolio optimization in this setting. Among the notable exceptions, we can

[1] For instance, bonds are not discussed in the landmark review *60 Years of Portfolio Optimization* by Kolm *et al.* (2014). More surprisingly, none of the 105 references cited in that survey is dedicated to bond portfolio optimization.

[2] Other extensions consider transaction costs, liquidity considerations, higher moments of the return distribution, risk parity approaches, regime-switching models, and alternative risk measures such as value-at-risk or expected shortfall.

[3] We exclude here CDS portfolios and credit portfolios, which have been comparatively better explored, particularly in the period preceding the global financial crisis.

[4] Conducted via Google Scholar using the keyword "*bond portfolio optimization*".

cite Konno and Watanabe (1996) on index tracking, Korn and Koziol (2006) on German sovereign bonds, Puhle (2008) on term structure models, Chandrasekhar (2009) on bond funds, Caldeira *et al.* (2016) on U.S. Treasury benchmarks, Deguest *et al.* (2018) on European sovereign bonds, Drenovak *et al.* (2021), and Luxenberg *et al.* (2024), the latter two focusing on corporate bond portfolios. Overall, these studies tend to rely on simplified representations of the fixed-income universe, most commonly using sovereign benchmark bonds or generic maturity buckets rather than individual securities.

Why this disconnect? In fact, the literature shifted away from portfolio construction toward the analysis of individual securities as early as the 1970s and 1980s:

> "*A number of early papers [...] have provided a preliminary analysis of bond portfolio construction problems shortly after the publication of the seminal paper by Markowitz (1952), but the literature has gradually shifted toward analysis of risk and performance of individual bonds [...]*" (Deguest *et al.*, 2018, page 6).

This shift is reflected in the tools that practitioners have developed and adopted. The dominant fixed-income analytics platforms — the Yield Book, which was originally developed at Salomon Brothers and later acquired by Citigroup and LSEG, and POINT, developed at Lehman Brothers and later acquired by Barclays and Bloomberg[5] — were built around the analytics of individual securities rather than portfolio optimization. Their core functionality centered on computing security-level risk metrics such as option-adjusted spread, modified duration, convexity, and rolldown, and aggregating these measures at the portfolio level for risk monitoring, scenario analysis, performance attribution, and index replication. For instance, the third edition of *Inside The Yield Book* does not contain the word *optimization* (Leibowitz *et al.*, 2013). Even when an optimization module existed — as it was the case with POINT — it was designed primarily for tracking error minimization and index replication rather than for mean-variance portfolio construction in the Markowitz sense. In short, the prevailing paradigm in fixed-income asset management has long been benchmark-relative risk budgeting and bond picking, not portfolio optimization[6]. This partly explains why the concept of bond portfolio optimization has remained the domain of specialized academics and professionals.

The divergence between equity and bond portfolio optimization also exists because applying standard asset allocation models to fixed-income portfolios presents several structural challenges that traditional mean-variance optimization cannot fully capture. One challenge is the estimation of expected returns. For any financial asset traded in a market, total return has two components: the income generated by the asset and the mark-to-market gain or loss resulting from price fluctuations. For equities, the income component is dividends, while the mark-to-market component reflects stock price appreciation or depreciation. Dividends are relatively predictable because they exhibit substantial persistence over time. The mark-to-market component is less predictable, but it can be approximated by a Gaussian distribution, despite well-documented asymmetries of equity returns[7]. In the case of bonds, income is generated by coupon payments, but the mark-to-market component is considerably more complex. It is driven by multiple sources of risk, including interest rate risk, credit spread risk, default risk, and liquidity conditions. Interest rate risk has a complex

[5] It is now integrated into PORT (Bloomberg's Portfolio & Risk Analytics).

[6] For instance, while bond portfolio management is extensively covered in the landmark handbooks edited by one of the foremost authorities in fixed income, Frank Fabozzi (Fabozzi and Pollack, 1983; Fabozzi, 2001; Fabozzi *et al.*, 2008), bond portfolio optimization has rarely a dedicated chapter. Instead, it tends to appear as a mathematical subtopic in the chapters devoted to index replication or liability matching.

[7] Negative equity returns tend to be less frequent but more severe than positive ones, resulting in negative skewness and excess kurtosis.

structure shaped by movements in the level, slope, and curvature of the yield curve. Modeling these dynamics has led to the development of a large number of term structure models. Credit risk introduces an additional layer of complexity. Beyond spread risk, which reflects changes in the market's assessment of creditworthiness, investors are exposed to default risk. Default risk is discontinuous by nature and is often modeled through jump processes. Consequently, estimating expected return is considerably more complex than in traditional equity portfolio models. Beyond modeling expected returns, the second challenge concerns risk measurement. Although imperfect, volatility and pairwise correlations are reasonably effective summaries of risk for diversified equity portfolios. In practice, quants typically rely on a linear factor model driven by style factors, such as size, value, momentum, quality, and low volatility, and sector exposures. In some cases, an empirical covariance matrix estimated from historical returns can be used directly as input for mean-variance optimization. The fixed-income case is more problematic for several reasons. First, bond volatility is non-stationary by construction. As a bond approaches maturity, its duration — and therefore its price sensitivity to interest rate movements — declines mechanically. Therefore, the volatility of a given bond decreases over time, even in the absence of any change in the underlying risk environment. For example, a newly issued 35-year bond is significantly more volatile than a 5-year bond. Yet, thirty years later, this bond has a remaining maturity of five years and behaves, in terms of interest rate sensitivity, essentially like a 5-year bond. This convergence of volatility toward zero at maturity is unique to fixed income and has no analogue in the equity world, where risk characteristics are often assumed to be relatively stable over moderate time horizons. As a result, a covariance matrix estimated from the historical returns of a fixed set of bonds becomes increasingly irrelevant as the bonds age. Moreover, this issue is exacerbated by the continuous turnover of the bond universe as securities mature and are replaced by new issuances. Second, the correlation structure among bonds is considerably more complex than in the equity case because it reflects several distinct and overlapping sources of co-movement. It is important to distinguish between intra-factor correlations, such as correlations among interest rates across maturities and currencies, correlations among credit spreads across sectors and rating categories, and correlations among default times, as well as cross-factor correlations between interest rates, credit spreads, and default times. These different correlation layers do not contribute equally across a bond investment universe, and their relative importance shifts markedly with credit quality. For high-quality sovereign bonds rated AAA, interest rate correlation dominates. For investment grade bonds rated in the BBB range, credit spread correlation becomes the primary driver. For high yield bonds rated CCC, the correlation structure is dominated by the dependence between default times. Finally, the third challenge is the implementation and execution of an optimized bond portfolio. Portfolio optimization produces a model portfolio, where exposures are expressed as weights or percentages of the portfolio value. However, to implement this model in practice, it must be translated into an investable (or tradable) portfolio. This process is considerably more complex for bonds than for equities for two main reasons. First, the minimum investment size for a bond is typically much larger than that for a stock. Concepts such as minimum tradable amounts and lot sizes play a critical role in bond portfolio construction, while one can generally buy a single share of any stock. Consequently, converting an optimized portfolio into an investable portfolio using rounding techniques is significantly more complex for bonds than for equities, and may result in large deviations from the theoretical optimum. Second, a significant proportion of bonds cannot be readily traded due to liquidity constraints. Unlike the stock market, the bond market is predominantly buy-and-hold. Many bonds, once absorbed by long-term investors at issuance, rarely trade again in the secondary market. This illiquidity means that the investable universe available to a portfolio manager may differ substantially from the theoretical universe used

to construct the model portfolio. These three challenges (the estimation of expected return, the non-stationarity of the risk structure, and the discrepancy between model and investable portfolios) explain why bond portfolio optimization has remained less developed than equity and multi-asset portfolio optimization.

The recent development of active fixed-income ETFs has generated renewed interest in bond portfolio optimization for several reasons. First, active ETFs are subject to transparency requirements that obligate managers to regularly disclose their holdings. This creates a need for disciplined, systematic, and repeatable portfolio construction processes. Second, since active ETF managers are evaluated against a benchmark, tracking error becomes a central and measurable concern that must be controlled in real time. Third, the market-making mechanism of ETFs introduces additional complexity. Authorized participants and market makers must efficiently create and redeem ETF shares. This imposes constraints on liquidity, lot size, and minimum tradable amount, which are naturally handled within an optimization framework. Fourth, the rapid growth of active fixed-income ETFs has intensified competition among managers, creating pressure to combine multiple sources of systematic alpha rather than relying on discretionary bond picking alone. Taken together, these factors suggest that the industrialization of active bond management through the ETF wrapper makes bond portfolio optimization increasingly useful.

This paper is structured as follows. Section Two is dedicated to bond portfolio optimization. We first discuss the application of the traditional mean-variance framework to an investment universe of individual bonds. Then, we identify several issues that make this setting fundamentally different from the equity case. First, an empirical covariance matrix poorly measures the risk of a bond portfolio, because volatility and correlation are non-stationary and depend on maturity and credit spread. Second, the structure of a bond investment universe differs markedly from those of equity or multi-asset investment universes. In particular, practitioners are highly sensitive to universe clustering and the notion of buckets. In equity markets, substituting one stock for another is generally difficult, since two companies remain distinct even when they operate under similar business models. This is less true for bonds. When a cluster or bucket is well-defined — for instance, AA-rated bonds in the utility sector with maturities in the 3–5Y range — substitution across securities becomes considerably more feasible. Third, we present the core optimization problems, with and without a benchmark. We consider both the $\boldsymbol{\ell}_1$- and $\boldsymbol{\ell}_2$-norm formulations and show how they can be solved with linear programming and quadratic programming, respectively. Fourth, we turn to more advanced bond optimization problems, with particular attention to the active share, which is an important and widely used metric in bond portfolio management. We also examine the distinction between model and investable portfolios, and illustrate how minimum tradable amount and lot size constraints introduce significant complexity when seeking an implementable optimal solution. Section Three presents a series of applications. We begin by illustrating the difference between $\boldsymbol{\ell}_1$- and $\boldsymbol{\ell}_2$-norm risk measures and their impact on the optimal bond portfolio in the context of a two-factor risk model. Then, we consider a more complex risk model — the Barra fixed-income multi-factor risk model — and compare it with the $\boldsymbol{\ell}_1$- and $\boldsymbol{\ell}_2$-norm solutions. We illustrate the differences in the corresponding efficient frontiers, and show the impact on tracking error volatility. The third part of Section 3 is devoted to active management, for which we develop a model of excess returns based on carry, rolldown, and repricing. We show how a portfolio manager's confidence in his views affects the optimized solution and shifts the efficient frontier. The fourth part addresses the classic problem of portfolio decarbonization, while the fifth part examines the impact of different clustering and bucketing methodologies on portfolio construction. The sixth and final part of Section Three illustrates the practical challenges of constructing investable portfolios. Section Four concludes.

2 Bond portfolio optimization

2.1 Traditional mean-variance optimization

When we think about portfolio optimization, we almost always think of the mean-variance optimization (MVO) model introduced by Markowitz (1952). Consider an investment universe of n assets. The modern formulation of MVO is:

$$w^\star = \arg\min \frac{1}{2} w^\top \Sigma w - \gamma w^\top (\mu - r\mathbf{1}_n) \qquad \text{s.t.} \qquad w \in \Omega \tag{1}$$

where μ and Σ denote the vector of expected returns and the covariance matrix of asset returns, r is the risk-free rate, and γ is the investor's risk tolerance. The set Ω defines the investment opportunities and the technical constraints. For instance, in the case of a long-only portfolio, we have $\Omega = \left\{w > \mathbf{0}_n : \mathbf{1}_n^\top w = 1\right\}$.

This type of optimization is widely used when working with an equity investment universe or a multi-asset investment universe. It is also applied to other asset classes, such as currencies, futures, or commodities. In this framework, risk is measured using the covariance matrix, which incorporates two dimensions: specific risk, captured by volatilities, and dependence or co-movement risk, captured by correlations. According to Perrin and Roncalli (2020), the success of mean-variance optimization is partly explained by the fact that Problem (1) can be formulated as a quadratic programming (QP) problem, which is relatively easy to solve numerically[8]. Moreover, the mean-variance optimization problem can be extended in a straightforward manner to more complex formulations that remain quadratic programming problems. For example, transaction costs, turnover management, and index sampling can be incorporated into MVO models and still preserve the QP structure through the use of augmented variables. Another common extension is mean-variance optimization relative to a benchmark. In this case, portfolio return is replaced by portfolio excess return, and the optimization problem becomes[9]:

$$w^\star = \arg\min \frac{1}{2} (w - b)^\top \Sigma (w - b) - \gamma (w - b)^\top \mu \qquad \text{s.t.} \qquad w \in \Omega \tag{3}$$

where b denotes the weight vector of the benchmark. Problem (3) is extensively used in the ETF industry, index replication, tilted portfolio construction, and active management with low tracking error. In particular, it has been the backbone of many ESG and climate-related portfolios, especially CTB and PAB solutions (Le Guenedal and Roncalli, 2022; Barahhou *et al.*, 2022; Roncalli, 2026).

Interestingly, the application of mean-variance optimization to fixed-income investment universes is relatively uncommon. When it is used, it is typically applied to aggregates such as bond baskets, bond futures, bond funds, or maturity buckets, rather than to individual securities. For example, mean-variance optimization may be implemented on an investment universe structured by maturity segments, typically 1-year, 1–3 year, 3–5 year, 5–7 year, 7–10 year and 10+ year bands. In the academic literature, bond portfolio optimization has not been extensively studied. When it is addressed, the scope of applications is generally limited and often diverges from the practical concerns of professional investors (Konno and Watanabe, 1996; Korn and Koziol, 2006; Puhle, 2008; Caldeira *et al.*, 2016).

[8] A quadratic programming problem is an optimization problem with a quadratic objective function and linear inequality constraints:

$$\begin{aligned} x^\star &= \arg\min \frac{1}{2} x^\top Q x - x^\top R \\ &\text{s.t.} \quad Sx \leq T \end{aligned} \tag{2}$$

Problem (1) is solved by setting $Q = \Sigma$ and $R = \gamma(\mu - r\mathbf{1}_n)$.

[9] We obtain a QP problem by setting $Q = \Sigma$ and $R = \Sigma b + \gamma\mu$.

2.2 Issues with fixed-income securities

In this section, we review the key challenges of implementing portfolio optimization with fixed-income securities. In particular, we focus on three primary issues: volatility risk, correlation risk, and the investment universe.

2.2.1 Volatility risk

In the Markowitz framework, covariance risk plays a central role. In general, we assume that asset returns follow a multi-factor risk model:

$$R(t) = \alpha + B\mathcal{F}(t) + \varepsilon(t) \tag{4}$$

where $R(t) = \left(R_1(t), \ldots, R_n(t)\right)$ is the vector of asset returns, $\mathcal{F}(t) = \left(\mathcal{F}_1(t), \ldots, \mathcal{F}_m(t)\right)$ is the vector of risk factors, and $\varepsilon(t) = \left(\varepsilon_1(t), \ldots, \varepsilon_n(t)\right)$ is the vector of idiosyncratic risks. The loading matrix B contains the beta coefficients: $B = \left(\beta_{i,j}\right)$ where $i \in \{1, \ldots, n\}$ and $j \in \{1, \ldots, m\}$. We generally assume that $\mathcal{F}(t) \sim \mathcal{N}(\psi, \Omega)$, $\varepsilon(t) \sim \mathcal{N}(0_n, D)$ and $\mathcal{F}(t) \perp \varepsilon(t)$. Under these assumptions, the covariance matrix of asset returns is given by:

$$\Sigma = B\Omega B^\top + D \tag{5}$$

In practice, the covariance matrix Σ is unknown and must be estimated. In mean-variance optimization, it is typically replaced by the historical covariance matrix, *i.e*, the empirical covariance matrix $\hat{\Sigma}$ or the factor-based covariance matrix $\hat{B}\hat{\Omega}\hat{B}^\top + \hat{D}$. Both approaches assume that asset returns are stationary, at least over a recent time interval $[t-h, t]$, where h is the time window used to calibrate the parameters of the risk model[10]. Stationarity is then a key assumption for implementing optimization problems (1) and (3).

Spot volatility The main difficulty with bonds is that the standard factor model (4) is not valid for such securities. For instance, in a two-factor model with interest rate and credit risk[11], the return of a bond can be approximated as:

$$R_i(t) = -\operatorname{MD}_i(t)\,\Delta r(t) - \operatorname{DTS}_i(t)\,\frac{\Delta s_i(t)}{s_i(t)} + \varepsilon_i(t) \tag{6}$$

where $\operatorname{MD}_i(t)$ and $\operatorname{DTS}_i(t)$ are the modified duration and the duration times spread of the bond, respectively. The stochastic component $\varepsilon_i(t)$ is the idiosyncratic component and we denote by $\tilde{\sigma}_i$ the specific volatility. In this case, the volatility of the bond return is given by the formula:

$$\sigma_i(t) = \sqrt{\operatorname{MD}_i^2(t)\,\sigma_r^2 + \operatorname{DTS}_i^2(t)\,\sigma_{s,i}^2 + \tilde{\sigma}_i^2} \tag{7}$$

Over a relevant time horizon, it is reasonable to assume that interest rate, credit spread and idiosyncratic volatilities σ_r, $\sigma_{s,i}$ and $\tilde{\sigma}_i$ are approximately stationary. However, this assumption is not valid for the factor loadings $\operatorname{MD}_i(t)$ and $\operatorname{DTS}_i(t)$. The modified duration and the duration-times spread decreases over time, while the duration times spread increases with the credit spread $s_i(t)$. For instance, in the case of a zero-coupon bond, we have:

$$\begin{cases} \operatorname{MD}_i(t) = T_i - t \\ \operatorname{DTS}_i(t) = (T_i - t)\,s_i(t) \end{cases}$$

[10] In practice, professionals typically use a one- to three-year time window for equities, a one- to five-year window for multi-asset classes, and a one- to twelve-month window for absolute return strategies based on futures.

[11] This model is presented in Appendix B.2 on page 90.

where T_i is the maturity date of the zero-coupon bond. By ignoring the specific component, we can consider two limiting cases:

1. If credit risk is negligible relative to interest rate risk, we obtain:

$$\sigma_i(t) = T_i\sigma_r - t\sigma_r$$

   The bond volatility is maximum at the issuance date and decreases linearly to zero as maturity approaches ($t \to T_i$).

2. If the interest rate risk is negligible relative to the credit risk, we obtain:

$$\sigma_i(t) = (T_i - t)\, s_i(t)\, \sigma_{s,i}$$

   With respect to time, the same qualitative conclusion holds. Volatility declines linearly as maturity approaches. However, a key difference emerges. Bond volatility now depends on the level of the credit spread $s_i(t)$. While the volatility parameters σ_r and $\sigma_{s,i}$ can reasonably be treated as constant over short horizons (their impact being of second order), the dependence on $s_i(t)$ is first order. As a result, bond volatility is highly sensitive to the credit spread level, which is closely related to the risk-neutral default probability. Assuming this quantity to be constant is therefore not appropriate.

Figure 1 shows the annualized volatility of a 50-year zero-coupon bond for different values of the parameters: $T_i = 50$, $\sigma_r = 1\%$, $s_i(t) = 50\,\text{bps}$, $\sigma_{s,i} = 50\%$ and $\tilde{\sigma}_i = 0$. As expected, the volatility decreases over time and converges to zero as $t \longrightarrow T_i$. Then, we consider two alternative specifications ($\sigma_r = 2\%$ and $s_i(t) = 250\,\text{bps}$) and illustrate their respective effects on the volatility $\sigma_i(t)$. In a similar way, Figure 2 shows the impact of the credit spread on the volatility of a 10-year zero-coupon bond[12].

In practice, bond volatility depends on both the interest rate factor and the credit factor. For highly-rated sovereign bonds, the interest rate contribution is the dominant driver. For corporate bonds, particularly those with lower credit ratings, it is the credit risk that tends to dominate. We illustrate these effects with two examples. In Figure 3, we consider the German Bund 6.5% July 2027, issued in July 1997 (ISIN: DE0001135044). This bond is of particular interest given its original maturity of 30 years. We compute the historical volatility from bond prices using a rolling window of 260 trading days (one year), and report the corresponding linear regression against time. As expected, the relationship is decreasing. Thirty years ago, the historical volatility was close to 10%, reflecting the long remaining maturity. By 2026, however, it has fallen below 2%, consistent with a remaining maturity of less than two years. This clearly illustrates how time to maturity drives volatility. However, certain periods cannot be fully explained by the duration factor alone. For instance, the 2008–2013 period was marked by the European sovereign debt crisis. This explains that the realized volatility exceeded the model-implied volatility obtained from the zero-coupon formula based solely on the interest rate risk factor. Similarly, Figure 4 shows the volatility of the Walmart bond 4.875% September 2029 (ISIN: XS0453133950). Once again, the linear regression confirms the expected decreasing slope. We also report the model-implied volatility from the zero-coupon formula based solely on the credit risk factor. The two curves are strongly correlated except during the 2020–2024 period, when interest rate risk becomes material due to increased interest rate volatility. Taken together, these examples demonstrate that bond volatility is governed by two time-varying bond characteristics — modified duration and duration times spread — and two market volatility factors — interest rate volatility and credit spread volatility. Any factor model for bonds must account for these features.

[12] We assume that the credit spread follows a geometric Brownian motion with $s_i(0) = \mu_{s,i} = 200\,\text{bps}$ and $\sigma_{s,i} = 50\%$, while $\sigma_r = 1\%$ and $\tilde{\sigma}_i = 0$.

Figure 1: Impact of the modified duration and the parameters σ_r and $s_i(t)$ on the volatility of a zero-coupon bond

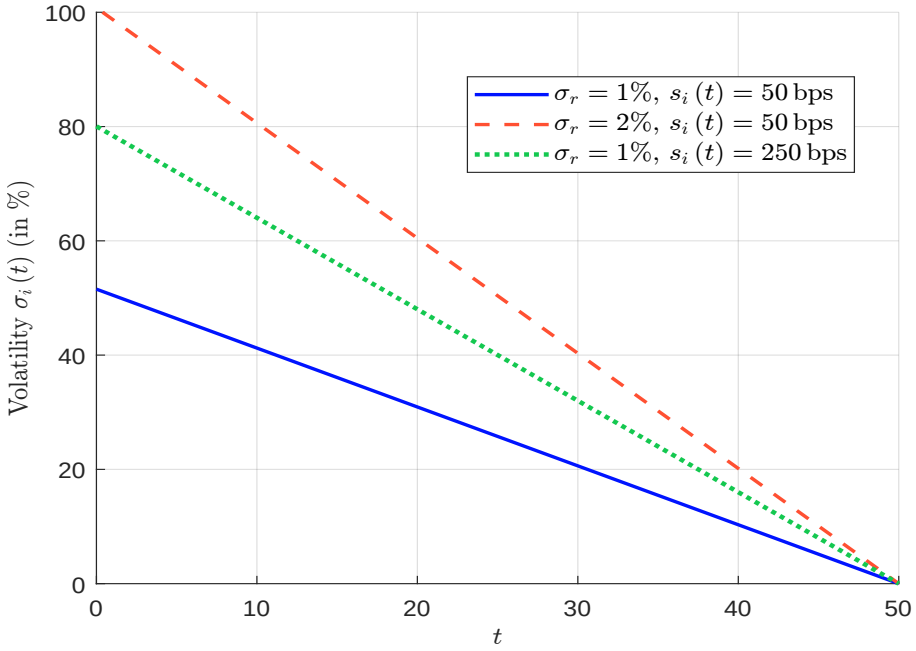

Figure 2: Impact of the modified duration and the credit spread on the volatility of a zero-coupon bond

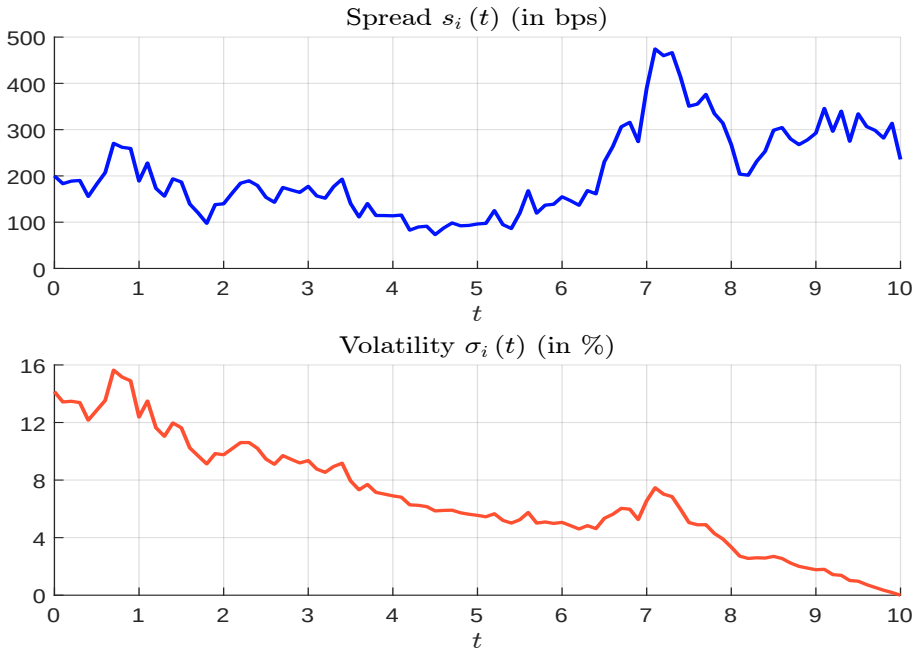

Figure 3: Volatility of the German Bund 6.5% July 2027 (ISIN: DE0001135044)

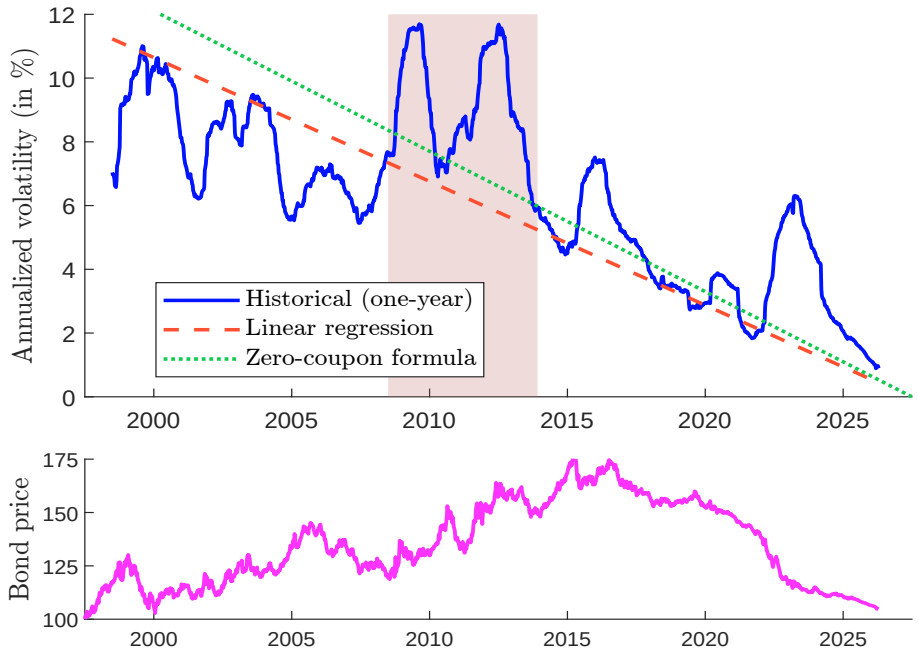

Figure 4: Volatility of the Walmart bond 4.875% September 2029 (ISIN: XS0453133950)

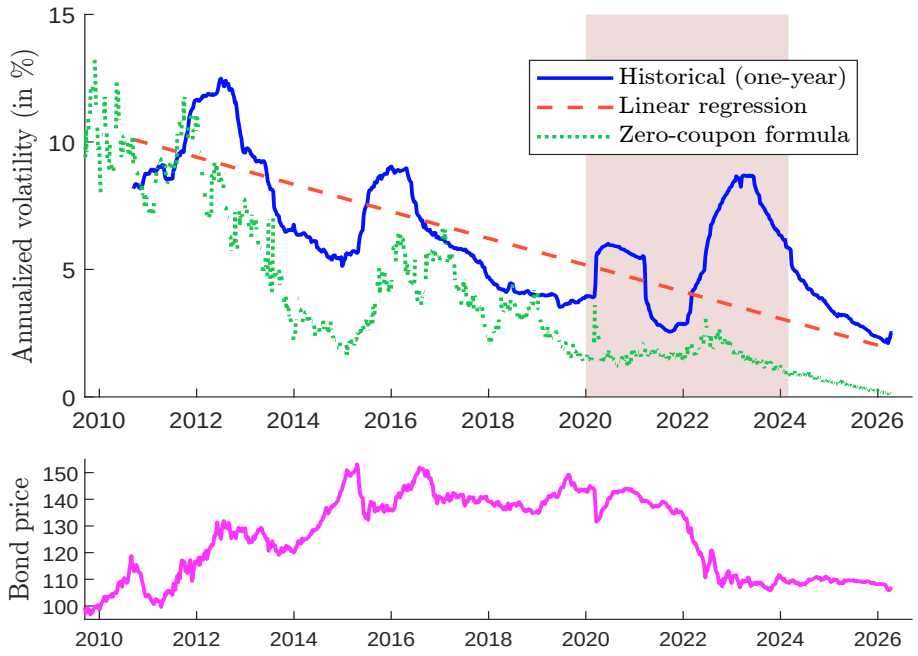

Window (or historical) volatility Because the bond return $R_i(t) \sim \mathcal{N}\left(0, \sigma_i(t)\right)$ is not stationary, the bond volatility over the period $[t_1, t_2]$ depends explicitly of the endpoints t_1 and t_2:

$$\sigma_i(t_1, t_2) = \sqrt{\overline{\mathrm{MD}_i^2}(t_1, t_2)\,\sigma_r^2 + \overline{\mathrm{DTS}_i^2}(t_1, t_2)\,\sigma_{s,i}^2 + \tilde{\sigma}_i^2} \tag{8}$$

where $\overline{\mathrm{MD}_i^2}(t_1, t_2)$ and $\overline{\mathrm{DTS}_i^2}(t_1, t_2)$ are the time average of the squared modified duration and squared duration times spread over the period $[t_1, t_2]$. In the case of a zero-coupon bond, we have:

$$\begin{cases} \overline{\mathrm{MD}_i^2}(t_1, t_2) = (T_i - t_2 - t_1)\,T_i + \dfrac{1}{3}\left(t_2^2 + t_2 t_1 + t_1^2\right) \\ \overline{\mathrm{DTS}_i^2}(t_1, t_2) = T_i^2 \overline{s_i^2}(t_1, t_2) - 2T_i \overline{t s_i^2}(t_1, t_2) + \overline{t^2 s_i^2}(t_1, t_2) \end{cases}$$

where $\overline{s_i^2}(t_1, t_2)$, $\overline{t s_i^2}(t_1, t_2)$, and $\overline{t^2 s_i^2}(t_1, t_2)$ are the time average of $s_i^2(t)$, $t s_i^2(t)$ and $t^2 s_i^2(t)$. Assuming that $t' > t$ and $h' \neq h$, we obtain the following properties:

$$\begin{cases} \sigma_i(t, t+h) \neq \sigma_i(t+h) \\ \sigma_i(t, t+h) \neq \sigma_i\left(t', t'+h\right) \\ \sigma_i(t, t+h) \neq \sigma_i\left(t, t+h'\right) \end{cases}$$

The first property means that the window (or historical) volatility differs from spot volatility. In particular, if we assume that the parameters are constant, we find that $\sigma_i(t+h) < \sigma_i(t, t+h)$. On average, the historical volatility tends to overestimate the spot volatility. The second property implies that the window volatility is also time-dependent. For example, the one-year rolling volatility is not stationary. The third property highlights the dependence of the historical volatility on the window length. For instance, a one-year historical volatility generally differs from three- or five-year measures. On average, we deduce that the historical volatility is an increasing function of the window length.

Table 1: Bias of the window volatility $\sigma_i(t-h, t)$ with respect to the spot volatility $\sigma_i(t)$

t	Decreasing spread			Increasing spread		
	1Y	5Y	10Y	1Y	5Y	10Y
10.0	4.7%	25.9%	57.3%	−0.9%	−6.0%	−13.1%
15.0	6.2%	34.4%	78.0%	0.6%	0.8%	−2.9%
20.0	8.7%	50.7%	119.4%	2.7%	11.0%	15.3%
25.0	14.9%	94.0%	237.4%	8.1%	36.5%	61.3%
26.0	17.7%	113.8%	292.8%	10.7%	48.9%	83.5%
27.0	22.1%	145.7%	382.2%	14.9%	69.5%	120.5%
28.0	31.0%	207.6%	554.9%	23.5%	111.1%	194.4%
29.0	58.5%	391.2%	1 059.4%	49.9%	237.2%	417.2%
29.5	115.6%	759.0%	2 058.0%	104.0%	491.8%	864.2%
30.0	$+\infty$	$+\infty$	$+\infty$	$+\infty$	$+\infty$	$+\infty$

To illustrate the behavior of window volatility relative to spot volatility, we consider a 30-year zero-coupon bond. We assume $\sigma_r = 30$ bps, $\sigma_{s,i} = 75\%$ and $\tilde{\sigma}_i = 0$. We compute $\sigma_i(t)$ and $\sigma_i(t-h, t)$ for three window lengths h: one, five and then years. Figure 5 shows the volatilities when the credit spread decreases linearly from 200 bps at inception date to 10 bps at maturity date, while Figure 6 shows the case where the credit spread increases linearly from 10 bps to 200 bps over the same period. We have also reported the relative

Figure 5: Window and spot volatilities (decreasing spread)

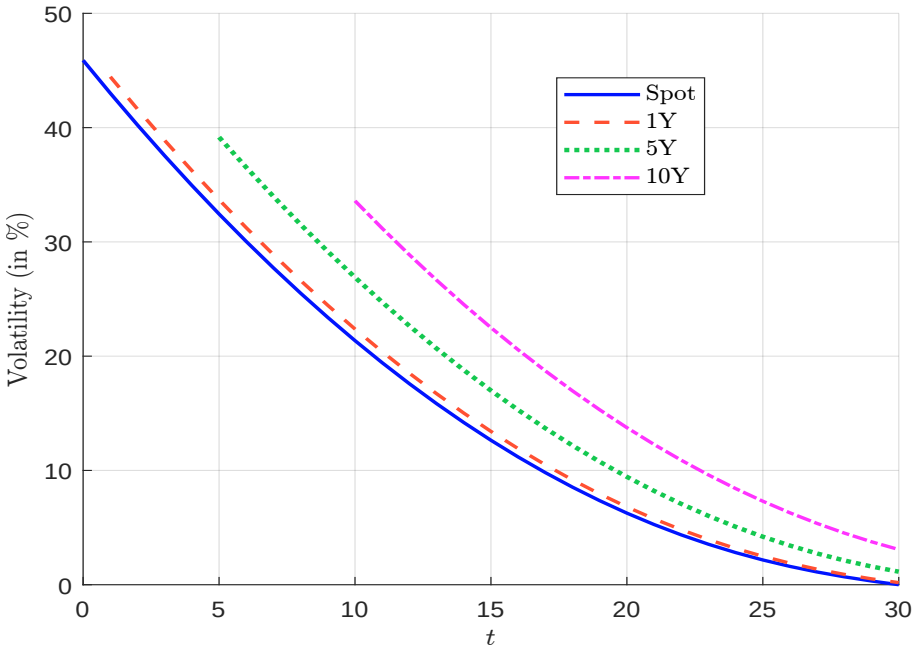

Figure 6: Window and spot volatilities (increasing spread)

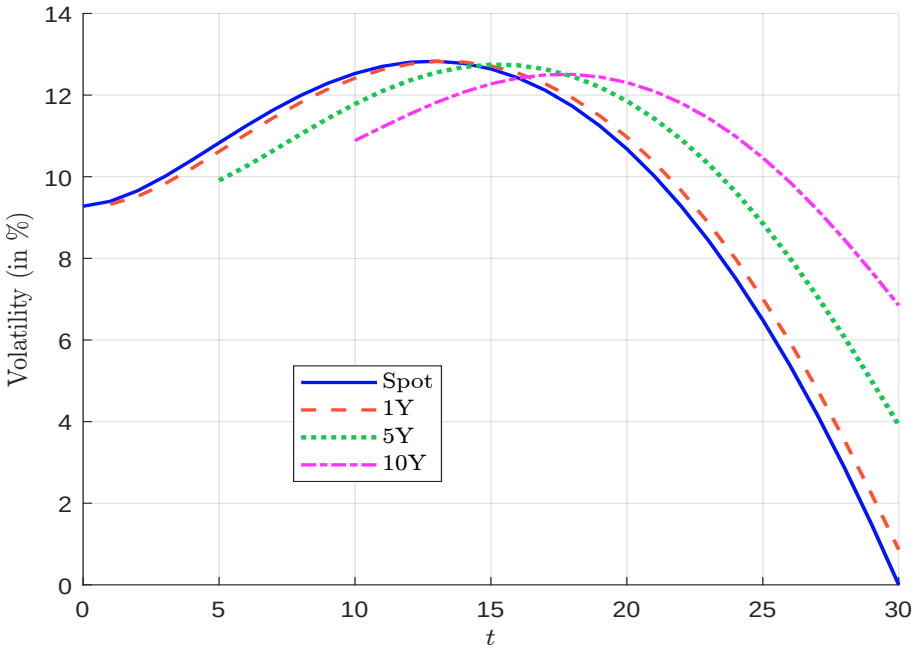

bias[13] of the window volatility in Table 1. The first case highlights a systematic lag between window volatility and spot volatility. The second case is more nuanced. For short maturities (the last ten years), the same lag is observed. For longer maturities (the first twenty years), however, the ordering of window volatilities is no longer monotonic. This is because the duration effect is offset by the increase in the credit spread. In both cases, the relative bias is largest for short maturities, and we get:

$$\lim_{t \to T} \frac{\sigma_i(t-h,t)}{\sigma_i(t)} = +\infty$$

The previous results have some implications for portfolio management. While it is common practice to estimate equity volatility using long historical windows, a shorter window is generally more appropriate for individual bonds. This difference stems from the non-stationary nature of bond volatility, which depends on time-varying factors such as duration and credit spreads. In equity markets, volatility is often assumed to exhibit mean reversion, which justifies the use of long estimation windows — typically one to three years — to obtain stable and representative measures. An exception is when considering the derivatives market or intra-day trading where equity volatility is better estimated using GARCH processes. By contrast, for individual bonds, volatility is largely driven by deterministic components linked to time to maturity. As a result, past observations over long horizons may not be representative of current or future risk. Using long windows for bonds therefore introduces a bias, as historical volatility tends to overestimate spot volatility and may obscure recent dynamics. Shorter windows, on the other hand, are better suited to capturing the current risk profile of the bond. More generally, the notion of volatility mean reversion, which is central in equity markets, does not directly apply to individual bonds. Bond volatility does not fluctuate around a stable long-term level but evolves structurally over time, reflecting the bond's aging.

2.2.2 Correlation risk

For equity portfolios, the standard practice is to use the covariance matrix (5) derived from multi-factor models. For instance, in the case of CAPM, the risk factor is the return of the market portfolio, and the covariance matrix is equal to:

$$\Sigma = \sigma_m^2 \beta\beta^\top + D \tag{9}$$

where $\beta = (\beta_1, \ldots, \beta_n)$, β_i is the (traditional) beta coefficient of stock i and σ_m is the market volatility. More sophisticated factor models can be used to incorporate size, value, momentum, and other risk factors. It is generally assumed that the risk factors are uncorrelated, and Equation (5) becomes:

$$\Sigma = \sigma_m^2 \beta\beta^\top + \sum_{j=2}^{m} \sigma_{(j)}^2 \beta_{(j)} \beta_{(j)}^\top + D \tag{10}$$

where $\beta_{(j)}$ and $\sigma_{(j)}$ are the vector of sensitivities and the volatility with respect to the j^{th} risk factor.

The same approach can be used for fixed-income securities, with the key distinction that the sensitivities are time-varying:

$$\Sigma(t) = B(t)\,\Omega B(t)^\top + D \tag{11}$$

[13] The bias is defined as the ratio $\left(\sigma_i(t-h,t) - \sigma_i(t)\right)/\sigma_i(t)$ and is expressed in %.

For instance, in the case of the two-factor model, we obtain the following covariance matrix[14]:

$$\Sigma(t) = \sigma_r^2 \,\mathrm{MD}(t)\,\mathrm{MD}(t)^\top + \big(\mathrm{DTS}(t) \odot \sigma_s\big) \odot \rho_s \odot \big(\mathrm{DTS}(t) \odot \sigma_s\big)^\top + D$$

It follows that the bond correlation is a linear combination of three correlations[15]:

$$\rho_{i,j}(t) = \varpi_{r,i,j}(t)\,\rho_{r,i,j} + \varpi_{s,i,j}(t)\,\rho_{s,i,j} + \tilde{\varpi}_{i,j}\tilde{\rho}_{i,j} \tag{12}$$

where $\rho_{r,i,j} = 1$, $\rho_{s,i,j} \in [0,1]$ and $\tilde{\rho}_{i,j} = 0$ for all $i \neq j$.

Figure 7: Bond correlation

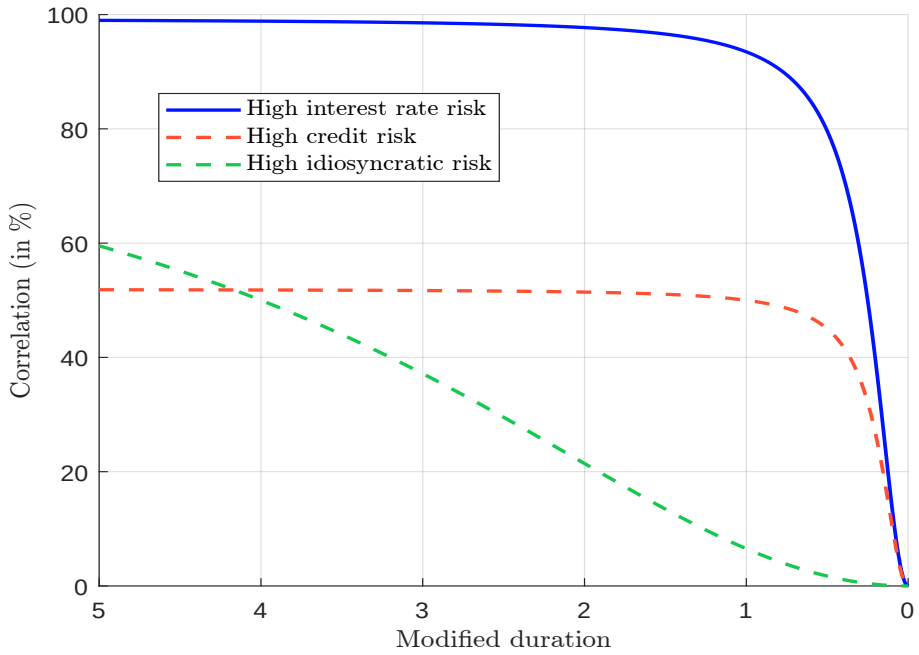

Using the previous framework, we can show that:

$$\frac{\partial \rho_{i,j}(t)}{\partial t} < 0 \quad \text{and} \quad \lim_{t \longrightarrow T_i} \rho_{i,j}(t) = 0$$

This implies that bond correlation is an increasing function of time to maturity, and vanishes as maturity is approached. Therefore, it tends to be higher for long-maturity bonds and lower for short-maturity bonds. This property is illustrated in Figure 7 using the following parameters: $\sigma_r = s_i = s_j = \tilde{\sigma}_i = \tilde{\sigma}_j = 50$ bps, $\sigma_{s,i} = \sigma_{s,j} = 50\%$ and $\rho_{s,i,j} = 50\%$. The relative contributions of interest rate, credit, and idiosyncratic risks determine the overall

[14] See Appendix B.2.4 on page 93.

[15] The weighting coefficients are:

$$\begin{cases} \varpi_{r,i,j}(t) = \dfrac{\sigma_r^2}{\sigma_i(t)\,\sigma_j(t)}\,\mathrm{MD}_i(t)\,\mathrm{MD}_j(t) \\ \varpi_{s,i,j} = \dfrac{\sigma_{s,i}\sigma_{s,j}}{\sigma_i(t)\,\sigma_j(t)}\,\mathrm{DTS}_i(t)\,\mathrm{DTS}_j(t) \\ \tilde{\varpi}_{i,j} = \dfrac{\tilde{\sigma}_i\tilde{\sigma}_j}{\sigma_i(t)\,\sigma_j(t)} \end{cases}$$

level of bond correlation. High interest rate risk tends to push bond correlation toward one[16], high idiosyncratic risk tends to push bond correlation toward zero[17], while high credit risk tends to align bond correlation with credit correlation[18]. These dynamics explain why bond correlation behaves differently across sovereign, corporate, and high-yield bonds, and why it varies over time depending on the dominant economic regime.

Remark 1. *This property can be illustrated by considering three fixed-income universes*[19]*: government bonds, investment-grade corporate bonds, and high-yield bonds. For each universe, we compute the one-year covariance matrix and perform a principal component analysis. Figure 8 shows the proportion of total variance explained by the first principal component. For government bonds, the first principal component explains approximately 95% of the variance, for investment-grade corporate bonds, about 80%, and for high-yield bonds, only 30%. The number of significant principal components, defined as those explaining more than 1% of the total variance, is equal to 2, 7 and 11, respectively. Therefore, only two common factors are needed to model US government bond returns from May 2025 to April 2026, whereas the universe of the US high yield bonds requires 11 independent risk factors. These empirical results have two main implications. First, the underlying risk structure is more complex for high-yield bonds than for government and investment-grade bonds. Second, idiosyncratic risk cannot be ignored in the high-yield universe.*

Figure 8: Proportion of total variance explained by principal components

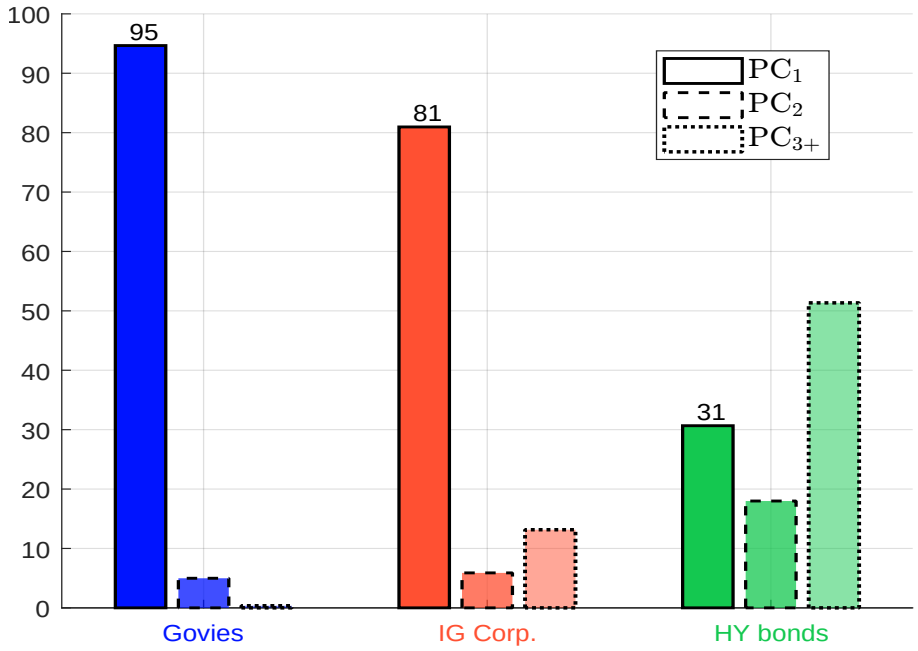

Source: ICE BofA & Authors' calculations.

[16] σ_r is set to 200 bps.
[17] $\tilde{\sigma}_i$ and $\tilde{\sigma}_j$ are set to 200 bps.
[18] s_i and s_j are set to 500 bps.
[19] We use the ICE BofA USD indices and filter US-domiciled securities. As of April 2026, we have 244 US govies, 7 382 US investment-grade corporate bonds and 1 274 US high yield bonds.

2.2.3 Investment universe

One major difference between equity and bond investment universes is the number of securities they contain. In equity indices, the relationship between issuers and securities is generally close to one-to-one, with one company corresponding to one listed stock. For example, the CAC 40 and the DAX are the main French and German equity benchmarks. Each index tracks the performance of the 40 largest listed companies in its respective market, and is therefore composed of exactly 40 stocks, each representing a single share class issued by a company. However, there are a few exceptions. Some companies issue multiple listed share classes with different voting rights or ownership structures. The most notable example is Alphabet, which has two listed share classes with different ticker symbols: GOOGL and GOOG. GOOGL corresponds to Class A shares, which carry voting rights under a one-share-one-vote structure, whereas GOOG corresponds to Class C shares, which have no voting rights. As a result, while the S&P 500 is designed to represent the 500 largest US companies, it typically contains between 503 and 506 stocks because some firms have multiple listed share classes.

Bond indices differ fundamentally because the one-issuer-one-security rule does not apply to fixed-income instruments. A single issuer can have dozens, or even hundreds, of outstanding bonds. For instance, governments typically maintain continuous issuance programs covering multiple maturities, coupon structures, and issuance dates. The same logic applies to financial institutions and corporate issuers, which often issue bonds across different currencies, maturities, seniority levels, and regulatory formats. As a result, the number of securities in a bond index is, on average, far greater than in an equity index covering a comparable investment universe (Table 2). For example, the MSCI EMU Index contains fewer than 250 stocks, whereas the ICE BofA EUR Corporate Index includes more than 4 000 individual bonds.

Table 2: Size of some common equity and bond indices

Equity		Fixed-income		
Index name	Size	Index name	Size	Issuer
Eurostoxx	≈ 250	ICE BofA EUR Corporate	≈ 4 500	≈ 850
FTSE Global AC	≈ 9 000	ICE BofA USD Corporate	≈ 11 500	≈ 1 400
MSCI ACWI	≈ 2 900	ICE BofA Global Corporate	≈ 20 000	≈ 2 500
MSCI ACWI IMI	≈ 9 000	ICE BofA Global High Yield	≈ 3 200	≈ 1 500
MSCI EM	≈ 1 400	ICE BofA USD High Yield	≈ 1 900	≈ 840
MSCI EMU	≈ 240	Bloomberg Global Aggregate Bond	≈ 32 000	≈ 3 200
MSCI USA	≈ 620	Bloomberg Euro Aggregate Bond	≈ 7 900	≈ 1 120
MSCI World	≈ 1 500	Bloomberg US Aggregate Bond	≈ 14 000	≈ 1 150
NIKKEI 225	225	JPM EMBI Global Diversified	≈ 1 050	≈ 150
Russell 1000	1 000	JPM GBI-EM Global Diversified	≈ 440	20
Russell 3000	3 000	iBoxx Euro Corporates	≈ 4 200	775
S&P 500	500	FTSE World Government Bond/WGBI	≈ 1 430	26
STOXX Europe 600	600	FTSE EMU Government Bond/EGBI	≈ 425	10
TOPIX	≈ 2 000	FTSE EM Government Bond/EMGBI	≈ 350	16

Source: Bloomberg, Factset & Authors' research.

This structural difference between the equity and bond universes has two important consequences for portfolio optimization. First, the dimensionality of the optimization problem is much larger in fixed income than in equities. A bond portfolio manager may need to optimize allocations across thousands of securities rather than a few hundred stocks. Traditional quadratic programming techniques, which are standard in equity portfolio optimization, can

be computationally expensive or numerically unstable in bond applications. For this reason, alternative formulations, such as linear programming, are frequently used in fixed-income portfolio management. Second, the statistical properties of bond universes present a greater challenge. Since multiple bonds are issued by the same borrower and are driven by same risk factors, many securities exhibit high correlations. Consequently, the covariance matrix of bond returns often contains groups of securities with correlations close to one[20]. This creates significant numerical difficulties. Thus, the covariance matrix is generally less well-conditioned for bonds than for equities due to the high dimensionality of the investment universe and the strong comovement among bonds issued by the same entity. In practice, this means fixed-income portfolio construction often requires regularization techniques to achieve a stable solution (Bruder *et al.*, 2013).

2.3 Alternative specifications of bond portfolio optimization

Unlike equity portfolios, where risk is generally assessed through volatility and correlation alone, the previous analysis shows that this approach is too restrictive for bond portfolios. Since bond risk is multi-dimensional by nature, bond portfolio construction is typically more complex, aiming to capture additional sources of risk beyond volatility. These may include measures such as modified duration, duration times spread, and liquidity metrics. In this framework, maturity risk, credit risk, and liquidity risk complement traditional volatility risk.

Another key difference from equity portfolio construction, which usually relies on an aggregate portfolio risk measure, is that bond portfolio construction generally uses a clustering approach. Specifically, the bond universe can be divided into groups based on characteristics such as currency, sector, credit quality and maturity band. The cluster (EUR, Financials, AAA to A−, 1Y–3Y), for example, represents euro-denominated bonds issued by financial-sector entities with credit ratings above A− and maturities ranging from one to three years. In this sense, a cluster can be viewed as a generalisation of the sector concept, incorporating multiple characteristics simultaneously. The multi-dimensional nature of risk and the use of clustering are ultimately the main features that differentiate bond portfolio construction from equity portfolio construction. In practice, however, the distinction between the risk dimension and the clustering dimension is somewhat artificial. For instance, both credit rating-based clusters and duration times spread relate to credit risk. As a result, some overlap may arise between risk optimisation and cluster matching.

2.3.1 Clustering

As said previously, clustering constitutes the backbone of bond portfolio optimization. In practice, it is extremely rare for portfolio managers to implement an optimization framework without introducing objectives or constraints related to predefined groups of securities. This reflects the inherently multi-dimensional nature of bond risk, which cannot be adequately captured by aggregate portfolio statistics alone. Clustering offers a structured approach to control exposures across critical dimensions such as currency, sector or credit quality.

Partition vs. overlapping clustering In fact, we distinguish between two types of clustering. Let $\mathcal{E} = \{1, \ldots, n\}$ be the bond investment universe. We denote by $\mathcal{G}_j$ the j^{th}

[20]Previously, we found that the first principal component explained 81% of the total variance in the ICE BofA US IG Corporate Bond universe. However, this estimate was overestimated by the presence of multiple securities issued by the same companies. After correcting for this issuer concentration bias, the proportion of variance explained falls to approximately 60%–70%.

cluster (or group) of bonds. We introduce the delta notation:

$$\delta_{i,j} = \mathbb{1}\left\{i \in \mathcal{G}_j\right\} = \begin{cases} 1 & \text{if } i \in \mathcal{G}_j \\ 0 & \text{if } i \notin \mathcal{G}_j \end{cases}$$

The first form of clustering corresponds to a partition of the investment universe. In this case, the clusters are mutually exclusive and collectively exhaustive. This means that each bond belongs to one and only one cluster, while the union of all the clusters reconstructs the full investment universe. Mathematically, a partition $\mathcal{P}$ is defined as follows:

$$\mathcal{P} = \left\{\mathcal{G}_j : \bigcup_{j=1}^{n_\mathcal{G}} \mathcal{G}_j = \mathcal{E} \wedge \mathcal{G}_j \cap \mathcal{G}_{j'} = \emptyset \text{ for } j \neq j'\right\}$$

This implies that $\sum_{j=1}^{n_\mathcal{G}} \delta_{i,j} = 1$ for all $i \in \mathcal{E}$. Examples of partition-based clustering include classifications credit rating buckets or maturity bands.

Besides partitions, the second type of clustering is overlapping clustering, in which a bond may belong to multiple groups simultaneously. This occurs naturally when clusters represent non-exclusive characteristics. For example, consider two binary characteristics: Euro-denominated (EUR vs. non-EUR) and Financial sector (FIN vs. non-FIN). Under a partition framework, the investment universe is divided into the four clusters: EUR×FIN, non-EUR×FIN, EUR×non-FIN, and non-EUR×non-FIN. By contrast, under an overlapping clustering framework, the same universe is represented by four independent groups: EUR, non-EUR, FIN and non-FIN. In this case, a bond belongs to several clusters simultaneously. For instance, a euro-denominated financial bond belongs to both the EUR and FIN groups.

Clustering-based risk contribution and score Let $M_{k,i}$ denote the k^{th} metric (or feature) of bond i. The portfolio score with respect to metric k is equal to the weighted average of the individual metrics:

$$\mathbb{S}_k(w) := M_k(w) = \sum_{i=1}^{n} w_i M_{k,i}$$

The contribution of cluster $\mathcal{G}_j$ to the portfolio score is defined as follows:

$$\mathbb{C}_{j,k}(w) = \sum_{i \in \mathcal{G}_j} w_i M_{k,i} = \sum_{i=1}^{n} w_i \delta_{i,j} M_{k,i}$$

where $\delta_{i,j} = \mathbb{1}\left\{i \in \mathcal{G}_j\right\}$. Under a partition framework, the sum of contributions is exactly equal to the portfolio score[21]:

$$\sum_{j=1}^{n_\mathcal{G}} \mathbb{C}_{j,k}(w) = \sum_{i=1}^{n} w_i M_{k,i} = \mathbb{S}_k(w)$$

Alongside the cluster contribution, one may also consider the cluster score:

$$\mathbb{S}_{j,k}(w) = \frac{\sum_{i \in \mathcal{G}_j} w_i M_{k,i}}{\sum_{i \in \mathcal{G}_j} w_i} = \frac{\sum_{i=1}^{n} w_i \delta_{i,j} M_{k,i}}{\sum_{i=1}^{n} w_i \delta_{i,j}}$$

[21] We have:

$$\sum_{j=1}^{n_\mathcal{G}} \mathbb{C}_{j,k}(w) = \sum_{j=1}^{n_\mathcal{G}} \sum_{i=1}^{n} w_i \delta_{i,j} M_{k,i} = \sum_{i=1}^{n} w_i \left(\sum_{j=1}^{n_\mathcal{G}} \delta_{i,j}\right) M_{k,i} = \sum_{i=1}^{n} w_i M_{k,i}$$

Let $w_j = \sum_{i=1}^n w_i \delta_{i,j}$ be the total weight of cluster $\mathcal{G}_j$. It follows that $\sum_{i=1}^n w_i \delta_{i,j} M_{k,i} = \mathbb{S}_{j,k}(w) \sum_{i=1}^n w_i \delta_{i,j}$. We can therefore deduce that the global score at the portfolio level is the weighted average of the cluster scores[22]:

$$\mathbb{S}_k(w) = \sum_{i=1}^n w_i M_{k,i} = \sum_{j=1}^{n_{\mathcal{G}}} w_j \mathbb{S}_{j,k}(w)$$

By combining the two decompositions, we obtain the following identity:

$$\mathbb{S}_k(w) = \sum_{j=1}^{n_{\mathcal{G}}} \mathbb{C}_{j,k}(w) = \sum_{j=1}^{n_{\mathcal{G}}} w_j \mathbb{S}_{j,k}(w)$$

Portfolio matching involves constructing a portfolio that satisfies pre-defined targets, based on cluster contributions:

$$\mathbb{C}_{j,k}(w) \approx \mathbb{C}_{j,k}^\star \Leftrightarrow \sum_{i=1}^n w_i \delta_{i,j} M_{k,i} - \mathbb{C}_{j,k}^\star \approx 0 \tag{13}$$

or on cluster scores:

$$\mathbb{S}_{j,k}(w) \approx \mathbb{S}_{j,k}^\star \Leftrightarrow \sum_{i=1}^n w_i \delta_{i,j} \left(M_{k,i} - \mathbb{S}_{j,k}^\star \right) \approx 0 \tag{14}$$

Table 3: Characteristics of the investment universe (Example #1)

Bond	#1	#2	#3	#4	#5	#6	#7	#8	#9
w_i (in %)	21	19	16	12	11	8	6	4	3
MD_i (in years)	3.16	6.48	3.54	9.23	6.40	2.30	8.12	7.96	5.48
DTS_i (in bps)	107	255	75	996	289	45	620	285	125
Cluster	1	1	1	2	2	2	3	3	3

The modified duration and the duration times spread are certainly the two most used risk metrics in fixed-income management. In the sequel, we denote the contributions as $\mathbb{C}_{\text{MD},j}(w)$ and $\mathbb{C}_{\text{DTS},j}(w)$, and the scores as $\text{MD}_j(w)$ and $\text{DTS}_j(w)$ (or $\mathbb{S}_{\text{MD},j}(w)$ and $\mathbb{S}_{\text{DTS},j}(w)$). Let us illustrate these concepts with the example described in Table 3. The investment universe consists of nine bonds. For each bond, we have indicated its weight w_i, its modified duration MD_i expressed in years, and its duration times spread DTS_i expressed in basis points. The investment universe is also divided into three clusters $\mathcal{G}_1$, $\mathcal{G}_2$, and $\mathcal{G}_3$. In Table 4, we report the weight, contribution and score of each cluster. For instance, the first cluster has a weight of 56%, a contribution of 45.35% to the portfolio MD and 28.58% to the portfolio DTS. The MD and DTS scores for the first group are 4.39 years and 148.07 bps, respectively. At the portfolio level, we have $\text{MD}(w) = 5.43$ and $\text{DTS}(w) = 290.18$. This example highlights how the decomposition of portfolio exposures across groups of bonds provides a more granular view of risk allocation than portfolio-level statistics alone.

[22] We have:

$$\sum_{i=1}^n w_i M_{k,i} = \sum_{j=1}^{n_{\mathcal{G}}} \sum_{i=1}^n w_i \delta_{i,j} M_{k,i} = \sum_{j=1}^{n_{\mathcal{G}}} \mathbb{S}_{j,k}(w) \sum_{i=1}^n w_i \delta_{i,j} = \sum_{j=1}^{n_{\mathcal{G}}} w_j \mathbb{S}_{j,k}(w)$$

Table 4: Weight, contribution and score of each cluster (Example #1)

$\mathcal{G}_j$	w_j (in %)	$\mathbb{C}_{\text{MD},j}(w)$ (in years)	(in %)	$\mathbb{S}_{\text{MD},j}(w)$ (in years)	$\mathbb{C}_{\text{DTS},j}(w)$ (in bps)	(in %)	$\mathbb{S}_{\text{DTS},j}(w)$ (in bps)
$\mathcal{G}_1$	56.00%	2.46	45.35%	4.39	82.92	28.58%	148.07
$\mathcal{G}_2$	31.00%	2.00	36.77%	6.44	154.91	53.38%	499.71
$\mathcal{G}_3$	13.00%	0.97	17.87%	7.46	52.35	18.04%	402.69
w	100.00%	5.43	100.00%	5.43	290.18	100.00%	290.18

2.3.2 Basic optimization problems

Without a benchmark We consider a generalization of the mean-variance framework defined by Equation (1):

$$w^\star = \arg\min \frac{1}{2}\mathcal{R}(w) - \gamma\mu(w) \tag{15}$$

where $\mathcal{R}(w)$ and $\mu(w)$ are the risk measure and expected return of the bond portfolio w, respectively. Since the risk of a bond portfolio depends on several factors, we assume that $\mathcal{R}(w)$ is a linear combination of individual risk measures:

$$\mathcal{R}(w) = \sum_{k=0}^{n_\mathcal{R}} \varphi_k \mathcal{R}_k(w)$$

where $\varphi_k \geq 0$ are non-negative weighting coefficients. The first risk measure corresponds to the portfolio variance: $\mathcal{R}_0(w) = \sigma^2(w) = w^\top \Sigma w$, while the other risk measures $\mathcal{R}_k$ for $k \geq 1$ are associated with a specific metric or feature. More specifically, the $\boldsymbol{\ell}_2$-norm risk measure $\mathcal{R}_k(w)$ is defined as:

$$\mathcal{R}_k(w) = \sum_{j=1}^{n_\mathcal{G}} \left(\mathbb{C}_{j,k}(w) - \mathbb{C}^\star_{j,k}\right)^2 = \sum_{j=1}^{n_\mathcal{G}} \left(\sum_{i=1}^{n} w_i \delta_{i,j} M_{k,i} - \mathbb{C}^\star_{j,k}\right)^2$$

where $\mathbb{C}_{j,k}(w)$ is the contribution of cluster $\mathcal{G}_j$ with respect to metric k and $\mathbb{C}^\star_{j,k}$ is the corresponding target value. In a similar way, we decompose the expected return as follows:

$$\mu(w) = \sum_{k=0}^{n_\mu} \phi_k \mu_k(w)$$

where $\phi_k \geq 0$ are non-negative weighting coefficients, and $\mu_k(w)$ is the k^{th} alpha source. The first alpha source corresponds to the portfolio carry: $\mu_0(w) = \mathcal{C}(w) = \sum_{i=1}^n w_i \mathcal{C}_i$. The remaining alpha sources are assumed to be linear with respect to the portfolio weights: $\mu_k(w) = \sum_{i=1}^n w_i \alpha_{k,i}$ for $k \geq 1$, where $\alpha_{k,i}$ denotes the k^{th} alpha signal for bond i.

Remark 2. *An alternative specification of the risk measure replaces cluster contributions by cluster scores. In this case, we have:*

$$\mathcal{R}_k(w) = \sum_{j=1}^{n_\mathcal{G}} \left(w_j \mathbb{S}_{j,k}(w) - w_j \mathbb{S}^\star_{j,k}\right)^2 = \sum_{j=1}^{n_\mathcal{G}} \left(\sum_{i=1}^{n} w_i \delta_{i,j} \left(M_{k,i} - \mathbb{S}^\star_{j,k}\right)\right)^2$$

The coefficient w_j is introduced to take into account the relative importance of the clusters.

Let us illustrate some basic optimization problems based on the previous framework. If we assume that $\varphi_k = \phi_k = 0$ for $k \geq 1$, we obtain the carry-volatility optimization problem:

$$w^\star = \arg\min \frac{1}{2} w^\top \Sigma w - \gamma \mathcal{C}(w)$$

If we assume that $\varphi_0 = 0$ and the two risk dimensions are the modified duration and the duration times spread, the objective function is maximizing the carry of the portfolio under a risk decomposition constraint[23]:

$$\begin{aligned} w^\star &= \arg\min \frac{\varphi_{\text{MD}}}{2} \sum_{j=1}^{n_{\mathcal{G}}} \left(\mathbb{C}_{\text{MD},j}(w) - \text{MD}_j^\star \right)^2 + \frac{\varphi_{\text{DTS}}}{2} \sum_{j=1}^{n_{\mathcal{G}}} \left(\mathbb{C}_{\text{DTS},j}(w) - \text{DTS}_j^\star \right)^2 - \mathcal{C}(w) \\ &\approx \arg\max \mathcal{C}(w) \text{ s.t. } w \in \Omega \end{aligned}$$

where $\text{MD}_j^\star$ and $\text{DTS}_j^\star$ are the target values of the contribution, and the set Ω is defined as:

$$\Omega = \left\{ w : \mathbb{C}_{\text{MD},j}(w) \approx \text{MD}_j^\star, \mathbb{C}_{\text{DTS},j}(w) \approx \text{DTS}_j^\star, j = 1, \ldots, n_{\mathcal{G}} \right\}$$

Of course, the matching quality of MD and DTS contributions depends on the values of φ_{MD} and φ_{DTS}.

Remark 3. *If $M_{k,i} = 1$, the metric correspond to the weight of the j^{th} group:*

$$Weight_j(w) = \sum_{i \in \mathcal{G}_j} w_i = \sum_{i=1}^{n} w_i \delta_{i,j}$$

In this case, we obtain:

$$\mathcal{R}(w) = \sum_{j=1}^{n_{\mathcal{G}}} \left(\left(\sum_{i \in \mathcal{G}_j} w_i \right) - w_j^\star \right)^2$$

This risk measure can be viewed as the $\boldsymbol{\ell}_2$-norm version of the active share applied to a set of clusters with pre-defined weights $w_j^\star$.

With a benchmark We now consider that the investment strategy has a benchmark b, and the objective of the portfolio manager is to minimize the active tracking risk. In this case, Problem (15) becomes:

$$w^\star = \arg\min \frac{1}{2} \mathcal{R}(w \mid b) - \gamma \mu(w \mid b) \tag{16}$$

where $\mathcal{R}(w \mid b)$ and $\mu(w \mid b)$ are the active risk measure and the expected excess return of the portfolio w relative to the benchmark b, respectively. Again, we write $\mathcal{R}(w \mid b) = \sum_{k=0}^{n_{\mathcal{R}}} \varphi_k \mathcal{R}_k(w \mid b)$ and $\mu(w \mid b) = \sum_{k=0}^{n_\mu} \phi_k \mu_k(w \mid b)$. Because there is a benchmark, the first risk measure becomes the tracking error variance: $\mathcal{R}_0(w \mid b) = \sigma^2(w \mid b) = (w - b)^\top \Sigma (w - b)$, while we define the other risk measures $\mathcal{R}_k(w \mid b)$ as follows:

$$\mathcal{R}_k(w \mid b) = \sum_{j=1}^{n_{\mathcal{G}}} \left(\mathbb{C}_{j,k}(w) - \mathbb{C}_{j,k}(b) \right)^2 = \sum_{j=1}^{n_{\mathcal{G}}} \left(\sum_{i=1}^{n} (w_i - b_i) \delta_{i,j} M_{k,i} \right)^2$$

[23] Without loss of generality, we set γ to one.

This is equivalent to imposing a target value that is exactly equal to the benchmark metric: $\mathbb{C}^{\star}_{j,k} = \mathbb{C}_{j,k}(b) = \sum_{i=1}^{n} b_i \delta_{i,j} M_{k,i}$. Regarding the expected excess return, we consider the excess carry $\mu_0(w \mid b) = \mathcal{C}(w \mid b) = \sum_{i=1}^{n}(w_i - b_i)\mathcal{C}_i$, while the other alpha sources are defined as $\mu_k(w \mid b) = \sum_{i=1}^{n}(w_i - b_i)\alpha_{k,i}$ for $k \geq 1$.

Remark 4. *In the case where we use the scores instead of the contributions, we obtain the following formula:*

$$\mathcal{R}_k(w \mid b) = \sum_{j=1}^{n_{\mathcal{G}}} \left(w_j \mathbb{S}_{j,k}(w) - w_j \mathbb{S}_{j,k}(b)\right)^2 = \sum_{j=1}^{n_{\mathcal{G}}} \left(\sum_{i=1}^{n} w_i \delta_{i,j} \left(M_{k,i} - \mathbb{S}_{j,k}(b)\right)\right)^2$$

Corresponding quadratic programming problems As explained by Perrin and Roncalli (2020), the success of a portfolio optimization method depends on several practical considerations: its operational feasibility, the computational time required to solve the problem, how easily the input parameters can be estimated, and the speed of convergence of the underlying algorithm. These considerations help to explain why many portfolio optimization models — many of them developed in academia — have never been widely adopted by practitioners, as they are often too complex to implement or computationally infeasible with existing numerical methods. In this context, the success of the mean-variance optimization model developed by Markowitz (1952) can be attributed to the relative simplicity of estimating or defining its inputs, particularly the covariance matrix, and the ability to efficiently compute solutions through quadratic programming (QP). Following the same rationale, we reformulate the basic optimization problems introduced previously as QP problems.

In Appendix B.5 on page 99, we show that the quadratic form of the objective function without a benchmark is:

$$\frac{1}{2}\mathcal{R}(w) - \gamma\mu(w) = \mathcal{QF}(w; Q, R, s)$$

where:

$$\begin{cases} Q = \varphi_0 \Sigma + \displaystyle\sum_{k=1}^{n_{\mathcal{R}}} \varphi_k \sum_{j=1}^{n_{\mathcal{G}}} \left(\delta_j \odot M_k\right)\left(\delta_j \odot M_k\right)^{\top} \\ R = \displaystyle\sum_{k=1}^{n_{\mathcal{R}}} \varphi_k M_k \odot \sum_{j=1}^{n_{\mathcal{G}}} \mathbb{C}^{\star}_{j,k}\delta_j + \gamma\left(\phi_0 \mathcal{C} + \sum_{k=1}^{n_{\mu}} \phi_k \alpha_k\right) \\ s = \dfrac{1}{2}\displaystyle\sum_{k=1}^{n_{\mathcal{R}}} \varphi_k \sum_{j=1}^{n_{\mathcal{G}}} \mathbb{C}^{\star 2}_{j,k} \end{cases} \tag{17}$$

If we use cluster scores instead of cluster contributions, the quadratic form is simplified and we have:

$$\begin{cases} Q = \varphi_0 \Sigma + \displaystyle\sum_{k=1}^{n_{\mathcal{R}}} \varphi_k \sum_{j=1}^{n_{\mathcal{G}}} \left(\delta_j \odot \left(M_k - \mathbb{S}^{\star}_{j,k}\right)\right)\left(\delta_j \odot \left(M_k - \mathbb{S}^{\star}_{j,k}\right)\right)^{\top} \\ R = \gamma\left(\phi_0 \mathcal{C} + \displaystyle\sum_{k=1}^{n_{\mu}} \phi_k \alpha_k\right) \\ s = 0 \end{cases} \tag{18}$$

If we include a benchmark, the objective function becomes:

$$\frac{1}{2}\mathcal{R}(w \mid b) - \gamma\mu(w \mid b) = \mathcal{QF}(w; Q, R, s)$$

where:

$$\begin{cases} Q = \varphi_0 \Sigma + \sum_{k=1}^{n_{\mathcal{R}}} \varphi_k \sum_{j=1}^{n_{\mathcal{G}}} \left(\delta_j \odot M_k\right) \left(\delta_j \odot M_k\right)^\top \\ R = \varphi_0 \Sigma b + \sum_{k=1}^{n_{\mathcal{R}}} \varphi_k \sum_{j=1}^{n_{\mathcal{G}}} \left(\delta_j \odot M_k\right) \left(\delta_j \odot M_k\right)^\top b + \gamma \left(\phi_0 \mathcal{C} + \sum_{k=1}^{n_\mu} \phi_k \alpha_k\right) \\ s = \frac{1}{2} \varphi_0 b^\top \Sigma b + \frac{1}{2} \sum_{k=1}^{n_{\mathcal{R}}} \varphi_k \sum_{j=1}^{n_{\mathcal{G}}} b^\top \left(\delta_j \odot M_k\right) \left(\delta_j \odot M_k\right)^\top b + \gamma \left(\phi_0 b^\top \mathcal{C} + \sum_{k=1}^{n_\mu} \phi_k b^\top \alpha_k\right) \end{cases} \tag{19}$$

In the case where we use cluster scores instead of cluster contributions, the quadratic form is:

$$\begin{cases} Q = \varphi_0 \Sigma + \sum_{k=1}^{n_{\mathcal{R}}} \varphi_k \sum_{j=1}^{n_{\mathcal{G}}} \left(\delta_j \odot \left(M_k - \mathbb{S}_{j,k}\left(b\right)\right)\right) \left(\delta_j \odot \left(M_k - \mathbb{S}_{j,k}\left(b\right)\right)\right)^\top \\ R = \varphi_0 \Sigma b + \gamma \left(\phi_0 \mathcal{C} + \sum_{k=1}^{n_\mu} \phi_k \alpha_k\right) \\ s = \frac{1}{2} \varphi_0 b^\top \Sigma b + \gamma \left(\phi_0 b^\top \mathcal{C} + \sum_{k=1}^{n_\mu} \phi_k b^\top \alpha_k\right) \end{cases} \tag{20}$$

The previous framework can easily be extended to take into account $\boldsymbol{\ell}_2$-norm penalization functions. For instance, if we incorporate the weight metric described on page 26, the quadratic form of this penalization function is:

$$\begin{aligned} \mathcal{P}\left(w\right) &= \sum_{j=1}^{n_{\mathcal{G}}} \left(\left(\sum_{i \in \mathcal{G}_j} w_i\right) - w_j^\star\right)^2 \\ &= \sum_{j=1}^{n_{\mathcal{G}}} \left(w^\top \delta_j - w_j^\star\right)^2 \\ &= \sum_{j=1}^{n_{\mathcal{G}}} w^\top \delta_j \delta_j^\top w - 2 w^\top \delta_j w_j^\star + {w_j^\star}^2 \\ &= \mathcal{QF}\left(w; 2\sum_{j=1}^{n_{\mathcal{G}}} \delta_j \delta_j^\top, 2\sum_{j=1}^{n_{\mathcal{G}}} \delta_j w_j^\star, \sum_{j=1}^{n_{\mathcal{G}}} {w_j^\star}^2\right) \end{aligned}$$

If the reference weights are those of the benchmark, we have $w_j^\star = \delta_j^\top b$. When the weight metric is applied to the individual securities instead of the clusters, we obtain:

$$\mathcal{P}\left(w\right) = \sum_{i=1}^{n} \left(w_i - b_i\right)^2 = \mathcal{QF}\left(w; 2I_n, 2b, bb^\top\right)$$

This is a special case of the previous quadratic form with a partition corresponding to the investment universe.

The transformation of the objective function into a quadratic form helps to numerically solve the optimization problem because we obtain a QP problem:

$$\begin{aligned} w^\star &= \arg\min \frac{1}{2} w^\top Q w - w^\top R \\ &\text{s.t.} \begin{cases} Aw = B \\ Cw \leq D \\ w^- \leq x \leq w^+ \end{cases} \end{aligned} \tag{21}$$

where the matrix Q and the vector R are given by the quadratic form. In this framework, imposing linear constraints becomes straightforward. A challenge arises, however, when constraints are formulated in terms of relative weights rather than absolute weights. Consider, for instance, the portfolio decarbonization example discussed in Roncalli (2026, page 1048). The carbon intensity of the j^{th} cluster is given by:

$$\boldsymbol{\mathcal{CI}}_j(w) = \frac{\sum_{i \in \mathcal{G}_j} w_i \boldsymbol{\mathcal{CI}}_j}{\sum_{i \in \mathcal{G}_j} w_i} = \frac{\left(\delta_j \odot \boldsymbol{\mathcal{CI}}\right)^\top w}{\delta_j^\top w}$$

Imposing the constraint $\boldsymbol{\mathcal{CI}}_j(w) \leq \boldsymbol{\mathcal{CI}}_j^\star$ is equivalent to the following inequality:

$$\begin{aligned} \boldsymbol{\mathcal{CI}}_j(w) &\leq \boldsymbol{\mathcal{CI}}_j^\star \Leftrightarrow \frac{\left(\delta_j \odot \boldsymbol{\mathcal{CI}}\right)^\top w}{\delta_j^\top w} \leq \boldsymbol{\mathcal{CI}}_j^\star \\ &\Leftrightarrow \left(\delta_j \odot \boldsymbol{\mathcal{CI}}\right)^\top w \leq \boldsymbol{\mathcal{CI}}_j^\star \left(\delta_j^\top w\right) \\ &\Leftrightarrow \left(\delta_j \odot \left(\boldsymbol{\mathcal{CI}} - \boldsymbol{\mathcal{CI}}_j^\star\right)\right)^\top w \leq 0 \end{aligned}$$

Hence, the constraint can be written in canonical QP form with $C = \left(\delta_j \odot \left(\boldsymbol{\mathcal{CI}} - \boldsymbol{\mathcal{CI}}_j^\star\right)\right)^\top$ and $D = 0$. The goal is therefore to systematically reformulate the optimization problem into a canonical QP framework.

2.3.3 Extension to ℓ_1-norm risk measures

As explained previously, the number of bonds in the investment universe can be extremely large, making the dimensionality of the optimization problem numerically challenging. In particular, the matrix Q contains n^2 elements, implying a memory requirement of $8n^2$ bytes, or equivalently $8n^2/1024^2$ megabytes when stored in double precision. For $n = 1\,000$, $5\,000$, $10\,000$, and $30\,000$, the size of the Q matrix is approximately 7.8 MB, 191 MB, 763 MB, and 6.7 GB, respectively. In this context, computing a numerical solution becomes increasingly challenging for large bond investment universes. Moreover, relying on a large covariance matrix with millions of variance and covariance terms is questionable[24], as portfolio risk is generally driven by a limited number of systematic risk factors. For this reason, practitioners often simplify the objective function by replacing $\boldsymbol{\ell}_2$-norm risk measures with $\boldsymbol{\ell}_1$-norm risk measures. At first glance, such a transformation may appear to involve a substantial loss of information. In practice, however, replacing a quadratic programming problem with a linear programming formulation significantly improves numerical tractability and enhances the interpretability of the solution. Moreover, replacing the $\boldsymbol{\ell}_2$-norm with the $\boldsymbol{\ell}_1$-norm fundamentally modifies the geometry of the optimization problem and its financial interpretation.

[24] If $n = 10\,000$, we get 50 millions of variance and covariance terms, and the growth is quadratic — doubling n multiplies the number of variance and covariance terms by 4.

The $\boldsymbol{\ell}_2$ penalty is quadratic. It increases rapidly with the magnitude of each deviation, so the optimizer is motivated to eliminate a small number of large mismatches. By contrast, the $\boldsymbol{\ell}_1$ penalty is linear. Each unit of deviation carries the same marginal cost regardless of its size. This encourages the optimizer to spread residual risk evenly across all buckets. In bond portfolio management, this distinction is financially significant. A portfolio with a single large deviation in one bucket exposes the manager to significant directional risk. An $\boldsymbol{\ell}_1$-optimized portfolio, on the other hand, tends to produce many small, diversified deviations across buckets. This is why we observe that the impact of parameter changes on the optimal solution is generally more transparent and predictable within this framework.

Without a benchmark The $\boldsymbol{\ell}_1$-norm optimization problem is closely related to the $\boldsymbol{\ell}_2$-norm optimization problem. We have:

$$w^\star = \arg\min \frac{1}{2}\mathcal{R}(w) - \gamma\mu(w) \tag{22}$$

where $\mathcal{R}(w)$ is now defined as an $\boldsymbol{\ell}_1$-norm risk measure, while the expected return of the bond portfolio remains the same[25]. Again, the aggregate risk measure is expressed as $\mathcal{R}(w) = \sum_{k=0}^{n_{\mathcal{R}}} \varphi_k \mathcal{R}_k(w)$, where the individual risk measures $\mathcal{R}_k$ for $k \geq 1$ are defined by:

$$\mathcal{R}_k(w) = \sum_{j=1}^{n_{\mathcal{G}}} \left| \mathbb{C}_{j,k}(w) - \mathbb{C}^\star_{j,k} \right| = \sum_{j=1}^{n_{\mathcal{G}}} \left| \sum_{i=1}^{n} w_i \delta_{i,j} M_{k,i} - \mathbb{C}^\star_{j,k} \right|$$

or by:

$$\mathcal{R}_k(w) = \sum_{j=1}^{n_{\mathcal{G}}} \left| w_j \mathbb{S}_{j,k}(w) - w_j \mathbb{S}^\star_{j,k}(w) \right| = \sum_{j=1}^{n_{\mathcal{G}}} \left| \sum_{i=1}^{n} w_i \delta_{i,j} \left(M_{k,i} - \mathbb{S}^\star_{j,k} \right) \right|$$

In this approach, the main challenge is defining a risk measure $\mathcal{R}_0(w)$ that plays an equivalent role to the variance in the classical mean-variance framework.

A first idea is to use the decomposition $\Sigma = LL^\top$ where L is a $n \times n$ matrix. We have:

$$\begin{aligned} w^\top \Sigma w &= w^\top L L^\top w \\ &= \left(L^\top w\right)^\top \left(L^\top w\right) \\ &= \left\| L^\top w \right\|_2^2 \end{aligned}$$

A natural $\boldsymbol{\ell}_1$-norm equivalent risk measure is then:

$$\begin{aligned} \mathcal{R}_k(w) &= \left\| L^\top w \right\|_1 \\ &= \sum_{j=1}^{n} \left| \sum_{i=1}^{n} L_{i,j} w_i \right| \end{aligned}$$

The choice of L is not unique. If Σ is strictly positive definite, we can use the Cholesky decomposition $\Sigma = PP^\top$ where P is a lower triangular matrix. In the case where Σ is positive semi-definite or has negative eigenvalues, the previous approach does not work. Therefore, we can use the eigendecomposition[26] $\Sigma = U\Lambda U^\top$ and set $L = U\Lambda^{1/2}$.

[25] We recall that $\mu(w) = \sum_{k=0}^{n_\mu} \phi_k \mu_k(w)$ with $\mu_0(w) = \mathcal{C}(w) = \sum_{i=1}^{n} w_i \mathcal{C}_i$ and $\mu_k(w) = \sum_{i=1}^{n} w_i \alpha_{k,i}$ for $k \geq 1$.

[26] We first transform Σ to remove the negative eigenvalues.

Remark 5. *Most of the time, practitioners do not use the full-rank matrix* $L = U\Lambda^{1/2}$ *because it is equivalent to assuming that* n *common risk factors are needed to assess the risk of the investment universe. In fact, this method is equivalent to a principal component analysis, and we usually retain only a few principal components. Let* $L_j = \left(L_{1,j}, \ldots, L_{n,j}\right)$ *be the* j^{th} *principal component vector. One generally replaces the previous risk measure with*[27]*:*

$$\mathcal{R}_0\left(w\right) = \sum_{j=1}^{m} \left|L_j^\top w\right|$$

where $m \ll n$*. The dimension reduction is particularly relevant because the memory requirement for the* L *matrix is now* $8nm$ *bytes instead of the* $8n^2$ *bytes for the* Q *matrix. For instance, if* $n = 30\,000$ *and* $m = 10$*, the memory requirement is reduced by a factor of* $3\,000$*! Besides the computational time and feasibility advantages, another interesting feature is that reducing the number of factors to* m *eliminates the noise of the covariance matrix. Thus, applying the* $\boldsymbol{\ell}_1$*-norm risk measure is equivalent to performing covariance denoising (Laloux et al., 1999).*

Another approach consists in approximating the covariance matrix using a suitable factor model, which leads to a risk measure expressed as a sum of $\boldsymbol{\ell}_1$-norms (see Appendix B.1 on page 90). For instance, under a two-factor model with uniform default correlation, we obtain the following formula[28]:

$$\mathcal{R}_{2\text{F}}\left(w\right) = \sigma_r \,\text{MD}^\top w + \sqrt{\rho}\upsilon_s^\top w + \sqrt{1-\rho}\left\|\upsilon_s \odot w\right\|_1$$

where σ_r is the interest rate volatility, $\text{MD} = \left(\text{MD}_1, \ldots, \text{MD}_n\right)$ is the vector of modified durations, ρ_s is the uniform correlation of credit spreads, $\upsilon_s = \left(\upsilon_{s,1}, \ldots, \upsilon_{s,n}\right)$ is the vector of credit spread risk, $\upsilon_{s,i} = \text{DTS}_i\,\sigma_{s,i}$ is the product of the DTS and the credit spread volatility. This formula has a clear financial structure:

- The first term captures interest rate risk, driven by the portfolio's aggregate duration.
- The second term captures the systematic component of credit spread risk.
- The third term captures the idiosyncratic component of credit spread risk, which depends on the individual credit spread volatilities.

With a benchmark Including a benchmark is straightforward since we simply replace the vector of weights w with the vector of active weights $w - b$. Nevertheless, we must be careful because while w is a positive vector[29], the vector $w - b$ contains both positive and negative values. As for the $\boldsymbol{\ell}_2$-norm optimization problem, the optimal solution satisfies:

$$w^\star = \arg\min \frac{1}{2}\mathcal{R}\left(w \mid b\right) - \gamma\mu\left(w \mid b\right) \tag{23}$$

where $\mathcal{R}\left(w \mid b\right) = \sum_{k=0}^{n_\mathcal{R}} \varphi_k \mathcal{R}_k\left(w \mid b\right)$ and $\mu\left(w \mid b\right) = \sum_{k=0}^{n_\mu} \phi_k \mu_k\left(w \mid b\right)$ are the active risk measure and the expected excess return of the portfolio w relative to the benchmark b, respectively. The individual risk measures $\mathcal{R}_k\left(w \mid b\right)$ are:

$$\mathcal{R}_0\left(w \mid b\right) = \left\|L^\top\left(w - b\right)\right\|_1 = \sum_{j=1}^{m}\left|\sum_{i=1}^{n} L_{i,j}\left(w_i - b\right)\right|$$

[27] For instance, if we consider a three-factor model, we have $\mathcal{R}_0\left(w\right) = \left|L_1^\top w\right| + \left|L_2^\top w\right| + \left|L_3^\top w\right|$.

[28] We use Equation (48) on page 92 and exploit the properties that MD_i, DTS_i, $\sigma_{s,i}$ and w_i are positive.

[29] We assume that $w_i \geq 0$, which imposes no short selling. This is standard in bond portfolio optimization because it is extremely difficult and costly to short bonds.

and:

$$\mathcal{R}_k\left(w \mid b\right) = \sum_{j=1}^{n_{\mathcal{G}}} \left| \sum_{i=1}^{n} \left(w_i - b_i\right) \delta_{i,j} M_{k,i} \right|$$

or:

$$\mathcal{R}_k\left(w \mid b\right) = \sum_{j=1}^{n_{\mathcal{G}}} \left| \sum_{i=1}^{n} w_i \delta_{i,j} \left(M_{k,i} - \mathbb{S}_{j,k}\left(b\right)\right) \right|$$

Regarding the expected excess return, $\mu_0\left(w \mid b\right) = \sum_{i=1}^{n}\left(w_i - b_i\right)\mathcal{C}_i$ and $\mu_k\left(w \mid b\right) = \sum_{i=1}^{n}\left(w_i - b_i\right)\alpha_{k,i}$ for $k \geq 1$.

Remark 6. *In the case of the two-factor risk model, the tracking error risk is defined as follows (see Appendix B.2.2 on page 91):*

$$\mathcal{R}_{2\mathrm{F}}\left(w \mid b\right) = \sigma_r \left|\mathrm{MD}^\top \left(w - b\right)\right| + \sqrt{\rho}\left|\upsilon_s^\top \left(w - b\right)\right| + \sqrt{1-\rho}\left\|\upsilon_s \odot \left(w - b\right)\right\|_1$$

Remark 7. *When practitioners include a benchmark, they often use active share as a proxy for tracking error risk:*

$$\mathcal{R}'_0\left(w \mid b\right) = \mathcal{AS}\left(w \mid b\right) = \frac{1}{2}\sum\nolimits_{i=1}^{n}\left|w_i - b_i\right| = \frac{1}{2}\left\|w - b\right\|_1$$

This is equivalent to setting $L = I_n$, meaning that the risk of each bond is entirely due to an idiosyncratic component of uniform magnitude across all bonds. While this assumption is clearly a simplification, active share remains widely used in practice for its transparency and ease of computation. However, it should be noted that active share measures positioning risk rather than market risk[30]*.*

Corresponding linear programming problems

Absolute value trick Using the $\boldsymbol{\ell}_1$-norm instead of the $\boldsymbol{\ell}_2$-norm allows us to reformulate the optimization problem as a linear programming (LP) problem. The idea is to use the absolute value trick. Let us assume that $c_i \geq 0$ for $i = 1, \ldots, n$. We have the following equivalence:

$$\min \sum_{i=1}^{n} c_i \left|f_i\left(x\right)\right| + g\left(x\right) \Leftrightarrow \begin{cases} \min & \displaystyle\sum_{i=1}^{n} c_i\tau_i + g\left(x\right) \\ \text{s.t.} & \begin{cases} \left|f_i\left(x\right)\right| \leq \tau_i \\ \tau_i \geq 0 \end{cases} \end{cases}$$

If $f_i\left(x\right)$ and $g\left(x\right)$ are linear functions, then the optimization problem becomes linear because $\left|f_i\left(x\right)\right| \leq \tau_i \Leftrightarrow -\tau_i \leq f_i\left(x\right) \wedge f_i\left(x\right) \leq \tau_i$.

We denote by x^* the solution of the first (unconstrained) problem and $(x^\star, \tau^\star)$ the solution of the second (constrained) problem. Since $\left|f_i\left(x\right)\right| \leq \tau_i$, we have:

$$\sum_{i=1}^{n} c_i \left|f_i\left(x\right)\right| + g\left(x\right) \leq \sum_{i=1}^{n} c_i\tau_i + g\left(x\right)$$

It follows that the constrained problem can never be better than the unconstrained problem. Let x be a feasible point in the unconstrained problem. We define $\tau_i = \left|f_i\left(x\right)\right|$. We deduce

[30] Two portfolios with identical active shares can have very different tracking errors if their active positions differ in duration times spread.

that $\left(x, \tau = \left|f(x)\right|\right)$ is a feasible point in the constrained problem, and the two problems have the same value:

$$\sum_{i=1}^{n} c_i \left|f_i(x)\right| + g(x) = \sum_{i=1}^{n} c_i \tau_i + g(x)$$

We deduce that the optimal value is:

$$\sum_{i=1}^{n} c_i \left|f_i(x^*)\right| + g(x^*) = \sum_{i=1}^{n} c_i \tau_i^* + g(x^*)$$

where $\tau_i^* = \left|f_i(x^*)\right|$. Because the constrained problem is never better than the unconstrained problem, we conclude that the optimal solution of the constrained problem is the optimal solution of the unconstrained problem:

$$(x^\star, \tau^\star) = \left(x^*, \tau^* = \left|f(x^*)\right|\right)$$

Linear programming and extended linear forms The standard formulation of a linear programming problem is:

$$\begin{aligned} x^\star &= \arg\min c^\top x \\ &\text{s.t.} \begin{cases} Ax = B \\ Cx \leq D \\ x^- \leq x \leq x^+ \end{cases} \end{aligned} \tag{24}$$

where x is a $n \times 1$ vector, c is a $n \times 1$ vector, A is a $n_A \times n$ matrix, B is a $n_A \times 1$ vector, C is a $n_C \times n$ matrix, D is a $n_C \times 1$ vector, and x^- and x^+ are two $n \times 1$ vectors. Unlike quadratic programming, where quadratic forms provide a natural and highly effective representation, the standard linear form $c^\top x + d$ is often insufficient for expressing and manipulating LP problems. To address this limitation, we introduce the following extended linear form:

$$\mathcal{LF}\left(x; c, d, C, D, x^-\right) = c^\top x + d + \mathbb{1}_\Omega(x)$$

where $\mathbb{1}_\Omega(x)$ is the convex indicator function[31] of $\Omega = \left\{x : Cx \leq D, x \geq x^-\right\}$. We have the following properties:

- The multiplication of an extended linear form by a positive scalar $\varphi \geq 0$ remains an extended linear form:

$$\varphi \cdot \mathcal{LF}\left(x; c, d, C, D, x^-\right) = \mathcal{LF}\left(x; \varphi c, \varphi d, C, D, x^-\right)$$

- The sum of two extended linear forms is an extended linear form. When considering the same variable, we obtain:

$$\mathcal{LF}\left(x; c_1, d_1, C_1, D_1, x_1^-\right) + \mathcal{LF}\left(x; c_2, d_2, C_2, D_2, x_2^-\right) = \mathcal{LF}\left(x; c, d, C, D, x^-\right)$$

  where:

$$c = c_1 + c_2,\ d = d_1 + d_2,\ C = \begin{bmatrix} C_1 \\ C_2 \end{bmatrix},\ D = \begin{bmatrix} D_1 \\ D_2 \end{bmatrix},\ \text{and } x^- = \max\left(x_1^-, x_2^-\right)$$

[31] This means that $\mathbb{1}_\Omega(x) = 0$ for $x \in \Omega$ and $\mathbb{1}_\Omega(x) = +\infty$ for $x \notin \Omega$.

When considering two distinct variables x and y, we get:

$$\mathcal{LF}\left(x; c_x, d_x, C_x, D_x, x^-\right) + \mathcal{LF}\left(y; c_y, d_y, C_y, D_y, y^-\right) = \mathcal{LF}\left(z; c_z, d_z, C_z, D_z, z^-\right)$$

where $z = \begin{bmatrix} x \\ y \end{bmatrix}$ is the augmented variable and:

$$c_z = \begin{bmatrix} c_x \\ c_y \end{bmatrix},\ d_z = d_x + d_y,\ C_z = \begin{bmatrix} C_x & \mathbf{0}_{n_{C_x}, n_y} \\ \mathbf{0}_{n_{C_y}, n_x} & C_y \end{bmatrix},\ D = \begin{bmatrix} D_x \\ D_y \end{bmatrix},\ \text{and } z^- = \begin{bmatrix} x^- \\ y^- \end{bmatrix}$$

We now examine the relationship between the absolute value trick and the extended linear form. Let $a = \left(a_{i,j}\right)$ and b be a $n \times m$ matrix and a $m \times 1$ vector. We have:

$$\begin{aligned}
\min \sum_{j=1}^{m} \left| \sum_{i=1}^{n} a_{i,j} x_i - b_j \right| \quad &\Leftrightarrow \quad \begin{cases} \min & \sum_{j=1}^{m} \tau_j \\ \text{s.t.} & \begin{cases} \left| \sum_{i=1}^{n} a_{i,j} x_i - b_j \right| \leq \tau_j \\ \tau_j \geq 0 \end{cases} \end{cases} \\
&\Leftrightarrow \quad \begin{cases} \min & \sum_{j=1}^{m} \tau_j \\ \text{s.t.} & \begin{cases} -\sum_{i=1}^{n} a_{i,j} x_i - \tau_j \leq -b_j \\ \sum_{i=1}^{n} a_{i,j} x_i - \tau_j \leq b_j \\ \tau_j \geq 0 \end{cases} \end{cases} \\
&\Leftrightarrow \quad \min \mathcal{LF}\left(z; c_z, d_z, C_z, D_z, z^-\right)
\end{aligned}$$

where the augmented variable is the $(n+m) \times 1$ vector $z = \begin{bmatrix} x \\ \tau \end{bmatrix}$. The other matrices are defined as[32]:

$$c_z = \begin{bmatrix} \mathbf{0}_n \\ \mathbf{1}_m \end{bmatrix},\ d_z = 0,\ C_z = \begin{bmatrix} -a^\top & -I_m \\ a^\top & -I_m \end{bmatrix},\ D_z = \begin{bmatrix} -b \\ b \end{bmatrix},\ \text{and } z^- = \begin{bmatrix} -\infty \cdot \mathbf{1}_n \\ \mathbf{0}_m \end{bmatrix}$$

LP bond optimization In Appendix B.6 on page 103, we show that the extended linear form of the objective function without a benchmark is:

$$\min \frac{1}{2} \mathcal{R}\left(w\right) - \gamma \mu\left(w\right) = \min \mathcal{LF}\left(z; c, d, C, D, z^-\right)$$

where the augmented variable is the $(n + m + n_{\mathcal{R}} n_{\mathcal{G}}) \times 1$ vector: $z = \left(w, \tau_{(0)}, \tau_{(1)}, \ldots, \tau_{(n_{\mathcal{R}})}\right)$. The objective is defined by $c_z = \left(-\gamma \left(\phi_0 \mathcal{C} + \sum_{k=1}^{n_\mu} \phi_k \alpha_k\right), \frac{1}{2}\varphi_0 \mathbf{1}_m, \frac{1}{2}\varphi_1 \mathbf{1}_{n_{\mathrm{G}}}, \ldots, \frac{1}{2}\varphi_{n_{\mathcal{R}}} \mathbf{1}_{n_{\mathrm{G}}}\right)$ and $d_z = 0$. The bounds are $z^- = \mathbf{0}_{n+m+n_{\mathcal{R}} \times n_{\mathcal{G}}}$. There are $2 \times (m + n_{\mathcal{R}} n_{\mathcal{G}})$ inequality con-

[32] Because the matrix forms of the inequalities are $-\sum_{i=1}^{n} a_{i,j} x_i - \tau_j \leq -b_j \Leftrightarrow -a^\top x - \tau \leq -b$ and $\sum_{i=1}^{n} a_{i,j} x_i - \tau_j \leq b_j \Leftrightarrow a^\top x - \tau \leq b$.

straints, defined by $D_z = \left(\mathbf{0}_m, \mathbf{0}_m, -\mathbb{C}_1^\star, \mathbb{C}_1^\star, \ldots, -\mathbb{C}_{n_\mathcal{R}}^\star, \mathbb{C}_{n_\mathcal{R}}^\star\right)$ and:

$$C_z = \begin{bmatrix} -L^\top & -I_m & & & \\ L^\top & -I_m & & & \\ -\left(\delta \odot M_1\right)^\top & & -I_{n_\mathcal{G}} & & \\ \left(\delta \odot M_1\right)^\top & & -I_{n_\mathcal{G}} & & \\ \vdots & & & \ddots & \\ -\left(\delta \odot M_{n_\mathcal{R}}\right)^\top & & & & -I_{n_\mathcal{G}} \\ \left(\delta \odot M_{n_\mathcal{R}}\right)^\top & & & & -I_{n_\mathcal{G}} \end{bmatrix}$$

where blanks are zeros. If we use cluster scores instead of cluster contributions, only C_z and D_z change. We have $D_z = \mathbf{0}_{2(m+n_\mathcal{R} n_\mathcal{G})}$ and:

$$C_z = \begin{bmatrix} -L^\top & -I_m & & & \\ L^\top & -I_m & & & \\ -\left(\delta \odot \left(M_1 - \mathbb{S}_1^\star\right)\right)^\top & & -I_{n_\mathcal{G}} & & \\ \left(\delta \odot \left(M_1 - \mathbb{S}_1^\star\right)\right)^\top & & -I_{n_\mathcal{G}} & & \\ \vdots & & & \ddots & \\ -\left(\delta \odot \left(M_{n_\mathcal{R}} - \mathbb{S}_{n_\mathcal{R}}^\star\right)\right)^\top & & & & -I_{n_\mathcal{G}} \\ \left(\delta \odot \left(M_{n_\mathcal{R}} - \mathbb{S}_{n_\mathcal{R}}^\star\right)\right)^\top & & & & -I_{n_\mathcal{G}} \end{bmatrix}$$

If we include a benchmark and add the active share risk measure, the objective function becomes:

$$\min \frac{1}{2}\mathcal{R}\left(w \mid b\right) - \gamma\mu\left(w \mid b\right) = \min \mathcal{LF}\left(z; c, d, C, D, z^-\right)$$

where the augmented variable is the $(2n + m + n_\mathcal{R} n_\mathcal{G})\times 1$ vector: $z = \left(w, \tau_{(0)}, \tau'_{(0)}, \tau_{(1)}, \ldots, \tau_{(n_\mathcal{R})}\right)$. The objective is defined by $c_z = \left(-\gamma\left(\phi_0\mathcal{C} + \sum_{k=1}^{n_\mu}\phi_k\alpha_k\right), \frac{1}{2}\varphi_0\mathbf{1}_m, \frac{1}{2}\varphi'_0\mathbf{1}_n, \frac{1}{2}\varphi_1\mathbf{1}_{n_\mathcal{G}}, \ldots, \frac{1}{2}\varphi_{n_\mathcal{R}}\mathbf{1}_{n_\mathcal{G}}\right)$ and $d_z = \gamma\left(\phi_0\mathcal{C} + \sum_{k=1}^{n_\mu}\phi_k\alpha_k\right)^\top b$. The bounds are $z^- = \mathbf{0}_{2n+m+n_\mathcal{R} n_\mathcal{G}}$. There are $2 \times (m + n + n_\mathcal{R} n_\mathcal{G})$ inequality constraints, defined by:

$$C_z = \begin{bmatrix} -L^\top & -I_m & & & & \\ L^\top & -I_m & & & & \\ -I_n & & -I_n & & & \\ I_n & & -I_n & & & \\ -\left(\delta \odot M_1\right)^\top & & & -I_{n_\mathcal{G}} & & \\ \left(\delta \odot M_1\right)^\top & & & -I_{n_\mathcal{G}} & & \\ \vdots & & & & \ddots & \\ -\left(\delta \odot M_{n_\mathcal{R}}\right)^\top & & & & & -I_{n_\mathcal{G}} \\ \left(\delta \odot M_{n_\mathcal{R}}\right)^\top & & & & & -I_{n_\mathcal{G}} \end{bmatrix} \text{ and } D_z = \begin{bmatrix} -L^\top b \\ L^\top b \\ -b \\ b \\ -\left(\delta \odot M_1\right)^\top b \\ \left(\delta \odot M_1\right)^\top b \\ \vdots \\ -\left(\delta \odot M_{n_\mathcal{R}}\right)^\top b \\ \left(\delta \odot M_{n_\mathcal{R}}\right)^\top b \end{bmatrix}$$

where blanks are zeros. If we use cluster scores instead of cluster contributions, only C_z and D_z change. We have $D_z = \mathbf{0}_{2(m+n+n_{\mathcal{R}}n_{\mathcal{G}})}$ and:

$$C_z = \begin{bmatrix} -L^\top & -I_m & & & \\ L^\top & -I_m & & & \\ -I_n & & -I_n & & \\ I_n & & -I_n & & \\ -\left(\delta \odot (M_1 - \mathbb{S}_1^\star)\right)^\top & & & -I_{n_{\mathcal{G}}} & \\ \left(\delta \odot (M_1 - \mathbb{S}_1^\star)\right)^\top & & & -I_{n_{\mathcal{G}}} & \\ \vdots & & & & \ddots \\ -\left(\delta \odot \left(M_{n_{\mathcal{R}}} - \mathbb{S}_{n_{\mathcal{R}}}^\star\right)\right)^\top & & & & -I_{n_{\mathcal{G}}} \\ \left(\delta \odot \left(M_{n_{\mathcal{R}}} - \mathbb{S}_{n_{\mathcal{R}}}^\star\right)\right)^\top & & & & -I_{n_{\mathcal{G}}} \end{bmatrix}$$

Comparison between LP and QP bond optimization As discussed earlier, the preference for LP over QP formulations is driven by computational considerations. The dimensions of each problem are:

Model	Variables	Objective function	Constraints
QP	n	$n^2 + n$	0
LP_1	$n + m + n_{\mathcal{R}}n_{\mathcal{G}}$	$n + m + n_{\mathcal{R}}n_{\mathcal{G}}$	$(2m + 2n_{\mathcal{R}}n_{\mathcal{G}}) \times (n + m + n_{\mathcal{R}}n_{\mathcal{G}})$
LP_2	$n + m + n_{\mathcal{R}}n_{\mathcal{G}}$	$n + m + n_{\mathcal{R}}n_{\mathcal{G}}$	$(2m + 2n_{\mathcal{R}}n_{\mathcal{G}}) \times (n + m + n_{\mathcal{R}}n_{\mathcal{G}})$
LP_3	$2n + m + n_{\mathcal{R}}n_{\mathcal{G}}$	$2n + m + n_{\mathcal{R}}n_{\mathcal{G}}$	$(2m + 2n + 2n_{\mathcal{R}}n_{\mathcal{G}}) \times (2n + m + n_{\mathcal{R}}n_{\mathcal{G}})$

where LP_1, LP_2, and LP_3 denote respectively the LP problem without benchmark, the LP problem with benchmark, and the LP problem with benchmark and active share. We recall that n is the number of bonds in the portfolio, m is the rank of the covariance matrix, $n_{\mathcal{G}}$ is the number of clusters, and $n_{\mathcal{R}}$ is the number of additional risk measures. Since $n_{\mathcal{R}} \leq 5$ and $n_{\mathcal{G}} \ll n$, we derive the following approximate orders of magnitude:

Model	Variables	Objective function	Constraints
QP	n	n^2	0
LP_1	$n + m$	$n + m$	$2mn + 2m^2$
LP_2	$n + m$	$n + m$	$2mn + 2m^2$
LP_3	$2n + m$	$2n + m$	$4n^2 + 6mn + 2m^2$

It is clear that the LP formulations are more computationally efficient than QP if and only if $m \ll n$, i.e. when the rank of the covariance matrix is small relative to the number of bonds. The most favourable case is $m = 0$, corresponding to the exclusion of covariance risk from the optimisation problem. In this case, the approximate dimensions reduce to:

Model	Variables	Objective function	Constraints
QP	n	n^2	0
LP_1	n	n	$2nn_{\mathcal{R}}n_{\mathcal{G}}$
LP_2	n	n	$2nn_{\mathcal{R}}n_{\mathcal{G}}$
LP_3	$2n$	$2n$	$4n^2$

In this case, LP_1 and LP_2 are substantially more efficient than QP, since their constraint matrices scale as $2nn_{\mathcal{R}}n_{\mathcal{G}}$, which is of order $\mathcal{O}(n)$ rather than $\mathcal{O}(n^2)$. To illustrate, consider a typical setup with MD and DTS risk measures, 10 sectors, and 4 maturity bands. We

obtain $2n_{\mathcal{R}}n_{\mathcal{G}} = 2 \times 2 \times 40 = 160$, which is negligible compared to a universe of $n > 1000$ bonds. However, LP_3 is an exception. The inclusion of the active share introduces an additional $2n$ rows in the constraint matrix, pushing the problem to order $\mathcal{O}\left(n^2\right)$ and making it comparable in cost to QP. This computational bottleneck is solved in the next section.

2.4 Advanced bond portfolio optimization

Previous sections focused on two classes of optimization problems and the numerical algorithms used to solve them: quadratic programming and linear programming. In this section, we extend the discussion to more advanced optimization techniques, such as the alternating direction method of multipliers (ADMM) and proximal operators. We also examine more complex optimization problems that involve discrete decision variables, requiring approaches such as integer programming and genetic algorithms.

2.4.1 Revisiting the ℓ_2-norm optimization problem

The idea is to exploit the separability of the objective function (Perrin and Roncalli, 2020, Third trick, page 18). For instance, we can split the risk measure into two components: $\mathcal{R}(w) = \mathcal{R}^{(1)}(w) + \mathcal{R}^{(2)}(w)$. Then, we can reformulate the optimization problem in ADMM form[33]:

$$\begin{aligned} \{w^\star, x^\star, y^\star\} &= \arg\min \underbrace{\frac{1}{2}\mathcal{R}^{(1)}(x) - \gamma\mu(x) + \mathbb{1}_\Omega(x)}_{f_x(x)} + \underbrace{\frac{1}{2}\mathcal{R}^{(2)}(y)}_{f_y(y)} \\ &\text{s.t.} \quad x = y = w \end{aligned}$$

The ADMM algorithm consists of the following three steps:

$$\begin{cases} x^{(k+1)} = \arg\min f_x^{(k+1)}(x) = \dfrac{1}{2}\mathcal{R}^{(1)}(x) - \gamma\mu(x) + \mathbb{1}_\Omega(x) + \dfrac{\theta}{2}\left\|x - y^{(k)} + u^{(k)}\right\|_2^2 \\ y^{(k+1)} = \arg\min f_y^{(k+1)}(y) = \dfrac{1}{2}\mathcal{R}^{(2)}(y) + \dfrac{\theta}{2}\left\|x^{(k+1)} - y + u^{(k)}\right\|_2^2 \\ u^{(k+1)} = u^{(k)} + \left(x^{(k+1)} - y^{(k+1)}\right) \end{cases}$$

where $\theta > 0$ is the augmented Lagrangian penalty parameter and $u^{(k)}$ is the dual variable. For instance, we can set $\mathcal{R}^{(1)}(w) = \sum_{k=1}^{n_{\mathcal{R}}} \varphi_k \mathcal{R}_k(w)$ and $\mathcal{R}^{(2)}(w) = \varphi_0 \mathcal{R}_0(w) = \varphi_0 w^\top \Sigma w$. With this splitting, the original optimization problem decomposes into two subproblems that are easier to solve.

An equivalent formulation of the previous problem can be derived using the fourth trick of Perrin and Roncalli (2020, page 18) by setting $y = L^\top x$, where L is obtained from the matrix decomposition $\Sigma = LL^\top$. It follows that :

$$y^\top y = \left(L^\top x\right)^\top \left(L^\top x\right) = x^\top LL^\top x = x^\top \Sigma x$$

We deduce that:

$$\begin{aligned} \{w^\star, x^\star, y^\star\} &= \arg\min \underbrace{\frac{1}{2}\mathcal{R}^{(1)}(x) - \gamma\mu(x) + \mathbb{1}_\Omega(x)}_{f_x(x)} + \underbrace{\frac{1}{2}\varphi_0 y^\top y}_{f_y(y)} \\ &\text{s.t.} \quad \begin{cases} L^\top x - y = 0_n \\ w = x \end{cases} \end{aligned}$$

[33] See Appendix B.7.1 on page 106 for a presentation of the ADMM algorithm.

The ADMM algorithm becomes:

$$\begin{cases} x^{(k+1)} = \arg\min f_x^{(k+1)}(x) = \frac{1}{2}\sum_{k=1}^{n_{\mathcal{R}}} \varphi_k \mathcal{R}_k(x) - \gamma\mu(x) + \mathbb{1}_\Omega(x) + \frac{\theta}{2}\left\|L^\top x - y^{(k)} + u^{(k)}\right\|_2^2 \\ y^{(k+1)} = \arg\min f_y^{(k+1)}(y) = \frac{1}{2}\varphi_0 y^\top y + \frac{\theta}{2}\left\|L^\top x^{(k+1)} - y + u^{(k)}\right\|_2^2 \\ u^{(k+1)} = u^{(k)} + \left(L^\top x^{(k+1)} - y^{(k+1)}\right) \end{cases}$$

Finally, a third approach can be derived using the second trick proposed by Perrin and Roncalli (2020, page 17). The idea is to separate the objective function from the constraints:

$$\begin{aligned} \{w^\star, x^\star, y^\star\} &= \arg\min \underbrace{\frac{1}{2}\mathcal{R}(x) - \gamma\mu(x)}_{f_x(x)} + \underbrace{\mathbb{1}_\Omega(y)}_{f_y(y)} \\ &\text{s.t.} \quad x = y = w \end{aligned}$$

The corresponding ADMM algorithm is:

$$\begin{cases} x^{(k+1)} = \arg\min f_x^{(k+1)}(x) = \frac{1}{2}\mathcal{R}(x) - \gamma\mu(x) + \frac{\theta}{2}\left\|x - y^{(k)} + u^{(k)}\right\|_2^2 \\ y^{(k+1)} = \arg\min f_y^{(k+1)}(y) = \mathbb{1}_\Omega(y) + \frac{\theta}{2}\left\|x^{(k+1)} - y + u^{(k)}\right\|_2^2 \\ u^{(k+1)} = u^{(k)} + \left(x^{(k+1)} - y^{(k+1)}\right) \end{cases}$$

The first step admits a straightforward analytical solution. Indeed, we have:

$$\begin{aligned} \frac{1}{2}\left\|x - y^{(k)} + u^{(k)}\right\|_2^2 &= \frac{1}{2}\left(x^\top - \left(y^{(k)} - u^{(k)}\right)^\top\right)\left(x - \left(y^{(k)} - u^{(k)}\right)\right) \\ &= \frac{1}{2}x^\top x - x^\top\left(y^{(k)} - u^{(k)}\right) + \frac{1}{2}\left(y^{(k)} - u^{(k)}\right)^\top\left(y^{(k)} - u^{(k)}\right) \\ &= \mathcal{QF}\left(x; I_n, y^{(k)} - u^{(k)}, \frac{1}{2}\left(y^{(k)} - u^{(k)}\right)^\top\left(y^{(k)} - u^{(k)}\right)\right) \end{aligned}$$

Using the quadratic form of $\frac{1}{2}\mathcal{R}(x) - \gamma\mu(x)$, we obtain:

$$\begin{aligned} f_x^{(k+1)}(x) &= \mathcal{QF}(x; Q, R, s) + \theta\mathcal{QF}\left(x; I_n, y^{(k)} - u^{(k)}, \frac{1}{2}\left(y^{(k)} - u^{(k)}\right)^\top\left(y^{(k)} - u^{(k)}\right)\right) \\ &= \mathcal{QF}\left(x; Q + \theta I_n, R + \theta\left(y^{(k)} - u^{(k)}\right), s + \frac{\theta}{2}\left(y^{(k)} - u^{(k)}\right)^\top\left(y^{(k)} - u^{(k)}\right)\right) \end{aligned}$$

and:

$$\arg\min f_x^{(k+1)}(x) \Leftrightarrow x^{(k+1)} = (Q + \theta I_n)^{-1}\left(R + \theta\left(y^{(k)} - u^{(k)}\right)\right)$$

Therefore, the x-update has a closed-form solution. The second step can be expressed as:

$$\begin{aligned} \arg\min f_y^{(k+1)}(y) &= \arg\min \mathbb{1}_\Omega(y) + \frac{\theta}{2}\left\|x^{(k+1)} - y + u^{(k)}\right\|_2^2 \\ &= \arg\min \theta\left(\frac{1}{\theta}\mathbb{1}_\Omega(y) + \frac{1}{2}\left\|y - x^{(k+1)} - u^{(k)}\right\|_2^2\right) \\ &= \mathbf{prox}_{\mathbb{1}_\Omega(y)}\left(x^{(k+1)} + u^{(k)}\right) \\ &= \mathcal{P}_\Omega\left(x^{(k+1)} + u^{(k)}\right) \end{aligned}$$

Because Ω corresponds to linear constraints (equality, inequality and bounds), the analytical projections given in Perrin and Roncalli (2020, page 21) can be used (affine set, hyperplane, half-space and box). When several linear constraints are combined, *i.e.* $\Omega = \left\{x \in \mathbb{R}^n : Ax = B, Cx \leq D, x^- \leq x \leq x^+\right\}$, Dykstra's algorithm provides an efficient numerical solution (Perrin and Roncalli, 2020, Algorithm 7, page 28). In this approach, quadratic programming is completely replaced by a succession of projections[34].

Remark 8. *The three ADMM formulations illustrate how a problem can be split into two subproblems that are easier to solve individually. Other possible splits depend on the specific structure of the bond portfolio optimization problem. Moreover, the above analysis can be easily extended to the optimization problem with a benchmark.*

2.4.2 Revisiting the ℓ_1-norm optimization problem

We note that the general bond portfolio optimization problem takes the form:

$$\begin{aligned} z^\star &= \arg\min c_z^\top z + d_z \\ &\text{s.t.} \quad z \in \Omega = \{z : A_z z = B_z, C_z z \leq D_z, z \geq \mathbf{0}_{n_z}\} \end{aligned}$$

Applying again the second trick of Perrin and Roncalli (2020, page 17), we have:

$$\begin{aligned} \{z^\star, x^\star, y^\star\} &= \arg\min \underbrace{c_z^\top x + d_z}_{f_x(x)} + \underbrace{\mathbb{1}_\Omega(y)}_{f_y(y)} \\ &\text{s.t.} \quad x = y = z \end{aligned}$$

The corresponding ADMM algorithm is:

$$\begin{cases} x^{(k+1)} = \arg\min f_x^{(k+1)}(x) = c_z^\top x + d_z + \dfrac{\theta}{2}\left\|x - y^{(k)} + u^{(k)}\right\|_2^2 \\ y^{(k+1)} = \arg\min f_y^{(k+1)}(y) = \mathbb{1}_\Omega(y) + \dfrac{\theta}{2}\left\|x^{(k+1)} - y + u^{(k)}\right\|_2^2 \\ u^{(k+1)} = u^{(k)} + \left(x^{(k+1)} - y^{(k+1)}\right) \end{cases}$$

We have:

$$f_x^{(k+1)}(x) = \mathcal{QF}\left(x; \theta I_{n_z}, -c_z + \theta\left(y^{(k)} - u^{(k)}\right), d_z + \frac{\theta}{2}\left(y^{(k)} - u^{(k)}\right)^\top\left(y^{(k)} - u^{(k)}\right)\right)$$

The solution of $\min f_x^{(k+1)}(x)$ is:

$$x^{(k+1)} = (\theta I_{n_z})^{-1}\left(-c_z + \theta\left(y^{(k)} - u^{(k)}\right)\right) = y^{(k)} - u^{(k)} - \frac{1}{\theta}c_z$$

We deduce that the optimal solution can be found using the following ADMM iteration:

$$\begin{cases} x^{(k+1)} = y^{(k)} - u^{(k)} - \dfrac{1}{\theta}c_z \\ y^{(k+1)} = \mathcal{P}_\Omega\left(x^{(k+1)} + u^{(k)}\right) \\ u^{(k+1)} = u^{(k)} + \left(x^{(k+1)} - y^{(k+1)}\right) \end{cases}$$

In this formulation, linear programming is entirely replaced by a projection onto Ω, which can be computed efficiently with the Dykstra's algorithm by exploiting the sparsity of C_z. The choice between linear programming or ADMM will depend on the dimension of the optimization problem.

[34] The algorithm is described on pages 109 and 110.

2.4.3 The active share problem

The ℓ_2-norm formulation When a benchmark is introduced, the objective function takes the following form:

$$\begin{array}{rcl} w^\star & = & \arg\min \mathcal{QF}\left(w; Q, R, s\right) \\ & \text{s.t.} & w \in \Omega \end{array}$$

where $\mathcal{QF}\left(w; Q, R, s\right) = \frac{1}{2}\mathcal{R}\left(w \mid b\right) - \gamma\mu\left(w \mid b\right)$ and Ω is the set of (equality, inequality and bound) constraints. Under the linearity assumption on all constraints, we obtain a standard QP problem. If we would like to control the active share of the portfolio, we can consider two equivalent formulations:

$$\begin{array}{rcl} w^\star\left(\lambda\right) & = & \arg\min \mathcal{QF}\left(w; Q, R, s\right) + \lambda\mathcal{AS}\left(w \mid b\right) \\ & \text{s.t.} & w \in \Omega \end{array} \tag{25}$$

or:

$$\begin{array}{rcl} w^\star\left(\mathcal{AS}^+\right) & = & \arg\min \mathcal{QF}\left(w; Q, R, s\right) \\ & \text{s.t.} & \left\{ \begin{array}{l} w \in \Omega \\ \mathcal{AS}\left(w \mid b\right) \leq \mathcal{AS}^+ \end{array} \right. \end{array} \tag{26}$$

where $\lambda \geq 0$ is the penalization coefficient and $\mathcal{AS}^+$ is the maximum level of active share. By standard duality arguments, these two formulations are equivalent in the sense that for every $\mathcal{AS}^+$, there exists a $\lambda \geq 0$ such that the two problems have the same solution, and vice versa.

To solve the active share problem without introducing a non-convex complementarity condition, we can first use the following decomposition:

$$w_i = b_i - \Delta w_i^- + \Delta w_i^+$$

where $0 \leq \Delta w_i^- \leq b_i$, $0 \leq \Delta w_i^+ \leq 1 - b_i$ and $\Delta w_i^- \Delta w_i^+ = 0$. Here Δw_i^- and Δw_i^+ capture the downward and upward deviations of portfolio weight w_i from the benchmark weight b_i. We deduce that:

$$\mathcal{AS}\left(w \mid b\right) = \frac{1}{2}\sum_{i=1}^n \left|w_i - b_i\right| = \frac{1}{2}\sum_{i=1}^n \left|\Delta w_i^+ - \Delta w_i^-\right| = \frac{1}{2}\sum_{i=1}^n \left(\Delta w_i^+ + \Delta w_i^-\right)$$

Unsing this decomposition, Problems (25) and (26) can be rewritten in terms of the augmented variable set $\left\{w, \Delta w^-, \Delta w^+\right\}$. The penalized formulation becomes[35]:

$$\begin{array}{rcl} \left\{w^\star, \Delta w^{-^\star}, \Delta w^{+^\star}\right\} & = & \arg\min \mathcal{QF}\left(w; Q, R, s\right) + \dfrac{\lambda}{2}\left(\mathbf{1}_n^\top \Delta w^- + \mathbf{1}_n^\top \Delta w^+\right) \\ & \text{s.t.} & \left\{ \begin{array}{l} w \in \Omega \\ I_n w + I_n \Delta w^- - I_n \Delta w^+ = b \\ \mathbf{0}_n \leq \Delta w^- \leq b \\ \mathbf{0}_n \leq \Delta w^+ \leq \mathbf{1}_n - b \end{array} \right. \end{array} \tag{27}$$

[35] The complementarity constraint $\Delta w^- \odot \Delta w^+ = \mathbf{0}_n$ vanishes because it is satisfied by any optimal solution. This is due to the convexity of the objective function and the linearity of the constraints.

while the constrained formulation becomes:

$$\left\{w^\star, \Delta w^{-^\star}, \Delta w^{+^\star}\right\} = \arg\min \mathcal{QF}\left(w; Q, R, s\right) \quad (28)$$
$$\text{s.t.} \begin{cases} w \in \Omega \\ \mathbf{1}_n^\top \Delta w^- + \mathbf{1}_n^\top \Delta w^+ \leq 2\mathcal{AS}^+ \\ I_n w + I_n \Delta w^- - I_n \Delta w^+ = b \\ \mathbf{0}_n \leq \Delta w^- \leq b \\ \mathbf{0}_n \leq \Delta w^+ \leq \mathbf{1}_n - b \end{cases}$$

Problems (27) and (28) remain QP and can be solved numerically via their augmented formulations. However, the number of variables increases to $3n$ and the quadratic cost of the matrix Q grows from n^2 to $9n^2$. This can pose a computational challenge when the benchmark already contains a large number of constituents.

The second approach is to use the ADMM formulation. The optimal solution $w^\star$ is equal to $x^\star$ or $y^\star$, where:

$$\{w^\star, x^\star, y^\star\} = \arg\min \underbrace{\mathcal{QF}\left(x; Q, R, s\right) + \mathbb{1}_\Omega\left(x\right)}_{f_x(x)} + \underbrace{\lambda\mathcal{AS}\left(y \mid b\right)}_{f_y(y)}$$
$$\text{s.t.} \quad x = y = w$$

or:

$$\{w^\star, x^\star, y^\star\} = \arg\min \underbrace{\mathcal{QF}\left(x; Q, R, s\right) + \mathbb{1}_\Omega\left(x\right)}_{f_x(x)} + \underbrace{\mathbb{1}_{\mathcal{AS}(y|b)\leq\mathcal{AS}^+}\left(y\right)}_{f_y(y)}$$
$$\text{s.t.} \quad x = y = w$$

The first problem is solved using the proximal of the $\boldsymbol{\ell}_1$ norm (Perrin and Roncalli, 2020, Section 3.3.3, page 22):

$$\mathbf{prox}_{f_y}\left(v\right) = b + \text{sign}\left(v - b\right) \odot \left(\left|v - b\right| - \frac{\lambda}{2\theta}\mathbf{1}_n\right)^+$$

while the second problem is solved using the proximal of the $\boldsymbol{\ell}_1$ ball with center b and radius $2\mathcal{AS}^+$ (Perrin and Roncalli, 2020, Appendix A.8.4, page 58):

$$\mathbf{prox}_{\mathcal{AS}(y|b)\leq\mathcal{AS}^+}\left(v\right) = v - \text{sign}\left(v - b\right) \odot \min\left(\left|v - b\right|, s^\star\right)$$

where $s^\star$ is the solution of the following equation:

$$s^\star = \left\{ s \in \mathbb{R} : \sum_{i=1}^n \left(\left|v_i - b_i\right| - s\right)^+ = 2\mathcal{AS}^+ \right\}$$

The $\boldsymbol{\ell}_1$-norm formulation In the case of the $\boldsymbol{\ell}_1$-norm optimization problem, the inclusion of the active share requires n slack variables, which highly increases the dimension of the inequality matrix C_z. From a numerical standpoint, the high sparsity of C_z can be exploited using sparse linear programming. We recall that the dimension of the matrix C_z is:

$$\dim C_z = \left(2m + 2n + 2n_{\mathcal{R}} n_{\mathcal{G}}\right) \times \left(2n + m + n_{\mathcal{R}} n_{\mathcal{G}}\right)$$

We deduce that the number of entries is:

$$\#\left(C_z\right) = 4n^2 + 6mn + 6n_{\mathcal{R}}n_{\mathcal{G}}n + 2m^2 + 4mn_{\mathcal{R}}n_{\mathcal{G}} + 2n_{\mathcal{R}}^2 n_{\mathcal{G}}^2$$

while the number of non-zero entries is:

$$\mathrm{nnz}\left(C_z\right) = 2mn + 4n + 2m + 2n_{\mathcal{R}}n_{\mathcal{G}} + 2n_{\mathcal{G}}n$$

The sparsity of C_z is then:

$$\begin{aligned}
\mathrm{sparsity}\left(C_z\right) &= 1 - \frac{mn + 2n + m + n_{\mathcal{R}}n_{\mathcal{G}} + n_{\mathcal{G}}n}{2n^2 + 3mn + 3n_{\mathcal{R}}n_{\mathcal{G}}n + m^2 + 2mn_{\mathcal{R}}n_{\mathcal{G}} + n_{\mathcal{R}}^2 n_{\mathcal{G}}^2} \\
&\approx 1 - \frac{n\left(m + n_{\mathcal{G}} + 2\right) + m}{2n^2 + 3mn + m^2} \\
&\approx 1 - \frac{m + n_{\mathcal{G}} + 2}{2n + 3m} \qquad \text{if } m \ll n
\end{aligned}$$

It follows that:

$$\lim_{n \longrightarrow \infty} \mathrm{sparsity}\left(C_z\right) = 1$$

Below, we report some numerical figures assuming that $n_{\mathcal{R}} = 5$ and $n_{\mathcal{G}} = 40$:

$\mathrm{sparsity}\left(C_z\right)$	$m = n$				$m = 50$			
$n = 1\,000$	85.2%				96.7%	96.7%	96.7%	96.7%
$n = 5\,000$		83.7%			99.1%	99.1%	99.1%	99.1%
$n = 10\,000$			83.5%		99.6%	99.6%	99.6%	99.6%
$n = 30\,000$				83.4%	99.8%	99.8%	99.8%	99.8%

Assuming the rank of the covariance matrix Σ is at most 50, the sparsity of C_z is already greater than 95%. Moreover, it exceeds 99% as soon as the number of bonds exceeds 5 000. These results confirm that C_z is a highly sparse matrix and can be exploited to dramatically reduce storage requirements and computational complexity.

Let $\{c_z, d_z, C_z, D_z\}$ be the matrices of the ℓ_1-norm problem without the active share risk measure. When the active share constraint is included, the bond portfolio optimization problem takes the following forms:

$$\begin{aligned}
z^\star &= \arg\min c_z^\top z + d_z + \lambda \mathcal{AS}\left(w \mid b\right) \\
&\text{s.t.} \quad z \in \Omega = \{z : A_z = B_z, C_z z \leq D_z, z \geq \mathbf{0}_{n_z}\}
\end{aligned}$$

or:

$$\begin{aligned}
z^\star &= \arg\min c_z^\top z + d_z \\
&\text{s.t.} \quad \left\{ \begin{array}{l} z \in \Omega \cap \Theta \\ \Omega = \{z : A_z = B_z, C_z z \leq D_z, z \geq \mathbf{0}_{n_z}\} \\ \Theta = \left\{z : \mathcal{AS}\left(w \mid b\right) \leq \mathcal{AS}^+\right\} \end{array} \right.
\end{aligned}$$

The corresponding ADMM formulations are:

$$\begin{aligned}
\{z^\star, x^\star, y^\star\} &= \arg\min \underbrace{c_z^\top x + d_z + \mathbf{1}_\Omega\left(x\right)}_{f_x(x)} + \underbrace{\lambda \mathcal{AS}\left(y \mid b\right)}_{f_y(y)} \\
&\text{s.t.} \quad x = y = z
\end{aligned}$$

and:

$$\begin{aligned}\{z^\star, x^\star, y^\star\} \quad &= \quad \arg\min \underbrace{c_z^\top x + d_z + \mathbb{1}_\Omega(x)}_{f_x(x)} + \underbrace{\mathbb{1}_{\mathcal{AS}(y|b)\leq \mathcal{AS}^+}(y)}_{f_y(y)} \\ &\text{s.t.} \quad x = y = z\end{aligned}$$

In both formulations, the x-update is solved via a nested ADMM subproblem, while the y-update corresponds to the proximal operator of $\lambda\mathcal{AS}\left(y \mid b\right)$ or $\mathbb{1}_\Theta(y)$ respectively. These were derived in closed form on page 41.

An alternative approach is to define the active share at the bucket level rather than at the security level. The idea is to group benchmark weights according to pre-defined buckets. For example, bonds can be grouped at the sector level. Given a bucket partition, the active share is defined as follows:

$$\mathcal{AS}_{\mathcal{B}}\left(w \mid b\right) = \frac{1}{2}\sum_{j=1}^{n_{\mathcal{B}}}\left|\sum_{i\in\mathcal{B}_j} w_i - \sum_{i\in\mathcal{B}_j} b_i\right| = \frac{1}{2}\sum_{j=1}^{n_{\mathcal{B}}}\left|\sum_{i=1}^{n}\zeta_{i,j}\left(w_i - b_i\right)\right|$$

where $\zeta_{i,j} = \mathbb{1}\left\{i \in \mathcal{B}_j\right\}$ and $\{\mathcal{B}_1, \ldots, \mathcal{B}_{n_{\mathrm{B}}}\}$ are the set of pre-defined buckets. The vector $z = \left(w, \tau_{(0)}, \tau'_{(0)}, \tau_{(1)}, \ldots, \tau_{(n\mathcal{R})}\right)$ is now of dimension $(n + m + n_{\mathcal{B}} + n_{\mathcal{R}}n_{\mathcal{G}}) \times 1$ rather than $(2n + m + n_{\mathcal{R}}n_{\mathcal{G}}) \times 1$. The objective function is defined by:

$$c_z = \left(-\gamma\left(\phi_0\mathcal{C} + \sum_{k=1}^{n_\mu}\phi_k\alpha_k\right), \frac{1}{2}\varphi_0\mathbf{1}_m, \frac{1}{2}\varphi'_0\mathbf{1}_{n_{\mathcal{B}}}, \frac{1}{2}\varphi_1\mathbf{1}_{n_{\mathcal{G}}}, \ldots, \frac{1}{2}\varphi_{n\mathcal{R}}\mathbf{1}_{n_{\mathcal{G}}}\right)$$

and $d_z = \gamma\left(\phi_0\mathcal{C} + \sum_{k=1}^{n_\mu}\phi_k\alpha_k\right)^\top b$. The lower bounds are $z^- = \mathbf{0}_{n+m+n_{\mathcal{B}}+n_{\mathcal{R}}n_{\mathcal{G}}}$. There are $2 \times (m + n_{\mathcal{B}} + n_{\mathcal{R}}n_{\mathcal{G}})$ inequality constraints, defined by:

$$C_z = \begin{bmatrix} -L^\top & -I_m & & & & \\ L^\top & -I_m & & & & \\ -\zeta^\top & & -I_{n_{\mathcal{B}}} & & & \\ \zeta^\top & & -I_{n_{\mathcal{B}}} & & & \\ -\left(\delta \odot M_1\right)^\top & & & -I_{n_{\mathcal{G}}} & & \\ \left(\delta \odot M_1\right)^\top & & & -I_{n_{\mathcal{G}}} & & \\ \vdots & & & & \ddots & \\ -\left(\delta \odot M_{n_{\mathcal{R}}}\right)^\top & & & & & -I_{n_{\mathcal{G}}} \\ \left(\delta \odot M_{n_{\mathcal{R}}}\right)^\top & & & & & -I_{n_{\mathcal{G}}} \end{bmatrix} \text{ and } D_z = \begin{bmatrix} -L^\top b \\ L^\top b \\ -\zeta^\top b \\ \zeta^\top b \\ -\left(\delta \odot M_1\right)^\top b \\ \left(\delta \odot M_1\right)^\top b \\ \vdots \\ -\left(\delta \odot M_{n_{\mathcal{R}}}\right)^\top b \\ \left(\delta \odot M_{n_{\mathcal{R}}}\right)^\top b \end{bmatrix}$$

Therefore, the complexity of the optimization problem is significantly reduced, becoming comparable to that of LP_1 or LP_2:

Model	Variables	Objective function	Constraints
LP_3	$2n + m + n_{\mathcal{R}}n_{\mathcal{G}}$	$2n + m + n_{\mathcal{R}}n_{\mathcal{G}}$	$(2m + 2n + 2n_{\mathcal{R}}n_{\mathcal{G}}) \times (2n + m + n_{\mathcal{R}}n_{\mathcal{G}})$
LP_4	$n + m + n_{\mathcal{B}} + n_{\mathcal{R}}n_{\mathcal{G}}$	$n + m + n_{\mathcal{B}} + n_{\mathcal{R}}n_{\mathcal{G}}$	$(2m + 2n_{\mathcal{B}} + 2n_{\mathcal{R}}n_{\mathcal{G}}) \times (n + m + n_{\mathcal{B}} + n_{\mathcal{R}}n_{\mathcal{G}})$
	$\approx n + m$	$\approx n + m$	$\approx 2mn + 2m^2$

2.4.4 Model portfolio vs. investable portfolio

Minimum trading volume and lot size Let q_i be the number of shares of asset i held in a portfolio, and p_i be its market price. The monetary value invested in asset i is $Q_i = q_i p_i$. By definition, the total portfolio value V is equal to the sum of all individual positions: $V = \sum_{i=1}^{n} Q_i = \sum_{i=1}^{n} q_i p_i$. Therefore, the portfolio weight of asset i is $w_i = \dfrac{Q_i}{V} = \dfrac{q_i p_i}{\sum_{j=1}^{n} q_j p_j}$. Thus, given a portfolio composition in terms of shares, the corresponding portfolio weights can always be calculated. In portfolio optimization, the primary decision variable is the weight w_i, not the number of shares q_i (or the monetary value Q_i). However, we can calculate these two quantities if we know the total capital V invested in the portfolio. Indeed, the monetary allocation is $Q_i = w_i V$, and the share allocation is $q_i = \dfrac{Q_i}{p_i} = \dfrac{w_i V}{p_i}$. A portfolio can then be represented equivalently by its weight allocation $(w_1, \ldots, w_n)$, its share allocation $(q_1, \ldots, q_n)$, or its monetary allocation $(Q_1, \ldots, Q_n)$. In theory, relative and nominal allocations are equivalent representations when fractional shares q_i are allowed. In practice, however, q_i and w_i belong to $\mathbb{N}$ and $\mathbb{R}^+$, respectively, which introduces rounding constraints. As a result, nominal allocations are generally not perfectly equivalent to relative allocations[36]:

$$\underbrace{\left\{ w : w_i \in \mathbb{R}^+, \sum_{i=1}^{n} w_i = 1 \right\}}_{\text{Relative allocation (weights)}} \quad \text{versus} \quad \underbrace{\left\{ q : q_i \in \mathbb{N}, \sum_{i=1}^{n} q_i p_i + \mathcal{C}_{ash} = V \right\}}_{\text{Nominal allocation (shares)}}$$

We introduce the cash amount $\mathcal{C}_{ash}$, which is the residual monetary value not invested in the assets. $\mathcal{C}_{ash}$ can be positive or negative. In this last case, this means that we borrow cash.

Consider an equity portfolio designed to replicate a benchmark with weights b. Assuming that fractional shares are not permitted and adopting a floor rounding approach, the number of shares invested in stock i is $q_i = \left\lfloor \dfrac{b_i V}{p_i} \right\rfloor$. The corresponding weight of stock i in the investable portfolio is then equal to $\tilde{w}_i = \dfrac{q_i p_i}{V}$. To quantify the deviation between the benchmark weights b and the investable portfolio weights $\tilde{w}$, we compute four different statistics:

1. Residual weight: $\tilde{w}_{\text{residual}} = 1 - \sum_{i=1}^{n} \tilde{w}_i$
2. Cash proportion: $\tilde{w}_{\text{cash}} = \mathcal{C}_{ash}/V$
3. Active share: $\mathcal{AS}\left(\tilde{w} \mid b\right) = \dfrac{1}{2} \sum_{i=1}^{n} |\tilde{w}_i - b_i|$
4. Tracking error volatility: $\sigma\left(\tilde{w} \mid b\right) = \sqrt{(\tilde{w} - b)^\top \Sigma (\tilde{w} - b)}$

Because of the floor rounding approach, one can show that $\tilde{w}_{\text{residual}} = \tilde{w}_{\text{cash}} = 2\mathcal{AS}\left(\tilde{w} \mid b\right)$. Figure 9 shows the distribution of constituent stock prices p_i in the MSCI World Index at the end of May 2026. The prices range from \$ 0.85 to \$ 122 200. However, 61.5% and 97.5% of stocks have prices below \$ 100 and \$ 1 000, respectively Moreover, only four stocks have

[36] We introduce the cash position $\mathcal{C}_{ash}$, which is defined as the residual amount of capital that is not invested in the assets. The cash position may be either positive or negative. A negative cash position indicates that cash has been borrowed to finance some positions ($\sum_{i=1}^{n} q_i p_i > V$).

Figure 9: Distribution of constituent stock prices p_i in the MSCI World Index (end of May 2026)

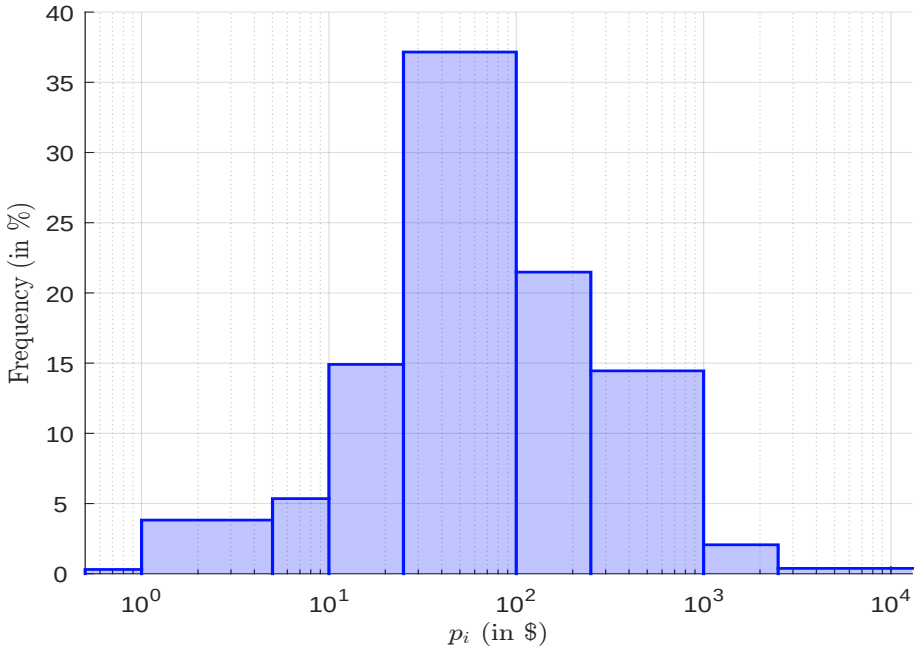

Figure 10: Active share $\mathcal{AS}\left(\tilde{w} \mid b\right)$ and tracking error volatility $\sigma\left(\tilde{w} \mid b\right)$ of investable portfolios (MSCI World Index, end of May 2026)

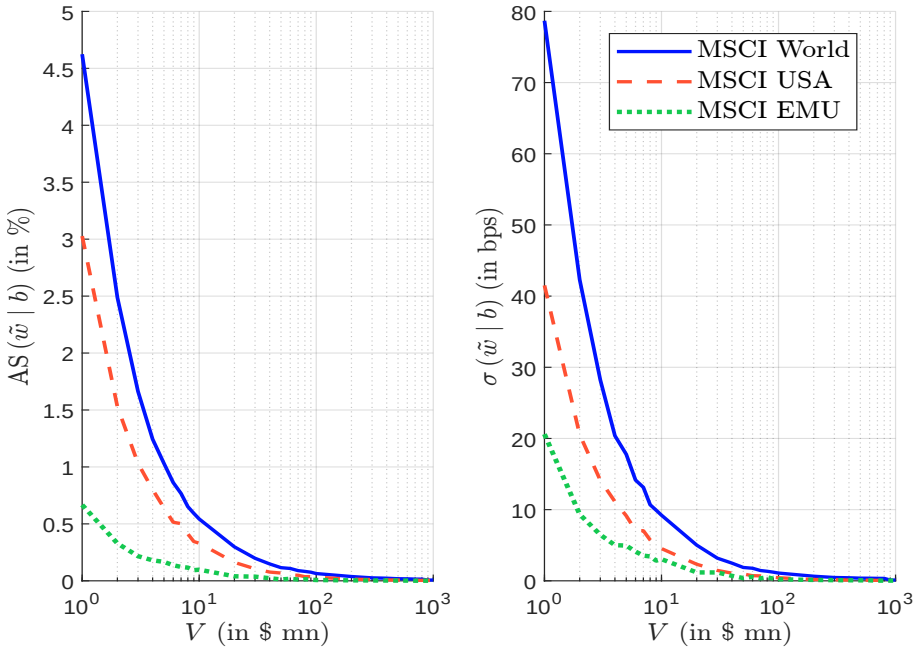

prices above \$ 5 000, representing 5 bps of the MSCI World Index allocation. In Figure 10, we report the active share and the tracking error volatility of investable portfolios with respect to the portfolio value V. Despite the integer-share constraint, the benchmark can be replicated with a high degree of accuracy. With \$ 10 million, the resulting active share is only 0.54%, while the tracking error volatility is approximately 9 bps. Increasing the portfolio value to \$ 100 million reduces the tracking error volatility to one basis point.

In the case of bonds, each security is associated with a minimum tradable amount (MT) and a lot size (LS). For example, a EUR investment-grade corporate bond is often traded with a minimum tradable amount of €100 000 and a lot size of €1 000. This means that this corporate bond can only be traded in amounts of €100 000, €101 000, €102 000, etc. Therefore, it cannot be traded in arbitrary amounts such as €50 000 or €102 500. Mathematically, we have:

$$q_i = x_i \operatorname{MT}_i + x_i y_i \operatorname{LS}_i$$

where MT_i and LS_i are the minimum tradable amount and lot size of bond i, $x_i \in \{0, 1\}$ and $y_i \in \mathbb{N}$ is the number of tradable lots. Let p_i be the notional price expressed as a percentage of the par value of the bond. We have:

$$Q_i = q_i p_i$$

For instance, if the par price is €100 and the current price is €95, then $p_i = 95\%$.

Figure 11: Distribution of minimum tradable amounts (G0BC Index, end of May 2026)

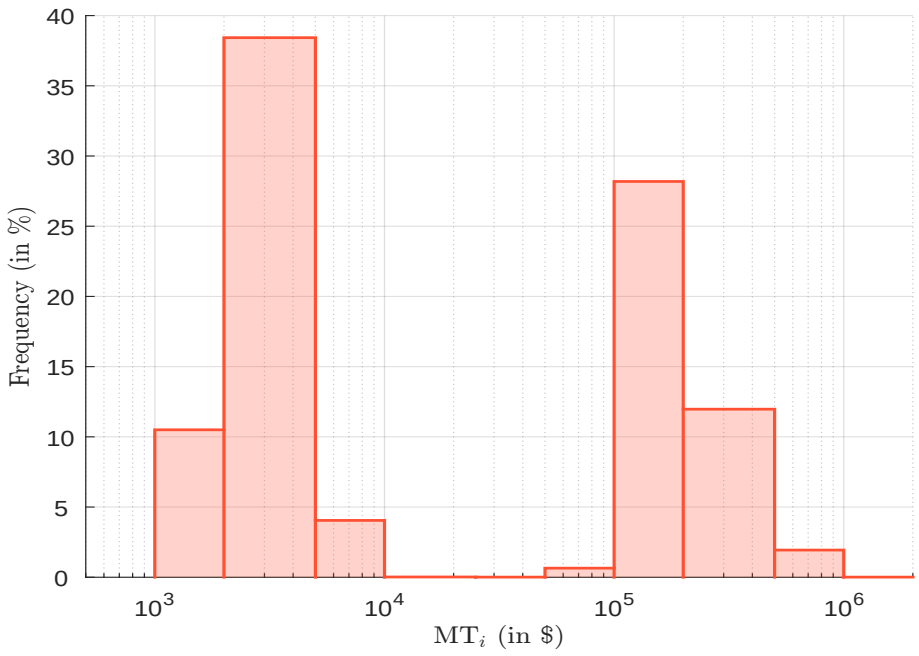

Source: ICE BofA & Authors' calculations.

Figure 11 shows the distribution of minimum tradable amounts for the ICE BofA Global Corporate Index (G0BC). As of the end of May 2026, the index contained 20 350 bonds. Four values of MT_i dominate the sample: 1 000, 2 000, 100 000, and 200 000 (see Table 21 on page 111). Regarding the lot size, it is generally a fraction of the minimum tradable amount. Table 5 reports the distribution of the ratio $\dfrac{\operatorname{LS}_i}{\operatorname{MT}_i}$. About 38% of bonds have a lot

size equal to half the minimum tradable amount, while about 31% have a ratio of one. In the remaining cases, the ratio is below 50%. In particular, the ratio is equal to 1% and 0.5% for 16.4% and 10.1% of bonds, respectively.

Table 5: Distribution of the lot size ratio $\frac{\text{LS}_i}{\text{MT}_i}$ (G0BC Index, end of May 2026)

$\frac{\text{LS}_i}{\text{MT}_i}$	$]0, 0.005[$	$\frac{1}{200}$	$]0.005, 0.01[$	$\frac{1}{100}$	$]0.01, 0.5[$	$\frac{1}{2}$	$]0.5, 1.0[$	1
Count	262	2 059	339	3 334	361	7 771	0	6 224
Frequency	1.29%	10.1%	1.67%	16.4%	1.77%	38.2%	0.00%	30.6%

Source: ICE BofA & Authors' calculations.

Let V be the total portfolio value and b the benchmark weights. The floor rounding approach applied to bonds is then defined by the following two equations. First, x_i indicates whether bond i can be included in the portfolio at its minimum tradable amount:

$$x_i = \min\left(\left\lfloor \frac{b_i V}{\text{MT}_i\, p_i} \right\rfloor, 1\right)$$

Second, the number of additional lots y_i that can be purchased on top of the minimum tradable amount is given by:

$$y_i = \left\lfloor \frac{(b_i V - x_i\, \text{MT}_i\, p_i)\, x_i}{\text{LS}_i\, p_i} \right\rfloor$$

The factor x_i in the numerator ensures that $y_i = 0$ when the bond is excluded from the investable portfolio ($x_i = 0$). Since the resulting tradable quantity of bond i is $q_i = x_i\, \text{MT}_i + x_i y_i\, \text{LS}_i$, the weight of bond i in the investable portfolio is equal to $\tilde{w}_i = \frac{q_i p_i}{V}$.

Figure shows the active share of the investable portfolio using the floor rounding approach. We note that the active share is much higher than in the equity case. For instance, the active share is equal to 46.84% when V is \$10 mn, whereas it was only 0.54% for the MSCI World. Using alternative methods[37] (nearest or threshold rounding) yields better results, but the order of magnitude remains comparable. For example, the required portfolio value to bring the active share below 10% is \$2.9 billion under floor rounding, \$1.45 billion under nearest rounding, and \$390 billion under threshold rounding.

Mixed integer programming We recall that the generic optimization problem is:

$$\begin{aligned} w^\star &= \arg\min \frac{1}{2}\mathcal{R}\left(w \mid b\right) - \gamma\mu\left(w \mid b\right) \\ &\text{s.t.} \quad \begin{cases} w \in \Omega \\ w_i \in [0,1] \end{cases} \end{aligned}$$

[37] The nearest rounding approach is a variant of the floor rounding approach in which the floor operator is replaced by the round operator. In the threshold rounding approach, the first step becomes $x_i = \mathbb{1}\{b_i V \leq \theta^\star\, \text{MT}_i\, p_i\}$, where the optimal parameter $\theta^\star$ is calibrated as follows: $\theta^\star = \arg\min \theta$ s.t. $\mathcal{C}_{ash} \geq 0$ and $\theta \in (0, 1]$.

Figure 12: Active share $\mathcal{AS}\left(\tilde{w} \mid b\right)$ of investable portfolios (G0BC Index, end of May 2026)

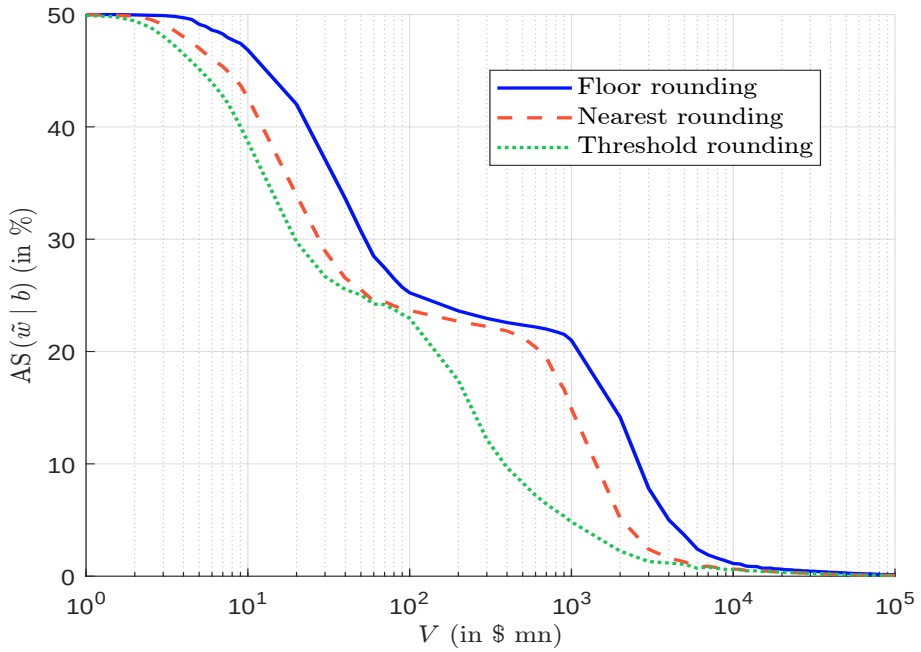

Source: ICE BofA & Authors' calculations.

In the case of investable portfolios, the optimization problem becomes:

$$\begin{aligned} \{x^\star, y^\star\} &= \arg\min \frac{1}{2}\mathcal{R}\left(\tilde{w} \mid b\right) - \gamma\mu\left(\tilde{w} \mid b\right) \\ &\text{s.t.} \begin{cases} q_i = x_i \,\mathrm{MT}_i + x_i y_i \,\mathrm{LS}_i \\ \tilde{w}_i = \dfrac{q_i p_i}{V} \\ x_i \in \{0,1\} \\ y_i \in \mathbb{N} \end{cases} \end{aligned} \tag{29}$$

This reformulation has an important consequence. The solution in w is replaced by the solution in (x, y), and the two problems behave differently with respect to scale. The first problem is invariant with respect to the total portfolio value, while the second is not:

$$V_1 \neq V_2 \Rightarrow \begin{cases} w^\star\left(V_1\right) = w^\star\left(V_2\right) \\ \left(x^\star\left(V_1\right), y^\star\left(V_1\right)\right) \neq \left(x^\star\left(V_2\right), y^\star\left(V_2\right)\right) \end{cases}$$

Problem (29) can be solved using specific algorithms dedicated to mixed integer linear (MILP) or quadratic (MIQP) programming. The MILP takes the generic form:

$$\begin{aligned} z^\star &= \arg\min c_z^\top z + d_z \\ &\text{s.t.} \begin{cases} C_z z \leq D_z \\ z_i \in \mathbb{Z} \text{ for some components } i \end{cases} \end{aligned}$$

while the objective function becomes $\frac{1}{2} z^\top Q_z z - z^\top R_z$ in the MIQP case.

Mixed-integer optimization has been the subject of extensive research over the past decades (Nemhauser and Wolsey, 1988; Conforti *et al.*, 2014). However, MILP and MIQP

are NP-hard optimization problems. Their computational complexity grows exponentially with problem size, making the exact solution of large instances challenging (Vielma, 2015; Bengio *et al.*, 2021). Modern exact solvers therefore combine several algorithmic techniques, including branch-and-bound (Land and Doig, 1960), cutting planes (Gomory, 1958), and branch-and-cut (Padberg and Rinaldi, 1991). These advances have increased the size of practical problems that can be solved, resulting in highly efficient commercial and open-source solvers such as CPLEX, FICO Xpress, Gurobi, Mosek and SCIP. The case of MIQP is generally more difficult than MILP because of the presence of quadratic terms in the objective function and convexity issues (Belotti *et al.*, 2013; Del Pia *et al.*, 2017). In the context of bond portfolio optimization, MILP have been used to problems such as small-scale portfolio construction, ETF creation and redemption baskets, and bond index sampling (Ben Slimane and Menchaoui, 2023; Alreshidi, 2019).

Remark 9. *Although exact methods remain the standard when optimality guarantees are required, they can be too computationally expensive for large-scale portfolio construction problems involving thousands of securities, numerous practical constraints, or non-convex/non-smooth features. For this reason, some practitioners and researchers have investigated meta-heuristic approaches, such as genetic algorithms (Ben Slimane, 2021). These methods sacrifice global optimality guarantees for reduced computational effort (Goldberg, 1989). Moreover, they often produce high-quality solutions for investable bond portfolio problems. Recently, quantum optimization has emerged as a promising alternative framework, although it is still at an early experimental stage. In the future, quantum methods may be competitive for certain classes of large combinatorial portfolio optimization problems (Abbas et al., 2024).*

3 Applications

This section presents several applications of bond portfolio optimization using the investment universes of three ICE BofA indices: the ICE BofA EUR Corporate Bond Index (ER00), the ICE BofA USD Corporate Bond Index (C0A0), and the ICE BofA Global Corporate Bond Index (G0BC). The examples compare tracking error volatility measured under the $\boldsymbol{\ell}_1$ and $\boldsymbol{\ell}_2$ norms, apply the BARRA factor model, demonstrate constrained optimization incorporating sector views, and highlight the role of bucketing and clustering techniques in portfolio construction.

3.1 ℓ_1- versus ℓ_2-norm risk measures

Our first application highlights the differences between portfolio optimization based on the $\boldsymbol{\ell}_1$ and $\boldsymbol{\ell}_2$ risk measures. Using a two-factor risk model, we seek to enhance the yield of the ICE BofA EUR Corporate Bond Index (ER00) subject to constraints on duration, duration times spread, issuer concentration, and active share. To this end, we first calibrate the covariance matrix Σ and then specify the optimization problem. We conclude by comparing the efficient frontiers obtained from the $\boldsymbol{\ell}_1$- and $\boldsymbol{\ell}_2$-norm optimization problems.

3.1.1 Two-factor risk model

Tracking error volatility We consider the two-factor risk model presented in Appendix B.2 on page 90. However, we now assume that the interest rate and credit spreads are correlated. The covariance matrix becomes:

$$\begin{aligned}\Sigma_{i,j} &= \mathrm{MD}_i\,\mathrm{MD}_j\,\sigma_r^2 + \mathrm{MD}_i\,\mathrm{MD}_j\,s_i\,(t)\,s_j\,(t)\,\rho_{s,i,j}\sigma_{s,i}\sigma_{s,j} + \\ &\quad \mathrm{MD}_i\,\mathrm{MD}_j\,s_j\,(t)\,\rho_{r,s,j}\sigma_r\sigma_{s,j} + \mathrm{MD}_j\,\mathrm{MD}_i\,s_i\,(t)\,\rho_{r,s,i}\sigma_r\sigma_{s,i}\end{aligned}$$

where $\rho_{r,s,i}$ is the correlation between $r(t)$ and $s_i(t)$. It follows that:

$$\begin{aligned}\Sigma_{i,j} &= \mathrm{MD}_i \,\mathrm{MD}_j\, \sigma_r^2 + \mathrm{DTS}_i(t)\,\mathrm{DTS}_j(t)\,\rho_{s,i,j}\sigma_{s,i}\sigma_{s,j} + \\ &\quad \mathrm{MD}_i\,\mathrm{DTS}_j(t)\,\rho_{r,s,j}\sigma_r\sigma_{s,j} + \mathrm{MD}_j\,\mathrm{DTS}_i(t)\,\rho_{r,s,i}\sigma_r\sigma_{s,i}\end{aligned}$$

where $\mathrm{DTS}_i(t) = \mathrm{MD}_i\, s_i(t)$. In matrix form, the covariance matrix can be written as follows:

$$\Sigma = \sigma_r^2\,\mathrm{MD}\,\mathrm{MD}^\top + \upsilon_s \odot \rho_s \odot \upsilon_s^\top + \sigma_r\left(\mathrm{MD}\left(\rho_{r,s}\odot\upsilon_s\right)^\top + \left(\rho_{r,s}\odot\upsilon_s\right)\mathrm{MD}^\top\right) \tag{30}$$

where ρ_s is the $n\times n$ correlation matrix between credit spreads and $\rho_{r,s}$ is the $n\times 1$ vector of correlations between the interest rate and credit spreads. Assuming that $\rho_{s,i,j}=\rho$ for all $i\neq j$ and $\rho_{r,s,i}=\eta$, we obtain:

$$\begin{aligned}\Sigma &= \sigma_r^2\,\mathrm{MD}\,\mathrm{MD}^\top + \rho\upsilon_s\upsilon_s^\top + \eta\sigma_r\left(\mathrm{MD}\,\upsilon_s^\top + \upsilon_s\,\mathrm{MD}^\top\right) + (1-\rho)\,\mathrm{diag}\left(\upsilon_s\odot\upsilon_s^\top\right) \\ &= B\Omega B^\top + D\end{aligned} \tag{31}$$

where:

$$\begin{cases} B = \begin{pmatrix} \mathrm{MD} & \upsilon_s \end{pmatrix} \\ \Omega = \begin{pmatrix} \sigma_r^2 & \eta\sigma_r \\ \eta\sigma_r & \rho \end{pmatrix} \\ D = (1-\rho)\,\mathrm{diag}\left(\upsilon_s\odot\upsilon_s^\top\right) \end{cases}$$

If $\rho\geq\eta^2$, the matrix Ω admits a Cholesky factorization $\Omega = LL^\top$ with:

$$L = \begin{pmatrix} \sigma_r & 0 \\ \eta & \sqrt{\rho-\eta^2} \end{pmatrix}$$

The expression of the tracking error variance is then equal to:

$$\begin{aligned}\sigma^2\left(w\mid b\right) &= (w-b)^\top\left(B\Omega B^\top + D\right)(w-b) \\ &= (w-b)^\top\left(BLL^\top B^\top + D\right)(w-b) \\ &= \left\|L^\top B^\top(w-b)\right\|_2^2 + (1-\rho)\left\|\upsilon_s\odot(w-b)\right\|_2^2\end{aligned}$$

Since we have:

$$\begin{aligned}L^\top B^\top(w-b) &= \begin{pmatrix} \sigma_r & \eta \\ 0 & \sqrt{\rho-\eta^2} \end{pmatrix}\begin{pmatrix} \mathrm{MD}^\top \\ \upsilon_s^\top \end{pmatrix}(w-b) \\ &= \begin{pmatrix} \sigma_r\,\mathrm{MD}^\top(w-b) + \eta\upsilon_s^\top(w-b) \\ \sqrt{\rho-\eta^2}\upsilon_s^\top(w-b) \end{pmatrix} \\ &= \begin{pmatrix} \sigma_r C_r + \eta C_s \\ \sqrt{\rho-\eta^2}C_s \end{pmatrix}\end{aligned}$$

where $C_r = \mathrm{MD}^\top(w-b)$ and $C_s = \upsilon_s^\top(w-b)$, the final expression of the quadratic $\boldsymbol{\ell}_2$-norm tracking error volatility is:

$$\sigma_{\boldsymbol{\ell}_2}\left(w\mid b\right) = \sqrt{\left(\sigma_r C_r + \eta C_s\right)^2 + \left(\rho-\eta^2\right)C_s^2 + (1-\rho)\left\|\upsilon_s\odot(w-b)\right\|_2^2} \tag{32}$$

while the linear $\boldsymbol{\ell}_1$-norm tracking error volatility is calculated with the upper bound:

$$\sigma_{\boldsymbol{\ell}_1}\left(w\mid b\right) = \left|\sigma_r C_r + \eta C_s\right| + \sqrt{\rho-\eta^2}\left|C_s\right| + \sqrt{1-\rho}\left\|\upsilon_s\odot(w-b)\right\|_1 \tag{33}$$

Calibration of the model We estimate the parameters using daily data from 3 January 2020 to 29 May 2026. For the interest rate factor, we use the German bond yield curve across seven tenors: 2Y, 5Y, 7Y, 10Y, 15Y, 20Y, and 30Y. The estimated annualized volatilities[38] of the yield variation are reported in the second column in Table 6. We note that the volatilities are very close across all tenors, yielding an average volatility of 78.91 bps. For the credit risk factor, we calculate the weighted average option-adjusted spread (OAS) for each sector within the ICE BofA EUR Corporate Bond Index (ER00). Table 7 shows the annualized volatility of the change in the logarithm of the OAS spread by sector. The real estate sector exhibits the lowest annualized volatility (21.02%), whereas the leisure sector has the highest volatility (45.63%). The average volatility of the credit spread across all sectors is 30.06%. We have also calculated the correlation between interest rates and credit spreads in Table 6. On average, the empirical correlation is −26.16%. Based on these estimates, we use the following baseline parameters: $\sigma_r = 80$ bps, $\sigma_s = 30\%$, $\rho = 80\%$, and $\eta = -25\%$.

Table 6: Yield volatility and correlation with credit spreads (Jan. 2020–May 2026)

Tenor	Volatility (in bps)	Correlation (in %)
2Y	79.51	−28.54
5Y	83.67	−26.63
7Y	81.15	−26.39
10Y	79.26	−24.89
15Y	76.83	−25.92
20Y	76.21	−25.64
30Y	75.73	−25.10
Average	78.91	−26.16

Table 7: Volatility of credit spreads by sector (Jan. 2020–May 2026)

Sector	Volatility (in %)	Sector	Volatility (in %)
Automotive	32.59	Leisure	45.63
Banking	34.40	Media	27.77
Basic Industry	27.12	Real Estate	21.02
Capital Goods	28.84	Retail	30.30
ConsumerGoods	29.50	Services	26.94
Energy	35.45	Technology & Electronics	31.56
Financial Services	32.33	Telecommunications	28.16
Healthcare	29.84	Transportation	26.36
Insurance	29.97	Utility	23.23
Average = 30.06			

3.1.2 Optimized portfolio and efficient frontier

We would like to replicate the ICE BofA EUR Corporate Bond Index as of the end of May 2026, subject to the following constraints:

- Increase duration by 0.20 to 0.50 year relative to the index;
- Limit concentration risk by capping the weight of issuers at 1%;

[38] All computations assume 252 business days per year to annualize the volatility.

- Impose a maximum active share of $\mathcal{AS}^+$;
- Impose the following constraints on duration times spread contributions:
  - Overweight the DTS of bonds in the 5Y bucket by at least 100 bps;
  - Overweight the DTS of bonds in the 7Y bucket by 25 to 100 bps;
  - Underweight the DTS of bonds in the 10Y+ bucket by −100 to −25 bps
  - Overweight the DTS of bonds in the financials sector by at least 100 bps;
  - Underweight the DTS of bonds rated A by −100 to −25 bps;
  - Overweight the DTS of bonds rated BBB by 25 to 100 bps;

The corresponding optimization problem is:

$$w^\star = \arg\min \frac{1}{2}\sigma^2\left(w \mid b\right) \tag{34}$$
$$\text{s.t.} \begin{cases} \mathbf{1}_n^\top w = 1 \\ w \geq \mathbf{0}_n \\ 0.20 \text{ yr} \leq \text{MD}\left(w\right) - \text{MD}\left(b\right) \leq 0.50 \text{ yr} \\ \sum_{i \in \mathcal{I}ssuer_j} w_i \leq 1\% \qquad \forall j = 1, \ldots, n_{\mathcal{I}ssuer} \\ \dfrac{1}{2}\displaystyle\sum_{i=1}^{n} \left|w_i - b_i\right| \leq \mathcal{AS}^+ \\ LB_k \leq \text{DTS}_{\mathfrak{B}_k}\left(w\right) - \text{DTS}_{\mathfrak{B}_k}\left(b\right) \leq UB_k \qquad \forall k = 1, \ldots, 6 \end{cases}$$

where $\text{DTS}_{\mathfrak{B}_k}\left(w\right) = \sum_{i \in \mathfrak{B}_k} w_i \,\text{DTS}_i$, $\mathfrak{B}_k$ is the k^{th} bucket (5Y, 7Y, 10Y+, Financials, A, and BBB), LB_k and UB_k are the lower and upper bound of DTS constraints. For instance, the sixth DTS constraint can be formulated as 25 bps $\leq \sum_{\mathfrak{R}_i \in \text{BBB}} \left(w_i - b_i\right) \text{DTS}_i \leq 100$ bps where $\mathfrak{R}_i$ is the credit rating of bond i. The optimization is implemented using linear programming for the $\boldsymbol{\ell}_1$ problem and quadratic programming with augmented variables for the $\boldsymbol{\ell}_2$ problems.

Table 8: $\boldsymbol{\ell}_1$-optimized bond portfolios (ER00 Index, end of May 2026)

Statistic	Benchmark	Active share limit $\mathcal{AS}^+$			
		25%	30%	40%	100%
Holdings	4 663	3 466	3 220	2 847	2 847
Active share (in %)		25.00	30.00	38.17	38.17
ENB (w)	3 940	425	372	284	284
Top 100 weight (in %)	5.36	29.22	33.97	41.89	41.89
$\sigma_{\boldsymbol{\ell}_1}\left(w \mid b\right)$ (in bps)		49.54	48.73	48.24	48.24
$\sigma_{\boldsymbol{\ell}_2}\left(w \mid b\right)$ (in bps)		16.06	15.61	16.11	16.11
Yield (in %)	3.47	3.53	3.47	3.45	3.45
$\beta_{\text{DTS}}\left(w \mid b\right)$	1.00	1.08	1.04	1.00	1.00
MD (in year)	4.48	4.68	4.68	4.68	4.68
5Y DTS (in bps)	92	192	192	192	192
7Y DTS (in bps)	101	126	126	126	126
10Y+ DTS (in bps)	48	4	0	0	0
Financials DTS (in bps)	128	228	228	228	228
A-rated DTS (in bps)	159	134	134	133	133
BBB-rated DTS (in bps)	193	249	218	218	218

Table 9: $\boldsymbol{\ell}_2$-optimized bond portfolios (ER00 Index, end of May 2026)

Statistic	Benchmark	Active share limit $\mathcal{AS}^+$			
		25%	30%	40%	100%
Holdings	4 663	3 506	3 966	4 469	4 609
Active share (in %)		25.00	29.94	39.40	49.36
ENB (w)	3 940	783	1 496	1 576	1 222
Top 100 weight (in %)	5.36	27.56	18.28	13.40	15.02
$\sigma_{\boldsymbol{\ell}_1}\left(w \mid b\right)$ (in bps)		51.48	51.45	56.30	60.90
$\sigma_{\boldsymbol{\ell}_2}\left(w \mid b\right)$ (in bps)		15.74	15.38	15.35	15.35
Yield (in %)	3.47	3.53	3.51	3.51	3.51
$\beta_{\text{DTS}}\left(w \mid b\right)$	1.00	1.07	1.05	1.04	1.04
MD (in year)	4.48	4.68	4.68	4.68	4.68
5Y DTS (in bps)	92	192	192	192	192
7Y DTS (in bps)	101	126	126	126	126
10Y+ DTS (in bps)	48	10	7	10	11
Financials DTS (in bps)	128	228	228	228	228
A-rated DTS (in bps)	159	134	134	134	134
BBB-rated DTS (in bps)	193	245	223	225	226

Table 8 and 9 report the results for different active share targets: 25%, 30%, 40% and 100% (no active share constraint). For each optimized portfolio, we evaluate the number of holdings, the active share, the effective number of bets[39], the top 100 concentration weight, the $\boldsymbol{\ell}_1$ and $\boldsymbol{\ell}_2$ tracking error volatilities, the portfolio yield, and the DTS beta[40]. The bottom panel outlines the specific portfolio constraints imposed on the modified duration and DTS contributions. The figures shows that the optimized portfolios are significantly more concentrated than the benchmark. While the 100 largest exposures account for only 5.36% of the benchmark, they represent 30–42% of the $\boldsymbol{\ell}_1$-optimized portfolios and 13–27% of the $\boldsymbol{\ell}_2$-optimized portfolios. This higher concentration is also reflected in the effective number of bets, which decreases from 3 940 in the benchmark to 280–430 for $\boldsymbol{\ell}_1$ and 780–1 580 for $\boldsymbol{\ell}_2$. Comparing the two optimization methods highlights a clear trade-off between sparsity and diversification:

- Constraint behavior
  Both methods exhibit similar behavior with respect to the portfolio constraints. Each method reaches the lower bound of the target duration (+0.20 years) and maximizes the allowable range of DTS positioning. This indicates that both optimizers fully exploit the constraint boundaries to minimize tracking error.

- Portfolio structure
  The main difference between the two methods lies in portfolio construction. The $\boldsymbol{\ell}_1$ solutions are considerably sparse and more concentrated, while the $\boldsymbol{\ell}_2$ solutions remain more diversified. This is evident from the top 100 weight concentration (35.5% for $\boldsymbol{\ell}_1$ versus 12.3% for $\boldsymbol{\ell}_2$ in the unconstrained active share case) and the effective number of bets (280–430 versus 780–1 580, respectively).

[39]The effective number of bets is the inverse of the Herfindahl index:

$$\text{ENB}\,(w) = \frac{1}{\sum_{i=1}^{n} w_i^2}$$

[40]The DTS beta is defined as follows:

$$\beta_{\text{DTS}}\left(w \mid b\right) = \frac{\sum_{i=1}^{n} w_i\,\text{DTS}_i}{\sum_{i=1}^{n} b_i\,\text{DTS}_i}$$

- Active share
  The active-share constraint affects the two approaches differently. The $\boldsymbol{\ell}_1$ portfolios cap out at 38.17% active share, even without an active share limit. By contrast, the $\boldsymbol{\ell}_2$ portfolios continue to increase active share as the constraint is relaxed, ultimately reaching 49.36%.

- Tracking error
  As expected, each method performs best according to its own objective function. The $\boldsymbol{\ell}_1$ portfolios achieve a lower $\boldsymbol{\ell}_1$ tracking error volatility (48–50 bps vs. 51–61 bps for the $\boldsymbol{\ell}_2$ portfolios). Conversely, $\boldsymbol{\ell}_2$ portfolios achieve a lower $\boldsymbol{\ell}_2$ tracking error volatility (15.3–15.8 bps vs. 15.6–16.1 bps for the $\boldsymbol{\ell}_1$ portfolios).

Nevertheless, these discrepancies in tracking error are relatively marginal. Overall, both optimization approaches produce portfolios with similar risk and return characteristics. Portfolio yields remain close to 3.5%, and DTS betas range from 1.04 to 1.08 across all solutions. Therefore, the primary distinction between $\boldsymbol{\ell}_1$- and $\boldsymbol{\ell}_2$-norm minimization lies in portfolio composition. $\boldsymbol{\ell}_1$ favors sparse and concentrated portfolios, while $\boldsymbol{\ell}_2$ promotes greater diversification, with only limited differences in risk and return characteristics.

Let us now draw the efficient frontier. The optimization problem becomes:

$$\begin{aligned} w^\star(\gamma) &= \arg\min \frac{1}{2}\sigma^2\left(w \mid b\right) - \gamma\mu\left(w \mid b\right) \\ &\text{s.t.} \quad w \in \Omega \end{aligned} \tag{35}$$

where Ω is the set of constraints defined in Equation (34), $\mu\left(w \mid b\right) = \sum_{i=1}^{n}\left(w_i - b_i\right)y_i$ is the excess yield of portfolio w with respect to the benchmark b, and y_i is the yield of bond i. The efficient frontiers are reported in Figures (23) and (24) on page 123. At first glance, the two frontiers appear quite different, but this comparison is misleading. Indeed, the values of $\sigma_{\boldsymbol{\ell}_1}\left(w \mid b\right)$ and $\sigma_{\boldsymbol{\ell}_2}\left(w \mid b\right)$ are not directly comparable since we have $\sigma_{\boldsymbol{\ell}_1}\left(w \mid b\right) \gg \sigma_{\boldsymbol{\ell}_2}\left(w \mid b\right)$. This is because the $\boldsymbol{\ell}_1$ tracking error volatility provides an upper-bound approximation of the $\boldsymbol{\ell}_2$ tracking error volatility. On average, we observe a scaling factor $\varphi \approx 3.2$ between the two norms. To provide a meaningful comparison, Figure 13 shows the two efficient frontiers by considering the scaled $\boldsymbol{\ell}_1$ tracking error volatility:

$$\tilde{\sigma}_{\boldsymbol{\ell}_1}\left(w \mid b\right) = \frac{1}{\varphi}\sigma_{\boldsymbol{\ell}_1}\left(w \mid b\right)$$

Once adjusted, the frontiers are remarkably close, with similar starting and ending points. The main distinction lies in their curvature, with the $\boldsymbol{\ell}_2$ solutions exhibiting a more pronounced convexity.

3.2 Barra multi-factor risk model

We use now a multi-factor risk model:

$$R(t) = \alpha + B\mathcal{F}(t) + \varepsilon(t)$$

where $R(t) = \left(R_1(t), \ldots, R_n(t)\right)$ is the vector of bond returns, $\mathcal{F}(t) = \left(\mathcal{F}_1(t), \ldots, \mathcal{F}_m(t)\right)$ is the vector of risk factors, and $\varepsilon(t) = \left(\varepsilon_1(t), \ldots, \varepsilon_n(t)\right)$ is the vector of idiosyncratic risks. The loading matrix B collects all the sensitivities: $B = \left(\beta_{i,j}\right)$ where $i \in \{1, \ldots, n\}$ and $j \in \{1, \ldots, m\}$. We assume that $\mathbb{E}\left[\mathcal{F}(t)\right] = \psi$, $\operatorname{cov}\left(\mathcal{F}(t)\right) = \Omega$, $\mathbb{E}\left[\varepsilon(t)\right] = \mathbf{0}_n$, $\operatorname{cov}\left(\varepsilon(t)\right) = D$ and $\mathcal{F}(t) \perp \varepsilon(t)$. Then, the covariance matrix of bond returns is:

$$\Sigma = B\Omega B^\top + D \tag{36}$$

Figure 13: Comparison of ℓ_1- and ℓ_2-norm efficient frontiers (ER00 Index, end of May 2026)

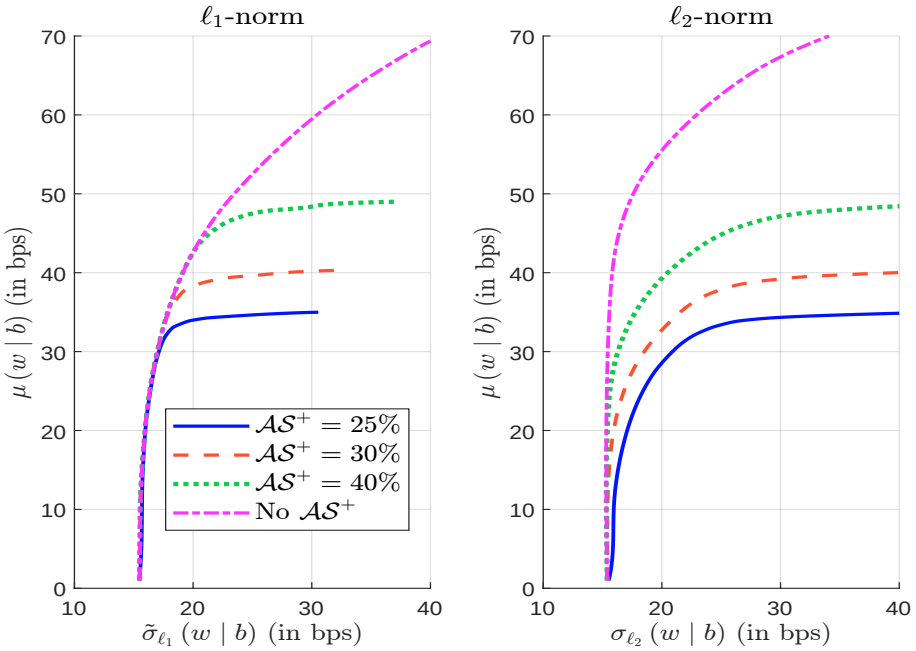

This specification corresponds to the Barra risk model (Barra, 2007). For fixed-income portfolios, the Barra model incorporates two main categories of common risk factors:

- Interest rate risk factors: shift, twist and butterfly (3 principal components), or maturity-based (1M, 3M, 6M, 1Y, 2Y, 5Y, 7Y, 10Y, 15Y, 20Y, 25Y, 30Y, 50Y).
- Credit spread risk factors: including both general market spread factors and sector-specific factors such as Energy (ENGY), Financials (FIN), Industrials (IND), and Utilities (UTL).

These risk factors are defined separately for each country or region. Consequently, the number of factors varies substantially across markets, reflecting differences in market depth and maturity. Here is the number of factors considered per area: AU(4), CA (5), CH (3), EM_CORP (12), EM_SOV (5), EUR_EMU_GOV (14), EUR_IMPVOL (1), EUR_SWAP (9), EU (39), GB (19), HK (1), JP (3), NO (3), NZ (2), SE (3), SG (1), and US (34). Therefore, the Barra model is much richer than the two-factor risk model that was studied in the previous section.

3.2.1 Comparison with the two-factor risk model

To illustrate the difference, we consider the same optimization problem as defined on page 52 (Equation 34), but use the Barra multi-factor risk model instead of our two-factor risk model. Results are given in Table 10. The impact of the DTS and the MD constraints remains the same. Indeed, all bounds except those of BBB-rated DTS are saturated in the same direction: MD +0.20 year, 5Y DTS +100 bps, 7Y DTS +25 bps, 10Y+ DTS −25 bps, Financials DTS +100 bps, and A-rated DTS −25 bps. In terms of financial performance, the portfolio yield $y(w)$ and the DTS beta $\beta_{\text{DTS}}(w \mid b)$ are higher, while the tracking error volatility $\sigma(w \mid b)$ is lower. However, the main difference concerns the portfolio structure. The active share reaches 87% with the Barra model, whereas it reached only 50% with the

Table 10: Tracking error minimization with specific risk (Barra model, ER00 Index, end of May 2026)

Statistic	Benchmark	Active share limit $\mathcal{AS}^+$			
		25%	30%	40%	100%
Holdings	4 663	3 463	3 244	2 786	643
Active share (in %)		25.00	30.00	40.00	87.39
ENB (w)	3 940	530	475	379	214
Top 100 weight (in %)	5.36	28.70	33.12	40.70	58.38
$\sigma\left(w \mid b\right)$ (in bps)		13.64	11.48	9.38	7.46
$\sigma_{\mathcal{F}}\left(w \mid b\right)$ (in bps)		11.50	9.13	6.70	4.23
$\sigma_{\epsilon}\left(w \mid b\right)$ (in bps)		2.14	2.35	2.67	3.23
Yield (in %)	3.47	3.63	3.63	3.63	3.66
$\beta_{\text{DTS}}\left(w \mid b\right)$	1.00	1.20	1.20	1.19	1.18
MD (in year)	4.48	4.68	4.68	4.68	4.68
5Y DTS (in bps)	92	192	192	192	192
7Y DTS (in bps)	101	126	126	126	126
10Y+ DTS (in bps)	48	23	23	23	23
Financials DTS (in bps)	128	228	228	228	228
A-rated DTS (in bps)	159	134	134	134	134
BBB-rated DTS (in bps)	193	289	286	277	267

$\boldsymbol{\ell}_2$-norm model. Moreover, the effective number of bets decreases with $\mathcal{AS}^+$ here, whereas it increased previously. The Barra model also produces more concentrated portfolios.

We define the contributions of common and specific risk factors using the Euler decomposition as follows:

$$\begin{aligned}
\sigma\left(w \mid b\right) &= \sum_{i=1}^{n} \left(w_i - b_i\right) \frac{\partial\, \sigma\left(w \mid b\right)}{\partial\, \left(w_i - b_i\right)} \\
&= \sum_{i=1}^{n} \left(w_i - b_i\right) \frac{1}{2} \frac{\left(2\Sigma\left(w - b\right)\right)_i}{\sigma\left(w \mid b\right)} \\
&= \underbrace{\frac{\left(w - b\right)^\top B\Omega B^\top \left(w - b\right)}{\sigma\left(w \mid b\right)}}_{\sigma_{\mathcal{F}}\left(w|b\right)} + \underbrace{\frac{\left(w - b\right)^\top D \left(w - b\right)}{\sigma\left(w \mid b\right)}}_{\sigma_{\varepsilon}\left(w|b\right)}
\end{aligned}$$

The two metrics $\sigma_{\mathcal{F}}\left(w \mid b\right)$ and $\sigma_{\varepsilon}\left(w \mid b\right)$ are reported in Table 10. We note that specific risk matters since $\sigma_{\varepsilon}\left(w \mid b\right) \approx$ 2–3 bps, representing about 28% of the tracking error volatility when the active share limit $\mathcal{AS}^+$ is 40%, and 43% when the active share limit is 100%. In the case of the $\boldsymbol{\ell}_2$-norm optimization, the decomposition is the following:

Statistic (in bps)	Active share limit $\mathcal{AS}^+$			
	25%	30%	40%	100%
$\sigma\left(w \mid b\right)$	15.74	15.38	15.35	15.35
$\sigma_{\mathcal{F}}\left(w \mid b\right)$	15.39	15.28	15.30	15.30
$\sigma_{\epsilon}\left(w \mid b\right)$	0.35	0.10	0.05	0.05

We recall that $\Omega = \begin{pmatrix} \sigma_r^2 & \eta\sigma_r \\ \eta\sigma_r & \rho \end{pmatrix}$ and $D = (1-\rho)\operatorname{diag}\left(\upsilon_s \odot \upsilon_s^\top\right)$. In fact, the specific risk of the $\boldsymbol{\ell}_2$-norm model is not truly idiosyncratic because the specific volatilities are very uniform and the default correlation is very high ($\rho = 80\%$). This explains its low contribution to the total tracking error volatility.

Remark 10. *Table 22 on page 112 shows the results of the Barra optimization when specific risk is excluded from the covariance matrix. As expected, the resulting portfolios are more concentrated. The effective number of bets decreases while the cumulative weight of the top 100 positions increases. This outcome is intuitive. When idiosyncratic risk is ignored, the optimizer no longer needs to diversify specific risk exposures and can therefore achieve its objectives using fewer securities.*

3.2.2 Yield maximization

Let us consider the problem of yield maximization $w^\star = \arg\max \mu\left(w \mid b\right)$. Results are reported below. Compared to tracking error minimization, we observe two effects: portfolios are more concentrated, and the tracking error volatility explodes while the modified duration constraint remains around at its lower bound (+0.20 year). We also remark that the active share constraint helps to mitigates these effects.

Table 11: Yield maximization (Barra model, ER00 Index, end of May 2026)

Statistic	Benchmark	Active share limit $\mathcal{AS}^+$			
		25%	30%	40%	100%
Holdings	4 663	3 502	3 261	2 786	104
Active share (in %)		25.00	30.00	40.00	97.85
ENB (w)	3 940	395	328	255	101
Top 100 weight (in %)	5.36	29.40	34.25	43.83	99.00
$\sigma\left(w \mid b\right)$ (in bps)		53.28	52.16	56.24	87.62
$\sigma_{\mathcal{F}}\left(w \mid b\right)$ (in bps)		51.97	50.80	54.79	85.01
$\sigma_{\epsilon}\left(w \mid b\right)$ (in bps)		1.31	1.36	1.45	2.61
Yield (in %)	3.47	3.80	3.85	3.93	4.18
$\beta_{\text{DTS}}\left(w \mid b\right)$	1.00	1.27	1.28	1.30	1.45
MD (in year)	4.48	4.74	4.72	4.68	4.68
5Y DTS (in bps)	92	192	192	192	192
7Y DTS (in bps)	101	126	126	126	126
10Y+ DTS (in bps)	48	23	23	23	23
Financials DTS (in bps)	128	228	228	228	234
A-rated DTS (in bps)	159	134	134	134	134
BBB-rated DTS (in bps)	193	293	293	293	293

3.2.3 Efficient frontier

The efficient frontier is shown in Figure 25 on page 124. It is close to the one obtained with the $\boldsymbol{\ell}_2$-norm model. However, the magnitude of the tracking error volatility differs. To analyze this, we match the tracking error volatilities $\sigma_{\boldsymbol{\ell}_2}\left(w \mid b\right)$ and $\sigma_{\mathcal{B}arra}\left(w \mid b\right)$ such that the $\boldsymbol{\ell}_2$- and Barra-optimized portfolios share the same excess yield $\mu\left(w \mid b\right)$. Figure 14 shows the scatter plot of the two tracking error volatilities. We observe the following relationship:

$$\begin{cases} \mu\left(w \mid b\right) \text{ low } \implies \sigma_{\mathcal{B}arra}\left(w \mid b\right) < \sigma_{\boldsymbol{\ell}_2}\left(w \mid b\right) \\ \mu\left(w \mid b\right) \text{ high } \implies \sigma_{\mathcal{B}arra}\left(w \mid b\right) > \sigma_{\boldsymbol{\ell}_2}\left(w \mid b\right) \end{cases}$$

As a result, the $\boldsymbol{\ell}_2$-norm model generates a higher tracking error when targeting low excess yields, whereas the Barra risk model generates a higher tracking error when targeting high excess yields.

Figure 14: Scatterplot of tracking error volatilities (ER00 Index, end of May 2026)

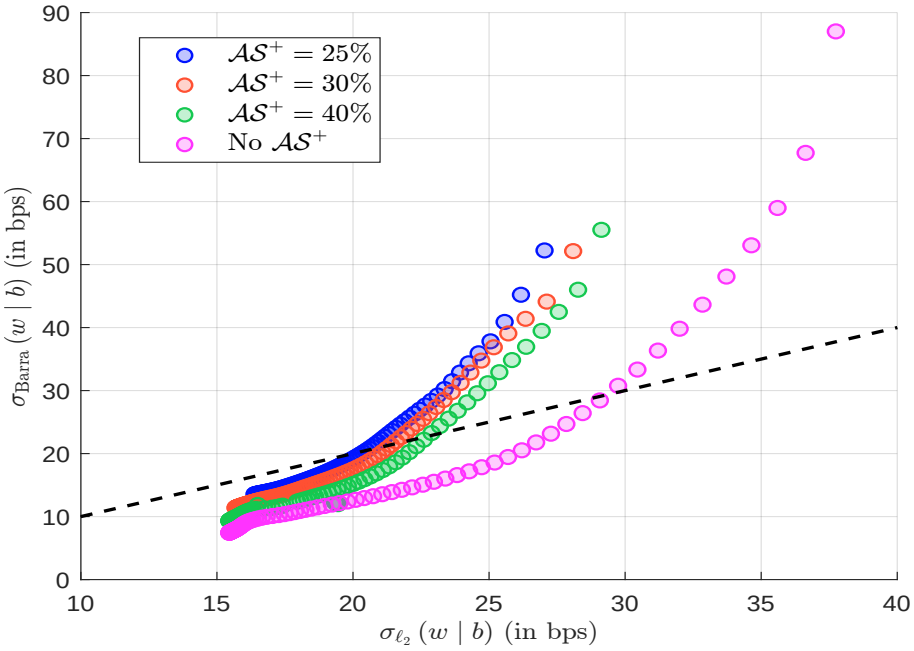

3.2.4 Extension to larger bond investment universes

The ER00 Index is a relatively small investment universe, containing approximately 4 600 bonds. To assess the impact of a larger opportunity set, we also examine two broader universes: the ICE BofA USD Corporate Bond Index (C0A0) and the ICE BofA Global Corporate Bond Index (G0BC). The results of the tracking error minimization and excess yield maximization problems are reported in Appendix C on pages 112–115. The behavior of the optimized portfolios for the C0A0 and G0BC universes differs somewhat from that observed for the ER00 universe. Because these universes contain substantially more securities, the optimizer has greater flexibility in constructing portfolios. As a result, when the objective is to minimize tracking error, it can achieve significantly lower tracking error volatility while maintaining a high degree of diversification. Conversely, when the objective is to maximize excess yield, the larger investment universe provides more opportunities to identify high yield bonds and concentrate active positions.

The benefits of a large investment universe can be illustrated using the efficient frontiers (Figures 26 and 27 on page 125). We observe that, given a target tracking error volatility, we can obtain significantly more excess return. For instance, Figure 15 compares the efficient frontiers when the active share limit is set to 30%. We clearly observe that C0A0-optimized portfolios dominate ER00-optimized portfolios, while G0BC-optimized portfolios dominate C0A0-optimized portfolios. Each time we double the number of securities, the excess yield is improved by at least 25%.

Remark 11. *The previous results may suggest that it is easy to outperform a bond index and generate alpha. In fact, we recall that there is a great deal of difference between model portfolios and investable portfolios. This aspect will be discussed later in Section 3.6 on page 71.*

Figure 15: Efficient frontier when $\mathcal{AS}^{+} = 30\%$ (end of May 2026, Barra risk model)

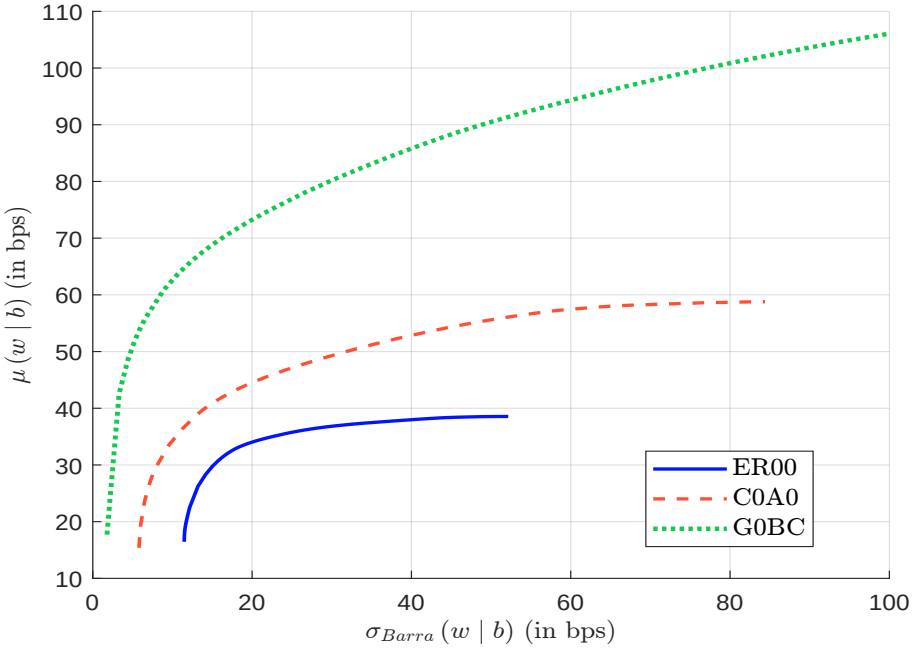

In summary, duration and DTS views can be efficiently implemented across all universes with limited tracking error, as active risk is mainly driven by factor exposures rather than specific risks. Relaxing the active share constraint and expanding the investment universe — particularly with C0A0 and G0BC — significantly improves the risk-return profile. This shifts the efficient frontier upward, enabling portfolios to generate higher excess yields for a given tracking error budget. However, these marginal gains diminish rapidly beyond moderate risk levels. Furthermore, broader universes like G0BC introduce additional currency and implementation complexities, particularly when managing the total number of portfolio holdings.

3.3 Active management

We adopt a top-down approach in which the portfolio is structured along two primary axes: maturity and sector. The idea is to simultaneously exploit relative value opportunities across maturities and sectors. Let $P_i(t)$ and T_i be the dirty price and maturity of bond i, respectively. The instantaneous return of bond i can be decomposed as follows[41]:

$$R_i(t) = -\sum_{k=1}^{K} \mathrm{KRD}_{i,k}(t)\, \mathrm{d}y_k(t) - \mathrm{SD}_i(t)\, \mathrm{d}s_i(t)$$

where $y_k(t)$ is the zero-coupon yield at maturity pillar k, $s_i(t)$ is the credit spread, $\mathrm{KRD}_{i,k}(t) = -\dfrac{\partial \ln P_i(t)}{\partial y_k(t)}$ is the key-rate duration of bond i at pillar k, and $\mathrm{SD}_i(t) = -\dfrac{\partial \ln P_i(t)}{\partial s_i(t)}$ is the spread duration of bond i. The first term captures exposure to movements in the yield curve, while the second term captures sensitivity to changes in the credit spread. To keep the model simple and tractable, we focus on the credit return component, but the extension

[41] We have:

$$R_i(t) = \frac{\mathrm{d}P_i(t)}{P_i(t)} = \mathrm{d}\ln P_i(t) = \sum_{k=1}^{K} \frac{\partial \ln P_i(t)}{\partial y_k(t)}\, \mathrm{d}y_k(t) + \frac{\partial \ln P_i(t)}{\partial s_i(t)}\, \mathrm{d}s_i(t)$$

to the full return decomposition is straightforward[42]. By approximating the spread change in relative terms, the return of bond i simplifies to:

$$R_i(t) \approx -\,\mathrm{SD}_i(t)\,\mathrm{d}s_i(t) \approx -\,\mathrm{DTS}_i(t)\,\frac{\Delta s_i(t)}{s_i(t)}$$

At the sector level, we get[43]:

$$R_{\mathcal{S}ector_j}(t) := R_{(j)}(t) \approx -\,\mathrm{DTS}_{(j)}(t)\,\frac{\Delta s_{(j)}(t)}{s_{(j)}(t)}$$

where $\mathrm{DTS}_{(j)}(t)$ and $s_{(j)}(t)$ are the benchmark-weighted DTS and credit spread of sector j, respectively. This sector-level return representation naturally leads to a one-factor risk model. Indeed, the covariance matrix between sector returns is given by $\Sigma = B\Omega B^\top$, where $B = \mathrm{diag}\left(-\,\mathrm{DTS}_{(1)}, \ldots, -\,\mathrm{DTS}_{(m)}\right)$ and Ω is the covariance matrix of relative spread changes across sectors.

3.3.1 A model of credit return decomposition

Let Δt be the holding period, which is typically one month. Over the interval $[t, t+\Delta t]$, the credit return of bond i can be decomposed into three economically meaningful components:

$$\begin{aligned} R_i(t) &\approx \underbrace{\mathrm{OAS}_i(t)\,\Delta t}_{\text{Carry}} + \underbrace{-\,\mathrm{SD}_i(t)\left(s_i(t+\Delta t) - s_i(t)\right)}_{\text{Rolldown}} + \underbrace{-\,\mathrm{SD}_i(t)\,\Delta\,\mathrm{OAS}_i(t)}_{\text{Repricing}} \\ &= \mathcal{C}arry_i(t) + \mathcal{R}olldown_i(t) + \mathcal{R}epricing_i(t) \end{aligned}$$

where $\mathrm{OAS}_i(t)$ is the option-adjusted spread of bond i at time t, $s_i(t+\Delta t) - s_i(t)$ is the change in the fitted credit spread due to the passage of time, and $\Delta\,\mathrm{OAS}_i(t) = \mathrm{OAS}_i(t+\Delta t) - \mathrm{OAS}_i(t)$ captures the residual idiosyncratic or market-driven spread change. Each component has a distinct economic interpretation (Hamdan *et al.*, 2016):

- Carry
  The investor earns $\mathrm{OAS}_i(t)\,\Delta t$ by simply holding the bond over the period and collecting the credit premium for default risk compensation, providing that no credit event occurs. This component is known and deterministic at time t.

- Rolldown
  As time passes, the bond's remaining maturity shortens from T_i to $T_i - \Delta t$. If the credit spread curve is upward-sloping, the bond naturally rolls down to a lower spread point, generating a price gain. This component is also observable ex-ante, given the current shape of the credit spread curve.

- Repricing
  The spread curve shifts between t and $t+\Delta t$ in an unpredictable manner. This parallel or non-parallel movement of $\mathrm{OAS}_i(t)$ generates an unexpected price gain or loss and is the primary source of return uncertainty over the holding period.

This decomposition is useful because it separates the predictable and structural return components (carry and rolldown) from the unpredictable, market-driven component (repricing).

[42] This is the generalization of our two-factor risk model.
[43] We use the notations (j) and $\mathcal{S}ector_j$ interchangeably to denote sector j.

Figure 16: Carry and rolldown components

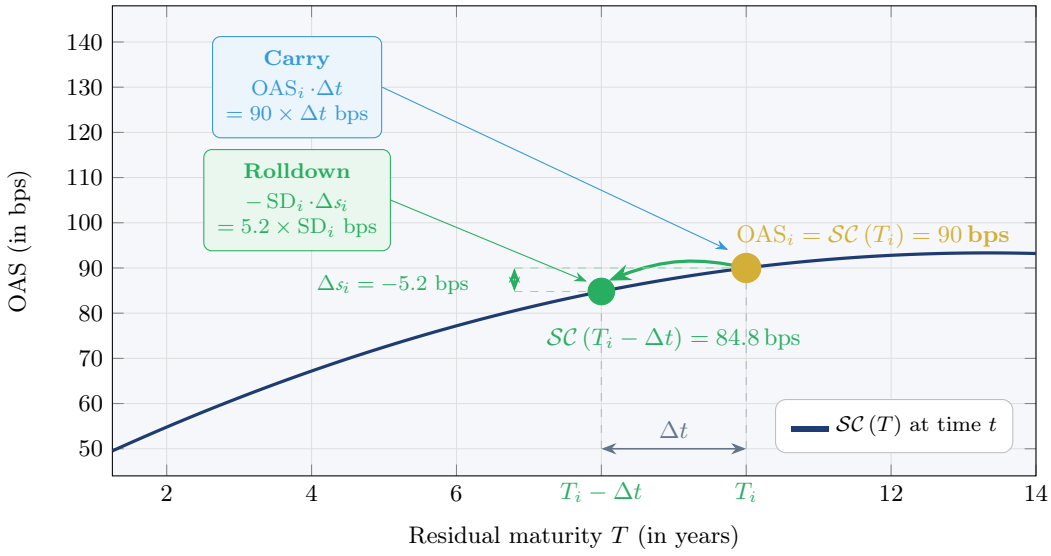

Aggregating across bonds within each sector j, the expected credit return at the sector level is given by:

$$\mu_{(j)} \approx \mathcal{C}arry_{(j)}(t) + \mathcal{R}olldown_{(j)}(t) + \mathbb{E}_t\left[\mathcal{R}epricing_{(j)}(t)\right]$$

While carry and rolldown are directly observable, forming a view on $\mathbb{E}_t\left[\mathcal{R}epricing_{(j)}(t)\right]$ — that is, forecasting the direction and magnitude of spread moves at the sector level — is precisely where active management plays its role.

Figure 17: Repricing component

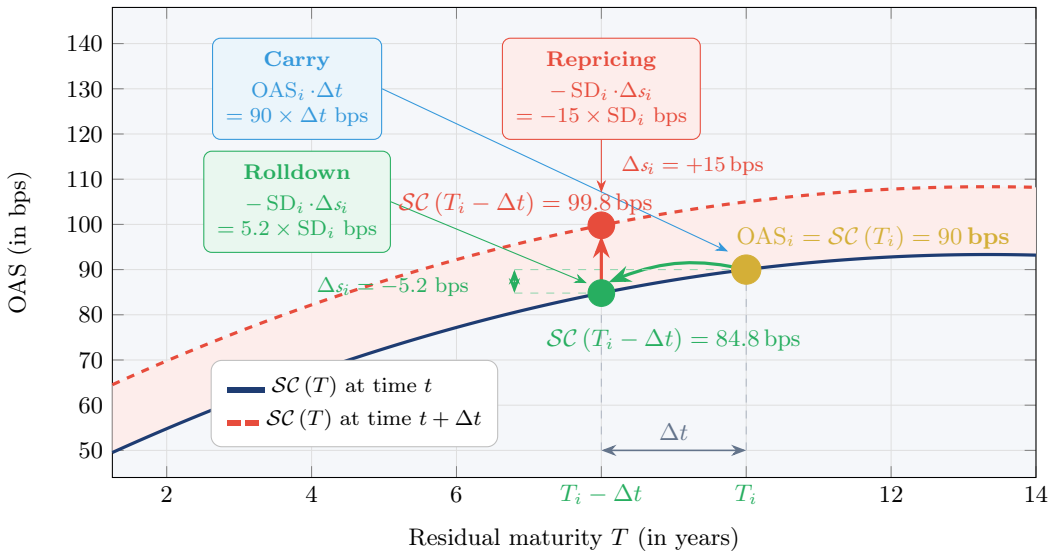

Remark 12. *This decomposition is illustrated in Figures 16 and 17. The central concept is the spread curve $\mathcal{SC}_t(T)$, which gives the credit spread of a bond with a remaining maturity*

T at time t. Over the holding period Δt, the bond's remaining maturity decreases from T to $T-\Delta t$. As a result, its spread shifts from $\mathcal{SC}_t(T)$ to $\mathcal{SC}_{t+\Delta t}(T-\Delta t)$. In addition to the carry, the investor therefore captures a mark-to-market return proportional to the spread difference $\mathcal{SC}_t(T)-\mathcal{SC}_{t+\Delta t}(T-\Delta t)$. This difference can be decomposed into two distinct components:

$$\underbrace{\mathcal{SC}_t(T)-\mathcal{SC}_{t+\Delta t}(T-\Delta t)}_{\textit{Mark-to-market}}=\underbrace{\mathcal{SC}_t(T)-\mathcal{SC}_t(T-\Delta t)}_{\textit{Rolldown}}+\underbrace{\mathcal{SC}_t(T-\Delta t)-\mathcal{SC}_{t+\Delta t}(T-\Delta t)}_{\textit{Repricing}}$$

The rolldown component measures the impact of the maturity, while the repricing component measures the reshaping impact of the spread curve[44].

Carry component Since $\mathcal{C}arry_i(t)=\mathrm{OAS}_i(t)\,\Delta t$, the sector-level carry is the benchmark-weighted average of the carry of the bonds belonging to sector j:

$$\mathcal{C}arry_{(j)}(t)=\frac{\sum_{i\in\mathcal{S}ector_j}w_i\cdot\mathcal{C}arry_i(t)}{\sum_{i\in\mathcal{S}ector_j}w_i}$$

Rolldown component To calculate the rolldown, we assume that the OAS of bond i depends on the following five determinants: the sector spread curve, the bond's maturity, its rating, its seniority, and its specific risk. We therefore formulate the following panel model with two sets of fixed effects:

$$\mathrm{OAS}_i=\sum_{j=1}^{m}\mathbb{1}\left\{i\in\mathcal{S}ector_j\right\}\mathcal{SC}_{(j)}(T_i)+\sum_{k=1}^{4}\mathbb{1}\left\{i\in\mathcal{R}ating_k\right\}\zeta_k+\sum_{k=1}^{3}\mathbb{1}\left\{i\in\mathcal{S}eniority_k\right\}\xi_k+\varepsilon_i$$

where $\mathcal{SC}_{(j)}(T)$ is the spread curve of sector j, ζ_k is the rating fixed effect (AAA, AA, A, or BBB), ξ_k is the seniority fixed effect (senior, secured, or subordinated), and ε_i is the idiosyncratic risk. The sector spread curve is parameterized using the Nelson-Siegel model:

$$\mathcal{SC}_{(j)}(T)=\beta_{0,j}+\beta_{1,j}\frac{1-\exp(-T/\tau)}{T/\tau}+\beta_{2,j}\left(\frac{1-\exp(-T/\tau)}{T/\tau}-\exp(-T/\tau)\right)$$

where $\beta_{0,j}$, $\beta_{1,j}$ and $\beta_{2,j}$ are the level, slope, and curvature parameters of sector j, while τ is the decay parameter common to all sectors. The parameter vector θ in this model consists of the $3m$ sector-specific parameters $(\beta_{0,j},\beta_{1,j},\beta_{2,j})$, the common decay parameter τ, the four rating fixed-effect coefficients ζ_k, and the three seniority fixed-effect coefficients ξ_k. Parameters are estimated by weighted least squares[45]:

$$\hat{\theta}=\arg\min\sum_{i=1}^{n}b_i\left(\mathrm{OAS}_i-\widehat{\mathrm{OAS}}_i\right)^2$$

where the fitted value is:

$$\widehat{\mathrm{OAS}}_i=\sum_{j=1}^{m}\mathbb{1}\left\{i\in\mathcal{S}ector_j\right\}\mathcal{SC}_{(j)}(T_i)+\sum_{k=1}^{4}\mathbb{1}\left\{i\in\mathcal{R}ating_k\right\}\zeta_k+\sum_{k=1}^{3}\mathbb{1}\left\{i\in\mathcal{S}eniority_k\right\}\xi_k$$

Once the parameters are estimated, the rolldown of bond i is computed as follows:

$$\mathcal{R}olldown_i(t)=-\mathrm{SD}_i(t)\left(\widehat{\mathcal{SC}}_{(j)}(T_i-\Delta t)-\widehat{\mathcal{SC}}_{(j)}(T_i)\right)$$

[44] For simplicity, we will use in the sequel the notation $\mathcal{SC}(T)$ instead of $\mathcal{SC}_t(T)$.
[45] We use the BBB/senior category as the reference point of the panel model.

where $\widehat{\mathcal{SC}}_{(j)}(T)$ is the estimated spread curve of the sector to which bond i belongs. The sector-level rolldown is then the benchmark-weighted average:

$$\mathcal{R}olldown_{(j)}(t) = \frac{\sum_{i \in \mathcal{S}ector_j} w_i \cdot \mathcal{R}olldown_i(t)}{\sum_{i \in \mathcal{S}ector_j} w_i}$$

Repricing component The future evolution of credit spreads is uncertain and cannot be forecasted deterministically. Therefore, we translate fund manager views into standardized spread scenarios scaled by the historical volatility of relative spread changes. For each sector, the fund manager assigns a qualitative view, which is encoded as a z-score:

Sector view	Interpretation	$\kappa_{(j)}$
$+++$	Strong expected spread tightening	-3.0
$++$	Moderate expected spread tightening	-2.0
$+$	Mild expected spread tightening	-1.0
Neutral	No directional view	0.0
$-$	Mild expected spread widening	$+1.0$
$--$	Moderate expected spread widening	$+2.0$
$---$	Strong expected spread widening	$+3.0$

For each sector j, the expected relative spread shock is defined as follows:

$$\mathbb{E}_t\left[\frac{\Delta s_{(j)}}{s_{(j)}}\right] = \lambda\kappa_{(j)}\sigma\left(\frac{\Delta s_{(j)}}{s_{(j)}}\right) = \lambda\kappa_{(j)}\sigma_{(j)}$$

where $\sigma_{(j)}$ is the historical volatility of relative spread changes, $\kappa_{(j)}$ encodes the qualitative sector view, and $\lambda \geq 0$ is a confidence scaling parameter that controls the weight assigned to active views. It can also be interpreted as the Sharpe ratio of the manager's views. For example, $\lambda = 0$ ignores all sector views, $\lambda = 0.25$ corresponds to moderate conviction, and $\lambda > 0.50$ corresponds to high conviction. The expected repricing return of sector j is then[46]:

$$\mathbb{E}_t\left[\mathcal{R}epricing_{(j)}(t)\right] = -\lambda\kappa_{(j)}\,\mathrm{DTS}_{(j)}\,\sigma_{(j)}$$

3.3.2 An example with sector views

We consider the investment universe defined by the ICE BofA Euro Corporate Index (ER00), which comprises 18 sectors: Automotive, Banking, Basic Industry, Capital Goods, Consumer Goods, Energy, Financial Services, Healthcare, Insurance, Leisure, Media, Real Estate, Retail, Services, Technology & Electronics, Telecommunications, Transportation, and Utility. To achieve greater allocation granularity, each sector is subdivided into five maturity buckets: 0–3Y, 3–5Y, 5–7Y, 7–10Y, and 10Y+. Active positioning can be therefore implemented at the sector $\times$ maturity level rather than at the sector level alone. In theory, there are $18 \times 5 = 90$ sector-maturity clusters. In practice, however, only 89 clusters are represented, because one maturity bucket is absent in a particular sector[47] (Table 29 on page 115). We assume that the portfolio manager expresses views on the ten sectors reported in Table 12. In addition, portfolio construction is subject to two constraints: a maximum active share of 10%, and a limit on sector-level DTS exposure, where each sector's DTS contribution may not exceed 130% of the corresponding benchmark contribution.

[46] Because $\mathbb{E}_t\left[\mathcal{R}epricing_{(j)}(t)\right] = -\,\mathrm{SD}_{(j)}(t)\,\mathbb{E}_t\left[\Delta\,\mathrm{OAS}_{(j)}(t)\right] = -\,\mathrm{DTS}_{(j)}(t)\,\mathbb{E}_t\left[\frac{\Delta s_{(j)}}{s_{(j)}}\right]$.

[47] This is the Services/10Y+ cluster.

Table 12: Sector views of the portfolio manager

Sector	Views
Banking	++
Financial Services	+
Insurance	+
Real Estate	+
Utility	+

Sector	Views
Capital Goods	−
Retail	−
Technology & Electronics	−
Telecommunications	−
Consumer Goods	−−

Let us first consider the maximization problem of the expected excess return:

$$w^\star(\lambda) = \arg\max \mu\left(w \mid b; \lambda\right)$$
$$\text{s.t.} \begin{cases} \mathcal{AS}\left(w \mid b\right) \leq 10\% \\ \sum_{i \in \mathcal{S}ector_j} w_i \,\mathrm{DTS}_i \leq 130\% \times \sum_{i \in \mathcal{S}ector_j} b_i \,\mathrm{DTS}_i \qquad \forall j = 1, \ldots, 18 \\ \mathbf{1}_m^\top w = 1 \\ w \geq \mathbf{0}_m \end{cases}$$

where w is the 89×1 vector of sector/maturity weights. Recall that the expected return in our model is given by:

$$\mu(w; \lambda) = \sum_{j=1}^{m} w_{(j)} \mathcal{C}arry_{(j)} + \sum_{j=1}^{m} w_{(j)} \mathcal{R}olldown_{(j)} + \lambda \sum_{j=1}^{m} w_{(j)} \mathcal{R}epricing_{(j)}$$

where $\mathcal{R}epricing_{(j)} = -\kappa_{(j)} \,\mathrm{DTS}_{(j)}\, \sigma_{(j)}$ represents the normalized expected repricing return when $\lambda = 1$. It follows that the expected excess return is equal to:

$$\begin{aligned} \mu\left(w \mid b; \lambda\right) &= \mu(w - b; \lambda) \\ &= \sum_{j=1}^{m} \left(w_{(j)} - b_{(j)}\right) \mathcal{C}arry_{(j)} + \sum_{j=1}^{m} \left(w_{(j)} - b_{(j)}\right) \mathcal{R}olldown_{(j)} + \\ &\quad \lambda \sum_{j=1}^{m} \left(w_{(j)} - b_{(j)}\right) \mathcal{R}epricing_{(j)} \end{aligned}$$

The optimization is performed across different values of λ. Results are reported in Table 13. One must be careful when interpreting these figures across different values of λ. If we consider two optimal portfolios $w^\star(\lambda_1)$ and $w^\star(\lambda_2)$ generated by two distinct values λ_1 and λ_2, we can easily compare their portfolio structure and risk profiles. However, directly comparing their return figures is more complex. Because $\mu(w; \lambda)$ and $\mu\left(w \mid b; \lambda\right)$ depend on the value of λ, the return components differ for the same portfolio under different values of λ. If $\lambda_1 \neq \lambda_2$, then $\mu(w; \lambda_1) \neq \mu(w; \lambda_2)$ and $\mu\left(w \mid b; \lambda_1\right) \neq \mu\left(w \mid b; \lambda_2\right)$. In fact, the difference in expected returns decomposes as:

$$\begin{aligned} \mu(w_2; \lambda_2) - \mu(w_1; \lambda_1) &= \sum_{j=1}^{m} \left(w_{(j),2} - w_{(j),1}\right) \left(\mathcal{C}arry_{(j)} + \mathcal{R}olldown_{(j)} + \lambda_1 \mathcal{R}epricing_{(j)}\right) \\ &\quad + (\lambda_2 - \lambda_1) \sum_{j=1}^{m} w_{(j),2} \mathcal{R}epricing_{(j)} \end{aligned}$$

The first term reflects the change in portfolio composition, valued at the confidence level λ_1, while the second term reflects the change in the confidence parameter itself, applied to the new portfolio w_2. When $\lambda = 0$, the expected return is 108 bps, which is entirely explained by the carry and rolldown components ($\mathcal{C}arry = 83$ bps, $\mathcal{R}olldown = 25$ bps). For $\lambda > 0$,

the carry-rolldown contribution falls below 108 bps, because the optimization now considers repricing in addition to carry and rolldown. For example, when $\lambda = 50\%$, the expected return increases to 168 bps, decomposed as follows: $\mathcal{C}arry = 80$ bps, $\mathcal{R}olldown = 24$ bps, and $\mathcal{R}epricing = 63$ bps. Thus, the choice of λ substantially impacts expected return and tracking error volatility while having a limited influence on portfolio concentration (measured by the number of holdings and effective bets). However, λ affects the sector and maturity allocation (see Tables 30–32 on page 116).

Table 13: Excess return maximization under a constraint of active share (active management, ER00 Index, end of May 2026)

Statistic	Benchmark	Confidence λ					
		0	10%	20%	30%	40%	50%
Portfolio structure							
Holdings	89	78	77	78	77	77	76
$\mathcal{AS}\left(w \mid b\right)$ (in %)		10	10	10	10	10	10
ENB (w)	32	29	29	27	27	27	27
Risk							
$\sigma\left(w \mid b\right)$ (in bps)		12.3	12.0	8.6	7.4	7.2	7.0
DTS (w) (in bps)	382	415	407	394	387	384	380
$\beta_{\text{DTS}}\left(w \mid b\right)$	1.00	1.09	1.07	1.03	1.01	1.01	1.00
Return							
$\mu\left(w;\lambda\right)$ (in bps)	101	108	118	130	142	155	168
$\mathcal{C}arry$		83	82	81	81	80	80
$\mathcal{R}olldown$		25	25	25	24	24	24
$\mathcal{R}epricing$		0	11	24	37	50	63
$\mu\left(w \mid b;\lambda\right)$ (in bps)		7	10	15	21	27	33
$\mathcal{C}arry$		5	4	3	3	2	2
$\mathcal{R}olldown$		2	1	1	1	1	0
$\mathcal{R}epricing$		0	5	11	18	24	31

We now consider the mean-variance optimization problem:

$$w^\star\left(\gamma,\lambda\right) = \arg\min \frac{1}{2}\sigma^2\left(w \mid b\right) - \gamma\mu\left(w \mid b;\lambda\right)$$
$$\text{s.t.} \begin{cases} \mathcal{AS}\left(w \mid b\right) \leq 10\% \\ \sum_{i\in\mathcal{S}ector_j} w_i \,\text{DTS}_i \leq 130\% \times \sum_{i\in\mathcal{S}ector_j} b_i \,\text{DTS}_i & \forall j = 1,\ldots,18 \\ \mathbf{1}_m^\top w = 1 \\ w \geq \mathbf{0}_m \end{cases}$$

where $\sigma^2\left(w \mid b\right) = \left(w-b\right)^\top B\Omega B^\top\left(w-b\right)$, $B = \text{diag}\left(-\text{DTS}_{(1)},\ldots,-\text{DTS}_{(m)}\right)$ and Ω is the covariance matrix of relative spread changes across the sector/maturity clusters. Results are reported in Figure 21. The efficient frontiers exhibit the expected concave profile, reflecting the fact that the marginal excess return diminishes with each additional unit of active risk. For low values of λ, which correspond to limited confidence in sector views, the trade-off between tracking error volatility and expected excess return remains relatively flat because the repricing component does little to differentiate portfolios across the risk spectrum. As λ increases[48], the efficient frontiers diverge progressively, revealing the growing

[48] We verify that the limit case $\gamma \to \infty$ corresponds to the solution of the excess return maximization (Table 13).

value of incorporating sector views into portfolio construction. Stronger convictions unlock higher expected excess returns at every level of tracking error. For example, with a tracking error of 2 bps, increasing conviction from $\lambda = 0\%$ to $\lambda = 50\%$ raises the expected active return from approximately 6 bps to 17 bps. This illustrates that performance enhancement from active sector views interacts with the active risk budget rather than being merely additive. The greater the risk a portfolio is permitted to take, the more valuable a well-calibrated set of views becomes.

Figure 18: Efficient frontier (active management, ER00 Index, end of May 2026)

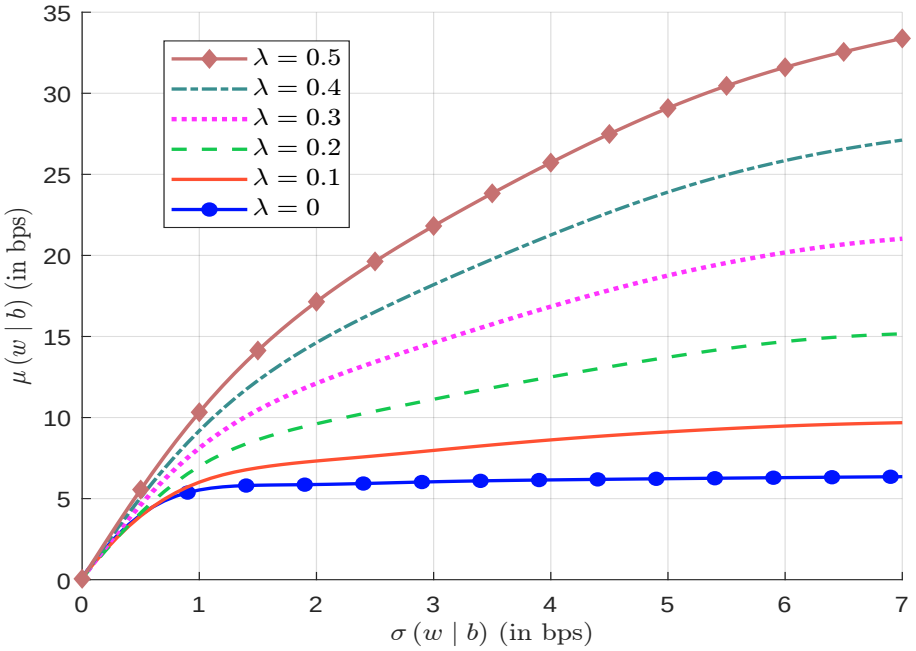

Remark 13. *The active management model presented in this section is very standard. It can be made more complex by considering other return engines. For example, Bajo Traver (2026, Equation 3.1) uses a four-component model that incorporates the convexity effect:*

$$R_i(t) = \mathcal{C}arry_i(t) + \mathcal{R}olldown_i(t) + \mathcal{R}epricing_i(t) + \mathcal{C}onvexity_i(t)$$

3.4 Portfolio decarbonization

One of the most common applications of bond portfolio optimization is the construction of benchmarks with enhanced sustainability characteristics. The underlying principle is generally the same. Starting from a well-established parent index, the index provider creates a sustainable benchmark by improving selected ESG metrics while maintaining risk and return characteristics similar to those of the original index (Ben Slimane *et al.*, 2019b,c). ESG integration can be implemented through several approaches, including scoring, screening, and optimization techniques. The objective is typically to replicate the parent index as closely as possible while achieving a superior ESG profile. For example, in portfolio decarbonization strategies, the carbon footprint of the portfolio is constrained to be lower than that of the benchmark. Let $\boldsymbol{\mathcal{CI}}_i$ be the carbon intensity of bond i. The carbon footprint of portfolio w is measured by its weighted average carbon intensity: $\boldsymbol{\mathcal{CI}}(w) = \sum_{i=1}^{n} w_i \boldsymbol{\mathcal{CI}}_i$. Portfolio decarbonization consists of imposing a minimum reduction in carbon intensity relative to a

benchmark: $\boldsymbol{\mathcal{CI}}(w) \leq (1-\boldsymbol{\mathcal{R}})\,\boldsymbol{\mathcal{CI}}(b)$. The value of the reduction rate is typically determined by the index provider. In some cases, however, it is given by regulation, as for climate transition benchmarks (CTB) and Paris-aligned benchmarks (PAB), which are subject to minimum decarbonization requirements. For instance, Barahhou *et al.* (2022) and Ben Slimane *et al.* (2023) propose minimizing the active credit risk and the active share of portfolio w with respect to benchmark b, subject to a carbon footprint reduction constraint:

$$\begin{aligned} w^\star &= \arg\min \frac{1}{2}\sum_{i=1}^{n}|w_i - b_i| + \varphi \sum_{j=1}^{n_{\mathcal{S}ector}} \left| \sum_{i\in\mathcal{S}ector_j} (w_i - b_i)\,\mathrm{DTS}_i \right| \\ \text{s.t.} &\quad \begin{cases} \boldsymbol{\mathcal{CI}}(w) \leq (1-\boldsymbol{\mathcal{R}})\,\boldsymbol{\mathcal{CI}}(b) \\ w \in \Omega_1 \cap \Omega_2 \end{cases} \end{aligned} \tag{37}$$

where $\boldsymbol{\mathcal{R}}$ is the reduction rate, $\Omega_1 \cap \Omega_2$ is a set of portfolio constraints, and φ is the trade-off parameter that controls the relative importance of the DTS component[49]. The first constraint set $\Omega_1 = \left\{w : \mathbf{1}_n^\top w = 1, \mathbf{0}_n \leq w \leq \mathbf{1}_n\right\}$ defines a fully invested long-only portfolio. The second constraint set Ω_2 controls the risk deviation between portfolio w and benchmark b. A typical specification is $\Omega_2 = \Omega_{2'} \cap \Omega_{2''} \cap \Omega_{2'''}$, where $\Omega_{2'} = \left\{w : \sum_{i=1}^{n}(w_i - b_i)\,\mathrm{MD}_i = 0\right\}$, $\Omega_{2''} = \left\{w : \forall j, \sum_{i\in\mathcal{B}ucket(j)}(w_i - b_i) = 0\right\}$ and $\Omega_{2'''} = \left\{w : \forall k, \sum_{i\in\mathcal{R}ating(k)}(w_i - b_i) = 0\right\}$. $\Omega_{2'}$ neutralizes the modified duration exposure at the portfolio level, whereas $\Omega_{2''}$ and $\Omega_{2'''}$ ensure that the portfolio allocation is the same as the benchmark per maturity buckets and rating categories, respectively.

Table 14: Sector allocation in % when the reduction rate is set at 50% (Barra model, G0BC Index, end of May 2026)

Sector	Index	$\boldsymbol{\mathcal{SC}}_1$	$\boldsymbol{\mathcal{SC}}_{1-2}$	$\boldsymbol{\mathcal{SC}}_{1-3}^{\mathrm{up}}$	$\boldsymbol{\mathcal{SC}}_{1-3}$
Communication Services	7.18	7.18	7.17	7.17	7.17
Consumer Discretionary	6.75	6.75	6.75	6.72	6.72
Consumer Staples	5.80	5.80	5.80	5.69	5.80
Energy	6.65	6.60	6.49	6.11	4.08
Financials	34.88	35.96	36.53	38.54	35.83
Health Care	7.82	7.82	7.83	7.82	7.82
Industrials	8.70	8.71	8.70	8.83	10.83
Information Technology	4.65	4.70	4.65	4.65	4.61
Materials	3.20	3.11	3.05	2.99	2.92
Real Estate	3.94	3.94	3.94	3.94	3.94
Utilities	10.42	9.43	9.09	7.54	10.29
$\mathcal{AS}(w \mid b)$ (in %)		3.02	3.66	6.81	15.04
$\sigma(w \mid b)$ (in bpd)		14.39	15.71	16.94	18.37

For reasonable reduction rates, Table 14 confirms the results of Barahhou (2022) that decarbonization has little impact on portfolio characteristics (DTS, MD, yield, sector allocation). However, when the reduction rate exceeds 50%, we observe a deformation of the portfolio structure. In particular, portfolio decarbonization is a strategy that is long financials and health care, and short energy and utilities when we consider scope 3 upstream emissions, while it becomes long industrials and short financials and energy when downstream emissions are included[50] (Luciani and Roncalli, 2026).

[49] φ is set to 50, implying that the trade-off is 1% of active share for 2 bps of DTS.
[50] See Tables 42–45 on pages 121–122.

Figure 19: Impact of the carbon scope on the active share (G0BC Index, end of May 2026)

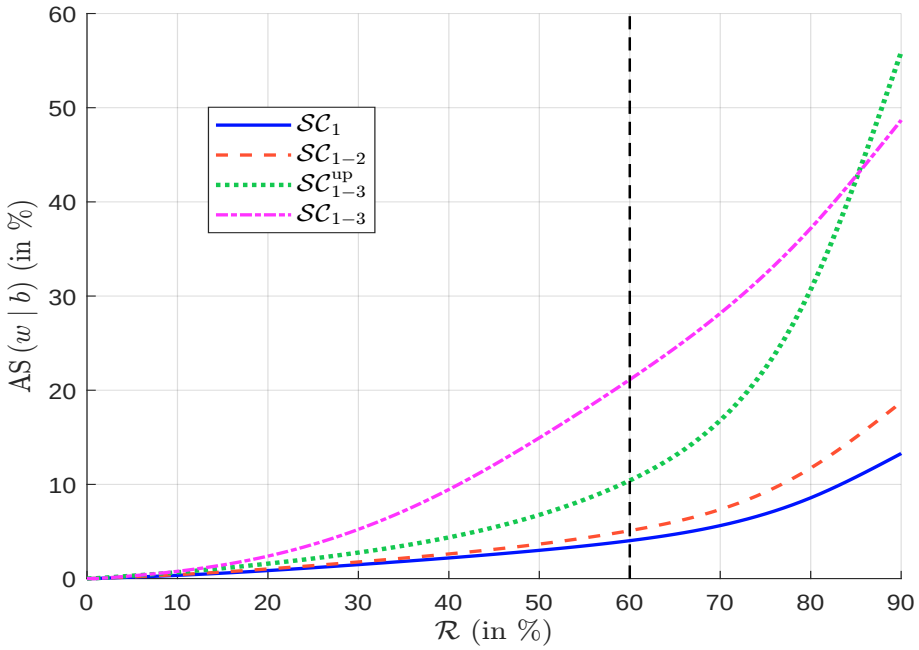

Source: ICE BofA, Trucost & Authors' calculations.

Figure 20: Impact of the carbon scope on the tracking error volatility (G0BC Index, end of May 2026)

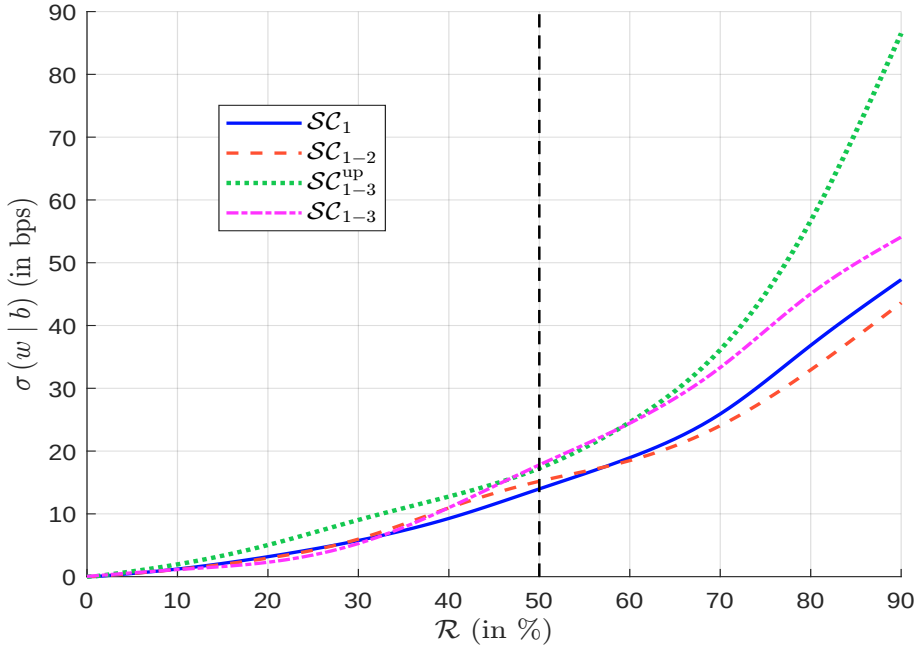

Source: ICE BofA, Trucost & Authors' calculations.

3.5 Clustering and bucketing methods

The concept of bucketing has a long history in fixed-income portfolio management. One of the earliest applications of mean-variance optimization to bond portfolios used maturity buckets instead of individual securities to determine the optimal allocation (Cheng, 1962). The importance of maturity segmentation remains central to fixed-income analysis and reporting. Most bond portfolio reports present key statistics across standard maturity bands, typically 0–1Y, 1–3Y, 3–5Y, 5–7Y, 7–10Y, and 10Y+. Bucketing has also become a standard tool for describing the credit risk profile of bond portfolios. In the investment-grade universe, the most common rating buckets are AAA, AA (including AA+ and AA−), A (including A+ and A−) and BBB (including BBB+ and BBB−). These dimensions can be naturally combined to define more granular classifications. For example, a maturity × rating framework partitions the investment universe into the following cells:

	0–1Y	1–3Y	3–5Y	5–7Y	7–10Y	10Y+
AAA						
AA						
A						
BBB						

The bucketing concept is closely related to the notion of risk factors. Its primary objective is to summarize a large bond universe consisting of thousands of securities into a limited number of representative cells. In practice, one of the most widely used approaches is based on four dimensions: Maturity × Rating × Sector × Currency. This framework provides an informative representation of the key sources of risk within a bond portfolio. More generally, statistical clustering techniques can be used to group securities by their characteristics or risk profiles, extending the traditional bucketing approach in a data-driven way (Focardi and Fabozzi, 2004).

The concept of bucketing is also closely related to security analysis and index replication. In practice, the characteristics and performance of an individual bond are often evaluated relative to its bucket or cluster. Bucketing plays also a central role in bond index tracking. One of the simplest and most widely used approaches to replicate a fixed-income benchmark is applying stratified sampling (or cell-based matching) to a partition of the investment universe. The objective is then to construct a portfolio whose aggregate exposures within each bucket closely match those of the benchmark. Stratified sampling has been applied to bond portfolios since Rudd (1980) introduced this methodology as a practical alternative to full replication. Since then, bucket-based replication techniques have become standard in fixed-income management (Gouzilh *et al.*, 2014). From this perspective, bucketing provides an implicit approach to tracking error control. Rather than minimizing an explicit mathematical measure of tracking error, the portfolio manager aligns the portfolio and benchmark exposures across a set of predefined buckets.

Consider the following optimization problem:

$$
\begin{aligned}
w^{\star} \quad = \quad & \arg\max \mu\left(w \mid b\right) \\
\text{s.t.} \quad & \begin{cases}
\mathrm{MD}\left(w\right) = \mathrm{MD}\left(b\right) \\
\mathrm{DTS}\left(w\right) = \mathrm{DTS}\left(b\right) \\
\mathcal{AS}\left(w \mid b\right) \leq 50\% \\
\sum_{i \in \mathcal{I}ssuer_j} w_i \leq 1\% \\
\mathbf{1}_n^{\top} w = 1 \\
\mathbf{0}_n \leq w \leq \mathbf{1}_n \\
w \in \Omega_{\mathfrak{B}ucket}
\end{cases}
\end{aligned}
$$

The objective is to maximize the excess yield of the portfolio $\mu\left(w \mid b\right)$ subject to the following constraints: the portfolio's modified duration and duration times spread must match those of the benchmark; the active share relative to the benchmark must not exceed 50%; issuer concentration risk is controlled by capping each issuer's aggregate exposure at 1%; and the weights must satisfy standard long-only and fully-invested constraints.

Table 15: Tracking error volatility $\sigma\left(w \mid b\right)$ in bps of clustering-based optimized portfolios (Barra model, G0BC Index, end of May 2026)

Bucket definition	$\left(\varphi^-, \varphi^+\right) = (0.5, 2.0)$	$\left(\varphi^-, \varphi^+\right) = (0.9, 1.1)$
No clustering	155.02	155.02
Currency	113.29	99.29
Maturity	155.02	151.91
Rating	155.00	162.47
Sector*	155.02	150.59
Sector	153.36	150.70
Currency × Maturity	112.91	99.12
Currency × Sector*	116.35	95.80
Rating × Sector	148.05	148.26
Currency × Maturity × Rating	112.41	103.70
Currency × Rating × Sector	110.69	68.97
Currency × Maturity × Rating × Sector*	108.75	81.51
Currency × Maturity × Rating × Sector	97.86	62.88

Using the G0BC investment universe, we obtain a solution with a tracking error volatility of 155 bps when no bucket restriction is imposed. We then define the following bucket-level restrictions:

- Currency: EUR, USD and others;
- Maturity: 0–3Y, 3–5Y, 5–7Y, 7–10Y, and 10Y+;
- Rating: AAA, AA, A and BBB;
- Sector*: Level 2 with 3 sectors (Financials, Corporates and Utilities) — or Sector: Level 3 with 18 sectors.

The number of buckets are $n_{\mathfrak{B}ucket^\star} = 3 \times 5 \times 4 \times 3 = 180$ and $n_{\mathfrak{B}ucket} = 3 \times 5 \times 4 \times 18 = 1\,080$, respectively. We then impose that the portfolio's aggregate weight within each bucket remains close to that of the benchmark. Specifically, we require that it stay within the following range:

$$\varphi^- \sum_{i \in \mathfrak{B}ucket_k} b_i \leq \sum_{i \in \mathfrak{B}ucket_k} w_i \leq \varphi^+ \sum_{i \in \mathfrak{B}ucket_k} b_i$$

Adding these constraints reduces $\sigma\left(w \mid b\right)$ to 108.75 bps with three sectors and 97.86 bps with 18 sectors when $\left(\varphi^-, \varphi^+\right) = (0.5, 2.0)$, confirming that finer bucket granularity yields tighter tracking. Table 15 reports results across some bucket-definition combinations.

Remark 14. *Portfolio managers often use MD or DTS bucket-level restrictions instead of weight-based restrictions. The bounds of these restrictions can be narrowed to further tighten tracking control. More generally, bucketing provides a flexible framework for managing tracking risk without explicitly optimizing it. Which bucket-level restrictions to impose — weight, MD, or DTS — depends on the relative importance of the underlying risk factors. For instance, weight and MD restrictions are usually more relevant for sovereign bond portfolios, while DTS restrictions are more appropriate for credit portfolios.*

3.6 Investable solutions

3.6.1 The mathematics of investable solutions

We now turn to the problem of computing investable portfolios[51]. For each bond i, we introduce a binary variable $x_i \in \{0,1\}$ defined by:

$$x_i = \begin{cases} 1 & \text{if bond } i \text{ is held in the portfolio} \\ 0 & \text{otherwise} \end{cases}$$

The tradable nominal is then given by:

$$q_i = x_i \,\mathrm{MT}_i + x_i y_i \,\mathrm{LS}_i$$

where MT_i and LS_i are the minimum tradable amount and lot size of bond i, respectively. Here, $y_i \in \mathbb{N}$ is the number of additional lots purchased. To ensure that no lots can be purchased when the bond is not selected, we impose the constraint:

$$0 \leq y_i \leq x_i y_i^+$$

where y_i^+ is an upper bound on the number of additional lots. A natural choice is:

$$y_i^+ = \left\lfloor \frac{q_i^+ - \mathrm{MT}_i}{\mathrm{LS}_i} \right\rfloor$$

where q_i^+ is calculated from the maximum weight allowed for bond i. We can then simplify the expression of q_i:

$$q_i = x_i \,\mathrm{MT}_i + y_i \,\mathrm{LS}_i$$

and we have:

$$\begin{cases} x_i = 0 \Rightarrow y_i = 0 \Rightarrow q_i = 0 \\ x_i = 1 \Rightarrow y_i \in \left\{0, 1, \ldots, y_i^+\right\} \Rightarrow q_i \in \left\{\mathrm{MT}_i, \mathrm{MT}_i + \mathrm{LS}_i, \ldots, \mathrm{MT}_i + y_i^+ \,\mathrm{LS}_i\right\} \end{cases}$$

Let V be the total portfolio value. The weight of bond i in the portfolio is:

$$\tilde{w}_i = \frac{q_i p_i}{V} = \frac{(x_i \,\mathrm{MT}_i + y_i \,\mathrm{LS}_i)\, p_i}{V} = x_i \frac{\mathrm{MT}_i \, p_i}{V} + y_i \frac{\mathrm{LS}_i \, p_i}{V}$$

where p_i is the dirty price of bond i. We note that $\tilde{w}_i$ is a linear combination of the integer variables x_i and y_i. As in the continuous case, constraints can be formulated directly in terms of the weights $\tilde{w}_i$ and then translated into equivalent constraints on x_i and y_i. We can also add two important types of constraints:

1. Cash constraint
   If the maximum allowable cash position is $\mathcal{C}_{ash}^+ \geq 0$, then we have:

$$V - \mathcal{C}_{ash}^+ \leq \sum_{i=1}^{n} q_i p_i \leq V$$

[51] Previously, exposures were expressed as a percentage under the following constraints: $w_i \in [0,1]$ and $\sum_{i=1}^n w_i = 1$. The optimiser does not generate null weights by construction, but we generally adopt the convention that small weights are forced to be zero: $w_i \leq \epsilon \Rightarrow w_i = 0$. In previous applications, we set ϵ to 10^{-6}.

We deduce that:

$$1 - c_{ash}^{+} \leq \sum_{i=1}^{n} \tilde{w}_i \leq 1$$

where:

$$c_{ash}^{+} = \frac{\mathcal{C}_{ash}^{+}}{V}$$

2. Cardinality constraint
   Since $x_i = 1$ if and only if bond i is held, the total number of holdings is:

$$\mathcal{N}_{holding} = \sum_{i=1}^{n} x_i$$

A lower and upper bound on portfolio size is then enforced by:

$$\mathcal{N}^{-} \leq \sum_{i=1}^{n} x_i \leq \mathcal{N}^{+}$$

More generally, we can impose minimum and maximum number of holdings for the cluster $\mathcal{G}_j$ as follows:

$$\mathcal{N}_j^{-} \leq \sum_{i \in \mathcal{G}_j} x_i \leq \mathcal{N}_j^{+}$$

Remark 15. *The yield maximization and $\boldsymbol{\ell}_1$-norm optimization problems can be reformulated as mixed integer linear programs (MILP) because the objective functions and portfolio constraints are linear. For the tracking error minimization and $\boldsymbol{\ell}_2$-norm optimization problems, we obtain a mixed integer quadratic program (MIQP). While MILPs are relatively easy to solve, MIQPs are time-consuming even with commercial solvers.*

3.6.2 One-step vs. two-step investable portfolios

We obtain the following optimization problem:

$$\begin{aligned} \{x^\star, y^\star\} \quad &= \quad \arg\min \frac{1}{2}\mathcal{R}\left(\tilde{w} \mid b\right) - \gamma\mu\left(\tilde{w} \mid b\right) \\ &\text{s.t.} \quad \begin{cases} \tilde{w}_i = x_i \dfrac{\mathrm{MT}_i\, p_i}{V} + y_i \dfrac{\mathrm{LS}_i\, p_i}{V} \\ x_i \in \{0, 1\} \\ y_i \in \{0, 1, \ldots, y_i^{+}\} \\ \{\tilde{w}, x, y\} \in \tilde{\Omega} \end{cases} \end{aligned} \tag{38}$$

Given an investment universe b, this *one-step approach* solves a single mixed-integer program to directly find the optimal integer allocations $\{x^\star, y^\star\}$. An alternative is the *two-step approach*, which first computes the continuous model portfolio $w^\star$ and then finds the investable portfolio $\{x^\star, y^\star\}$ closest to it. The first step is the standard continuous optimization problem:

$$\begin{aligned} w^\star \quad &= \quad \arg\min \frac{1}{2}\mathcal{R}\left(w \mid b\right) - \gamma\mu\left(w \mid b\right) \\ &\text{s.t.} \quad \begin{cases} w \in \Omega \\ \mathbf{0}_n \leq w \leq \mathbf{1}_n \end{cases} \end{aligned} \tag{39}$$

The second step then seeks the investable portfolio that best replicates $w^\star$. One natural

Figure 21: One-step vs. two-step investable portfolio optimization

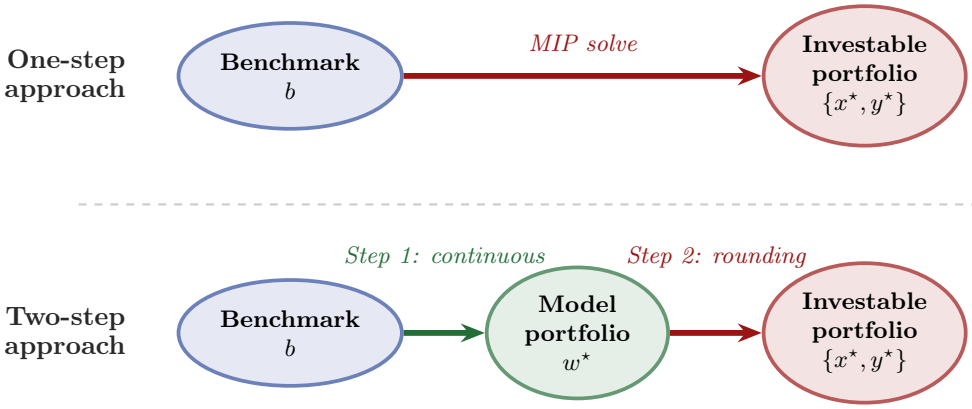

formulation minimizes the active share $\mathcal{AS}\left(\tilde{w} \mid w^\star\right)$ under the same optimization constraints plus the integer constraints:

$$\begin{aligned} \{x^\star, y^\star\} \quad &= \quad \arg\min \frac{1}{2} \sum_{i=1}^{n} |\tilde{w}_i - w_i^\star| \\ &\text{s.t.} \quad \begin{cases} \tilde{w}_i = x_i \dfrac{\mathrm{MT}_i \, p_i}{V} + y_i \dfrac{\mathrm{LS}_i \, p_i}{V} \\ x_i \in \{0, 1\} \\ y_i \in \{0, 1, \ldots, y_i^+\} \\ \{\tilde{w}, x, y\} \in \tilde{\Omega} \end{cases} \end{aligned} \tag{40}$$

The feasible set $\tilde{\Omega}$ of this second step is therefore a subset of Ω — $\tilde{\Omega} \subset \Omega$. For instance, imposing a cash constraint and bounds on the number of holdings gives:

$$\tilde{\Omega} = \left\{ \tilde{w} \in \Omega : 1 - c^+ \leq \mathbf{1}_n^\top \tilde{w} \leq 1, \mathcal{N}^- \leq \mathbf{1}_n^\top x \leq \mathcal{N}^+ \right\}$$

This second optimization is referred to as *implementation gap minimization*.

Remark 16. *The implementation gap corresponds to the active share between the investable portfolio and the model portfolio:*

$$\mathcal{IG}_{ap} = \mathcal{AS}\left(\tilde{w} \mid w^\star\right) = \frac{1}{2V} \sum_{i=1}^{n} |x_i^\star \, \mathrm{MT}_i \, p_i + y_i^\star \, \mathrm{LS}_i \, p_i - w_i^\star V|$$

It can be calculated for the two approaches (Figure 21).

3.6.3 Example

We consider the yield maximization problem presented in Section 3.2.2 on page 57. We recall that the corresponding constraints are:

- Increase duration by 0.20 to 0.50 year relative to the index;
- Limit concentration risk by capping the weight of issuers at 1%;
- Impose a maximum active share of $\mathcal{AS}^+$;

- Impose the following constraints on duration times spread contributions:
  - Overweight the DTS of bonds in the 5Y bucket by at least 100 bps;
  - Overweight the DTS of bonds in the 7Y bucket by 25 to 100 bps;
  - Underweight the DTS of bonds in the 10Y+ bucket by −100 to −25 bps
  - Overweight the DTS of bonds in the financials sector by at least 100 bps;
  - Underweight the DTS of bonds rated A by −100 to −25 bps;
  - Overweight the DTS of bonds rated BBB by 25 to 100 bps;

In addition to these continuous constraints, we impose the following integer constraints:

- The maximum cash ratio c^+ is set to 2%.
- The total portfolio value V takes the values 50 mn, 100 mn, 500 mn, and 1 bn.
- We consider two cases: one with no holding constraint, and one requiring at least 150 holdings.

Without active share limit Results for the ER00 Index are reported in Tables 16, 17 and 18. When there is no active share constraint, it is easy to find an investable portfolio close to the model portfolio, using either the one-step or two-step approach. In fact, investable portfolios achieve the same yield as the optimal continuous portfolio. Moreover, the cash constraint is never reached. The results are quite similar when we consider the C0A0 and G0BC indices (see Tables 34–40 on pages 117–120). However, we note that the cash constraint is reached using the two-step approach with the G0BC investment universe.

Table 16: Optimal investable portfolios (Barra model, ER00 Index, end of May 2026, one-step approach, no cardinality constraint, no active share limit)

Statistic	Benchmark	Continuous	50 mn	100 mn	500 mn	1 bn
Holdings	4 663	104	115	114	116	119
Active share (in %)		97.85	97.67	97.74	97.75	97.66
ENB (w)	3 940	101	108	104	102	102
Top 100 weight (in %)	5.36	99.00	94.34	97.11	98.47	98.39
$\sigma\left(w \mid b\right)$ (in bps)		87.62	90.31	90.95	88.19	87.38
$\sigma_{\mathcal{F}}\left(w \mid b\right)$ (in bps)		85.01	87.96	88.55	85.62	84.86
$\sigma_{\epsilon}\left(w \mid b\right)$ (in bps)		2.61	2.35	2.41	2.57	2.52
Yield (in %)	3.47	4.18	4.17	4.18	4.18	4.18
$\beta_{\text{DTS}}\left(w \mid b\right)$	1.00	1.45	1.46	1.46	1.45	1.45
MD (in year)	4.48	4.68	4.68	4.69	4.68	4.68
5Y DTS (in bps)	92	192	192	192	192	192
7Y DTS (in bps)	101	126	126	126	126	126
10Y+ DTS (in bps)	48	23	23	23	23	23
Financials DTS (in bps)	128	234	235	230	234	233
A-rated DTS (in bps)	159	134	134	134	134	134
BBB-rated DTS (in bps)	193	293	293	293	293	293
c_{ash} (in %)			0.00	0.00	0.00	0.00
$\mathcal{C}_{ash}$ (in €)			1 648	2 108	2	62
$\mathcal{IG}_{ap}$ (in %)			9.26	4.59	1.57	1.55

Table 17: Optimal investable portfolios (Barra model, ER00 Index, end of May 2026, one-step approach, at least 150 holdings, no active share limit)

Statistic	Benchmark	Continuous	50 mn	100 mn	500 mn	1 bn
Holdings	4 663	104	150	150	151	150
Active share (in %)		97.85	97.60	97.68	97.67	97.65
ENB (w)	3 940	101	109	105	103	102
Top 100 weight (in %)	5.36	99.00	93.90	96.79	98.33	98.40
$\sigma\left(w \mid b\right)$ (in bps)		87.62	88.11	91.26	88.23	87.37
$\sigma_{\mathcal{F}}\left(w \mid b\right)$ (in bps)		85.01	85.71	88.86	85.67	84.86
$\sigma_{\epsilon}\left(w \mid b\right)$ (in bps)		2.61	2.40	2.39	2.56	2.51
Yield (in %)	3.47	4.18	4.17	4.18	4.18	4.18
$\beta_{\text{DTS}}\left(w \mid b\right)$	1.00	1.45	1.46	1.46	1.46	1.45
MD (in year)	4.48	4.68	4.68	4.69	4.68	4.68
5Y DTS (in bps)	92	192	192	192	192	192
7Y DTS (in bps)	101	126	126	126	126	126
10Y+ DTS (in bps)	48	23	23	23	23	23
Financials DTS (in bps)	128	234	233	231	234	233
A-rated DTS (in bps)	159	134	134	134	134	134
BBB-rated DTS (in bps)	193	293	293	293	293	293
c_{ash} (in %)			0.00	0.00	0.00	0.00
$\mathcal{C}_{ash}$ (in €)			2	2 054	189	825
$\mathcal{IG}_{ap}$ (in %)			7.64	4.74	1.26	1.58

Table 18: Optimal investable portfolios (Barra model, ER00 Index, end of May 2026, two-step approach, no cardinality constraint, no active share limit)

Statistic	Benchmark	Continuous	50 mn	100 mn	500 mn	1 bn
Holdings	4 663	104	113	112	111	114
Active share (in %)		97.85	96.77	97.37	97.67	97.60
ENB (w)	3 940	101	110	106	102	103
Top 100 weight (in %)	5.36	99.00	94.07	96.71	98.56	97.92
$\sigma\left(w \mid b\right)$ (in bps)		87.62	85.43	86.93	87.48	87.31
$\sigma_{\mathcal{F}}\left(w \mid b\right)$ (in bps)		85.01	82.95	84.41	84.89	84.80
$\sigma_{\epsilon}\left(w \mid b\right)$ (in bps)		2.61	2.49	2.53	2.59	2.51
Yield (in %)	3.47	4.18	4.09	4.15	4.17	4.17
$\beta_{\text{DTS}}\left(w \mid b\right)$	1.00	1.45	1.44	1.45	1.45	1.45
MD (in year)	4.48	4.68	4.68	4.68	4.68	4.68
5Y DTS (in bps)	92	192	192	192	192	192
7Y DTS (in bps)	101	126	126	126	126	126
10Y+ DTS (in bps)	48	23	23	23	23	23
Financials DTS (in bps)	128	234	228	233	233	235
A-rated DTS (in bps)	159	134	127	131	134	134
BBB-rated DTS (in bps)	193	293	292	293	293	293
c_{ash} (in %)			1.92	0.78	0.18	0.25
$\mathcal{C}_{ash}$ (in k€)			961.1	777.4	900.4	2 479
$\mathcal{IG}_{ap}$ (in %)			4.53	1.92	0.38	0.97

The framework admits several natural extensions. In the one-step approach, the objective function can be modified to account for the return earned on residual cash:

$$\{x^\star, y^\star\} = \arg\max \sum_{i=1}^{n} \tilde{w}_i \mu_i + r_{cash} \left(1 - \sum_{i=1}^{n} \tilde{w}_i\right) \tag{41}$$

where r_{cash} is the cash return. Similarly, the two-step implementation gap minimization can be extended to penalize excess cash holdings:

$$\{x^\star, y^\star\} = \arg\min \frac{1}{2} \sum_{i=1}^{n} |\tilde{w}_i - w_i^\star| + \varphi \left(1 - \sum_{i=1}^{n} \tilde{w}_i\right) \tag{42}$$

where $\varphi \geq 0$ is a penalty parameter governing the trade-off between the implementation gap and residual cash. As φ increases, the optimizer progressively reduces residual cash at the cost of a wider implementation gap. Results are reported in Tables 19, 37 and 41. We also note that the portfolio yield has increased, especially for the G0BC Index.

Table 19: Optimal investable portfolios (Barra model, ER00 Index, end of May 2026, two-step approach, no cardinality constraint, no active share limit, $\varphi = 1$)

Statistic	Benchmark	Continuous	50 mn	100 mn	500 mn	1 bn
Holdings	4 663	104	129	168	118	347
Active share (in %)		97.85	97.58	97.61	97.63	97.50
ENB (w)	3 940	101	108	105	102	103
Top 100 weight (in %)	5.36	99.00	94.24	96.81	98.56	98.23
$\sigma\left(w \mid b\right)$ (in bps)		87.62	83.11	86.94	87.35	87.19
$\sigma_{\mathcal{F}}\left(w \mid b\right)$ (in bps)		85.01	80.56	84.40	84.76	84.67
$\sigma_{\epsilon}\left(w \mid b\right)$ (in bps)		2.61	2.55	2.54	2.60	2.52
Yield (in %)	3.47	4.18	4.15	4.17	4.18	4.18
$\beta_{\text{DTS}}\left(w \mid b\right)$	1.00	1.45	1.44	1.45	1.45	1.45
MD (in year)	4.48	4.68	4.69	4.69	4.68	4.68
5Y DTS (in bps)	92	192	192	192	193	192
7Y DTS (in bps)	101	126	126	126	126	126
10Y+ DTS (in bps)	48	23	23	23	23	22
Financials DTS (in bps)	128	234	228	232	234	234
A-rated DTS (in bps)	159	134	134	134	134	134
BBB-rated DTS (in bps)	193	293	290	293	293	293
c_{ash} (in %)			0.00	0.00	0.00	0.00
$\mathcal{C}_{ash}$ (in €)			389	644	940	1 882
$\mathcal{IG}_{ap}$ (in %)			5.49	2.32	0.46	1.09

Numerical experiments offer valuable insights into the performance of investable portfolio formulations. The one-step approach is remarkably robust. Regardless of the size of the portfolio or investment universe, the resulting investable portfolio is close to the continuous solution in terms of expected yield and risk exposure. This confirms that integer constraints introduce only marginal distortions in practice. As expected, the implementation gap narrows as the size of the portfolio increases because larger portfolios can spread capital across a greater number of bonds, more faithfully replicating the continuous solution. Beyond size, the structure and liquidity of the investment universe also play a decisive role. The gap remains negligible for concentrated, liquid universes, such as C0A0. However, it is more difficult to replicate broader, multi-currency universes, such as G0BC, due to greater

heterogeneity in lot sizes and minimum tradable amounts. To mitigate these errors, the implementation gap minimization approach uses the available cash budget as an additional degree of freedom to systematically absorb discrepancies arising from lot size constraints. Together, the one-step and two-step approaches highlight the fundamental trade-off in investable portfolio construction: maximizing expected yield versus faithfully reproducing the optimal continuous allocation.

With active share limit Introducing constraints on active share complicates optimization and does not always guarantee a solution. This issue arises even in the continuous case. We can divide the set of constraints into two groups:

$$\begin{cases} w \in \Omega \\ \dfrac{1}{2}\sum_{i=1}^{n} |w_i - b_i| \leq \mathcal{AS}^+ \end{cases}$$

In fact, the maximum active share $\mathcal{AS}^+$ must be sufficiently high to guarantee the existence of a solution. Assuming that $w \in \Omega \neq \emptyset$, this means that $\mathcal{AS}^+ \notin [0,1]$ but $\mathcal{AS}^+ \in [\mathcal{AS}^\star_-, 1]$. For example, in the previous applications (Sections 3.1 and 3.2 on pages 49–59), we chose four values of $\mathcal{AS}^+$: 25%, 30%, 40%, and 100%. This is because $\mathcal{AS}^\star_- \approx 17\%$ in the case of the ER00 Index. Therefore, no solution exists if $\mathcal{AS}^+$ is set to 10% or 15%, which explains why all the applications begin at $\mathcal{AS}^+ = 25\%$. In the discrete case, the set of constraints becomes:

$$\begin{cases} \tilde{w} \in \tilde{\Omega}_w = \Omega \\ \{x, y\} \in \tilde{\Omega}_{x,y} = \left\{ x_i = 0, 1; y_i = 0, 1, \ldots, y_i^+ \right\} \\ \tilde{w}_i = x_i \dfrac{\mathrm{MT}_i\, p_i}{V} + y_i \dfrac{\mathrm{LS}_i\, p_i}{V} \\ \dfrac{1}{2}\sum_{i=1}^{n} |\tilde{w}_i - b_i| \leq \mathcal{AS}^+ \end{cases}$$

Assuming that $\tilde{w} \in \tilde{\Omega}_w \cap \{x, y\} \in \tilde{\Omega}_{x,y} \neq \emptyset$, we obtain $\mathcal{AS}^+ \in [\mathcal{AS}^*_-(V), 1]$, where $\mathcal{AS}^*_-(V) \geq \mathcal{AS}^\star_-$. The lower bound on the maximum active share is higher than in the continuous case by construction and depends on the portfolio value V. However, because of the tradability constraints on the investable portfolio, we may face situations where $\mathcal{AS}^*_-(V) \gg \mathcal{AS}^\star_-$.

From a numerical standpoint, the lower bounds are calculated using the following optimization problems:

$$\begin{aligned} \mathcal{AS}^\star_- \quad = \quad & \inf \frac{1}{2}\sum_{i=1}^{n} |w_i - b_i| \\ & \text{s.t.} \quad w \in \Omega \end{aligned}$$

and:

$$\begin{aligned} \mathcal{AS}^*_-(V) \quad = \quad & \inf \frac{1}{2}\sum_{i=1}^{n} |\tilde{w}_i - b_i| \\ & \text{s.t.} \quad \begin{cases} \tilde{w} \in \tilde{\Omega}_w \\ \{x, y\} \in \tilde{\Omega}_{x,y} \\ \tilde{w}_i = x_i \dfrac{\mathrm{MT}_i\, p_i}{V} + y_i \dfrac{\mathrm{LS}_i\, p_i}{V} \end{cases} \end{aligned}$$

We have $\lim_{V \to \infty} \mathcal{AS}^*_-(V) = \mathcal{AS}^\star_-$.

Figure 22: Relationship between the lower bound of the maximum active share and the portfolio value (ER00 Index, end of May 2026)

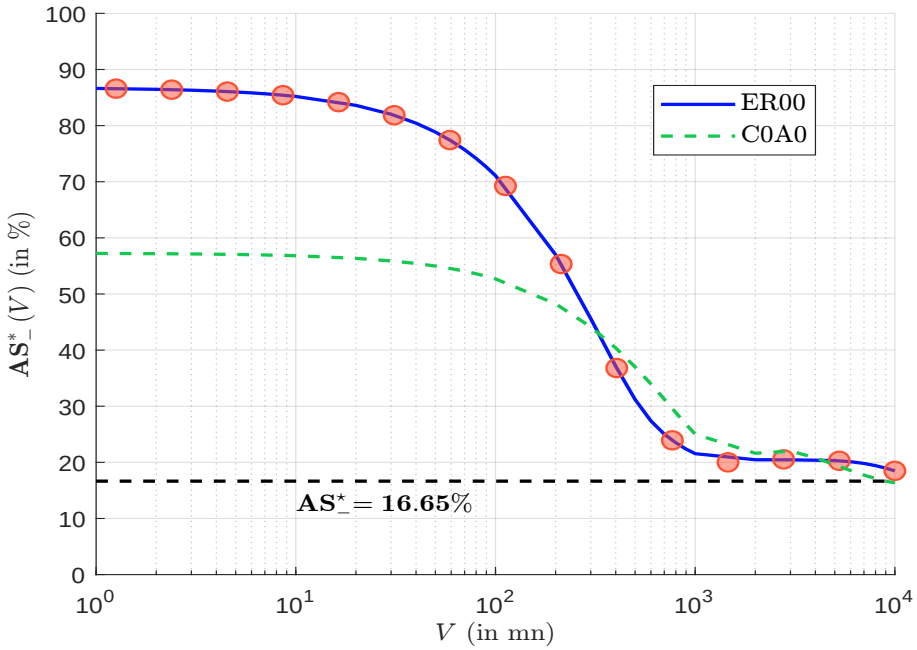

In Table 20, we report the estimated values of $\mathcal{AS}^{\star}_{-}$ and $\mathcal{AS}^{*}_{-}(V)$. The continuous minimum active share $\mathcal{AS}^{\star}_{-}$ is equal to 16.65%, 12.02%, and 9.81% for the ER00, C0A0, and G0BC indices, respectively. The magnitude of $\mathcal{AS}^{\star}_{-}$ depends primarily on the number of securities in the investment universe. By contrast, the magnitude of $\mathcal{AS}^{*}_{-}(V)$ depends on three factors: the number of securities, the trading characteristics of the universe, and the portfolio value V. The continuous minimum active share tends to be lower when the investment universe is large because the optimizer has more flexibility in the security selection process. This explains why $\mathcal{AS}^{\star}_{-}$ is lower for G0BC than for ER00 (9.81% vs. 16.65%). For investable portfolios, the distribution of minimum tradable amounts and lot sizes plays an additional role alongside the number of holdings. For example, if the average minimum tradable amount is \$1 000 in one universe and \$100 000 in another, then the first universe is more flexible. This makes it easier to construct an investable portfolio. Portfolio value V also matters, since a larger portfolio can accommodate more bonds at their minimum tradable sizes. Because of the interplay of these three factors, $\mathcal{AS}^{*}_{-}(V)$ does not vary monotonically across universes or portfolio sizes (Figure 22). For instance, $\mathcal{AS}^{*}_{-}(V)$ is lower for C0A0 than for ER00 at a portfolio size of \$50 million, but higher at \$1 billion (Table 20). This reversal occurs because minimum tradable amounts are generally lower for C0A0 than for ER00, favouring C0A0 at small portfolio sizes, whereas ER00 has fewer holdings than C0A0. This difference becomes the dominant factor at larger portfolio sizes.

Table 20: Lower bound of the maximum active share (end of May 2026)

Index	Holdings	$\mathcal{AS}^{\star}_{-}$	$\mathcal{AS}^{*}_{-}(V)$			
			50 mn	100 mn	500 mn	1 bn
ER00	4 663	16.65%	79.95%	68.13%	30.73%	21.68%
C0A0	11 507	12.02%	58.08%	50.59%	36.99%	23.78%
G0BC	20 350	9.81%	84.72%	83.09%	52.30%	41.20%

4 Conclusion

The academic quest to apply quantitative allocation models to fixed income began shortly after the advent of mean-variance optimization, pioneered by Cheng (1962), who adapted the Markowitz framework to determine the optimal maturity distribution of debt issues. Despite this early foundation, subsequent academic literature shifted away from portfolio optimization toward specialized single-security analytics. On the practitioner side, interest in bond portfolio optimization remained slower to develop. It is only sparsely present in the *Yield Book* and the broader body of work of Martin Leibowitz, who was one of the foremost authorities in fixed-income securities and a pioneer in liability-driven investment and maturity matching (Bernstein, 2007). Against this backdrop, the objective of this paper is to present a comprehensive framework for bond portfolio optimization at the individual security level. By synthesizing the existing literature on the subject, this study aims to highlight the practical solutions currently available to market participants. Rather than introducing novel concepts, this paper is intended to serve as a reference guide for practitioners and academics navigating the field of bond portfolio optimization.

We first show that the limited adoption of bond portfolio optimization is structural rather than merely historical. Three fundamental challenges distinguish fixed-income optimization from its equity and multi-asset counterparts. The first challenge involves risk measurement. Bond volatility and correlation are non-stationary by construction. As a bond approaches maturity, its duration — and therefore its sensitivity to interest rate changes — decreases mechanically, causing the volatility to converge to zero. Similarly, bond correlation depends on several sources of co-movement, such as correlation between interest rates, correlation between credit spreads, and correlation between default times. These properties make the empirical covariance matrix, which is the standard input of mean-variance optimization, unreliable as bonds age. Another important consequence is that the standard deviation of bond returns is not necessarily an appropriate measure of bond risk. Similarly, tracking error volatility may not be the most appropriate metric for measuring the tracking risk of a bond portfolio relative to a benchmark. For instance, practitioners often use other concepts such as modified duration and duration times spread instead of price-based metrics to define bond risk. The second challenge concerns the structure of the investment universe. Bond indices are considerably larger and more heterogeneous than their equity counterparts. A single issuer may have dozens of outstanding securities that differ in terms of maturity, coupon, seniority, and currency. Moreover, the composition of the index changes continuously as bonds are issued and mature. This complexity makes direct application of classical portfolio optimization difficult and explains why practitioners have traditionally relied on bucket matching, duration control, and security selection rather than on formal mathematical optimization. The third challenge is the gap between a model portfolio and an investable portfolio. Unlike equities, bonds are subject to minimum tradable amount and lot size constraints. These trading constraints and liquidity issues of the bond market make the rounding of continuous weights into integer positions a non-trivial problem, particularly for smaller portfolio sizes. This can lead to substantial deviation from the theoretical optimum.

To address these challenges, we develop a unified optimization framework that accommodates the structural specificities of fixed-income markets. We consider a family of optimization problems with and without a benchmark, under alternative risk factor models and various practical constraints. Our framework is based on a generic formulation of the risk measure as a linear combination of several risk metrics, including volatility risk, duration risk, and spread risk. In a similar way, we consider several sources of expected returns that can be incorporated into the objective function. As a parsimonious yet realistic representation of bond risk, we focus on a two-factor model based on modified duration and duration

times spread. This model captures the dominant role of interest rate and credit spread risk while remaining tractable. For more sophisticated applications, we also consider multi-factor risk models, which allow for a richer decomposition of portfolio risk into common factor and specific risk contributions. A central methodological contribution of this paper is the distinction between ℓ_1-norm and ℓ_2-norm portfolio optimization problems. We show how these formulations can be cast as linear and quadratic programming problems, respectively, using the properties of quadratic and extended linear forms. Moreover, we illustrate how combining ℓ_1 and ℓ_2 norms results in richer and more flexible optimization problems. In addition to linear and quadratic programming techniques, we show how specific algorithms, such as the alternating direction method of multipliers and proximal operators, can solve challenging bond optimization problems. We pay particular attention to the active share constraint, which plays a central role in fixed-income portfolio management. Unlike its equity counterpart, the active share of a bond portfolio is mechanically high due to the large size and continuous turnover of bond indices. Therefore, it must be handled carefully during the optimization. Finally, to bridge the gap between the model and investable portfolios, we show how the continuous optimization problem can be extended to a mixed-integer program that explicitly considers minimum tradable amounts and lot size constraints. We also discuss one-step and two-step approaches to solving this problem in practice (single-step discrete optimization vs. implementation gap minimization).

The second part of the paper presents a series of empirical applications conducted on the ICE BofA Corporate Bond indices (EUR, USD, and Global), which illustrate the practical relevance of the methodological choices discussed above. These three indices contain 4 663, 11 507, and 20 350 securities at the end of May 2026, respectively, which gives a sense of the scale of the optimization problems considered. The first application compares ℓ_1- and ℓ_2-norm solutions and shows that, while they lead to similar risk-return profiles, they produce different portfolio structures. The ℓ_1 solutions tend to be sparser and more concentrated, while the ℓ_2 solutions are more diversified. We also illustrate how the two norms generate fundamentally different concepts of tracking error risk with significant implications for portfolio construction. The second application considers the Barra multi-factor risk model and confirms that the choice of the risk model has a significant impact. Richer factor models generally produce lower tracking error, but they can also lead to more concentrated active portfolios and allow for a finer decomposition of portfolio risk into common factor and specific risk contributions. Comparing the efficient frontiers obtained with the ℓ_2-norm risk model and the Barra multi-factor model further shows that tracking error volatilities in bond markets are highly definition-dependent, much more than in equity markets. The third application addresses active portfolio management, where expected excess returns are decomposed into carry, rolldown, and repricing components. We show how these components can be integrated into a systematic optimization framework. Using sector views formulated by the portfolio manager, we illustrate that the shape of the efficient frontier is highly sensitive to the degree of confidence assigned to those views. The fourth application considers the classical problem of portfolio decarbonization and shows that significant reductions in carbon intensity can be achieved at a modest cost in terms of tracking error if the optimization problem is structured properly. The fifth application examines the sensitivity of portfolio construction to alternative clustering and bucketing methodologies. It confirms that the choice of segmentation significantly impacts the resulting portfolio. This underscores the importance of aligning the optimization architecture with the investment process. In particular, we show how bucketing methodologies can serve as a practical tool for portfolio managers to control the tracking risk of their portfolios in a transparent and interpretable way. The sixth and final application reveals that the construction of investable portfolios is a primary issue in fixed-income optimization. Converting continuous weights

into integer positions subject to minimum tradable amounts, lot size constraints, and cash management requirements, introduces substantial deviations from the theoretical optimum. This issue is particularly acute for smaller portfolio sizes, and must be managed explicitly within the optimization process rather than treated as a post-processing afterthought. This issue is particularly acute when active share constraints are imposed because the interaction between cardinality and active share creates additional combinatorial complexity.

Looking ahead, several factors suggest that bond portfolio optimization will become increasingly central to fixed-income asset management. One of the major historical obstacles to its development has been computational feasibility. In equity markets, portfolio optimization could be applied to relatively small investment universes. For instance, country indices such as the CAC 40, the FTSE 100, the DAX 30, MSCI indices, and even the S&P 500 Index were tractable with quadratic programming from an early stage (Perrin and Roncalli, 2020). In fixed income, by contrast, bond indices typically contain thousands of securities, making the optimization problem considerably more challenging. Yet the past two decades have fundamentally changed this landscape. Genetic algorithms, which were indispensable for solving investable portfolio problems a decade ago, have largely been replaced by mixed-integer programming solvers, due to dramatic increases in computational power and the maturation of numerical optimization libraries. Looking further ahead, the emergence of quantum computing promises to make bond portfolio optimization faster, more scalable, and more accessible. This could remove the computational barriers that have historically constrained its adoption, opening the door to optimization at a scale and speed that are currently out of reach. The rapid growth of the active fixed-income ETF market is the second factor driving renewed interest in bond portfolio optimization. The ETF structure prioritizes benchmarking and transparency, regardless of the management style (active or passive). Benchmarking requires the continuous measurement, control, and reporting of tracking error risk. Meanwhile, ETF transparency obligations demand a disciplined, fully auditable investment process. A formal optimization framework naturally and efficiently meets these requirements by producing systematic, reproducible, and well-documented portfolio decisions. In addition, the market-making mechanism that underpins ETF liquidity requires this same level of systematic and operationally robust portfolio construction, as authorized participants must be able to efficiently create and redeem shares using a well-defined and replicable process. Beyond these structural requirements, rapid growth and increasing competition in the active ETF space pressure managers to combine multiple sources of systematic alpha in a scalable and consistent manner, rather than relying solely on discretionary bond selection. This is a challenge that the emerging *quantamental* approach seeks to address by blending quantitative and fundamental analysis. Taken together, these forces make portfolio optimization essential for any asset manager seeking to develop and scale a competitive, active fixed-income ETF franchise.

These institutional drivers raise a more fundamental issue. Tracking error risk in fixed income is difficult to measure because it is highly definition-dependent. Unlike in equity markets, where a covariance matrix estimated from historical returns provides a reasonably consistent measure of risk, the bond market offers no such simple benchmark. Our results illustrate this ambiguity. For the same portfolio, the $\boldsymbol{\ell}_1$ tracking error can be roughly three times larger than the $\boldsymbol{\ell}_2$ tracking error, and both differ from the figures obtained under a richer multi-factor model. This raises a rarely asked, yet central, question in fixed-income risk management: What precisely does tracking error measure? Is it primarily interest rate risk, reflecting duration mismatches with the benchmark? Or is it spread risk, capturing divergences in credit exposure? Or, in the case of lower-quality credit, is it default risk, reflecting differences in the probability and severity of issuer-specific losses? Each of these dimensions requires a different risk model. Moreover, the relevant definition is unlikely to

be universal. It must adapt to the investment universe. For sovereign bonds, where credit risk is generally limited, interest rate risk naturally dominates the definition of tracking error. For investment grade corporate bonds, spread risk becomes increasingly important alongside duration risk. For high yield bonds, default risk and idiosyncratic credit events play a significant role. A tracking error measure that ignores these dimensions may give a misleading picture of the true risk. As the active fixed-income ETF market continues to grow, and ex-ante tracking error becomes contractual and regulatory information rather than an internal risk metric, this ambiguity cannot be considered a technical detail. We believe that rethinking how tracking error risk is defined will become increasingly central to the future of bond portfolio optimization.

References

Abbas, A., Ambainis, A., Augustino, B., ..., and Zoufal, C. (2024). Challenges and Opportunities in Quantum Optimization. *Nature Reviews Physics*, 6(12), p. 718-735.

Alreshidi, N. (2019). *Two-Stage Mixed Integer Stochastic Programming and Its Application to Bond Portfolio Optimization*. PhD Dissertation, Florida Institute of Technology.

Bajo Traver, M. (2026). Break-Even Yield in Fixed-Income Portfolios: A Unifying Framework for Carry and Risk-Based Allocation. *SSRN*, 6480378, 48 pages.

Barahhou, I., Ben Slimane, M., Oulid Azouz, N., and Roncalli, T. (2022). Net Zero Investment Portfolios — Part 1. The Comprehensive Integrated Approach. *SSRN*, 4283998.

Barra (2007). *Barra Risk Model*. 202 pages.

Bekkers, N., Doeswijk, R. Q., and Lam, T. (2009). Strategic Asset Allocation: Determining the Optimal Portfolio with Ten asset classes. *Journal of Wealth Management*, 12(3), pp. 61-77.

Belotti, P., Kirches, C., Leyffer, S., Linderoth, J., Luedtke, J., and Mahajan, A. (2013). Mixed-integer Nonlinear Optimization. *Acta Numerica*, 22, pp. 1-131.

Ben Slimane, M. (2021). Bond Index Tracking with Genetic Algorithms. *Amundi Working Paper*, 108, 53 pages.

Ben Slimane, M., De Jong, M., Dumas, J. M., Fredj, H., Sekine, T., and Srb, M. (2019). Traditional and Alternative Factors in Investment Grade Corporate Bond Investing. *Amundi Working Paper*, 78, 88 pages.

Ben Slimane, M., Brard, E., Le Guenedal, T., Roncalli, T., and Sekine, T. (2019). ESG Investing in Fixed Income: It's Time to Cross the Rubicon. *SSRN*, 3683477, 23 pages.

Ben Slimane, M., Le Guenedal, T., Roncalli, T., and Sekine, T. (2019). ESG Investing in Corporate Bonds: Mind the Gap. *SSRN*, 3683472, 61 pages.

Ben Slimane, M., Lucius, D., Roncalli, T., and Xu, J. (2023). Net Zero Investment Portfolios — Part 2. The Core-Satellite Approach. *SSRN*, 4611418.

Ben Slimane, M., and Menchaoui, G. (2023). Bond Portfolio Optimisation and Mixed Integer Programming. *Amundi Working Paper*, 152, 26 pages.

Bengio, Y., Lodi, A., and Prouvost, A. (2021). Machine Learning for Combinatorial Optimization: A Methodological Tour d'Horizon. *European Journal of Operational Research*, 290(2), pp. 405-421.

Bernstein, P. L. (2007). *Capital Ideas Evolving*. John Wiley & Sons.

Bessler, W., Opfer, H., and Wolff, D. (2017). Multi-asset Portfolio Optimization and Out-of-sample Performance: An Evaluation of Black–Litterman, Mean-variance, and Naïve Diversification Approaches. *European Journal of Finance*, 23(1), pp. 1-30.

Boyd, S., Parikh, N., Chu, E., Peleato, B., and Eckstein, J. (2011). Distributed Optimization and Statistical Learning via the Alternating Direction Method of Multipliers. *Foundations and Trends® in Machine learning*, 3(1), pp. 1-122.

Bruder, B., Dao, T. L., Richard, J. C., and Roncalli, T. (2011). Trend Filtering Methods for Momentum Strategies. *SSRN*, 2289097.

Bruder, B., Gaussel, N., Richard, J. C., and Roncalli, T. (2013). Regularization of Portfolio Allocation. *SSRN*, 2767358.

Caldeira, J. F., Moura, G. V., and Santos, A. A. (2016). Bond Portfolio Optimization using Dynamic Factor Models. *Journal of Empirical Finance*, 37, pp. 128-158.

Chandrasekhar, R. (2009). Fixed-income Portfolio Optimization. *University of Texas at Austin, Master of Science in Engineering Report*, 81 pages.

Cheng, P. L. (1962). Optimum Bond Portfolio Selections. *Management Science*, 8(4), pp. 490-499.

Conforti, M., Cornuéjols, G., and Zambelli, G. (2014). *Integer Programming*. Graduate Texts in Mathematics, 271, Springer.

Deguest, R., Fabozzi, F., Martellini, L., and Milhau, V. (2018). Bond Portfolio Optimization in the Presence of Duration Constraints. *Journal of Fixed Income*, 28(1), pp. 6-26.

DeMiguel, V., Garlappi, L., and Uppal, R. (2009). Optimal Versus Naive Diversification: How Inefficient is the 1/N Portfolio Strategy?. *Review of Financial Studies*, 22(5), pp. 1915-1953.

Del Pia, A., Dey, S. S., and Molinaro, M. (2017). Mixed-integer Quadratic Programming is in NP. *Mathematical Programming*, 162(1), pp. 225-240.

Drenovak, M., Ranković, V., Urošević, B., and Jelic, R. (2021). Bond Portfolio Management under Solvency II Regulation. *European Journal of Finance*, 27(9), pp. 857-879.

Dykstra, R. L. (1983). An Algorithm for Restricted Least Squares Regression. *Journal of the American Statistical Association*, 78(384), pp. 837-842.

Elton, E. J., Gruber, M. J., Brown, S. J., and Goetzmann, W. N. (2009). *Modern Portfolio Theory and Investment Analysis*. John Wiley & Sons.

Fabozzi, F. J. (2001). *Bond Portfolio Management*. Wiley, 728 pages.

Fabozzi, F. J., Focardi, S. M., and Kolm, P. N. (2010). *Quantitative Equity Investing: Techniques and Strategies*. John Wiley & Sons.

Fabozzi, F. J., Martellini, L., and Priaulet, P. (2008). *Advanced Bond Portfolio Management*. Wiley, 576 pages.

Fabozzi, F. J., and Pollack, I. M. (1983). *The Handbook of Fixed-Income Securities*. Dow Jones-Irwin (Homewood, Illinois).

Focardi, S. M., and Fabozzi, F. J. (2004). A Methodology for Index Tracking based on Time-series Clustering. *Quantitative Finance*, 4(4), pp. 417-425.

Gabay, D., and Mercier, B. (1976). A Dual Algorithm for the Solution of Nonlinear Variational Problems via Finite Element Approximation. *Computers & Mathematics with Applications*, 2(1), pp. 17-40.

Goldberg, D. E. (1989). *Genetic Algorithms in Search, Optimization, and Machine Learning*. Addison-Wesley.

Gomory, R. E. (1958). Outline of an Algorithm for Integer Solutions to Linear Programs. *Bulletin of the American Mathematical Society*, 64(5), pp. 275-278.

Gouzilh, L., de Jong, M., Lebaupain, T., and Wu, H. (2014). The Art of Tracking Corporate Bond Indices. *Amundi Working Paper*, 42, 21 pages.

Hamdan, R., Pavlowsky, F., Roncalli, T., and Zheng, B. (2016). A Primer on Alternative Risk Premia. *SSRN*, 2766850.

Jusselin, P., Lezmi, E., Malongo, H., Masselin, C., Roncalli, T., and Dao, T. L. (2017). Understanding the Momentum Risk Premium: An In-depth Journey Through Trend-following Strategies. *SSRN*, 3042173, 102 pages.

Koijen, R. S., Moskowitz, T. J., Pedersen, L. H., and Vrugt, E. B. (2018). Carry. *Journal of Financial Economics*, 127(2), pp. 197-225.

Kolm, P. N., Tütüncü, R., and Fabozzi, F. J. (2014). 60 Years of Portfolio Optimization: Practical Challenges and Current Trends. *European Journal of Operational Research*, 234(2), pp. 356-371.

Konno, H., and Watanabe, H. (1996). Bond Portfolio Optimization Problems and Their Applications to Index Tracking: A Partial Optimization Approach. *Journal of the Operations Research Society of Japan*, 39(3), pp. 295-306.

Korn, O., and Koziol, C. (2006). Bond Portfolio Optimization: A Risk-return Approach. *Journal of Fixed Income*, 15(4), pp. 48-60.

Laloux, L., Cizeau, P., Bouchaud, J. P., and Potters, M. (1999). Noise Dressing of Financial Correlation Matrices. *Physical Review Letters*, 83(7), pp. 1467-1470.

Land, A. H., and Doig, A. G. (1960). An Automatic Method of Solving Discrete Programming Problems. *Econometrica*, 28(3), pp. 497-520.

Le Guenedal, T., and Roncalli, T. (2022). Portfolio Construction with Climate Risk Measures. In Jurczenko, E. (Ed.), *Climate Investing: New Strategies and Implementation Challenges*, Wiley, December 2022, pp. 49-86.

Ledoit, O., and Wolf, M. (2004). Honey, I Shrunk the Sample Covariance Matrix. *Journal of Portfolio Management*, 30(4), pp. 110-119.

Leibowitz, M. L., Homer, S., Bova, A. and Kogelman, S. (2013). *Inside the Yield Book: The Classic That Created the Science of Bond Analysis*. Third edition, John Wiley & Sons (first edition published in 1972).

Luciani, F., and Roncalli, T. (2026). From Transition to Physical Risk: Rethinking Portfolio Management. *SSRN*, 6366120.

Luxenberg, E., Schiele, P., and Boyd, S. (2024). Robust Bond Portfolio Construction via Convex-Concave Saddle Point Optimization. *Journal of Optimization Theory and Applications*, 201(3), pp. 1089-1115.

Markowitz, H. M. (1952), Portfolio Selection. *Journal of Finance*, 7(1), pp. 77-91.

Nemhauser, G. L., and Wolsey, L. A. (1988). *Integer and Combinatorial Optimization*. Interscience Series in Discrete Mathematics and Optimization, 18, Wiley.

Padberg, M., and Rinaldi, G. (1991). A Branch-and-cut Algorithm for the Resolution of Large-scale Symmetric Traveling Salesman Problems. *SIAM Review*, 33(1), pp. 60-100.

Parikh, N., and Boyd, S. (2014). Proximal Algorithms. *Foundations and Trends® in Optimization*, 1(3), pp. 127-239.

Perrin, S., and Roncalli, T. (2020). Machine Learning Optimization Algorithms & Portfolio Allocation. In Jurczenko, E. (Ed.), *Machine Learning for Asset Management: New Developments and Financial Applications*, Wiley, Chapter 8, pp. 261-328.

Puhle, M. (2008). *Bond Portfolio Optimization*. Springer.

Roncalli, T. (2017). Alternative Risk Premia: What Do We Know?. In Jurczenko, E. (Ed.), *Factor Investing: From Traditional to Alternative Risk Premia*, Elsevier.

Roncalli, T. (2026). *Handbook of Sustainable Finance*. *SSRN*, 4277875.

Rudd, A. (1980). Optimal Selection of Passive Portfolios. *Financial Management*, 9(1), pp. 57-66.

Tibshirani, R. J. (2017). Dykstra's Algorithm, ADMM, and Coordinate Descent: Connections, Insights, and Extensions. In Guyon, I., Luxburg, U.V., Bengio, S., Wallach, H., Fergus, R., Vishwanathan, S., and Garnett, R. (Eds), *Advances in Neural Information Processing Systems*, 30, pp. 517-528.

Tütüncü, R. H., and Koenig, M. (2004). Robust Asset Allocation. *Annals of Operations Research*, 132(1), pp. 157-187..

Vielma, J. P. (2015). Mixed Integer Linear Programming Formulation Techniques. *Siam Review*, 57(1), pp. 3-57.

A Notations

- $\mathbf{0}_n$ is the vector of zeros.
- $\mathbf{1}_n$ is the vector of ones.
- e_i is the unit vector, i.e. $[e_i]_i = 1$ and $[e_i]_j = 0$ for all $j \neq i$.
- $x \odot y$ is the Hadamard element-wise product: $[x \odot y]_{i,j} = [x]_{i,j} [y]_{i,j}$. The product $x \odot y$ exists if x and y are compatible, *i.e.*, the number of rows and columns are either 1 or n.
- $A^\dagger$ is the Moore-Penrose pseudo-inverse matrix of A.
- $A \otimes B$ is the kronecker product, where each entry $A_{i,j}$ is replaced by the block matrix $A_{i,j} \cdot B$
- $\mathbb{1}_\Omega(x)$ is the convex indicator function of Ω: $\mathbb{1}_\Omega(x) = 0$ for $x \in \Omega$ and $\mathbb{1}_\Omega(x) = +\infty$ for $x \notin \Omega$.
- $\mathcal{A}_{ffineset}[A, B]$ is the affine set $\{x \in \mathbb{R}^n : Ax = B\}$.
- $\mathcal{AS}(w \mid b) = \frac{1}{2}\sum_{i=1}^n |w_i - b_i|$ is the active share of Portfolio w with respect to Benchmark b.
- $\mathcal{AS}_2(w \mid b) = \frac{1}{2}\sum_{i=1}^n (w_i - b_i)^2$ is the $\boldsymbol{\ell}_2$-norm version of the active share $\mathcal{AS}(w \mid b) = \frac{1}{2}\sum_{i=1}^n |w_i - b_i|$.
- $\mathcal{AS}_{\mathcal{B}}(w \mid b) = \frac{1}{2}\sum_{j=1}^{n_{\mathcal{B}}} \left|\sum_{i \in \mathcal{B}_j} w_i - \sum_{i \in \mathcal{B}_j} b_i\right|$ is the active share applied to the set of pre-defined buckets $\{\mathcal{B}_1, \ldots, \mathcal{B}_{n_{\mathrm{B}}}\}$.
- $\alpha_{k,i}$ is the k^{th} alpha signal for bond i, while $\alpha_k = (\alpha_{k,1}, \ldots, \alpha_{k,n})$ is the corresponding $n \times 1$ vector across all bonds. We also note α the corresponding $n_\mu \times n$ matrix.
- $b = (b_1, \ldots, b_n)$ is the vector of benchmark weights.
- $\mathcal{B}_{ox}\left[x^-, x^+\right]$ is the box $\left\{x \in \mathbb{R}^n : x^- \leq x \leq x^+\right\}$.
- $\mathcal{B}_p(c, r)$ is the $\boldsymbol{\ell}_p$-ball $\left\{x \in \mathbb{R}^n : \|x - c\|_p \leq r\right\}$.
- $\beta_{\mathrm{DTS}}(w \mid b)$ is the DTS beta of portfolio w relative to benchmark b.
- $c_{ash}$is the cash ratio.
- $\mathcal{C}_{ash}$ is the cash position.
- $\mathcal{C}_i$ is the carry of bond i, while $\mathcal{C} = (\mathcal{C}_1, \ldots, \mathcal{C}_n)$ is the corresponding $n \times 1$ vector across all bonds.
- $\mathbb{C}^\star_{j,k}$ is the target contribution for the j^{th} cluster and the k^{th} risk measure, while $\mathbb{C}^\star_k = \left(\mathbb{C}^\star_{1,k}, \ldots, \mathbb{C}^\star_{n_G,k}\right)$ is the corresponding $n_G \times 1$ vector across all clusters.
- $\boldsymbol{\mathcal{CI}}_i$ is the carbon intensity of bond i, while $\boldsymbol{\mathcal{CI}} = (\boldsymbol{\mathcal{CI}}_1, \ldots, \boldsymbol{\mathcal{CI}}_n)$ is the corresponding $n \times 1$ vector across all bonds.

- D is the diagonal matrix of idiosyncratic variances.
- DTS_i is the duration times spread of Bond i.
- $\delta_{j,i}$ is the indicator function: $\mathbb{1}\left\{i \in \mathcal{G}_j\right\}$, while $\delta_j = \left(\delta_{j,1}, \ldots, \delta_{j,n}\right)$ is the corresponding $n \times 1$ vector across all bonds. We also note δ the corresponding $n_{\mathcal{G}} \times n$ matrix.
- $\text{ENB}\left(w\right)$ is the effective number of bets.
- $\mathcal{G}_j$ is the j^{th} cluster or group of bonds.
- $\mathcal{H}_{alfspace}\left[c, d\right]$ is the half-space $\left\{x \in \mathbb{R}^n : c^\top x \leq d\right\}$.
- $\mathcal{H}_{yperplane}\left[a, b\right]$ is the hyperplane $\left\{x \in \mathbb{R}^n : a^\top x = b\right\}$.
- i is the bond index $(i = 1, \ldots, n)$.
- $\mathcal{IG}_{ap}$ is the implementation gap ratio.
- j is the cluster index $(j = 1, \ldots, n_{\mathcal{G}})$.
- k is the metric index (for the risk measure, $k = 1, \ldots, n_{\mathcal{R}}$, while for the alpha signal, $k = 1, \ldots, n_{\mu}$).
- $\boldsymbol{\ell}_1\left(x\right) = \left\|x\right\|_1 = \left|x_1\right| + \left|x_2\right| + \cdots + \left|x_n\right|$ is the $\boldsymbol{\ell}_1$-norm.
- $\boldsymbol{\ell}_2\left(x\right) = \left\|x\right\|_2 = \sqrt{x_1^2 + x_2^2 + \cdots + x_n^2}$ is the $\boldsymbol{\ell}_2$-norm.
- $\mathcal{LF}\left(x; c, d\right)$ is the linear form $c^\top x + d$.
- LS_i is the lot size of bond i.
- $M_{k,i}$ is the k^{th} metric (or feature) of bond i, while $M_k = \left(M_{k,1}, \ldots, M_{k,n}\right)$ is the corresponding $n \times 1$ vector across all bonds. We also note M the corresponding $n_{\mathcal{G}} \times n$ matrix.
- MD_i is the modified duration of Bond i.
- MT_i is the minimum tradable amount of bond i.
- $\mu = \left(\mu_1, \ldots, \mu_n\right)$ is the vector of expected return.
- $\mu\left(w\right) = w^\top \mu$ is the expected return of Portfolio w.
- $\mu\left(w \mid b\right) = \left(w - b\right)^\top \mu$ is the expected excess return of Portfolio w with respect to Benchmark b.
- $\mu_k\left(w\right)$ is the k^{th} alpha signal of portfolio w.
- n is the number of assets in the investment universe.
- $\mathbf{prox}_f\left(v\right)$ is the proximal operator of $f\left(x\right)$: $\mathbf{prox}_f\left(v\right) = \arg\min_x \left\{f\left(x\right) + \frac{1}{2}\left\|x - v\right\|_2^2\right\}$.
- $\mathcal{P}_\Omega\left(v\right)$ is the projection of v onto the set Ω: $\mathcal{P}_\Omega\left(v\right) = \arg\min_{x \in \Omega} \frac{1}{2}\left\|x - v\right\|_2^2 = \mathbf{prox}_{\mathbb{1}_\Omega(x)}\left(v\right)$.
- ϕ_k is the weight of the k^{th} alpha signal in the objective function.
- φ_k is the weight of the k^{th} risk measure in the objective function.

- $q_i = x_i \operatorname{MT}_i + x_i y_i \operatorname{LS}_i$ is the tradable nominal.
- $QF\left(x; Q, R, s\right)$ is the quadratic form $\frac{1}{2} x^\top Q x - x^\top R + s$.
- r is the risk-free interest rate.
- $\mathcal{R}\left(w\right)$ is the global risk measure.
- $\mathcal{R}_k\left(w\right)$ is the k^{th} risk measure for portfolio w.
- ρ_s is the $n \times n$ correlation matrix between credit spreads.
- s_i is the credit spread of Bond i.
- $\mathbb{S}_n$ is the unit simplex with dimension n.
- $\mathbb{S}_k\left(w\right)$ is the portfolio score with respect to metric k: $\mathbb{S}_k\left(w\right) = M_k\left(w\right) = \sum_{i=1}^{n} w_i M_{k,i}$.
- $\mathbb{S}^\star_{j,k}$ is the target score for the j^{th} cluster and the k^{th} risk measure, while $\mathbb{S}^\star_k = \left(\mathbb{S}^\star_{1,k}, \ldots, \mathbb{S}^\star_{n_G,k}\right)$ is the corresponding $n_G \times 1$ vector across all clusters.
- $\Sigma = \left[\rho_{i,j}\sigma_i\sigma_j\right]_{i,j=1}^{i,j=1}$ is the covariance matrix where σ_i is the volatility of Asset i and $\rho_{i,j}$ is the correlation between Asset i and Asset j.
- $\sigma\left(w\right) = \sqrt{w^\top \Sigma w}$ is the volatility of Portfolio w.
- $\sigma\left(w \mid b\right) = \sqrt{\left(w - b\right)^\top \Sigma \left(w - b\right)}$ is the tracking error volatility of Portfolio w with respect to Benchmark b.
- $\sigma_{s,i}$ is the volatility of the credit spread.
- $\mathcal{T}\left(v, x^-, x^+\right) = \max\left(x^-, \min\left(x, x^+\right)\right)$ is the truncation operator.
- τ is the slack variable of the absolute value trick.
- $\boldsymbol{\tau}\left(x \mid \tilde{x}\right) = \sum_{i=1}^{n} \left|x_i - \tilde{x}_i\right|$ is the turnover between Portfolios x and $\tilde{x}$. The maximum acceptable turnover is denoted by $\boldsymbol{\tau}^+$.
- $\upsilon_{s,i} = \operatorname{DTS}_i \sigma_{s,i}$ is the credit spread risk, and $\upsilon_s = \left(\upsilon_{s,1}, \ldots, \upsilon_{s,n}\right)$ is the corresponding $n \times 1$ vector across all bonds.
- V is the total portfolio value.
- $w = \left(w_1, \ldots, w_n\right)$ is the vector of portfolio weights.
- $\tilde{w}_i = x_i \frac{\operatorname{MT}_i p_i}{V} + y_i \frac{\operatorname{LS}_i p_i}{V}$ is the discrete weight of bond i in the investable portfolio, whose value is V.
- $x_i \in \{0, 1\}$ is a binary variable equal to 1 if bond i is held in the portfolio, 0 otherwise.
- y_i is the number of lots purchased.

B Mathematical appendix

B.1 Approximation and upper bound of portfolio tracking error volatility

Let w and b denote the vectors of portfolio and benchmark weights. Let Σ be the covariance matrix of bond returns. The tracking error volatility is given by:

$$\sigma\left(w \mid b\right) = \sqrt{\left(w-b\right)^{\top} \Sigma \left(w-b\right)}$$

The portfolio return volatility is obtained by setting $b = \mathbf{0}_n$:

$$\sigma\left(w\right) = \sigma\left(w \mid \mathbf{0}_n\right) = \sqrt{w^{\top} \Sigma w}$$

We assume that $\Sigma \approx \sum_{j=1}^{m} p_j p_j^{\top}$ where p_j is a vector of dimension n. We deduce that:

$$\begin{aligned}
\sigma^2\left(w \mid b\right) &= \left(w-b\right)^{\top} \left(\sum_{j=1}^{m} p_j p_j^{\top}\right) \left(w-b\right) \\
&= \sum_{j=1}^{m} \left(p_j^{\top} \left(w-b\right)\right)^2 \\
&= \sum_{j=1}^{m} \left|p_j^{\top} \left(w-b\right)\right|^2
\end{aligned}$$

and:

$$\sigma^2\left(w\right) = \sum_{j=1}^{m} \left|p_j^{\top} w\right|^2$$

We impose $p_j \geq \mathbf{0}_n$. In the case $m = 1$, we get:

$$\sigma\left(w \mid b\right) = \left\|p \odot \left(w-b\right)\right\|_1 \leq \sum_{i=1}^{n} p_i \left|w_i - b_i\right| \tag{43}$$

In the case $m \geq 2$, a convenient upper bound is:

$$\sigma\left(w \mid b\right) \leq \sum_{j=1}^{m} p_j^{\top} \left|w-b\right| \tag{44}$$

B.2 A two-factor model for interest rate and credit risk

B.2.1 Analytical expression of the covariance matrix

We consider an investment universe of n zero-coupon bonds. Let $B_i\left(t, T_i\right)$ be the price at time t of the i^{th} bond with maturity T_i. We have $B_i\left(t, T_i\right) = \exp\left(-\int_t^{T_i} \left(r\left(u\right) + s_i\left(u\right)\right) \, \mathrm{d}u\right)$. We deduce that:

$$\mathrm{d} \ln B_i\left(t, T_i\right) = -\operatorname{MD}_i \, \mathrm{d}r\left(t\right) - \operatorname{MD}_i \, \mathrm{d}s_i\left(t\right) \tag{45}$$

where $\operatorname{MD}_i = T_i - t$ is the remaining duration, r_t is the (risk-free) interest rate and $s_i\left(t\right)$ is the credit spread. This specification yields a two-factor model with two risk factors: one

factor capturing the yield curve risk and the other representing the credit or default risk[52]. If we assume that these two risk factors are uncorrelated, we deduce that:

$$\sigma^2\left(\mathrm{d}\ln B_i\left(t,T_i\right)\right)=\mathrm{MD}_i^2\,\sigma^2\left(\mathrm{d}r\left(t\right)\right)+\mathrm{MD}_i^2\,\sigma^2\left(\mathrm{d}s_i\left(t\right)\right)$$

where $\sigma^2\left(\mathrm{d}r\left(t\right)\right)$ and $\sigma^2\left(\mathrm{d}s_i\left(t\right)\right)$ are the variance of the interest rate risk and the default risk. We set $\sigma_r^2=\sigma^2\left(\mathrm{d}r\left(t\right)\right)$ and $\sigma_{s,i}^2=\sigma^2\left(\mathrm{d}\ln s_i\left(t\right)\right)$. It follows that:

$$\sigma\left(\mathrm{d}\ln B_i\left(t,T_i\right)\right)=\mathrm{MD}_i\sqrt{\sigma_r^2+s_i^2\left(t\right)\sigma_{s,i}^2}$$

The bond volatility is a linear function of the duration and is increasing with respect to the interest rate volatility, the credit spread and the spread volatility. This formula extends naturally to the covariance matrix. Let $\rho_{s,i,j}$ be the correlation between $\mathrm{d}\ln s_i\left(t\right)$ and $\mathrm{d}\ln s_j\left(t\right)$. We have:

$$\begin{aligned}\Sigma_{i,j} &= \operatorname{cov}\left(\mathrm{d}\ln B_i\left(t,T_i\right),\mathrm{d}\ln B_j\left(t,T_j\right)\right)\\ &= \operatorname{cov}\left(-\mathrm{MD}_i\ \mathrm{d}r\left(t\right),-\mathrm{MD}_j\ \mathrm{d}r\left(t\right)\right)+\operatorname{cov}\left(-\mathrm{MD}_i\ \mathrm{d}s_i\left(t\right),-\mathrm{MD}_j\ \mathrm{d}s_j\left(t\right)\right)+\\ &\quad \operatorname{cov}\left(-\mathrm{MD}_i\ \mathrm{d}r\left(t\right),-\mathrm{MD}_j\ \mathrm{d}s_j\left(t\right)\right)+\operatorname{cov}\left(-\mathrm{MD}_i\ \mathrm{d}s_i\left(t\right),-\mathrm{MD}_j\ \mathrm{d}r\left(t\right)\right)\\ &= \mathrm{MD}_i\,\mathrm{MD}_j\,\sigma_r^2+\mathrm{MD}_i\,\mathrm{MD}_j\,s_i\left(t\right)s_j\left(t\right)\rho_{s,i,j}\sigma_{s,i}\sigma_{s,j}\end{aligned}$$

In matrix form, the covariance matrix can be written as:

$$\Sigma=\sigma_r^2\,\mathrm{MD}\,\mathrm{MD}^\top+\upsilon_s\odot\rho_s\odot\upsilon_s^\top \tag{46}$$

where $\mathrm{MD}=\left(\mathrm{MD}_1,\ldots,\mathrm{MD}_n\right)$ is the vector of durations, $\upsilon_s=\left(\upsilon_{s,1},\ldots,\upsilon_{s,n}\right)$, $\upsilon_{s,i}=\mathrm{MD}_i\,s_i\left(t\right)\sigma_{s,i}$ and ρ_s is the correlation matrix of credit spread shocks.

B.2.2 Approximation of portfolio tracking error volatility

Let us assume that $\rho_{s,i,j}=\rho$ for all $i\neq j$. We obtain:

$$\begin{aligned}\Sigma &= \sigma_r^2\,\mathrm{MD}\,\mathrm{MD}^\top+\rho\upsilon_s\upsilon_s^\top+\left(1-\rho\right)\operatorname{diag}\left(\upsilon_s\odot\upsilon_s^\top\right)\\ &= \left(\sigma_r\,\mathrm{MD}\right)\left(\sigma_r\,\mathrm{MD}\right)^\top+\left(\sqrt{\rho}\upsilon_s\right)\left(\sqrt{\rho}\upsilon_s\right)^\top+\left(1-\rho\right)\operatorname{diag}\left(\upsilon_s\odot\upsilon_s^\top\right)\end{aligned}$$

We deduce that:

$$\begin{aligned}\sigma^2\left(w\mid b\right) &= \left(w-b\right)^\top\left(\sigma_r^2\,\mathrm{MD}\,\mathrm{MD}^\top+\rho\upsilon_s\upsilon_s^\top+\left(1-\rho\right)\operatorname{diag}\left(\upsilon_s\odot\upsilon_s^\top\right)\right)\left(w-b\right)\\ &= \sigma_r^2\left|\mathrm{MD}^\top\left(w-b\right)\right|^2+\rho\left|\upsilon_s^\top\left(w-b\right)\right|^2+\left(1-\rho\right)\left\|\upsilon_s\odot\left(w-b\right)\right\|_2^2\end{aligned}$$

Therefore, the quadratic $\boldsymbol{\ell}_2$-norm tracking error volatility is:

$$\sigma\left(w\mid b\right)=\sqrt{\sigma_r^2\left|\mathrm{MD}^\top\left(w-b\right)\right|^2+\rho\left|\upsilon_s^\top\left(w-b\right)\right|^2+\left(1-\rho\right)\left\|\upsilon_s\odot\left(w-b\right)\right\|_2^2} \tag{47}$$

[52] This model can be extended by incorporating additional risk factors. For instance, Ben Slimane *et al.* (2019a) explicitly account for liquidity risk and propose the following factor model:

$$R_i\left(t\right)=-\mathrm{MD}_i\left(t\right)\Delta r\left(t\right)-\mathrm{DTS}_i\left(t\right)R_{s,i}\left(t\right)+\mathrm{LTP}_i\left(t\right)R_{L,i}\left(t\right)+\varepsilon_i\left(t\right)$$

where $\mathrm{LTP}_i\left(t\right)$ is the liquidity-time-price factor, $R_{L,i}\left(t\right)$ captures the return component driven by liquidity dynamics and $\varepsilon_i\left(t\right)$ is the idiosyncratic risk.

while the linear $\boldsymbol{\ell}_1$-norm tracking error volatility is calculated with the upper bound[53]:

$$\sigma\left(w \mid b\right) = \sigma_r \left|\mathrm{MD}^\top \left(w - b\right)\right| + \sqrt{\rho}\left|\upsilon_s^\top \left(w - b\right)\right| + \sqrt{1-\rho}\left\|\upsilon_s \odot \left(w - b\right)\right\|_1 \tag{48}$$

B.2.3 Bond volatility

We remind that the daily bond return at time t is equal to[54]:

$$R_i\left(t\right) = -\mathrm{MD}_i\left(t\right)\Delta r\left(t\right) - \mathrm{DTS}_i\left(t\right)R_{s,i}\left(t\right) + \varepsilon_i\left(t\right) \tag{49}$$

where $\Delta r\left(t\right) \sim \mathcal{N}\left(0, \sigma_r^2\right)$, $R_{s,i}\left(t\right) \sim \mathcal{N}\left(0, \sigma_{s,i}^2\right)$ and $\varepsilon_i\left(t\right) \sim \mathcal{N}\left(0, \tilde{\sigma}_i^2\left(t\right)\right)$. Moreover, we assume that the three stochastic components $\Delta r\left(t\right)$, $R_{s,i}\left(t\right)$ and $\varepsilon_i\left(t\right)$ are independent. It follows that:

$$R_i\left(t\right) \sim \mathcal{N}\left(0, \sigma_i^2\left(t\right)\right)$$

where $\sigma_i^2\left(t\right)$ is the instantaneous daily variance:

$$\sigma_i^2\left(t\right) = \mathrm{MD}_i^2\left(t\right)\sigma_r^2 + \mathrm{DTS}_i^2\left(t\right)\sigma_{s,i}^2 + \tilde{\sigma}_i^2 \tag{50}$$

Let us now compute the standardized integrated variance over the period $[t_1, t_2]$. We have:

$$\begin{aligned}
\sigma_i^2\left(t_1, t_2\right) &= \frac{1}{t_2 - t_1}\int_{t_1}^{t_2}\left(\mathrm{MD}_i^2\left(t\right)\sigma_r^2 + \mathrm{DTS}_i^2\left(t\right)\sigma_{s,i}^2 + \tilde{\sigma}_i^2\right)\mathrm{d}t \\
&= \overline{\mathrm{MD}_i^2}\left(t_1, t_2\right)\sigma_r^2 + \overline{\mathrm{DTS}_i^2}\left(t_1, t_2\right)\sigma_{s,i}^2 + \tilde{\sigma}_i^2
\end{aligned} \tag{51}$$

where $\overline{\mathrm{MD}_i^2}\left(t_1, t_2\right)$ and $\overline{\mathrm{DTS}_i^2}\left(t_1, t_2\right)$ are the average of the square of the modified duration and the duration times spread over the period $[t_1, t_2]$:

$$\begin{cases}
\overline{\mathrm{MD}_i^2}\left(t_1, t_2\right) = \dfrac{1}{t_2 - t_1}\int_{t_1}^{t_2}\mathrm{MD}_i^2\left(t\right)\,\mathrm{d}t \\
\overline{\mathrm{DTS}_i^2}\left(t_1, t_2\right) = \dfrac{1}{t_2 - t_1}\int_{t_1}^{t_2}\mathrm{DTS}_i^2\left(t\right)\,\mathrm{d}t
\end{cases}$$

In the case of a zero-coupon bond, we have:

$$\begin{aligned}
\overline{\mathrm{MD}_i^2}\left(t_1, t_2\right) &= \frac{1}{t_2 - t_1}\int_{t_1}^{t_2}\left(T_i - t\right)^2\,\mathrm{d}t \\
&= \frac{1}{t_2 - t_1}\left[-\frac{1}{3}\left(T_i - t\right)^3\right]_{t_1}^{t_2} \\
&= \frac{1}{3}\left(3T_i^2 - 3T_i\left(t_2 + t_1\right) + \left(t_2^2 + t_2 t_1 + t_1^2\right)\right) \\
&= \left(T_i - t_2 - t_1\right)T_i + \frac{1}{3}\left(t_2^2 + t_2 t_1 + t_1^2\right)
\end{aligned}$$

[53] We use the following relationship $\sigma\left(w \mid b\right) \leq \sigma_r\left|\mathrm{MD}^\top\left(w - b\right)\right| + \sqrt{\rho}\left|\upsilon_s^\top\left(w - b\right)\right| + \sqrt{1-\rho}\left\|\upsilon_s \odot \left(w - b\right)\right\|_2$ and the inequality $\left\|x\right\|_2 \leq \left\|x\right\|_1$.

[54] We denote by $R_{s,i}\left(t\right) = \dfrac{\Delta s_i\left(t\right)}{s_i\left(t\right)}$ the daily relative variation of the credit spread.

and:

$$\begin{aligned}\overline{\mathrm{DTS}_i^2}(t_1,t_2) &= \frac{1}{t_2-t_1}\int_{t_1}^{t_2}(T_i-t)^2 s_i^2(t)\,\mathrm{d}t \\ &= \frac{1}{t_2-t_1}\int_{t_1}^{t_2}\left(T_i^2-2T_it+t^2\right)s_i^2(t)\,\mathrm{d}t \\ &= T_i^2\overline{s_i^2}(t_1,t_2)-2T_i\overline{ts_i^2}(t_1,t_2)+\overline{t^2s_i^2}(t_1,t_2)\end{aligned}$$

where $\overline{s_i^2}(t_1,t_2)$, $\overline{ts_i^2}(t_1,t_2)$, and $\overline{t^2s_i^2}(t_1,t_2)$ are the time average of $s_i^2(t)$, $ts_i^2(t)$ and $t^2s_i^2(t)$. Finally, we obtain:

$$\begin{aligned}\sigma_i^2(t_1,t_2) &= \left((T_i-t_2-t_1)T_i+\frac{1}{3}\left(t_2^2+t_2t_1+t_1^2\right)\right)\sigma_r^2+ \\ &\quad \left(T_i^2\overline{s_i^2}(t_1,t_2)-2T_i\overline{ts_i^2}(t_1,t_2)+\overline{t^2s_i^2}(t_1,t_2)\right)\sigma_{s,i}^2+\tilde{\sigma}_i^2\end{aligned} \tag{52}$$

Remark 17. *If the spread is constant over* $[t_1,t_2]$ — $s_i(t)=s_i$, *the expression of* $\overline{\mathrm{DTS}_i^2}(t_1,t_2)$ *reduces to* $\overline{\mathrm{DTS}_i^2}(t_1,t_2)=\overline{\mathrm{MD}_i^2}(t_1,t_2)\,s_i^2$ *and we have:*

$$\sigma_i^2(t_1,t_2)=\left((T_i-t_2-t_1)T_i+\frac{1}{3}\left(t_2^2+t_2t_1+t_1^2\right)\right)\left(\sigma_r^2+s_i^2\sigma_{s,i}^2\right)+\tilde{\sigma}_i^2 \tag{53}$$

B.2.4 Bond correlation matrix

For the two-factor model defined by Equation (49), the covariance between bonds i and j is given by:

$$\Sigma_{i,j}(t)=\mathrm{MD}_i(t)\,\mathrm{MD}_j(t)\,\sigma_r^2+\mathrm{DTS}_i(t)\,\mathrm{DTS}_j(t)\,\rho_{s,i,j}\sigma_{s,i}\sigma_{s,j}$$

for $i\neq j$ and $\Sigma_{i,i}=\sigma_i^2(t)$, where $\rho_{s,i,j}$ denotes the correlation between the credit spreads of bonds i and j. The corresponding matrix form is:

$$\Sigma(t)=\mathrm{MD}(t)\,\sigma_r^2\,\mathrm{MD}(t)^\top+\left(\mathrm{DTS}(t)\odot\sigma_s\right)\odot\rho_s\odot\left(\mathrm{DTS}(t)\odot\sigma_s\right)^\top+D \tag{54}$$

where $D=\mathrm{diag}\left(\tilde{\sigma}_1^2,\ldots,\tilde{\sigma}_n^2\right)$ is a diagonal matrix, $\mathrm{MD}(t)=\left(\mathrm{MD}_1(t),\ldots,\mathrm{MD}_n(t)\right)$, $\mathrm{DTS}(t)=\left(\mathrm{DTS}_1(t),\ldots,\mathrm{DTS}_n(t)\right)$ and $\sigma_s=\left(\sigma_{s,1},\ldots,\sigma_{s,n}\right)$. Another decomposition of Σ is:

$$\begin{aligned}\Sigma(t) &= \left(\sigma_r\,\mathrm{MD}(t)\right)\odot\rho_r\odot\left(\sigma_r\,\mathrm{MD}(t)\right)^\top+\left(\mathrm{DTS}(t)\odot\sigma_s\right)\odot\rho_s\odot\left(\mathrm{DTS}(t)\odot\sigma_s\right)^\top+ \\ &\quad \tilde{\sigma}\odot\tilde{\rho}\odot\tilde{\sigma}^\top \\ &= \upsilon_r(t)\odot\rho_r\odot\upsilon_r(t)^\top+\upsilon_s(t)\odot\rho_s\odot\upsilon_s(t)^\top+\tilde{\upsilon}\odot\tilde{\rho}\odot\tilde{\upsilon}^\top\end{aligned} \tag{55}$$

where $\rho_r=\mathbf{1}_n\mathbf{1}_n^\top$, $\tilde{\rho}=I_n$, $\upsilon_r(t)=\sigma_r\,\mathrm{MD}(t)$, $\upsilon_s(t)=\mathrm{DTS}(t)\odot\sigma_s$ and $\tilde{\upsilon}=\tilde{\sigma}$. This decomposition shows that the bond covariance matrix is driven by three distinct correlation structures:

1. A rank-one correlation matrix ρ_r: all bond returns depend on the short-term interest rate, meaning that they are perfectly positively correlated on this risk dimension;
2. A general correlation matrix ρ_s between credit spreads;
3. A zero correlation matrix $\tilde{\rho}$ between uncorrelated idiosyncratic risks.

Finally, we obtain the following formula for the bond correlation:

$$\rho_{i,j}(t)=\frac{\mathrm{MD}_i(t)\,\mathrm{MD}_j(t)\,\rho_{r,i,j}\sigma_r^2+\mathrm{DTS}_i(t)\,\mathrm{DTS}_j(t)\,\rho_{s,i,j}\sigma_{s,i}\sigma_{s,j}+\tilde{\rho}_{i,j}\tilde{\sigma}_i\tilde{\sigma}_j}{\sigma_i(t)\,\sigma_j(t)} \tag{56}$$

B.3 Linear and quadratic programming

B.3.1 Linear programming

Definition The canonical form of a linear program is:

$$\begin{array}{rcl} x^\star & = & \arg\max c^\top x \\ & \text{s.t.} & \left\{ \begin{array}{l} Sx \leq T \\ x \geq \mathbf{0}_n \end{array} \right. \end{array}$$

where x is a $n \times 1$ vector, c is a $n \times 1$ vector, S is a $n_S \times n$ matrix, and T is a $n_S \times 1$ vector. A minimization linear programming (LP) problem can be cast into a maximization LP problem because $\min c^\top x \equiv \max -c^\top x$. A maximization LP problem is in standard form if it is written as:

$$\begin{array}{rcl} x^\star & = & \arg\max c^\top x \\ & \text{s.t.} & \left\{ \begin{array}{l} Sx = T \\ x \geq \mathbf{0}_n \end{array} \right. \end{array}$$

We notice that a canonical problem can always be put into a standard form by introducing the slack variables ξ:

$$Sx \leq T \Leftrightarrow \left\{ \xi \geq \mathbf{0}_{n_S} : Sx + I_{n_S} \xi = T \right\}$$

We obtain the following LP problem:

$$\begin{array}{rcl} y^\star & = & \arg\max d^\top y \\ & \text{s.t.} & \left\{ \begin{array}{l} My = N \\ y \geq \mathbf{0}_n \end{array} \right. \end{array}$$

where $d = \left(c, \mathbf{0}_{n_S}\right)$, $y = (x, \xi)$, $M = \begin{pmatrix} S & I_{n_S} \end{pmatrix}$ and $N = T$. The technique of slack variables[55] can also be used when the constraint is $Sx \geq T$ and we have $Sx - \xi = T$. If we introduce lower and upper bounds ($x^- \leq x \leq x^+$), we can use the change of variable $y = x - x^-$. It follows that $y \geq \mathbf{0}_n$ and $I_n y \leq x^+ - x^-$. Since we have $x = x^- + y$, we obtain $c^\top x = c^\top x^- + c^\top y$ and $Sx \leq T \Leftrightarrow Sy \leq T - Sx^-$. Finally,we deduce that:

$$\left\{ \begin{array}{rcl} x^\star & = & \arg\max c^\top x \\ & \text{s.t.} & \left\{ \begin{array}{l} Sx \leq T \\ x \geq \mathbf{0}_n \end{array} \right. \end{array} \right. \Longleftrightarrow \left\{ \begin{array}{rcl} y^\star & = & \arg\max c^\top y \\ & \text{s.t.} & \left\{ \begin{array}{l} \begin{pmatrix} S \\ I_n \end{pmatrix} y \leq \begin{pmatrix} T - Sx^- \\ x^+ - x^- \end{pmatrix} \\ y \geq \mathbf{0}_n \end{array} \right. \end{array} \right.$$

If some variables $x_i \in \mathbb{R}$, we can write $x_i = y_i - z_i$ where $y_i \geq 0$ and $z_i \geq 0$.

The previous analysis shows that we can always transform a general LP problem into a canonical or standard form. This is why most numerical packages consider the following general formulation:

$$\begin{array}{rcl} x^\star & = & \arg\min c^\top x \\ & \text{s.t.} & \left\{ \begin{array}{l} Ax = B \\ Cx \leq D \\ x^- \leq x \leq x^+ \end{array} \right. \end{array} \tag{57}$$

[55] When we rewrite an inequality by substracting new variables, these last ones are also called surplus variables.

where x is a $n \times 1$ vector, c is a $n \times 1$ vector, A is a $n_A \times n$ matrix, B is a $n_A \times 1$ vector, C is a $n_C \times n$ matrix, D is a $n_C \times 1$ vector, and x^- and x^+ are two $n \times 1$ vectors. If $n_A = 0$, there is no equality constraints. Similarly, there is no inequality constraints if $n_C = 0$. If there is no lower bounds or/and upper bounds, this implies that $x^- = -\infty \cdot \mathbf{1}_n$ and $x^+ = \infty \cdot \mathbf{1}_n$. A solution x is said to be feasible if it satisfies all the constraints of the linear program (57). The set of feasible solutions is called the feasible space Ω:

$$\Omega = \left\{x \in \mathbb{R}^n : Ax = B, Cx \leq D, x^- \leq x \leq x^+\right\}$$

Since $Ax = B$ and $Cx \leq D$ define two convex sets (a hyperplane and a closed half-space), Ω is a convex set. If Ω is not empty and $c^\top x$ is bounded below, then there is an optimal solution.

Duality If the primal problem is maximizing $c^\top x$ subject to $Ax \leq b$ and $x \geq \mathbf{0}_n$, then the dual problem is defined as:

$$\begin{aligned} x^\star &= \arg\min b^\top y \\ &\text{s.t.} \begin{cases} A^\top y \geq c \\ y \geq \mathbf{0}_m \end{cases} \end{aligned} \tag{58}$$

We notice that:

- The dual problem has a linear programming form;
- The maximization problem and the $\leq$ inequality type are changed into a minimization problem and a $\geq$ inequality type;
- Each dual variable y_j may be assigned to a corresponding primal constraint $\sum_{i=1}^n A_{j,i} x_i \leq b_j$;
- The roles of the vectors c and b are switched: c becomes the right-hand side of the constraints and b the coefficients of the objective function;
- The matrix A of the inequality constraints is transposed.

Let $\Omega_x = \{x : Ax \leq b, x \geq \mathbf{0}_n\}$ and $\Omega_y = \left\{y : A^\top y \geq c, y \geq \mathbf{0}_m\right\}$ be the primal and dual feasible spaces. The weak duality theorem states that[56]:

$$\forall x \in \Omega_x, y \in \Omega_y : c^\top x \leq b^\top y$$

This means that the objective value of the dual problem is an upper bound on the objective value of the primal problem, and vice versa. Using this property, we can also formulate the strong duality theorem: A primal feasible solution $x^\star$ is optimal if and only if there exists a dual feasible solution $y^\star$ such that $c^\top x^\star = b^\top y^\star$. We also deduce that $y^\star$ is the optimal solution of the dual LP problem.

B.3.2 Quadratic programming

Definition A quadratic programming (QP) problem is an optimization problem with a quadratic objective function and linear inequality constraints:

$$\begin{aligned} x^\star &= \arg\min \frac{1}{2} x^\top Q x - x^\top R \\ &\text{s.t.} \quad Sx \leq T \end{aligned} \tag{59}$$

[56] If $x \geq \mathbf{0}_n$ and $\alpha \geq \beta$, we have $\alpha^\top x \geq \beta^\top x$ because $\alpha_i x_i \geq \beta_i x_i$ and $\sum_{i=1}^n \alpha_i x_i \geq \sum_{i=1}^n \beta_i x_i$. Using the constraints $Ax \leq b$ and $A^\top y \geq c$, we deduce that $c^\top x = x^\top c \leq x^\top A^\top y = (Ax)^\top y \leq b^\top y$.

where x is a $n \times 1$ vector, Q is a $n \times n$ matrix and R is a $n \times 1$ vector. We note that the system of constraints $Sx \leq T$ allows specifying linear equality constraints[57] $Ax = B$ or weight constraints $x^- \leq x \leq x^+$. Most numerical packages then consider the following formulation:

$$\begin{aligned} x^\star &= \arg\min \frac{1}{2} x^\top Q x - x^\top R \\ &\text{s.t.} \begin{cases} Ax = B \\ Cx \leq D \\ x^- \leq x \leq x^+ \end{cases} \end{aligned} \tag{60}$$

because the problem (60) is equivalent to the canonical problem (59) with the following system of linear inequalities:

$$\begin{bmatrix} -A \\ A \\ C \\ -I_n \\ I_n \end{bmatrix} x \leq \begin{bmatrix} -B \\ B \\ D \\ -x^- \\ x^+ \end{bmatrix}$$

If the space Ω defined by $Sx \leq T$ is non-empty and if Q is a symmetric positive definite matrix, the solution exists because the function $f(x) = \frac{1}{2} x^\top Q x - x^\top R$ is convex. In the general case where Q is a square matrix, the solution may not exist.

Duality The Lagrange function is:

$$\mathcal{L}(x; \lambda) = \frac{1}{2} x^\top Q x - x^\top R + \lambda^\top (Sx - T)$$

We deduce that the dual problem is defined by:

$$\begin{aligned} \lambda^\star &= \arg\max \left\{ \inf_x \mathcal{L}(x; \lambda) \right\} \\ &\text{s.t.} \quad \lambda \geq 0 \end{aligned}$$

We note that $\partial_x \mathcal{L}(x; \lambda) = Qx - R + S^\top \lambda$. The solution to the problem $\partial_x \mathcal{L}(x; \lambda) = 0$ is then $x = Q^{-1}\left(R - S^\top \lambda\right)$. We obtain:

$$\begin{aligned} \inf_x \mathcal{L}(x; \lambda) &= \frac{1}{2}\left(R^\top - \lambda^\top S\right) Q^{-1}\left(R - S^\top \lambda\right) - \left(R^\top - \lambda^\top S\right) Q^{-1} R + \\ &\quad \lambda^\top \left(S Q^{-1}\left(R - S^\top \lambda\right) - T\right) \\ &= \frac{1}{2} R^\top Q^{-1} R - \lambda^\top S Q^{-1} R + \frac{1}{2} \lambda^\top S Q^{-1} S^\top \lambda - R^\top Q^{-1} R + \\ &\quad 2\lambda^\top S Q^{-1} R - \lambda^\top S Q^{-1} S^\top \lambda - \lambda^\top T \\ &= -\frac{1}{2} \lambda^\top S Q^{-1} S^\top \lambda + \lambda^\top \left(S Q^{-1} R - T\right) - \frac{1}{2} R^\top Q^{-1} R \end{aligned}$$

The dual program is another quadratic program:

$$\begin{aligned} \lambda^\star &= \arg\min \frac{1}{2} \lambda^\top \bar{Q} \lambda - \lambda^\top \bar{R} \\ &\text{s.t.} \quad \lambda \geq 0 \end{aligned} \tag{61}$$

where $\bar{Q} = S Q^{-1} S^\top$ and $\bar{R} = S Q^{-1} R - T$.

[57] This is equivalent to imposing that $Ax \geq B$ and $Ax \leq B$.

B.4 Linear and quadratic forms

B.4.1 Linear form

Definition Let $c = (c_1, \ldots, c_n)$ be a n-dimensional column vector. A linear form is a homogeneous polynomial of degree one:

$$\mathcal{LF}(x_1, \ldots, x_n) = \sum_{i=1}^{n} c_i x_i = c^\top x$$

We use the notation $\mathcal{LF}(x; c) = c^\top x = x^\top c$ to define a canonical linear form. A generalized linear form (or affine form) includes a scalar term:

$$\mathcal{LF}(x; c, d) = c^\top x + d$$

Main properties We have the following properties:

- The multiplication of a linear form by a scalar φ remains a linear form:

$$\varphi \cdot \mathcal{LF}(x; c, d) = \mathcal{LF}(x; \varphi c, \varphi d)$$

- The sum of two linear forms is a linear form:

$$\mathcal{LF}(x; c_1, d_1) + \mathcal{LF}(x; c_2, d_2) = \mathcal{LF}(x; c_1 + c_2, d_1 + d_2)$$

- The product of two canonical linear forms is a bilinear form:

$$\mathcal{LF}(x; c_1) \cdot \mathcal{LF}(y; c_2) = \mathcal{BF}\left(x, y; c_1 c_2^\top\right)$$

  where the bilinear form is defined by $\mathcal{BF}(x, y; A) = x^\top A y$.

B.4.2 Quadratic form

Definition In mathematics, a quadratic form is a polynomial whose terms are all of degree two:

$$\mathcal{QF}(x_1, \ldots, x_n) = \sum_{i=1}^{n} \sum_{j=1}^{n} a_{i,j} x_i x_j = x^\top A x$$

where $A = \left(a_{i,j}\right)$ is a $n \times n$ matrix. Since $x^\top A x$ is a scalar, we have $\left(x^\top A x\right)^\top = x^\top A^\top x$ and:

$$\mathcal{QF}(x_1, \ldots, x_n) = \frac{1}{2}\left(x^\top A x + x^\top A^\top x\right) = \frac{1}{2} x^\top \left(A + A^\top\right) x = \frac{1}{2} x^\top Q x$$

where $Q = A + A^\top$ is a symmetric matrix. We use the notation $\mathcal{QF}(x; Q) = \frac{1}{2} x^\top Q x$ to define a canonical quadratic form. A generalized quadratic form includes terms with degrees one and zero[58]:

$$\mathcal{QF}(x; Q, R, s) = \frac{1}{2} x^\top Q x - x^\top R + s$$

[58] We add the one-degree polynomial $-x^\top R$ instead of $x^\top R$ in order to match the canonical form of a QP problem.

Main properties We list here some properties that are helpful when considering portfolio optimization:

- The multiplication of a quadratic form by a nonnegative scalar $\varphi \geq 0$ remains a quadratic form:
$$\varphi \cdot \mathcal{QF}(x; Q, R, s) = \mathcal{QF}(x; \varphi Q, \varphi R, \varphi s)$$
- The sum of two quadratic forms is a quadratic form:
$$\mathcal{QF}(x; Q_1, R_1, s_1) + \mathcal{QF}(x; Q_2, R_2, s_2) = \mathcal{QF}(x; Q_1 + Q_2, R_1 + R_2, s_1 + s_2)$$
- A quadratic form applied to the difference vector $x - y$ is a quadratic form in x:
$$\begin{aligned}
\mathcal{QF}(x - y; Q, R, s) &= \frac{1}{2}(x - y)^\top Q(x - y) - (x - y)^\top R + s \\
&= \frac{1}{2}\left(x^\top Qx - 2x^\top Qy + y^\top Qy\right) - x^\top R + y^\top R + s \\
&= \frac{1}{2}x^\top Qx - x^\top(R + Qy) + \frac{1}{2}y^\top Qy + y^\top R + s \\
&= \mathcal{QF}\left(x; Q, R + Qy, \frac{1}{2}y^\top Qy + y^\top R + s\right)
\end{aligned}$$
and a quadratic form in y:
$$\begin{aligned}
\mathcal{QF}(x - y; Q, R, s) &= \frac{1}{2}y^\top Qy - y^\top(Qx - R) + \frac{1}{2}x^\top Qx - x^\top R + s \\
&= \mathcal{QF}\left(y; Q, Qx - R, \frac{1}{2}x^\top Qx - x^\top R + s\right)
\end{aligned}$$
- When Q is a diagonal matrix, the quadratic form reduces to:
$$\mathcal{QF}(x; Q, R, S) = \frac{1}{2}\sum_{i=1}^{n} q_{i,i}x_i^2 - \sum_{i=1}^{n} r_i x_i + c$$
We deduce that:
$$\frac{1}{2}\sum_{i=1}^{n} q_i x_i^2 = \mathcal{QF}\left(x; \mathcal{D}(q), \mathbf{0}_n, 0\right)$$
where $q = (q_1, \ldots, q_n)$ is a $n \times 1$ vector and $\mathcal{D}(q) = \text{diag}(q)$.
- Using the previous properties, we have:
$$\frac{1}{2}\sum_{i=1}^{n} q_i (x_i - y_i)^2 = \mathcal{QF}\left(x - y; \mathcal{D}(q), \mathbf{0}_n, 0\right) = \mathcal{QF}\left(x; \mathcal{D}(q), \mathcal{D}(q)\, y, \frac{1}{2}y^\top \mathcal{D}(q)\, y\right)$$
- The square of a weighted sum is also a quadratic form:
$$\frac{1}{2}\left(\sum_{i=1}^{n} q_i x_i\right)^2 = \frac{1}{2}\left(x^\top q\right)\left(x^\top q\right)^\top = \frac{1}{2}x^\top\left(qq^\top\right)x^\top = \mathcal{QF}\left(x; \mathcal{T}(q), \mathbf{0}_n, 0\right)$$
where $\mathcal{T}(q) = qq^\top$ is the outer product of q with itself.

- We deduce that:

$$\frac{1}{2}\left(\sum_{i=1}^{n} q_i\left(x_i - y_i\right)\right)^2 = \mathcal{QF}\left(x-y; \mathcal{T}\left(q\right), \mathbf{0}_n, 0\right) = \mathcal{QF}\left(x; \mathcal{T}\left(q\right), \mathcal{T}\left(q\right) y, \frac{1}{2} y^\top \mathcal{T}\left(q\right) y\right)$$

- The previous results can be extended when we consider partial sums:

$$\sum_{i\in\Omega} q_i x_i = \sum_{i=1}^{n} \mathbb{1}\left\{i \in \Omega\right\} \cdot q_i x_i = \sum_{i=1}^{n} \left(\omega_i q_i\right) x_i$$

where $\omega_i = \mathbb{1}\left\{i \in \Omega\right\}$. In a matrix form, we have $\sum_{i\in\Omega} q_i x_i = \left(\omega \odot q\right)^\top x$ where $\omega = (\omega_1, \ldots, \omega_n)$. We deduce that:

$$\begin{cases} \frac{1}{2}\sum_{i\in\Omega} q_i x_i^2 = \mathcal{QF}\left(x; \mathcal{D}\left(\omega \odot q\right), \mathbf{0}_n, 0\right) \\ \frac{1}{2}\sum_{i\in\Omega} q_i \left(x_i - y_i\right)^2 = \mathcal{QF}\left(x; \mathcal{D}\left(\omega \odot q\right), \mathcal{D}\left(\omega \odot q\right) y, \frac{1}{2} y^\top \mathcal{D}\left(\omega \odot q\right) y\right) \\ \frac{1}{2}\left(\sum_{i\in\Omega} q_i x_i\right)^2 = \mathcal{QF}\left(x; \mathcal{T}\left(\omega \odot q\right), \mathbf{0}_n, 0\right) \\ \frac{1}{2}\left(\sum_{i\in\Omega} q_i \left(x_i - y_i\right)\right)^2 = \mathcal{QF}\left(x; \mathcal{T}\left(\omega \odot q\right), \mathcal{T}\left(\omega \odot q\right) y, \frac{1}{2} y^\top \mathcal{T}\left(\omega \odot q\right) y\right) \end{cases}$$

We notice that $\mathcal{D}\left(\omega \odot q\right) = \operatorname{diag}\left(\omega \odot q\right) = \mathcal{D}\left(\omega\right)\mathcal{D}\left(q\right)$ and $\mathcal{T}\left(\omega \odot q\right) = \left(\omega \odot q\right)\left(\omega \odot q\right)^\top = \left(\omega\omega^\top\right) \odot qq^\top = \mathcal{T}\left(\omega\right) \odot \mathcal{T}\left(q\right)$.

B.5 Equivalent QP problems of basic optimization problems

B.5.1 Without a benchmark

Let us assume that we can express each risk measure $\mathcal{R}_k\left(w\right)$ by a quadratic form $\mathcal{QF}\left(w; Q_k, R_k, s_k\right)$. We deduce that the global risk measure is also a quadratic form:

$$\begin{aligned} \frac{1}{2}\mathcal{R}\left(w\right) &= \frac{1}{2}\sum_{k=0}^{n_{\mathcal{R}}} \varphi_k \mathcal{R}_k\left(w\right) \\ &= \sum_{k=0}^{n_{\mathcal{R}}} \frac{1}{2}\varphi_k \mathcal{QF}\left(w; Q_k, R_k, s_k\right) \\ &= \sum_{k=0}^{n_{\mathcal{R}}} \mathcal{QF}\left(w; \frac{1}{2}\varphi_k Q_k, \frac{1}{2}\varphi_k R_k, \frac{1}{2}\varphi_k s_k\right) \\ &= \mathcal{QF}\left(w; \frac{1}{2}\sum_{k=0}^{n_{\mathcal{R}}} \varphi_k Q_k, \frac{1}{2}\sum_{k=0}^{n_{\mathcal{R}}} \varphi_k R_k, \frac{1}{2}\sum_{k=0}^{n_{\mathcal{R}}} \varphi_k s_k\right) \end{aligned}$$

For $k = 0$, we have:

$$\mathcal{R}_0\left(w\right) = w^\top \Sigma w = \mathcal{QF}\left(w; 2\Sigma, \mathbf{0}_n, 0\right)$$

while for $k > 1$, we have:

$$\begin{aligned}
\mathcal{R}_k(w) &= \sum_{j=1}^{n_{\mathcal{G}}} \left(\mathbb{C}_{j,k}(w) - \mathbb{C}^{\star}_{j,k}\right)^2 \\
&= \sum_{j=1}^{n_{\mathcal{G}}} \left(\sum_{i=1}^{n} w_i \delta_{i,j} M_{k,i} - \mathbb{C}^{\star}_{j,k}\right)^2 \\
&= \sum_{j=1}^{n_{\mathcal{G}}} \left(w^\top \left(\delta_j \odot M_k\right) - \mathbb{C}^{\star}_{j,k}\right)^2 \\
&= \sum_{j=1}^{n_{\mathcal{G}}} \left(w^\top \left(\delta_j \odot M_k\right) - \mathbb{C}^{\star}_{j,k}\right)\left(w^\top \left(\delta_j \odot M_k\right) - \mathbb{C}^{\star}_{j,k}\right)^\top \\
&= \sum_{j=1}^{n_{\mathcal{G}}} \left(w^\top \left(\delta_j \odot M_k\right) - \mathbb{C}^{\star}_{j,k}\right)\left(\left(\delta_j \odot M_k\right)^\top w^\top - \mathbb{C}^{\star}_{j,k}\right) \\
&= \sum_{j=1}^{n_{\mathcal{G}}} w^\top \left(\delta_j \odot M_k\right)\left(\delta_j \odot M_k\right)^\top w^\top - 2\mathbb{C}^{\star}_{j,k} w^\top \left(\delta_j \odot M_k\right) + \mathbb{C}^{\star^2}_{j,k} \\
&= \sum_{j=1}^{n_{\mathcal{G}}} \mathcal{QF}\left(w; 2\left(\delta_j \odot M_k\right)\left(\delta_j \odot M_k\right)^\top, 2\mathbb{C}^{\star}_{j,k}\left(\delta_j \odot M_k\right), \mathbb{C}^{\star^2}_{j,k}\right) \\
&= \mathcal{QF}\left(w; 2\sum_{j=1}^{n_{\mathcal{G}}} \left(\delta_j \odot M_k\right)\left(\delta_j \odot M_k\right)^\top, 2M_k \odot \sum_{j=1}^{n_{\mathcal{G}}} \mathbb{C}^{\star}_{j,k}\delta_j, \sum_{j=1}^{n_{\mathcal{G}}} \mathbb{C}^{\star^2}_{j,k}\right)
\end{aligned}$$

Regarding the expected return, we have:

$$\begin{aligned}
\mu(w) &= \sum_{k=0}^{n_\mu} \phi_k \mu_k(w) \\
&= \phi_0 \mathcal{QF}\left(w; \mathbf{0}_{n,n}, -\mathcal{C}, 0\right) + \sum_{k=1}^{n_\mu} \phi_k \mathcal{QF}\left(w; \mathbf{0}_{n,n}, -\alpha_k, 0\right) \\
&= \mathcal{QF}\left(w; \mathbf{0}_{n,n}, -\phi_0\mathcal{C} - \sum_{k=1}^{n_\mu} \phi_k \alpha_k, 0\right)
\end{aligned}$$

We deduce that the quadratic form of the objective function is:

$$\begin{aligned}
\frac{1}{2}\mathcal{R}(w) - \gamma\mu(w) &= \frac{1}{2}\left(\varphi_0 w^\top \Sigma w + \sum_{k=1}^{n_{\mathcal{R}}} \varphi_k \mathcal{R}_k(w)\right) - \gamma\left(\phi_0 w^\top \mathcal{C} + \sum_{k=1}^{n_\mu} \phi_k \mu_k(w)\right) \\
&= \frac{1}{2}\varphi_0 \mathcal{QF}(w; 2\Sigma, \mathbf{0}_n, 0) + \\
&\quad \frac{1}{2}\sum_{k=1}^{n_{\mathcal{R}}} \varphi_k \mathcal{QF}\left(w; 2\sum_{j=1}^{n_{\mathcal{G}}} \left(\delta_j \odot M_k\right)\left(\delta_j \odot M_k\right)^\top, 2M_k \odot \sum_{j=1}^{n_{\mathcal{G}}} \mathbb{C}^{\star}_{j,k}\delta_j, \sum_{j=1}^{n_{\mathcal{G}}} \mathbb{C}^{\star^2}_{j,k}\right) - \\
&\quad \gamma\mathcal{QF}\left(w; \mathbf{0}_{n,n}, -\phi_0\mathcal{C} - \sum_{k=1}^{n_\mu} \phi_k\alpha_k, 0\right) \\
&= \mathcal{QF}(w; Q, R, s)
\end{aligned}$$

where:

$$\begin{cases} Q = \varphi_0 \Sigma + \sum_{k=1}^{n_{\mathcal{R}}} \varphi_k \sum_{j=1}^{n_{\mathcal{G}}} \left(\delta_j \odot M_k\right) \left(\delta_j \odot M_k\right)^\top \\ R = \sum_{k=1}^{n_{\mathcal{R}}} \varphi_k M_k \odot \sum_{j=1}^{n_{\mathcal{G}}} \mathbb{C}_{j,k}^\star \delta_j + \gamma \left(\phi_0 \mathcal{C} + \sum_{k=1}^{n_\mu} \phi_k \alpha_k\right) \\ s = \dfrac{1}{2} \sum_{k=1}^{n_{\mathcal{R}}} \varphi_k \sum_{j=1}^{n_{\mathcal{G}}} \mathbb{C}_{j,k}^{\star^2} \end{cases}$$

If we use cluster scores instead of cluster contributions, then:

$$\mathcal{R}_k\left(w\right) = \sum_{j=1}^{n_{\mathcal{G}}} \left(\sum_{i=1}^{n} w_i \delta_{i,j} \left(M_{k,i} - \mathbb{S}_{j,k}^\star\right)\right)^2$$

This is equivalent to the risk measure $\mathcal{R}_k\left(w \mid b\right) = \sum_{j=1}^{n_{\mathcal{G}}} \left(\sum_{i=1}^{n} w_i \delta_{i,j} M_{k,i} - \mathbb{C}_{j,k}^\star\right)^2$ where $M_{k,i}$ is replaced by $M_{k,i} - \mathbb{S}_{j,k}^\star$ and $\mathbb{C}_{j,k}^\star = 0$. It follows that:

$$\mathcal{R}_k\left(w\right) = \mathcal{QF}\left(w; 2\sum_{j=1}^{n_{\mathcal{G}}} \left(\delta_j \odot \left(M_k - \mathbb{S}_{j,k}^\star\right)\right) \left(\delta_j \odot \left(M_k - \mathbb{S}_{j,k}^\star\right)\right)^\top, \mathbf{0}_n, 0\right)$$

We deduce that the quadratic form of the objective function becomes:

$$\frac{1}{2}\mathcal{R}\left(w\right) - \gamma\mu\left(w\right) = \mathcal{QF}\left(w; Q, R, s\right)$$

where:

$$\begin{cases} Q = \varphi_0 \Sigma + \sum_{k=1}^{n_{\mathcal{R}}} \varphi_k \sum_{j=1}^{n_{\mathcal{G}}} \left(\delta_j \odot \left(M_k - \mathbb{S}_{j,k}^\star\right)\right) \left(\delta_j \odot \left(M_k - \mathbb{S}_{j,k}^\star\right)\right)^\top \\ R = \gamma \left(\phi_0 \mathcal{C} + \sum_{k=1}^{n_\mu} \phi_k \alpha_k\right) \\ s = 0 \end{cases}$$

B.5.2 With a benchmark

The quadratic forms of the risk measures become:

$$\begin{aligned} \mathcal{R}_0\left(w \mid b\right) &= \left(w - b\right)^\top \Sigma \left(w - b\right) \\ &= \mathcal{QF}\left(w - b; 2\Sigma, \mathbf{0}_n, 0\right) \\ &= \mathcal{QF}\left(w; 2\Sigma, 2\Sigma b, b^\top \Sigma b\right) \end{aligned}$$

and:

$$\begin{aligned}
\mathcal{R}_k\left(w \mid b\right) &= \sum_{j=1}^{n_{\mathcal{G}}}\left(\sum_{i=1}^{n}\left(w_i - b_i\right)\delta_{i,j}M_{k,i}\right)^2 \\
&= \sum_{j=1}^{n_{\mathcal{G}}}\left(\left(w-b\right)^\top\left(\delta_j \odot M_k\right) - 0\right)^2 \\
&= \mathcal{QF}\left(w-b; 2\sum_{j=1}^{n_{\mathcal{G}}}\left(\delta_j \odot M_k\right)\left(\delta_j \odot M_k\right)^\top, \mathbf{0}_n, 0\right) \\
&= \mathcal{QF}\left(w; Q, Qb, \frac{1}{2}b^\top Qb\right)
\end{aligned}$$

where $Q = 2\sum_{j=1}^{n_{\mathcal{G}}}\left(\delta_j \odot M_k\right)\left(\delta_j \odot M_k\right)^\top$. Regarding the expected excess return, we have:

$$\begin{aligned}
\mu\left(w \mid b\right) &= \sum_{k=0}^{n_\mu}\phi_k\mu_k\left(w \mid b\right) \\
&= \mathcal{QF}\left(w-b; \mathbf{0}_{n,n}, -\phi_0\mathcal{C} - \sum_{k=1}^{n_\mu}\phi_k\alpha_k, 0\right) \\
&= \mathcal{QF}\left(w; \mathbf{0}_{n,n}, -\phi_0\mathcal{C} - \sum_{k=1}^{n_\mu}\phi_k\alpha_k, -\phi_0 b^\top\mathcal{C} - \sum_{k=1}^{n_\mu}\phi_k b^\top\alpha_k\right)
\end{aligned}$$

Finally, we obtain:

$$\frac{1}{2}\mathcal{R}\left(w \mid b\right) - \gamma\mu\left(w \mid b\right) = \mathcal{QF}\left(w; Q, R, s\right)$$

where:

$$\begin{cases}
Q = \varphi_0\Sigma + \sum_{k=1}^{n_{\mathcal{R}}}\varphi_k\sum_{j=1}^{n_{\mathcal{G}}}\left(\delta_j \odot M_k\right)\left(\delta_j \odot M_k\right)^\top \\
R = \varphi_0\Sigma b + \sum_{k=1}^{n_{\mathcal{R}}}\varphi_k\sum_{j=1}^{n_{\mathcal{G}}}\left(\delta_j \odot M_k\right)\left(\delta_j \odot M_k\right)^\top b + \gamma\left(\phi_0\mathcal{C} + \sum_{k=1}^{n_\mu}\phi_k\alpha_k\right) \\
s = \frac{1}{2}\varphi_0 b^\top\Sigma b + \frac{1}{2}\sum_{k=1}^{n_{\mathcal{R}}}\varphi_k\sum_{j=1}^{n_{\mathcal{G}}}b^\top\left(\delta_j \odot M_k\right)\left(\delta_j \odot M_k\right)^\top b + \gamma\left(\phi_0 b^\top\mathcal{C} + \sum_{k=1}^{n_\mu}\phi_k b^\top\alpha_k\right)
\end{cases}$$

In the case where we use cluster scores instead of cluster contributions, the quadratic form is:

$$\begin{cases}
Q = \varphi_0\Sigma + \sum_{k=1}^{n_{\mathcal{R}}}\varphi_k\sum_{j=1}^{n_{\mathcal{G}}}\left(\delta_j \odot \left(M_k - \mathbb{S}_{j,k}\left(b\right)\right)\right)\left(\delta_j \odot \left(M_k - \mathbb{S}_{j,k}\left(b\right)\right)\right)^\top \\
R = \varphi_0\Sigma b + \gamma\left(\phi_0\mathcal{C} + \sum_{k=1}^{n_\mu}\phi_k\alpha_k\right) \\
s = \frac{1}{2}\varphi_0 b^\top\Sigma b + \gamma\left(\phi_0 b^\top\mathcal{C} + \sum_{k=1}^{n_\mu}\phi_k b^\top\alpha_k\right)
\end{cases}$$

B.6 Equivalent LP problems of basic optimization problems

B.6.1 Without a benchmark

We first transform the various risk measures into the extended linear form $\mathcal{LF}\left(z;c,d,C,D,z^{-}\right)$. For $k \geq 1$, we have:

$$\mathcal{R}_k\left(w\right) = \sum_{j=1}^{n_{\mathcal{G}}} \left| \sum_{i=1}^{n} w_i \delta_{i,j} M_{k,i} - \mathbb{C}_{j,k}^{\star} \right| = \sum_{j=1}^{n_{\mathcal{G}}} \left| \sum_{i=1}^{n} \left(\delta_{i,j} M_{k,i}\right) w_i - \mathbb{C}_{j,k}^{\star} \right|$$

We deduce that $z = \begin{bmatrix} w \\ \tau_{(k)} \end{bmatrix}$ is the augmented variable, $\tau_{(k)}$ is a $n_{\mathcal{G}} \times 1$ vector, $c_z = \begin{bmatrix} \mathbf{0}_n \\ \mathbf{1}_{n_{\mathcal{G}}} \end{bmatrix}$, $d_z = 0$, $C_z = \begin{bmatrix} -\left(\delta \odot M_k\right)^{\top} & -I_{n_{\mathcal{G}}} \\ \left(\delta \odot M_k\right)^{\top} & -I_{n_{\mathcal{G}}} \end{bmatrix}$, $D_z = \begin{bmatrix} -\mathbb{C}_k^{\star} \\ \mathbb{C}_k^{\star} \end{bmatrix}$, and $z^{-} = \mathbf{0}_{n+n_{\mathcal{G}}}$. In the case where we use the cluster scores:

$$\mathcal{R}_k\left(w\right) = \sum_{j=1}^{n_{\mathcal{G}}} \left| \sum_{i=1}^{n} w_i \delta_{i,j} \left(M_{k,i} - \mathbb{S}_{j,k}^{\star}\right) \right|$$

we obtain the same parameterization with the following modifications:

$$C_z = \begin{bmatrix} -\left(\delta \odot \left(M_k - \mathbb{S}_k^{\star}\right)\right)^{\top} & -I_{n_{\mathcal{G}}} \\ \left(\delta \odot \left(M_k - \mathbb{S}_k^{\star}\right)\right)^{\top} & -I_{n_{\mathcal{G}}} \end{bmatrix} \quad \text{and} \quad D_z = \begin{bmatrix} \mathbf{0}_{n_{\mathcal{G}}} \\ \mathbf{0}_{n_{\mathcal{G}}} \end{bmatrix}$$

For $k = 0$, we have:

$$\mathcal{R}_0\left(w\right) = \sum_{j=1}^{m} \left| \sum_{i=1}^{n} L_{i,j} w_i \right|$$

We deduce that $z = \begin{bmatrix} w \\ \tau_{(0)} \end{bmatrix}$ is the augmented variable, $\tau_{(0)}$ is a $m \times 1$ vector, $c_z = \begin{bmatrix} \mathbf{0}_n \\ \mathbf{1}_m \end{bmatrix}$, $d_z = 0$, $C_z = \begin{bmatrix} -L^{\top} & -I_m \\ L^{\top} & -I_m \end{bmatrix}$, $D_z = \begin{bmatrix} \mathbf{0}_m \\ \mathbf{0}_m \end{bmatrix}$, and $z^{-} = \mathbf{0}_{n+m}$. Regarding the expected return:

$$\mu\left(w\right) = \phi_0 \sum_{i=1}^{n} w_i \mathcal{C}_i + \sum_{k=1}^{n_{\mu}} \phi_k \sum_{i=1}^{n} w_i \alpha_{k,i}$$

we obtain $z = w$, $c_z = \phi_0 \mathcal{C} + \sum_{k=1}^{n_{\mu}} \phi_k \alpha_k$, $d_z = 0$, and $z^{-} = \mathbf{0}_n$.

The aggregation of the different linear forms gives $\mathcal{LF}\left(z;c,d,C,D,z^{-}\right)$ where the augmented variable is the $(n + m + n_{\mathcal{R}} n_{\mathcal{G}}) \times 1$ vector: $z = \left(w, \tau_{(0)}, \tau_{(1)}, \ldots, \tau_{(n_{\mathcal{R}})}\right)$. The objective function is defined by $c_z = \left(-\gamma\left(\phi_0 \mathcal{C} + \sum_{k=1}^{n_{\mu}} \phi_k \alpha_k\right), \frac{1}{2}\varphi_0 \mathbf{1}_m, \frac{1}{2}\varphi_1 \mathbf{1}_{n_{\mathcal{G}}}, \ldots, \frac{1}{2}\varphi_{n_{\mathcal{R}}} \mathbf{1}_{n_{\mathcal{G}}}\right)$ and $d_z = 0$. The bounds are $z^{-} = \mathbf{0}_{n+m+n_{\mathcal{R}} n_{\mathcal{G}}}$. There are $2 \times (m + n_{\mathcal{R}} n_{\mathcal{G}})$ inequality

constraints, defined by $D_z = \left(\mathbf{0}_m, \mathbf{0}_m, -\mathbb{C}_1^\star, \mathbb{C}_1^\star, \ldots, -\mathbb{C}_{n_\mathcal{R}}^\star, \mathbb{C}_{n_\mathcal{R}}^\star\right)$ and:

$$C_z = \begin{bmatrix} -L^\top & -I_m & & & \\ L^\top & -I_m & & & \\ -\left(\delta \odot M_1\right)^\top & & -I_{n_\mathcal{G}} & & \\ \left(\delta \odot M_1\right)^\top & & -I_{n_\mathcal{G}} & & \\ \vdots & & & \ddots & \\ -\left(\delta \odot M_{n_\mathcal{R}}\right)^\top & & & & -I_{n_\mathcal{G}} \\ \left(\delta \odot M_{n_\mathcal{R}}\right)^\top & & & & -I_{n_\mathcal{G}} \end{bmatrix}$$

where blanks are zeros. This can be written in block form:

$$C_z = \begin{bmatrix} \begin{pmatrix} -1 \\ 1 \end{pmatrix} \otimes L^\top & \begin{pmatrix} -1 \\ -1 \end{pmatrix} \otimes I_m & \mathbf{0} \\ \begin{pmatrix} -1 \\ 1 \end{pmatrix} \otimes \mathcal{M} & \mathbf{0} & I_{n_\mathcal{R}} \otimes \begin{pmatrix} -1 \\ -1 \end{pmatrix} \otimes I_{n_\mathcal{G}} \end{bmatrix}$$

where $\mathcal{M} = \begin{bmatrix} \left(\delta \odot M_1\right)^\top \\ \vdots \\ \left(\delta \odot M_{n_\mathcal{R}}\right)^\top \end{bmatrix}$ is the $(n_\mathcal{R} n_\mathcal{G}) \times n$ vertical stack. We have:

$$C_z \in \mathbb{R}^{2(m+n_\mathcal{R} n_\mathcal{G}) \times (n+m+n_\mathcal{R} n_\mathcal{G})}$$

with the following split:

$$\dim C_z = \begin{bmatrix} 2m \times n & 2m \times m & 2m \times n_\mathcal{R} n_\mathcal{G} \\ 2n_\mathcal{R} n_\mathcal{G} \times n & 2n_\mathcal{R} n_\mathcal{G} \times m & 2n_\mathcal{R} n_\mathcal{G} \times n_\mathcal{R} n_\mathcal{G} \end{bmatrix}$$

B.6.2 With a benchmark

We first transform the various risk measures into the extended linear form $\mathcal{LF}\left(z; c, d, C, D, z^-\right)$. For $k \geq 1$, we have:

$$\mathcal{R}_k\left(w \mid b\right) = \sum_{j=1}^{n_\mathcal{G}} \left| \sum_{i=1}^{n} \left(w_i - b_i\right) \delta_{i,j} M_{k,i} \right| = \sum_{j=1}^{n_\mathcal{G}} \left| \sum_{i=1}^{n} \left(\delta_{i,j} M_{k,i}\right) w_i - \left(\delta_{i,j} M_{k,i}\right) b_i \right|$$

We deduce that $z = \begin{bmatrix} w \\ \tau_{(k)} \end{bmatrix}$ is the augmented variable, $\tau_{(k)}$ is a $n_\mathcal{G} \times 1$ vector, $c_z = \begin{bmatrix} \mathbf{0}_n \\ \mathbf{1}_{n_\mathcal{G}} \end{bmatrix}$, $d_z = 0$, $C_z = \begin{bmatrix} -\left(\delta \odot M_k\right)^\top & -I_{n_\mathcal{G}} \\ \left(\delta \odot M_k\right)^\top & -I_{n_\mathcal{G}} \end{bmatrix}$, $D_z = \begin{bmatrix} -\left(\delta \odot M_k\right)^\top b \\ \left(\delta \odot M_k\right)^\top b \end{bmatrix}$, and $z^- = \mathbf{0}_{n+n_\mathcal{G}}$. In the case where we use the cluster scores:

$$\mathcal{R}_k\left(w \mid b\right) = \sum_{j=1}^{n_\mathcal{G}} \left| \sum_{i=1}^{n} w_i \delta_{i,j} \left(M_{k,i} - \mathbb{S}_{j,k}^\star\right) \right|$$

we obtain the same parameterization with the following modifications:

$$C_z = \begin{bmatrix} -\left(\delta \odot \left(M_k - \mathbb{S}_k^\star\right)\right)^\top & -I_{n_\mathcal{G}} \\ \left(\delta \odot \left(M_k - \mathbb{S}_k^\star\right)\right)^\top & -I_{n_\mathcal{G}} \end{bmatrix} \quad \text{and} \quad D_z = \begin{bmatrix} \mathbf{0}_{n_\mathcal{G}} \\ \mathbf{0}_{n_\mathcal{G}} \end{bmatrix}$$

For $k = 0$, we have:

$$\mathcal{R}_0\left(w \mid b\right) = \sum_{j=1}^{m} \left| \sum_{i=1}^{n} L_{i,j} \left(w_i - b\right) \right|$$

We deduce that $z = \begin{bmatrix} w \\ \tau_{(0)} \end{bmatrix}$ is the augmented variable, $\tau_{(0)}$ is a $m \times 1$ vector, $c_z = \begin{bmatrix} \mathbf{0}_n \\ \mathbf{1}_m \end{bmatrix}$, $d_z = 0$, $C_z = \begin{bmatrix} -L^\top & -I_m \\ L^\top & -I_m \end{bmatrix}$, $D_z = \begin{bmatrix} -L^\top b \\ L^\top b \end{bmatrix}$, and $z^- = \mathbf{0}_{n+m}$. If we use the active share approach, we have:

$$\mathcal{R}'_0\left(w \mid b\right) = \frac{1}{2} \sum_{i=1}^{n} \left| w_i - b \right|$$

We deduce that $z = \begin{bmatrix} w \\ \tau'_{(0)} \end{bmatrix}$ is the augmented variable, $\tau'_{(0)}$ is a $n \times 1$ vector, $c_z = \begin{bmatrix} \mathbf{0}_n \\ \mathbf{1}_n \end{bmatrix}$, $d_z = 0$, $C_z = \begin{bmatrix} -I_n & -I_n \\ I_n & -I_n \end{bmatrix}$, $D_z = \begin{bmatrix} -b \\ b \end{bmatrix}$, and $z^- = \mathbf{0}_{n+m}$. Regarding the expected return:

$$\mu\left(w \mid b\right) = \phi_0 \sum_{i=1}^{n} \left(w_i - b_i\right) \mathcal{C}_i + \sum_{k=1}^{n_\mu} \phi_k \sum_{i=1}^{n} \left(w_i - b_i\right) \alpha_{k,i}$$

we obtain $z = w$, $c_z = \phi_0 \mathcal{C} + \sum_{k=1}^{n_\mu} \phi_k \alpha_k$, $d_z = -c_z^\top b$, and $z^- = \mathbf{0}_n$.

In the case of the two-factor risk model, we have:

$$\mathcal{R}_{\text{2F}}\left(w \mid b\right) = \sigma_r \left| \text{MD}^\top \left(w - b\right) \right| + \sqrt{\rho} \left| \upsilon_s^\top \left(w - b\right) \right| + \sqrt{1-\rho} \left\| \upsilon_s \odot \left(w - b\right) \right\|_1$$

We deduce that $z = \begin{bmatrix} w \\ \tau_{(\text{2F})} \end{bmatrix}$ is the augmented variable, $\tau_{(\text{2F})}$ is a $(2+n) \times 1$ vector, c_z is a $(2+2n) \times 1$ vector, $d_z = 0$, C_z is a $(4+2n) \times (2+2n)$ matrix, D_z is a $(4+2n) \times 1$ vector, and $z^- = \mathbf{0}_{2+2n}$. More specifically, we have:

$$c_z = \begin{bmatrix} \mathbf{0}_n \\ \sigma_r \\ \sqrt{\rho} \\ \sqrt{1-\rho} \cdot \mathbf{1}_n \end{bmatrix}, C_z = \begin{bmatrix} -\text{MD}^\top & -1 & 0 & \mathbf{0}_{1,n} \\ \text{MD}^\top & -1 & 0 & \mathbf{0}_{1,n} \\ -\upsilon_s^\top & 0 & -1 & \mathbf{0}_{1,n} \\ \upsilon_s^\top & 0 & -1 & \mathbf{0}_{1,n} \\ -\text{diag}\left(\upsilon_s\right) & \mathbf{0}_{n,1} & \mathbf{0}_{n,1} & -I_n \\ \text{diag}\left(\upsilon_s\right) & \mathbf{0}_{n,1} & \mathbf{0}_{n,1} & -I_n \end{bmatrix}, \text{ and } D_z = \begin{bmatrix} -\text{MD}^\top b \\ \text{MD}^\top b \\ -\upsilon_s^\top b \\ \upsilon_s^\top b \\ -\upsilon_s \odot b \\ \upsilon_s \odot b \end{bmatrix}$$

We assume that we aggregate the different risk measures $\left(\mathcal{R}_0, \mathcal{R}'_0, \mathcal{R}_1, \ldots, \mathcal{R}_{n_\mathcal{R}}\right)$ and alpha sources $\left(C, \mu_1, \ldots, \mu_{n_\mu}\right)$. We obtain an extended linear form $\mathcal{LF}\left(z; c, d, C, D, z^-\right)$ where the augmented variable is the $(2n + m + n_\mathcal{R} n_\mathcal{G}) \times 1$ vector: $z = \left(w, \tau_{(0)}, \tau'_{(0)}, \tau_{(1)}, \ldots, \tau_{(n_\mathcal{R})}\right)$. The objective function is defined by:

$$c_z = \left(-\gamma \left(\phi_0 \mathcal{C} + \sum_{k=1}^{n_\mu} \phi_k \alpha_k \right), \frac{1}{2}\varphi_0 \mathbf{1}_m, \frac{1}{2}\varphi'_0 \mathbf{1}_n, \frac{1}{2}\varphi_1 \mathbf{1}_{n_\mathcal{G}}, \ldots, \frac{1}{2}\varphi_{n_\mathcal{R}} \mathbf{1}_{n_\mathcal{G}} \right)$$

and $d_z = \gamma\left(\phi_0\mathcal{C} + \sum_{k=1}^{n_\mu}\phi_k\alpha_k\right)^\top b$. The bounds are $z^- = \mathbf{0}_{2n+m+n_\mathcal{R}n_\mathcal{G}}$. There are $2\times(m+n+n_\mathcal{R}n_\mathcal{G})$ inequality constraints defined by:

$$C_z = \begin{bmatrix} -L^\top & -I_m & & & & \\ L^\top & -I_m & & & & \\ -I_n & & -I_n & & & \\ I_n & & -I_n & & & \\ -(\delta\odot M_1)^\top & & & -I_{n_\mathcal{G}} & & \\ (\delta\odot M_1)^\top & & & -I_{n_\mathcal{G}} & & \\ \vdots & & & & \ddots & \\ -(\delta\odot M_{n_\mathcal{R}})^\top & & & & & -I_{n_\mathcal{G}} \\ (\delta\odot M_{n_\mathcal{R}})^\top & & & & & -I_{n_\mathcal{G}} \end{bmatrix} \text{ and } D_z = \begin{bmatrix} -L^\top b \\ L^\top b \\ -b \\ b \\ -(\delta\odot M_1)^\top b \\ (\delta\odot M_1)^\top b \\ \vdots \\ -(\delta\odot M_{n_\mathcal{R}})^\top b \\ (\delta\odot M_{n_\mathcal{R}})^\top b \end{bmatrix}$$

where blanks are zeros. This can be written in block form:

$$C_z = \begin{bmatrix} \begin{pmatrix} -1 \\ 1 \end{pmatrix}\otimes L^\top & \begin{pmatrix} -1 \\ -1 \end{pmatrix}\otimes I_m & \mathbf{0} & \mathbf{0} \\ \begin{pmatrix} -1 \\ 1 \end{pmatrix}\otimes I_n & \mathbf{0} & \begin{pmatrix} -1 \\ -1 \end{pmatrix}\otimes I_n & \mathbf{0} \\ \begin{pmatrix} -1 \\ 1 \end{pmatrix}\otimes \mathcal{M} & \mathbf{0} & \mathbf{0} & I_{n_\mathcal{R}}\otimes\begin{pmatrix} -1 \\ -1 \end{pmatrix}\otimes I_{n_\mathcal{G}} \end{bmatrix}$$

where $\mathcal{M} = \begin{bmatrix} (\delta\odot M_1)^\top \\ \vdots \\ (\delta\odot M_{n_\mathcal{R}})^\top \end{bmatrix}$ is the $(n_\mathcal{R}n_\mathcal{G})\times n$ vertical stack. We have:

$$C_z \in \mathbb{R}^{2(m+n+n_\mathcal{R}n_\mathcal{G})\times(2n+m+n_\mathcal{R}n_\mathcal{G})}$$

with the following split:

$$\dim C_z = \begin{bmatrix} 2m\times n & 2m\times m & 2m\times n & 2m\times n_\mathcal{R}n_\mathcal{G} \\ 2n\times n & 2n\times m & 2n\times n & 2n\times n_\mathcal{R}n_\mathcal{G} \\ 2n_\mathcal{R}n_\mathcal{G}\times n & 2n_\mathcal{R}n_\mathcal{G}\times m & 2n_\mathcal{R}n_\mathcal{G}\times n & 2n_\mathcal{R}n_\mathcal{G}\times n_\mathcal{R}n_\mathcal{G} \end{bmatrix}$$

B.7 Optimization algorithms

This section provides technical details on the different optimization algorithms used in Section 2.4 on page 37, which is dedicated to advanced bond portfolio optimization. For a comprehensive treatment of ADMM, proximal operators, and Dykstra's algorithm, the reader is referred to Perrin and Roncalli (2020). The presentation on genetic algorithms is adapted from Ben Slimane (2021), while the discussion on mixed integer programming comes from Ben Slimane and Menchaoui (2023).

B.7.1 Alternating direction method of multipliers

The alternating direction method of multipliers (ADMM) is an algorithm introduced by Gabay and Mercier (1976) to solve optimization problems which can be expressed as:

$$\begin{aligned} \{x^\star, y^\star\} &= \arg\min_{(x,y)} f_x(x) + f_y(y) \\ &\text{s.t.} \quad Ax + By = c \end{aligned} \tag{62}$$

where $A \in \mathbb{R}^{p\times n}$, $B \in \mathbb{R}^{p\times m}$, $c \in \mathbb{R}^p$, and the functions $f_x : \mathbb{R}^n \to \mathbb{R} \cup \{+\infty\}$ and $f_y : \mathbb{R}^m \to \mathbb{R} \cup \{+\infty\}$ are proper closed convex functions. Boyd *et al.* (2011) show that the ADMM algorithm consists of the following three steps:

1. The x-update is:

$$x^{(k+1)} = \arg\min_x \left\{ f_x^{(k+1)}(x) = f_x(x) + \frac{\theta}{2} \left\| Ax + By^{(k)} - c + u^{(k)} \right\|_2^2 \right\} \tag{63}$$

2. The y-update is:

$$y^{(k+1)} = \arg\min_y \left\{ f_y^{(k+1)}(y) = f_y(y) + \frac{\theta}{2} \left\| Ax^{(k+1)} + By - c + u^{(k)} \right\|_2^2 \right\} \tag{64}$$

3. The u-update is:

$$u^{(k+1)} = u^{(k)} + \left(Ax^{(k+1)} + By^{(k+1)} - c \right) \tag{65}$$

In this approach, $u^{(k)}$ is the dual variable of the primal residual $r = Ax + By - c$ and θ is the $\boldsymbol{\ell}_2$-norm penalty variable. The parameter θ can be constant or may change at each iteration. The ADMM algorithm benefits from the dual ascent principle and the method of multipliers. The difference with the latter is that the x- and y-updates are performed in an alternating way. In practice, ADMM may be slow to converge with high accuracy, but is fast to converge if we consider modest accuracy. This is why ADMM is a good candidate for solving large-scale optimization problems, where high accuracy does not necessarily lead to a better solution.

B.7.2 Proximal operator

The x- and y-update steps of the ADMM algorithm require solving a $\boldsymbol{\ell}_2$-norm penalized optimization problem. Proximal operators are special cases of this type of problem when the matrices A or B correspond to the identity matrix I_n or its opposite $-I_n$. Let $f : \mathbb{R}^n \to \mathbb{R} \cup \{+\infty\}$ be a proper closed convex function. The proximal operator $\mathbf{prox}_f(v) : \mathbb{R}^n \to \mathbb{R}^n$ is defined by:

$$\mathbf{prox}_f(v) = x^\star = \arg\min_x \left\{ f_v(x) = f(x) + \frac{1}{2} \|x - v\|_2^2 \right\} \tag{66}$$

Since the function $f_v(x) = f(x) + \frac{1}{2}\|x - v\|_2^2$ is strongly convex, it has a unique minimum for every $v \in \mathbb{R}^n$ (Parikh and Boyd, 2014). By construction, the proximal operator defines a point $x^\star$ which is a trade-off between minimizing $f(x)$ and being close to v. When $f(x) = \mathbb{1}_\Omega(x)$ is the indicator function, the proximal operator is the Euclidean projection onto Ω:

$$\mathbf{prox}_f(v) = \arg\min_x \left\{ \mathbb{1}_\Omega(x) + \frac{1}{2} \|x - v\|_2^2 \right\} = \arg\min_{x\in\Omega} \left\{ \|x - v\|_2^2 \right\} = \mathcal{P}_\Omega(v)$$

where $\mathcal{P}_\Omega(v)$ is the standard projection of v onto Ω. Parikh and Boyd (2014) interpret then proximal operators as a generalization of the Euclidean projection.

Here, we give the results of Parikh and Boyd (2014) for some simple polyhedra:

Notation	Ω	$\mathcal{P}_{\Omega}(v)$
$\mathcal{A}_{ffineset}[A,B]$	$Ax=B$	$v-A^{\dagger}(Av-B)$
$\mathcal{H}_{yperplane}[a,b]$	$a^{\top}x=b$	$v-\frac{\left(a^{\top}v-b\right)}{\|a\|_2^2}a$
$\mathcal{H}_{alfspace}[c,d]$	$c^{\top}x\leq d$	$v-\frac{\left(c^{\top}v-d\right)_+}{\|c\|_2^2}c$
$\mathcal{B}_{ox}\left[x^-,x^+\right]$	$x^-\leq x\leq x^+$	$\mathcal{T}\left(v;x^-,x^+\right)$

where $A^{\dagger}$ is the Moore-Penrose pseudo-inverse of A, and $\mathcal{T}\left(v;x^-,x^+\right)$ is the truncation operator. If we consider the $\boldsymbol{\ell}_p$-norm function $f(x)=\|x\|_p$, we have[59]:

p	$\mathbf{prox}_{\lambda f}(v)$
$p=1$	$\mathcal{S}(v;\lambda)=\operatorname{sign}(v)\odot\left(\lvert v\rvert-\lambda\mathbf{1}_n\right)_+$
$p=2$	$\left(1-\frac{\lambda}{\max\left(\lambda,\|v\|_2\right)}\right)v$
$p=\infty$	$\operatorname{sign}(v)\odot\mathbf{prox}_{\lambda\max x}\left(\lvert v\rvert\right)$

We can show that the projection onto the $\boldsymbol{\ell}_p$ ball can be deduced from the proximal operator of the $\boldsymbol{\ell}_q$-norm function. Let $\mathcal{B}_p(c,\lambda)=\left\{x\in\mathbb{R}^n:\|x-c\|_p\leq\lambda\right\}$ be the $\boldsymbol{\ell}_p$ ball with center c and radius λ. We have:

p	$\mathcal{P}_{\mathcal{B}_p(\mathbf{0}_n,\lambda)}(v)$	q
$p=1$	$v-\operatorname{sign}(v)\odot\mathbf{prox}_{\lambda\max x}\left(\lvert v\rvert\right)$	$q=\infty$
$p=2$	$v-prox_{\lambda\|x\|_2}(v)$	$q=2$
$p=\infty$	$\mathcal{T}(v;-\lambda,\lambda)$	$q=1$

B.7.3 Dykstra's algorithm

We consider the proximal optimization problem where the function $f(x)$ is the convex sum of basic functions $f_j(x)$:

$$x^{\star}=\arg\min_x\left\{\sum_{j=1}^m f_j(x)+\frac{1}{2}\|x-v\|_2^2\right\}$$

and the proximal of each basic function is known. Following Dykstra (1983), the solution can be found by solving the following algorithm:

1. The x-update is:
$$x^{(k+1)}=\mathbf{prox}_{f_{j(k)}}\left(x^{(k)}+z^{(k+1-m)}\right)$$
2. The z-update is:
$$z^{(k+1)}=x^{(k)}+z^{(k+1-m)}-x^{(k+1)}$$

[59] In the case of the pointwise maximum function $f(x)=\max x$, we have $\mathbf{prox}_{\lambda\max x}(v)=\min(v,s^{\star})$ where $s^{\star}$ is the solution of the equation $s^{\star}=\left\{s\in\mathbb{R}:\sum_{i=1}^n(v_i-s)_+=\lambda\right\}$.

where $x^{(0)} = v$, $z^{(k)} = \mathbf{0}_n$ for $k < 0$ and $j(k) = \mod(k+1, m)$ denotes the modulo operator taking values in $\{1, \ldots, m\}$. The variable $x^{(k)}$ is updated at each iteration while the residual $z^{(k)}$ is updated every m iterations. This implies that the basic function $f_j(x)$ is related to the residuals $z^{(j)}$, $z^{(j+m)}$, $z^{(j+2m)}$, etc. Following Tibshirani (2017), it is better to write the Dykstra's algorithm by using two iteration indices k and j. The main index k refers to the cycle, whereas the sub-index j refers to the function/constraint number:

1. The x-update is:
$$x^{(k+1,j)} = \mathbf{prox}_{f_j}\left(x^{(k+1,j-1)} + z^{(k,j)}\right) \tag{67}$$
2. The z-update is:
$$z^{(k+1,j)} = x^{(k+1,j-1)} + z^{(k,j)} - x^{(k+1,j)} \tag{68}$$

where $x^{(1,0)} = v$, $z^{(k,j)} = \mathbf{0}_n$ for $k = 0$ and $x^{(k+1,0)} = x^{(k,m)}$. The Dykstra's algorithm is particularly efficient when we consider the projection problem:

$$x^\star = \mathcal{P}_\Omega(v)$$

where:

$$\Omega = \Omega_1 \cap \Omega_2 \cap \cdots \cap \Omega_m$$

Indeed, the solution is found by replacing Equation (67) with:

$$x^{(k+1,j)} = \mathcal{P}_{\Omega_j}\left(x^{(k+1,j-1)} + z^{(k,j)}\right) \tag{69}$$

Let us consider the case $\Omega = \{x \in \mathbb{R}^n : Cx \leq D\}$ where the number of inequality constraints is equal to m. We can write $\Omega = \Omega_1 \cap \Omega_2 \cap \cdots \cap \Omega_m$ where $\Omega_j = \left\{x \in \mathbb{R}^n : c_{(j)}^\top x \leq d_{(j)}\right\}$, $c_{(j)}^\top$ corresponds to the j^{th} row of C and $d_{(j)}$ is the j^{th} element of D. Since $\mathcal{P}_{\Omega_j}$ is the half-space projection, the Dykstra's algorithm for solving the proximal problem with linear inequality constraints is the following:

- The x-update is:
$$x^{(k+1,j)} = x^{(k+1,j-1)} + z^{(k,j)} - \frac{\left(c_{(j)}^\top x^{(k+1,j-1)} + c_{(j)}^\top z^{(k,j)} - d_{(j)}\right)_+}{\left\|c_{(j)}\right\|_2^2} c_{(j)}$$
- The z-update is:
$$z^{(k+1,j)} = x^{(k+1,j-1)} + z^{(k,j)} - x^{(k+1,j)}$$

Consider the set $\Omega = \left\{x \in \mathbb{R}^n : Ax = B, Cx \leq D, x^- \leq x \leq x^+\right\}$. We can decompose Ω as the intersection of three basic convex sets: $\Omega = \Omega_1 \cap \Omega_2 \cap \Omega_3$ where $\Omega_1 = \{x \in \mathbb{R}^n : Ax = B\}$, $\Omega_2 = \{x \in \mathbb{R}^n : Cx \leq D\}$ and $\Omega_3 = \left\{x \in \mathbb{R}^n : x^- \leq x \leq x^+\right\}$. The Dykstra's algorithm becomes[60]:

1. $x_0^{(k+1)} \leftarrow x_3^{(k)}$
2. $x_1^{(k+1)} \leftarrow x_0^{(k+1)} + z_1^{(k)} - A^\dagger\left(Ax_0^{(k+1)} + Az_1^{(k)} - B\right)$

[60] We initialize $x_1^{(0)}, x_2^{(0)}, x_3^{(0)} \leftarrow v$ and $z_1^{(0)}, z_2^{(0)}, z_3^{(0)} \leftarrow \mathbf{0}_n$.

3. $z_1^{(k+1)} \leftarrow x_0^{(k+1)} + z_1^{(k)} - x_1^{(k+1)}$
4. $x_2^{(k+1)} \leftarrow \mathcal{P}_{\Omega_2}\left(x_1^{(k+1)} + z_2^{(k)}\right)$ using the previous algorithm to solve the proximal problem with linear inequality constraints
5. $z_2^{(k+1)} \leftarrow x_1^{(k+1)} + z_2^{(k)} - x_2^{(k+1)}$
6. $x_3^{(k+1)} \leftarrow \mathcal{T}\left(x_2^{(k+1)} + z_3^{(k)}; x^-, x^+\right)$
7. $z_3^{(k+1)} \leftarrow x_2^{(k+1)} + z_3^{(k)} - x_3^{(k+1)}$

C Additional results

C.1 Tables

Table 21: Minimum tradable amount (G0BC Index, end of May 2026)

MT_i	Currency							Total
	AUD	CAD	CHF	EUR	GBP	JPY	USD	
0.01				1				1
1						1	2	3
100		3						3
1 000	43	806		347	52		1 646	2 894
2 000		92		1			7 684	7 777
5 000		118	452				17	587
10 000	307	1		1			8	317
20 000							1	1
25 000							1	1
50 000			2	4	77		2	85
100 000	34	12	43	4 235	774	4	150	5 252
125 000				7				7
150 000		99		18	1		218	336
200 000	122	38	60	44	17		2 044	2 325
250 000	32			3			251	286
500 000	15	1						16
1 000 000	31	1		2		56	29	119
2 000 000						1		1
5 000 000	1							1
10 000 000	1					3		4
100 000 000						333		333
140 000 000	1							1
Total	587	1 171	557	4 663	921	398	12 053	20 350

Source: ICE BofA & Authors' calculations.

Table 22: Tracking error minimization without specific risk (Barra model, ER00 Index, end of May 2026)

Statistic	Benchmark	Active share limit $\mathcal{AS}^+$			
		25%	30%	40%	100%
Holdings	4 663	3 444	3 234	2 784	137
Active share (in %)		25.00	30.00	40.00	97.12
ENB (w)	3 940	447	370	276	112
Top 100 weight (in %)	5.36	29.22	33.97	43.59	92.03
$\sigma\left(w \mid b\right)$ (in bps)		12.04	9.61	7.01	3.77
$\sigma_{\mathcal{F}}\left(w \mid b\right)$ (in bps)		12.04	9.61	7.01	3.77
$\sigma_{\epsilon}\left(w \mid b\right)$ (in bps)		0.00	0.00	0.00	0.00
Yield (in %)	3.47	3.63	3.63	3.63	3.61
$\beta_{\text{DTS}}\left(w \mid b\right)$	1.00	1.21	1.21	1.18	1.16
MD (in year)	4.48	4.68	4.68	4.68	4.68
5Y DTS (in bps)	92	192	192	192	192
7Y DTS (in bps)	101	126	126	126	126
10Y+ DTS (in bps)	48	23	23	23	23
Financials DTS (in bps)	128	228	228	228	228
A-rated DTS (in bps)	159	134	134	134	112
BBB-rated DTS (in bps)	193	289	289	271	268

Table 23: Tracking error minimization with specific risk (Barra model, C0A0 Index, end of May 2026)

Statistic	Benchmark	Active share limit $\mathcal{AS}^+$			
		25%	30%	40%	100%
Holdings	11 507	8 717	8 193	7 037	3 393
Active share (in %)		25.00	30.00	40.00	73.22
ENB (w)	7 121	784	763	672	417
Top 100 weight (in %)	4.79	24.49	25.73	29.04	39.51
$\sigma\left(w \mid b\right)$ (in bps)		6.71	5.80	4.96	4.22
$\sigma_{\mathcal{F}}\left(w \mid b\right)$ (in bps)		4.49	3.66	2.79	1.93
$\sigma_{\epsilon}\left(w \mid b\right)$ (in bps)		2.22	2.14	2.17	2.29
Yield (in %)	5.13	5.28	5.28	5.28	5.27
$\beta_{\text{DTS}}\left(w \mid b\right)$	1.00	1.09	1.09	1.09	1.08
MD (in year)	6.49	6.69	6.69	6.69	6.69
5Y DTS (in bps)	48	148	148	148	148
7Y DTS (in bps)	67	92	92	92	92
10Y+ DTS (in bps)	299	262	260	254	247
Financials DTS (in bps)	133	233	233	233	233
A-rated DTS (in bps)	203	178	178	178	178
BBB-rated DTS (in bps)	283	345	346	342	330

Table 24: Tracking error minimization without specific risk (Barra model, C0A0 Index, end of May 2026)

Statistic	Benchmark	Active share limit $\mathcal{AS}^+$			
		25%	30%	40%	100%
Holdings	11 507	8 689	8 073	6 891	186
Active share (in %)		25.00	30.00	40.00	98.36
ENB (w)	7 121	506	440	320	123
Top 100 weight (in %)	4.79	27.91	32.41	41.84	85.81
$\sigma\left(w \mid b\right)$ (in bps)		4.59	3.67	2.60	0.77
$\sigma_{\mathcal{F}}\left(w \mid b\right)$ (in bps)		4.59	3.67	2.60	0.77
$\sigma_{\epsilon}\left(w \mid b\right)$ (in bps)		0.00	0.00	0.00	0.00
Yield (in %)	5.13	5.29	5.29	5.26	5.20
$\beta_{\text{DTS}}\left(w \mid b\right)$	1.00	1.10	1.10	1.09	1.07
MD (in year)	6.49	6.69	6.69	6.69	6.69
5Y DTS (in bps)	48	148	148	148	148
7Y DTS (in bps)	67	92	92	92	92
10Y+ DTS (in bps)	299	262	254	252	255
Financials DTS (in bps)	133	233	233	233	233
A-rated DTS (in bps)	203	178	178	178	162
BBB-rated DTS (in bps)	283	356	356	350	349

Table 25: Yield maximization (Barra model, C0A0 Index, end of May 2026)

Statistic	Benchmark	Active share limit $\mathcal{AS}^+$			
		25%	30%	40%	100%
Holdings	11 507	8 861	8 272	7 016	103
Active share (in %)		25.00	30.00	40.00	99.29
ENB (w)	7 121	401	342	260	101
Top 100 weight (in %)	4.79	28.75	33.50	43.11	99.06
$\sigma\left(w \mid b\right)$ (in bps)		77.74	88.64	102.99	148.58
$\sigma_{\mathcal{F}}\left(w \mid b\right)$ (in bps)		75.56	86.48	100.31	143.76
$\sigma_{\epsilon}\left(w \mid b\right)$ (in bps)		2.18	2.17	2.69	4.81
Yield (in %)	5.13	5.64	5.72	5.85	6.25
$\beta_{\text{DTS}}\left(w \mid b\right)$	1.00	1.27	1.30	1.33	1.52
MD (in year)	6.49	6.94	6.99	6.99	6.69
5Y DTS (in bps)	48	148	148	148	148
7Y DTS (in bps)	67	92	92	92	92
10Y+ DTS (in bps)	299	270	274	274	274
Financials DTS (in bps)	133	252	271	269	434
A-rated DTS (in bps)	203	178	178	178	178
BBB-rated DTS (in bps)	283	383	383	383	383

Table 26: Tracking error minimization with specific risk (Barra model, G0BC Index, end of May 2026)

Statistic	Benchmark	Active share limit $\mathcal{AS}^+$			
		25%	30%	40%	100%
Holdings	20 350	14 810	13 946	12 284	8 661
Active share (in %)		25.00	30.00	40.00	60.12
ENB (w)	12 788	1 273	1 167	1 075	920
Top 100 weight (in %)	3.10	16.13	17.43	19.16	22.08
$\sigma\left(w \mid b\right)$ (in bps)		1.94	1.78	1.62	1.54
$\sigma_{\mathcal{F}}\left(w \mid b\right)$ (in bps)		1.25	1.09	0.91	0.75
$\sigma_{\epsilon}\left(w \mid b\right)$ (in bps)		0.70	0.69	0.71	0.79
Yield (in %)	4.62	4.80	4.80	4.79	4.78
$\beta_{\text{DTS}}\left(w \mid b\right)$	1.00	1.19	1.19	1.18	1.18
MD (in year)	5.83	6.07	6.06	6.06	6.05
5Y DTS (in bps)	62	162	162	162	162
7Y DTS (in bps)	75	100	100	100	100
10Y+ DTS (in bps)	224	199	199	199	199
Financials DTS (in bps)	133	233	233	233	233
A-rated DTS (in bps)	190	165	165	165	165
BBB-rated DTS (in bps)	255	355	355	355	355

Table 27: Tracking error minimization without specific risk (Barra model, G0BC Index, end of May 2026)

Statistic	Benchmark	Active share limit $\mathcal{AS}^+$			
		25%	30%	40%	100%
Holdings	20 350	14 652	13 592	11 675	19 629
Active share (in %)		25.00	30.00	40.00	63.72
ENB (w)	12 788	687	591	444	333
Top 100 weight (in %)	3.10	25.48	29.51	37.91	46.55
$\sigma\left(w \mid b\right)$ (in bps)		0.69	0.47	0.20	0.17
$\sigma_{\mathcal{F}}\left(w \mid b\right)$ (in bps)		0.69	0.47	0.20	0.17
$\sigma_{\epsilon}\left(w \mid b\right)$ (in bps)		0.00	0.00	0.00	0.00
Yield (in %)	4.62	4.75	4.75	4.76	4.76
$\beta_{\text{DTS}}\left(w \mid b\right)$	1.00	1.17	1.17	1.15	1.13
MD (in year)	5.83	6.11	6.09	6.03	6.03
5Y DTS (in bps)	62	162	162	162	162
7Y DTS (in bps)	75	100	100	100	100
10Y+ DTS (in bps)	224	199	199	191	182
Financials DTS (in bps)	133	233	233	233	233
A-rated DTS (in bps)	190	165	165	165	149
BBB-rated DTS (in bps)	255	355	351	336	322

Table 28: Yield maximization (Barra model, G0BC Index, end of May 2026)

Statistic	Benchmark	Active share limit $\mathcal{AS}^+$			
		25%	30%	40%	100%
Holdings	20 350	14 953	13 837	11 981	106
Active share (in %)		25.00	30.00	40.00	99.70
ENB (w)	12 788	416	345	264	102
Top 100 weight (in %)	3.10	27.43	32.31	41.95	98.60
$\sigma\left(w \mid b\right)$ (in bps)		126.26	144.34	149.80	238.86
$\sigma_{\mathcal{F}}\left(w \mid b\right)$ (in bps)		125.05	143.11	148.17	236.06
$\sigma_{\epsilon}\left(w \mid b\right)$ (in bps)		1.20	1.23	1.63	2.80
Yield (in %)	4.62	5.59	5.74	5.95	6.63
$\beta_{\text{DTS}}\left(w \mid b\right)$	1.00	1.22	1.24	1.31	1.53
MD (in year)	5.83	6.06	6.09	6.33	6.33
5Y DTS (in bps)	62	162	162	162	162
7Y DTS (in bps)	75	100	100	100	100
10Y+ DTS (in bps)	224	184	187	191	199
Financials DTS (in bps)	133	233	248	283	428
A-rated DTS (in bps)	190	165	165	165	165
BBB-rated DTS (in bps)	255	355	355	355	355

Table 29: Benchmark weight breakdown by sector and maturity (active management, ER00 Index, end of May 2026)

Sector	0–3Y	3–5Y	5–7Y	7–10Y	10Y+	Total
Automotive	2.11%	1.48%	0.81%	0.47%	0.22%	5.09%
Banking	10.03%	9.56%	4.98%	2.97%	0.12%	27.65%
Basic Industry	1.10%	1.20%	0.98%	0.58%	0.29%	4.14%
Capital Goods	1.18%	1.14%	0.73%	0.61%	0.34%	3.98%
Consumer Goods	1.35%	1.63%	1.33%	1.09%	0.88%	6.28%
Energy	0.90%	0.98%	0.88%	0.50%	0.36%	3.61%
Financial Services	1.97%	1.95%	0.96%	0.90%	0.25%	6.02%
Healthcare	1.19%	1.37%	1.03%	0.62%	1.09%	5.31%
Insurance	1.15%	0.79%	0.82%	1.26%	0.13%	4.16%
Leisure	0.14%	0.17%	0.19%	0.12%	0.13%	0.74%
Media	0.31%	0.26%	0.43%	0.17%	0.39%	1.55%
Real Estate	1.18%	1.53%	1.31%	0.72%	0.27%	5.00%
Retail	0.58%	0.72%	0.53%	0.47%	0.21%	2.51%
Services	0.46%	0.37%	0.35%	0.09%		1.27%
Technology & Electronics	0.71%	0.55%	0.52%	0.20%	0.13%	2.11%
Telecommunications	1.04%	1.01%	1.24%	1.14%	0.77%	5.21%
Transportation	1.09%	1.12%	0.99%	0.84%	0.50%	4.54%
Utility	2.47%	2.44%	2.35%	2.35%	1.23%	10.85%
Total	28.95%	28.25%	20.42%	15.08%	7.29%	100.00%

Table 30: Active weights in % by maturity buckets (active management, ER00 Index, $\lambda = 0$)

Sector	0–3Y	3–5Y	5–7Y	7–10Y	10Y+	Total
Positive views						
Banking (++)	0.00	0.00	0.00	0.00	0.00	0.00
Financial Services (+)	−0.00	0.00	1.29	0.00	−0.00	1.29
Insurance (+)	−0.00	−0.00	0.00	0.71	0.00	0.71
Real Estate (+)	−0.00	2.90	0.00	−0.00	−0.27	2.63
Utility (+)	−0.78	0.00	0.00	0.08	0.00	−0.69
Negative views						
Capital Goods (−)	−1.18	−0.00	0.00	0.00	−0.00	−1.18
Retail (−)	−0.58	−0.00	0.00	0.54	0.00	−0.04
Technology & Electronics (−)	−0.00	0.00	0.46	0.00	−0.00	0.46
Telecommunications (−)	−1.04	0.00	0.00	0.00	0.00	−1.04
Consumer Goods (−−)	−1.35	−0.00	0.00	0.00	−0.00	−1.35
Other sectors	−4.59	1.66	1.89	0.46	−0.22	−0.80
Net allocation change	−9.51	4.55	3.64	1.80	−0.49	0.00

Table 31: Active weights in % by maturity buckets (active management, ER00 Index, $\lambda = 0.20$)

Sector	0–3Y	3–5Y	5–7Y	7–10Y	10Y+	Total
Positive views						
Banking (++)	0.00	0.00	3.54	0.00	0.84	4.38
Financial Services (+)	0.00	0.00	1.29	0.00	0.00	1.29
Insurance (+)	0.00	0.00	0.00	0.71	0.00	0.71
Real Estate (+)	0.00	1.97	0.00	0.00	−0.00	1.97
Utility (+)	0.00	0.00	0.00	0.00	0.00	0.00
Negative views						
Capital Goods (−)	−1.09	0.00	−0.00	−0.61	−0.34	−2.03
Retail (−)	−0.58	−0.00	0.00	0.00	−0.21	−0.79
Technology & Electronics (−)	0.00	0.00	0.00	−0.00	−0.13	−0.13
Telecommunications (−)	−0.00	0.00	0.00	−0.00	−0.77	−0.77
Consumer Goods (−−)	−1.35	−1.63	−1.33	−1.09	−0.88	−6.28
Other sectors	−0.00	0.00	1.25	0.41	0.00	1.66
Net allocation change	−3.02	0.34	4.74	−0.57	−1.49	0.00

Table 32: Active weights in % by maturity buckets (active management, ER00 Index, $\lambda = 0.50$)

Sector	0–3Y	3–5Y	5–7Y	7–10Y	10Y+	Total
Positive views						
Banking (++)	0.00	0.00	3.54	0.00	0.84	4.38
Financial Services (+)	0.00	0.00	1.29	0.00	0.00	1.29
Insurance (+)	0.00	0.00	0.00	0.71	0.00	0.71
Real Estate (+)	0.00	1.97	0.00	0.00	−0.00	1.97
Utility (+)	0.00	0.00	0.00	0.00	0.00	0.00
Negative views						
Capital Goods (−)	−0.00	−0.00	−0.73	−0.61	−0.34	−1.67
Retail (−)	−0.00	−0.00	−0.00	−0.47	−0.21	−0.68
Technology & Electronics (−)	−0.00	−0.00	−0.48	−0.20	−0.13	−0.81
Telecommunications (−)	−0.00	−0.00	−0.00	−1.14	−0.77	−1.91
Consumer Goods (−−)	−0.00	−1.63	−1.33	−1.09	−0.88	−4.93
Other sectors	0.00	0.00	1.25	0.41	0.00	1.66
Net allocation change	−0.00	0.34	3.53	−2.38	−1.49	0.00

Table 33: DTS contributions in bps of optimized portfolios (active management, ER00 Index, end of May 2026)

Sector	Benchmark	Confidence λ					
		0	10%	20%	30%	40%	50%
Positive views							
Banking (++)	86	86	111	111	111	111	111
Financial Services (+)	22	28	28	28	28	28	28
Insurance (+)	20	27	27	27	27	27	27
Real Estate (+)	24	32	32	32	32	32	32
Utility (+)	49	48	49	49	49	49	49
Negative views							
Capital Goods (−)	12	11	9	5	6	6	4
Retail (−)	9	12	9	6	7	4	4
Technology & Electronics (−)	8	10	6	6	5	5	2
Telecommunications (−)	23	22	16	16	9	9	9
Consumer Goods (−−)	24	23	9	0	0	0	1
Other sectors	104	115	111	113	113	113	113
Portfolios DTS	382	415	407	394	387	384	380

Table 34: Optimal investable portfolios (Barra model, C0A0 Index, end of May 2026, one-step approach, no cardinality constraint, no active share limit)

Statistic	Benchmark	Continuous	50 mn	100 mn	500 mn	1 bn
Holdings	11 507	103	118	108	109	129
Active share (in %)		99.29	99.25	99.27	99.29	99.15
ENB (w)	7 121	101	102	102	101	107
Top 100 weight (in %)	4.79	99.06	98.74	98.78	99.01	95.07
$\sigma\left(w \mid b\right)$ (in bps)		148.58	147.61	147.65	148.42	146.39
$\sigma_{\mathcal{F}}\left(w \mid b\right)$ (in bps)		143.76	142.84	142.89	143.62	141.72
$\sigma_{\epsilon}\left(w \mid b\right)$ (in bps)		4.81	4.76	4.76	4.80	4.68
Yield (in %)	5.13	6.25	6.25	6.25	6.25	6.24
$\beta_{\text{DTS}}\left(w \mid b\right)$	1.00	1.52	1.52	1.52	1.52	1.53
MD (in year)	6.49	6.69	6.70	6.70	6.69	6.69
5Y DTS (in bps)	48	158	157	157	158	156
7Y DTS (in bps)	67	92	92	92	92	92
10Y+ DTS (in bps)	299	274	274	274	274	274
Financials DTS (in bps)	133	434	433	433	434	439
A-rated DTS (in bps)	203	178	178	178	178	178
BBB-rated DTS (in bps)	283	383	383	383	383	383
c_{ash} (in %)			0.00	0.00	0.00	0.00
$\mathcal{C}_{ash}$ (in \$)			159	850	892	3 531
$\mathcal{IG}_{ap}$ (in %)			0.48	0.40	0.06	5.35

Table 35: Optimal investable portfolios (Barra model, C0A0 Index, end of May 2026, one-step approach, at least 150 holdings, no active share limit)

Statistic	Benchmark	Continuous	50 mn	100 mn	500 mn	1 bn
Holdings	11 507	103	151	162	150	151
Active share (in %)		99.29	99.18	99.22	99.28	99.14
ENB (w)	7 121	101	102	102	101	107
Top 100 weight (in %)	4.79	99.06	98.61	98.72	99.00	95.05
$\sigma\left(w \mid b\right)$ (in bps)		148.58	147.49	147.48	148.40	146.37
$\sigma_{\mathcal{F}}\left(w \mid b\right)$ (in bps)		143.76	142.74	142.73	143.60	141.69
$\sigma_{\epsilon}\left(w \mid b\right)$ (in bps)		4.81	4.74	4.75	4.80	4.67
Yield (in %)	5.13	6.25	6.25	6.25	6.25	6.24
$\beta_{\text{DTS}}\left(w \mid b\right)$	1.00	1.52	1.52	1.52	1.52	1.53
MD (in year)	6.49	6.69	6.69	6.69	6.69	6.69
5Y DTS (in bps)	48	158	157	157	158	156
7Y DTS (in bps)	67	92	92	92	92	92
10Y+ DTS (in bps)	299	274	273	273	274	274
Financials DTS (in bps)	133	434	433	433	434	439
A-rated DTS (in bps)	203	178	178	178	178	178
BBB-rated DTS (in bps)	283	383	383	383	383	383
c_{ash} (in %)			0.00	0.00	0.00	0.00
$\mathcal{C}_{ash}$ (in \$)			369.04	827.21	237.46	53.17
$\mathcal{IG}_{ap}$ (in %)			0.54	0.44	0.07	5.35

Table 36: Optimal investable portfolios (Barra model, C0A0 Index, end of May 2026, two-step approach, no cardinality constraint, no active share limit)

Statistic	Benchmark	Continuous	50 mn	100 mn	500 mn	1 bn
Holdings	11 507	103	108	108	106	120
Active share (in %)		99.29	99.23	99.25	99.27	98.73
ENB (w)	7 121	101	103	102	101	107
Top 100 weight (in %)	4.79	99.06	98.76	98.82	99.02	95.52
$\sigma\left(w \mid b\right)$ (in bps)		148.58	147.29	147.38	148.38	142.71
$\sigma_{\mathcal{F}}\left(w \mid b\right)$ (in bps)		143.76	142.53	142.61	143.58	137.88
$\sigma_{\epsilon}\left(w \mid b\right)$ (in bps)		4.81	4.76	4.76	4.80	4.83
Yield (in %)	5.13	6.25	6.24	6.24	6.25	6.17
$\beta_{\text{DTS}}\left(w \mid b\right)$	1.00	1.52	1.52	1.52	1.52	1.49
MD (in year)	6.49	6.69	6.69	6.69	6.69	6.69
5Y DTS (in bps)	48	158	158	158	158	157
7Y DTS (in bps)	67	92	92	92	92	92
10Y+ DTS (in bps)	299	274	274	274	274	262
Financials DTS (in bps)	133	434	432	432	433	425
A-rated DTS (in bps)	203	178	176	176	178	175
BBB-rated DTS (in bps)	283	383	383	383	383	383
c_{ash} (in %)			0.08	0.04	0.01	1.03
$\mathcal{C}_{ash}$ (in k\$)			38.9	40.4	39.8	10 278
$\mathcal{IG}_{ap}$ (in %)			0.26	0.23	0.04	3.45

Table 37: Optimal investable portfolios (Barra model, C0A0 Index, end of May 2026, two-step approach, no cardinality constraint, no active share limit, $\varphi = 1$)

Statistic	Benchmark	Continuous	50 mn	100 mn	500 mn	1 bn
Holdings	11 507	103	120	112	113	193
Active share (in %)		99.29	99.25	99.26	99.27	99.19
ENB (w)	7 121	101	102	102	101	107
Top 100 weight (in %)	4.79	99.06	98.76	98.81	99.02	95.55
$\sigma\left(w \mid b\right)$ (in bps)		148.58	147.40	147.35	148.36	142.19
$\sigma_{\mathcal{F}}\left(w \mid b\right)$ (in bps)		143.76	142.64	142.58	143.56	137.35
$\sigma_{\epsilon}\left(w \mid b\right)$ (in bps)		4.81	4.76	4.77	4.80	4.84
Yield (in %)	5.13	6.25	6.25	6.25	6.25	6.22
$\beta_{\text{DTS}}\left(w \mid b\right)$	1.00	1.52	1.52	1.52	1.52	1.50
MD (in year)	6.49	6.69	6.69	6.69	6.69	6.69
5Y DTS (in bps)	48	158	158	158	158	159
7Y DTS (in bps)	67	92	92	93	92	93
10Y+ DTS (in bps)	299	274	274	274	274	263
Financials DTS (in bps)	133	434	433	433	433	424
A-rated DTS (in bps)	203	178	177	177	177	178
BBB-rated DTS (in bps)	283	383	383	383	383	383
c_{ash} (in %)			0.00	0.00	0.00	0.00
$\mathcal{C}_{ash}$ (in \$)			330	286	531	146
$\mathcal{IG}_{ap}$ (in %)			0.30	0.26	0.05	3.97

Table 38: Optimal investable portfolios (Barra model, G0BC Index, end of May 2026, one-step approach, no cardinality constraint, no active share limit)

Statistic	Benchmark	Continuous	50 mn	100 mn	500 mn	1 bn
Holdings	20 350	106	117	110	115	133
Active share (in %)		99.70	99.66	99.68	99.68	99.64
ENB (w)	12 788	102	105	104	104	105
Top 100 weight (in %)	3.10	98.60	96.69	97.41	97.31	96.15
$\sigma\left(w \mid b\right)$ (in bps)		238.86	269.78	237.47	239.38	235.42
$\sigma_{\mathcal{F}}\left(w \mid b\right)$ (in bps)		236.06	267.29	234.69	236.68	232.62
$\sigma_{\epsilon}\left(w \mid b\right)$ (in bps)		2.80	2.48	2.78	2.69	2.80
Yield (in %)	4.62	6.63	6.53	6.58	6.61	6.61
$\beta_{\text{DTS}}\left(w \mid b\right)$	1.00	1.53	1.51	1.53	1.55	1.54
MD (in year)	5.83	6.33	6.33	6.33	6.33	6.33
5Y DTS (in bps)	62	162	162	162	162	162
7Y DTS (in bps)	75	100	102	100	100	100
10Y+ DTS (in bps)	224	199	198	199	199	199
Financials DTS (in bps)	133	428	433	435	442	429
A-rated DTS (in bps)	190	165	165	165	165	165
BBB-rated DTS (in bps)	255	355	355	355	355	355
c_{ash} (in %)			0.00	0.00	0.00	0.00
$\mathcal{C}_{ash}$ (in \$)			3	967	3 325	132
$\mathcal{IG}_{ap}$ (in %)			15.42	7.70	5.22	7.40

Table 39: Optimal investable portfolios (Barra model, G0BC Index, end of May 2026, one-step approach, at least 150 holdings, no active share limit)

Statistic	Benchmark	Continuous	50 mn	100 mn	500 mn	1 bn
Holdings	20 350	106	150	150	151	150
Active share (in %)		99.70	99.61	99.65	99.67	99.65
ENB (w)	12 788	102	105	104	104	105
Top 100 weight (in %)	3.10	98.60	96.53	97.25	97.45	96.28
$\sigma\left(w \mid b\right)$ (in bps)		238.86	270.73	237.00	240.98	235.53
$\sigma_{\mathcal{F}}\left(w \mid b\right)$ (in bps)		236.06	268.27	234.21	238.23	232.73
$\sigma_{\epsilon}\left(w \mid b\right)$ (in bps)		2.80	2.46	2.79	2.75	2.80
Yield (in %)	4.62	6.63	6.53	6.58	6.61	6.61
$\beta_{\text{DTS}}\left(w \mid b\right)$	1.00	1.53	1.50	1.53	1.54	1.54
MD (in year)	5.83	6.33	6.32	6.33	6.33	6.33
5Y DTS (in bps)	62	162	162	162	162	162
7Y DTS (in bps)	75	100	101	100	100	100
10Y+ DTS (in bps)	224	199	198	199	199	199
Financials DTS (in bps)	133	428	435	432	439	429
A-rated DTS (in bps)	190	165	165	165	165	165
BBB-rated DTS (in bps)	255	355	355	355	355	355
c_{ash} (in %)			0.00	0.00	0.00	0.00
$\mathcal{C}_{ash}$ (in \$)			38.58	807.44	19 860	9 217
$\mathcal{IG}_{ap}$ (in %)			14.96	7.86	4.81	7.23

Table 40: Optimal investable portfolios (Barra model, G0BC Index, end of May 2026, two-step approach, no cardinality constraint, no active share limit)

Statistic	Benchmark	Continuous	50 mn	100 mn	500 mn	1 bn
Holdings	20 350	106	126	115	127	136
Active share (in %)		99.70	98.61	98.66	98.62	98.62
ENB (w)	12 788	102	111	107	106	108
Top 100 weight (in %)	3.10	98.60	93.16	96.15	96.42	95.23
$\sigma\left(w \mid b\right)$ (in bps)		238.86	232.28	238.43	241.17	235.70
$\sigma_{\mathcal{F}}\left(w \mid b\right)$ (in bps)		236.06	229.43	235.68	238.42	232.95
$\sigma_{\epsilon}\left(w \mid b\right)$ (in bps)		2.80	2.85	2.75	2.75	2.76
Yield (in %)	4.62	6.63	6.24	6.44	6.48	6.46
$\beta_{\text{DTS}}\left(w \mid b\right)$	1.00	1.53	1.46	1.50	1.51	1.49
MD (in year)	5.83	6.33	6.08	6.26	6.11	6.03
5Y DTS (in bps)	62	162	162	162	164	162
7Y DTS (in bps)	75	100	100	101	100	100
10Y+ DTS (in bps)	224	199	199	185	189	175
Financials DTS (in bps)	133	428	416	422	428	434
A-rated DTS (in bps)	190	165	161	163	160	165
BBB-rated DTS (in bps)	255	355	355	355	355	355
c_{ash} (in %)			2.00	2.00	2.00	2.00
$\mathcal{C}_{ash}$ (in k\$)			999.9	1 999.8	10 000	20 000
$\mathcal{IG}_{ap}$ (in %)			11.35	4.61	2.14	4.19

Table 41: Optimal investable portfolios (Barra model, G0BC Index, end of May 2026, two-step approach, no cardinality constraint, no active share limit, $\varphi = 1$)

Statistic	Benchmark	Continuous	50 mn	100 mn	500 mn	1 bn
Holdings	20 350	106	141	182	117	283
Active share (in %)		99.70	99.52	99.40	99.67	99.62
ENB (w)	12 788	102	108	106	104	105
Top 100 weight (in %)	3.10	98.60	94.72	95.94	97.30	96.65
$\sigma\left(w \mid b\right)$ (in bps)		238.86	249.64	237.29	245.17	234.09
$\sigma_{\mathcal{F}}\left(w \mid b\right)$ (in bps)		236.06	246.99	234.54	242.45	231.29
$\sigma_{\epsilon}\left(w \mid b\right)$ (in bps)		2.80	2.65	2.75	2.72	2.80
Yield (in %)	4.62	6.63	6.34	6.49	6.51	6.59
$\beta_{\text{DTS}}\left(w \mid b\right)$	1.00	1.53	1.47	1.51	1.55	1.51
MD (in year)	5.83	6.33	6.10	6.32	6.31	6.03
5Y DTS (in bps)	62	162	175	162	175	164
7Y DTS (in bps)	75	100	100	100	100	100
10Y+ DTS (in bps)	224	199	197	199	198	180
Financials DTS (in bps)	133	428	403	419	431	434
A-rated DTS (in bps)	190	165	165	165	164	164
BBB-rated DTS (in bps)	255	355	354	354	355	355
c_{ash} (in %)			0.00	0.00	0.01	0.00
$\mathcal{C}_{ash}$ (in \$)			436	875	67 491	0.00
$\mathcal{IG}_{ap}$ (in %)			12.36	5.62	3.14	5.20

Table 42: Sector allocation in % (Barra model, G0BC Index, end of May 2026, scope $\boldsymbol{\mathcal{SC}}_1$)

Sector	Index	Reduction rate $\boldsymbol{\mathcal{R}}$							
		10%	30%	40%	50%	60%	70%	80%	90%
Communication Services	7.18	7.18	7.19	7.19	7.18	7.18	7.17	7.17	7.17
Consumer Discretionary	6.75	6.75	6.75	6.75	6.75	6.75	6.75	6.75	6.67
Consumer Staples	5.80	5.80	5.80	5.80	5.80	5.80	5.80	5.80	5.80
Energy	6.65	6.65	6.65	6.65	6.60	6.36	6.36	6.55	5.68
Financials	34.88	34.77	35.35	35.68	35.96	36.35	36.96	37.57	38.92
Health Care	7.82	7.82	7.82	7.82	7.82	7.82	7.82	7.82	7.82
Industrials	8.70	8.70	8.71	8.71	8.71	8.70	8.70	8.55	8.79
Information Technology	4.65	4.65	4.67	4.66	4.70	4.74	4.70	4.66	4.66
Materials	3.20	3.20	3.16	3.12	3.11	3.00	2.98	2.66	2.46
Real Estate	3.94	3.94	3.94	3.94	3.94	3.94	3.94	3.94	3.94
Utilities	10.42	10.53	9.96	9.67	9.43	9.35	8.81	8.53	8.09

Source: ICE BofA, Trucost & Authors' calculations.

Table 43: Sector allocation in % (Barra model, G0BC Index, end of May 2026, scope $\boldsymbol{\mathcal{SC}}_{1-2}$)

Sector	Index	Reduction rate $\boldsymbol{\mathcal{R}}$							
		10%	30%	40%	50%	60%	70%	80%	90%
Communication Services	7.18	7.17	7.18	7.17	7.17	7.17	7.17	7.17	7.17
Consumer Discretionary	6.75	6.75	6.75	6.75	6.75	6.75	6.70	6.66	6.62
Consumer Staples	5.80	5.80	5.80	5.80	5.80	5.80	5.80	5.80	5.77
Energy	6.65	6.65	6.65	6.65	6.49	6.33	5.94	4.71	2.62
Financials	34.88	34.84	35.63	36.07	36.53	37.41	38.26	38.83	41.18
Health Care	7.82	7.82	7.82	7.83	7.83	7.83	7.83	7.82	7.82
Industrials	8.70	8.70	8.70	8.70	8.70	8.70	8.60	8.41	8.25
Information Technology	4.65	4.66	4.66	4.66	4.65	4.66	4.65	4.65	4.60
Materials	3.20	3.20	3.11	3.06	3.05	2.95	2.78	2.46	2.03
Real Estate	3.94	3.94	3.94	3.94	3.94	3.94	3.94	4.63	5.39
Utilities	10.42	10.46	9.75	9.36	9.09	8.45	8.34	8.85	8.56

Source: ICE BofA, Trucost & Authors' calculations.

Table 44: Sector allocation in % (Barra model, G0BC Index, end of May 2026, scope $\boldsymbol{\mathcal{SC}}^{\text{up}}_{1-3}$)

Sector	Index	Reduction rate $\boldsymbol{\mathcal{R}}$							
		10%	30%	40%	50%	60%	70%	80%	90%
Communication Services	7.18	7.17	7.17	7.17	7.17	7.17	7.17	7.16	6.84
Consumer Discretionary	6.75	6.75	6.75	6.75	6.72	6.64	6.50	5.43	1.79
Consumer Staples	5.80	5.80	5.80	5.78	5.69	5.57	4.74	3.40	1.50
Energy	6.65	6.65	6.65	6.26	6.11	4.77	2.89	2.08	1.82
Financials	34.88	35.03	36.35	37.20	38.54	38.81	41.32	46.84	59.76
Health Care	7.82	7.82	7.82	7.82	7.82	7.82	7.82	8.60	12.04
Industrials	8.70	8.70	8.70	8.82	8.83	10.08	11.10	11.04	6.10
Information Technology	4.65	4.65	4.65	4.65	4.65	4.65	4.63	4.42	2.45
Materials	3.20	3.19	3.10	3.03	2.99	3.02	2.86	2.65	2.59
Real Estate	3.94	3.94	3.94	3.94	3.94	3.89	3.83	3.66	2.23
Utilities	10.42	10.30	9.06	8.58	7.54	7.58	7.14	4.72	2.89

Source: ICE BofA, Trucost & Authors' calculations.

Table 45: Sector allocation in % (Barra model, G0BC Index, end of May 2026, scope $\boldsymbol{\mathcal{SC}}_{1-3}$)

Sector	Index	Reduction rate $\boldsymbol{\mathcal{R}}$							
		10%	30%	40%	50%	60%	70%	80%	90%
Communication Services	7.18	7.18	7.17	7.17	7.17	7.17	7.17	7.17	7.17
Consumer Discretionary	6.75	6.75	6.75	6.72	6.72	6.72	6.72	6.20	4.47
Consumer Staples	5.80	5.80	5.80	5.80	5.80	5.80	5.80	5.80	5.25
Energy	6.65	6.65	6.02	5.27	4.08	4.05	3.84	2.92	2.00
Financials	34.88	34.88	34.94	35.55	35.83	34.96	33.06	33.17	33.42
Health Care	7.82	7.82	7.82	7.82	7.82	7.82	7.82	7.82	7.82
Industrials	8.70	8.70	9.17	9.71	10.83	11.65	13.82	15.40	18.92
Information Technology	4.65	4.65	4.65	4.64	4.61	4.61	4.62	4.64	4.63
Materials	3.20	3.20	3.04	2.97	2.92	2.91	2.84	2.68	2.50
Real Estate	3.94	3.94	3.94	3.94	3.94	3.94	3.94	3.94	3.87
Utilities	10.42	10.42	10.72	10.41	10.29	10.37	10.38	10.25	9.95

Source: ICE BofA, Trucost & Authors' calculations.

C.2 Figures

Figure 23: ℓ_1-norm efficient frontier (ER00 Index, end of May 2026)

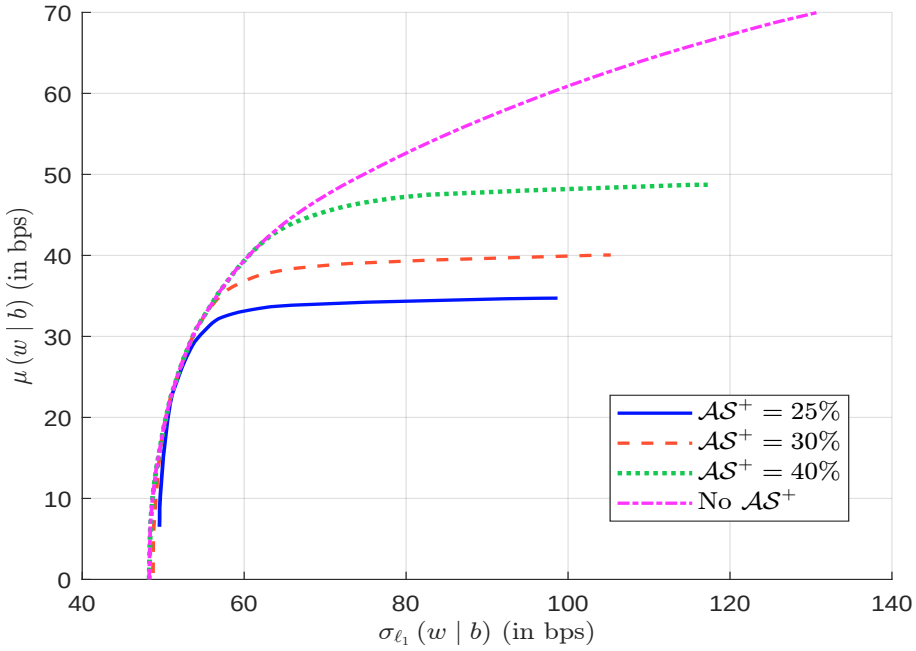

Figure 24: ℓ_2-norm efficient frontier (ER00 Index, end of May 2026)

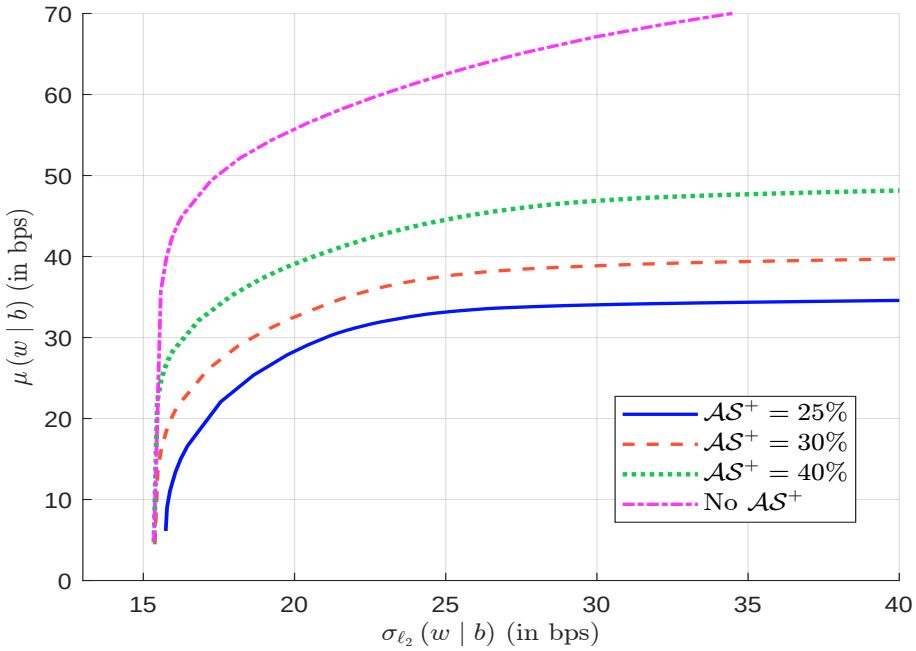

Figure 25: Efficient frontier (ER00 Index, end of May 2026, Barra risk model)

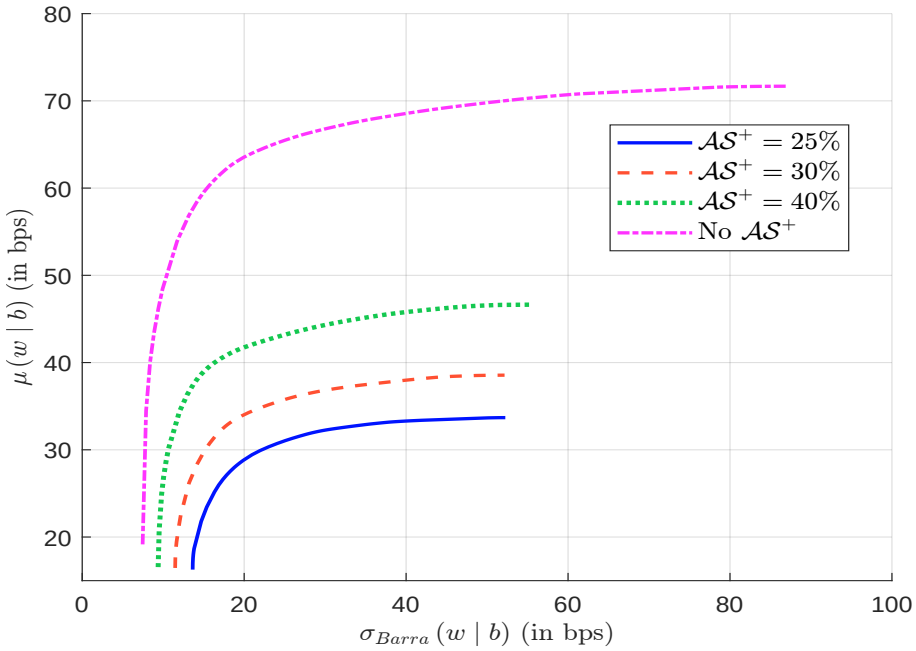

Figure 26: Efficient frontier (C0A0 Index, end of May 2026, Barra risk model)

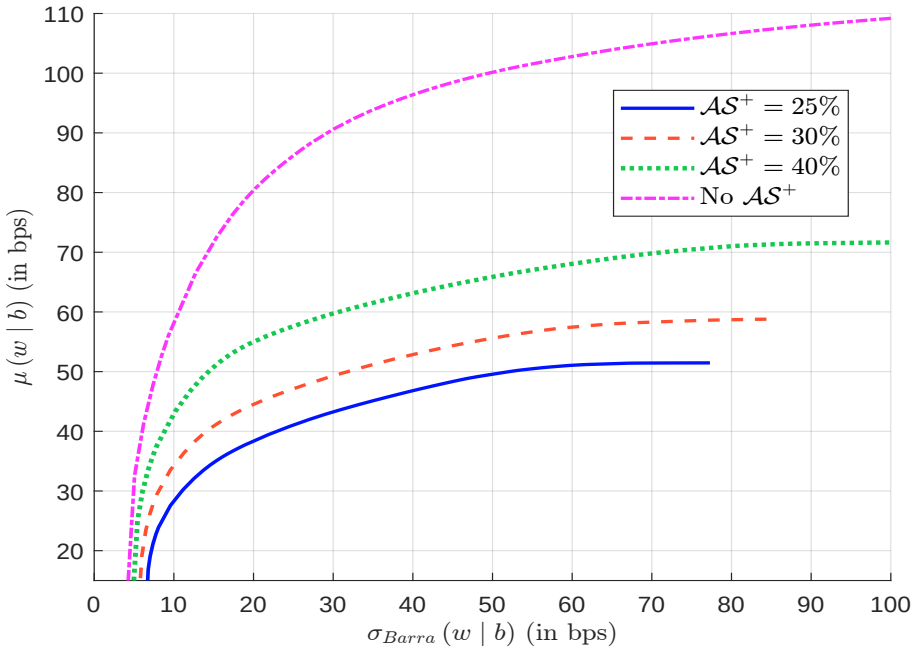

Figure 27: Efficient frontier (G0BC Index, end of May 2026, Barra risk model)

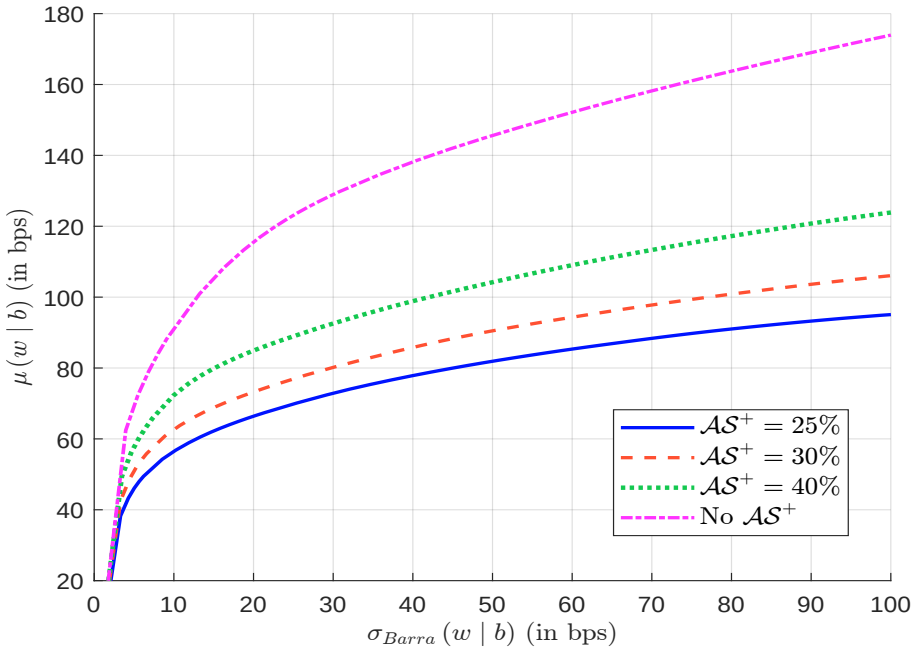

Chief Editor

Monica DEFEND
Head of Amundi Investment Institute

Editors

Marie BRIÈRE
Head of Investors' Intelligence & Academic Partnership

Thierry RONCALLI
Head of Quant Portfolio Strategy

Investment Institute

WORKING PAPER 191 | **JULY 2026**

Find out more about Amundi Investment Institute Publications

Visit our Research Center

SCAN ME

Amundi
Investment Solutions

Trust must be earned